RICE UNIVERSITY

THE EFFECTS OF IMPURITIES ON THE PLASTIC DEFORMATION OF MOLYBDENUM SINGLE CRYSTALS

by

LARRY DON WHITMIRE

A THESIS SUBMITTED
IN PARTIAL FULFILLMENT OF THE
REQUIREMENTS FOR THE DEGREE OF

DOCTOR OF PHILOSOPHY

Thesis Director's signature:

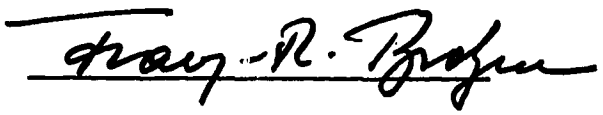

Houston, Texas

(June, 1966)

TABLE OF CONTENTS

INTRODUCTION

Plastic deformation of metals proceeds by the movement of dislocations. When a dislocation moves, it must overcome obstacles. These are of two types; long range and short range, depending on the extent of their stress fields. If the stress field of an obstacle is in the order of 10 atomic diameters or greater, it is termed a "long range" obstacle. Short range obstacles have stress fields less than 10 atomic diameters.

The stress on a segment of a dislocation is equal to the applied stress plus the algebraic sum of all the internal stress fields in the crystal at the point in question. If the movement of the particular segment of dislocation being considered is opposed mainly by a short range obstacle, thermal energy helps the dislocation overcome the obstacle. The dislocation segment is then said to be thermally activated. Thermal activation plays no role in overcoming long range obstacles. Examples of short range obstacles are Peierls-Nabarro stress (or intrinsic resistance of the crystal lattice to dislocation motion), forest dislocations, weak impurity pinning points, motion of jogs and cross-slip of screw dislocations. Dislocations on parallel slip planes or large precipitate particles are examples of long range or athermal obstacles. If the flow stress of a metal does not vary with temperature, the motion of the dislocations is considered to be opposed only by the long range stress fields in the metal.

Metals which have a body-centered cubic crystal structure are characterized by a rapid increase in the flow stress with decreasing temperature. This rise in stress is much greater than the change in the elastic constants with temperature. No one explanation for this strong temperature dependence in the b.c.c. metals has satisfied all of the experimental observations. Among the theories proposed to explain the strong temperature and strain-rate dependence of the flow stress of b.c.c. metals are:

1. Intersection of dislocations [1].
2. Overcoming the Peierls-Nabarro stress [2,3,4,5].
3. Motion of jogs [6,7,8].
4. Interaction with impurities [9,10,11].
5. Cross-slip [12,13,14].

All of the theories have current advocates who construe certain experimental evidence as proof that one single mechanism controls the rate of motion of the dislocations. Since the movement of dislocations determines the plastic deformation, a correct model should predict the temperature and strain-rate dependence of the flow stress.

Considerable experimental evidence indicates that the movement of dislocations in b.c.c. metals is a thermally activated process at low temperature. By assuming that a single process is

rate controlling and by applying the usual arguments of rate theory, Mott[15] has written the strain-rate $\dot{\epsilon}$ as:

$$(1) \qquad \dot{\epsilon} = NAb\nu e^{-\Delta G/kT} = \dot{\epsilon}_o e^{-\Delta G/kT}$$

In this equation N is the number of activated sites per unit volume, A is the area swept out by an activated segment of dislocation, b is the Burger's vector of the dislocation, ν is the vibrational frequency of the dislocation, k is Boltzmann's constant, T is the absolute temperature, and ΔG is the difference in the Gibbs free energy in the activated and equilibrium states. Recently Schoeck[16] has discussed the thermodynamics of dislocation motion and noted several errors that have appeared in the literature. The correct value of ΔG in equation (1) is the change in G to bring a dislocation from its equilibrium position isothermally to the saddle-point with the lowest activation energy and is given by[16]:

$$(2) \qquad \Delta G = \Delta g(\bar{\tau}) - \bar{\tau}\ell bd(\bar{\tau})$$

Here $\Delta g(\bar{\tau})$ is the change in G due to local atomic misfit, $\bar{\tau}$ is the effective stress on the segment of dislocation given by the applied stress less the internal stress at the point of activation, ℓ is the length of dislocation segment being activated, b is the Burger's vector, and $d(\bar{\tau})$ is the distance the dislocation moves in going from its equilibrium position to the saddle-point.

A quantity called the activation volume, V, has been introduced in the literature and is defined as

$$V = b\ell d(\bar{\tau}) \tag{3}$$

With this definition of V, the second term in equation (2) can be written as $\bar{\tau}V(\bar{\tau})$ and can be interpreted as the work done by the effective stress $\bar{\tau}$ in moving the dislocation from the equilibrium position to the saddle-point configuration. Substituting equations (2) and (3) into equation (1), we get

$$\dot{\epsilon} = \dot{\epsilon}_o e^{-[\Delta g(\bar{\tau}) - \bar{\tau}V(\bar{\tau})]/kT} \tag{4}$$

Equation (4) can be written in logarithmic form as follows:

$$kT(\ln \dot{\epsilon}/\dot{\epsilon}_o) = -\Delta g(\tau) + \bar{\tau}V(\bar{\tau}) \tag{5}$$

The differentiation of equation (5) with respect to $\bar{\tau}$ at constant temperature and dislocation structure gives

$$kT\left[\frac{\partial \ln \dot{\epsilon}/\dot{\epsilon}_o}{\partial \bar{\tau}}\right]_{T,\epsilon} = -\frac{\partial \Delta g(\bar{\tau})}{\partial \bar{\tau}} + V(\bar{\tau}) + \bar{\tau}\frac{\partial V(\bar{\tau})}{\partial \bar{\tau}} \tag{6}$$

Since the internal structure has been assumed constant, the change in the effective stress $\bar{\tau}$ is equal to the change in the applied stress τ_a and

$$kT\left[\frac{\partial \ln \dot{\epsilon}/\dot{\epsilon}_o}{\partial \tau_a}\right]_{T,\epsilon} = -\frac{\partial \Delta g(\bar{\tau})}{\partial \tau_a} + V(\bar{\tau}) + \bar{\tau}\frac{\partial V(\bar{\tau})}{\partial \tau_a} \tag{7}$$

Because of the stress dependence of $\Delta g(\bar{\tau})$ and $V(\bar{\tau})$ the L.H.S. of equation (7) has been taken by some authors [17,18] to define an "effective activation volume", V^*. Schoeck [16] has shown that if the dislocations are assumed to be in equilibrium at the saddle point position the stress dependence of $\Delta g(\bar{\tau})$ and $V(\bar{\tau})$ can be eliminated from equation (7) and the above distinction between V and V^* is not justified. Schoeck also implied that V can be determined directly from experiment by the equation

$$(8) \qquad \left.\frac{kT[\partial \ln \dot{\epsilon}/\dot{\epsilon}_o]}{\partial \tau_a}\right|_{T,\epsilon} = V = -\frac{\partial \Delta G}{\partial \tau_a}$$

In order to illustrate the information required to determine the activation volume from equation (8), it has been re-written as

$$(9) \qquad V = kT[\partial \ln \dot{\epsilon}/\partial \tau_a]_{T,\epsilon} - kT[\partial \ln \dot{\epsilon}_o/\partial \tau_a]_{T,\epsilon}$$

It is apparent from equation (9) that V can be determined from the standard strain-rate change at constant temperature method only if additional information on the variation of $\dot{\epsilon}_o$ with stress is available. Usually the assumption is made that $\dot{\epsilon}_o$ does not vary with stress and the last term in equation (9) is zero. This assumption was made for the present tests although recent results indicated that $\dot{\epsilon}_o$ may vary considerably with stress in the low strain region [12,16]. Even with the above limitations Schoeck has concluded that the activation volume should have a

characteristic value and stress dependence for each dislocation mechanism and should be helpful in determining the mechanism controlling the rate of dislocation motion.

A characteristic property of b.c.c. metals is the strong influence of impurities on their plastic properties. Exactly how the impurities change the plastic properties is not certain, as is evident from the proposed theories for the rate controlling mechanism in the movement of dislocations. Since it is now possible to grow single crystals of b.c.c. metals of very high purity, the possibility of testing the influence of minute quantities of impurities on the plastic deformation of b.c.c. metals without the influence of grain boundaries has been considered. Other distinctive properties of the b.c.c. metals are the high stacking-fault energy and the multiplicity of slip systems. These two properties result in macroscopically observable differences in the plastic properties of b.c.c. and f.c.c. metals.

To study the effect of impurities, single crystals of molybdenum were grown with various degrees of purity. All of the single crystals were so pure that quantitative differences in the purity levels could not be determined by chemical analyses, and the resistivity at liquid helium temperature was used as a qualitative measure of the differences in purity of the crystals.

In order to minimize the orientation effects and to maximize the resolved shear stress on a particular slip system, the tests in this investigation were conducted by deforming the single crystals in direct shear. (A review of the technique may be found in the literature [19].)

The effects of small amounts of impurities on the plastic deformation of molybdenum were studied by observing their influence on the stress-strain curve and activation volume for deformation in the low temperature region. Maximum resolved shear stress was placed on the (110) - $[1\bar{1}1]$ system during all tests.

Background Material

The following survey of the literature covers only a few of the many investigations conducted into the behavior of dislocations in metals. Since the present tests are concerned with the effect of impurities on the plastic deformation of molybdenum, only those theories, models, and experiments which are more or less directly related to the interaction of impurities and dislocations in the b.c.c. structure are considered. Even with this limitation, many publications are not included because of the vast amount of work that has been done in this area.

Heslop and Petch[2] studied the effect of C and N in solution in polycrystalline iron. The flow stress was considered to be composed of two components; one was a function of the grain size, and the other, termed the frictional stress, was a function of the temperature and impurity content. Increasing the C and N concentration was found to have an athermal effect on the frictional stress, and, from this observation, Heslop and Petch concluded that a high Peierls-Nabarro force was responsible for the temperature dependence of the flow stress.

Basinski and Christian[3] measured the difference in flow stress for a strain-rate change at constant temperature, $\Delta\sigma)_T$, for polycrystalline iron. At 180° K the change in flow stress

$\Delta\sigma)_T$ was approximately constant with stress, and $\Delta\sigma)_T$ increased or decreased linearly with stress for temperatures of 78° and 273° K, respectively. At 20% strain, $(1/T)\Delta\sigma)_T$ was found to be a linearly decreasing function of increasing temperature. They concluded that the density of rate controlling obstacles was not changed during deformation. Only two obstacles were considered to satisfy these requirements—a uniform distribution of impurities and the Peierls-Nabarro barriers. Because of the similarity between carburized and annealed specimens, the Peierls-Nabarro barriers were assumed to be the controlling factors. They maintained that the Peierls-Nabarro barriers were only minor functions of temperature, and that thermal activation over a more or less constant barrier explained the results.

Conrad and Frederick[4] also investigated the effect of temperature and strain rate on the flow stress of polycrystalline iron and obtained results similar to Basinski and Christian[3]. The variation of the activation energy and activation volume with stress was considered to be independent of the strain, interstitial content and impurity distribution. A change in the flow parameters $(\Delta\sigma/\Delta \ln \dot{\epsilon})_T$ and $(\Delta\sigma/\Delta T)_{\dot{\epsilon}}$ with strain was attributed to an increase in the frequency factor $\dot{\epsilon}_o$, or more specifically, to the mobile dislocation density contributing to the deformation.

Wellings and Maddin[20] found the yield stress in "high purity" polycrystalline and single crystals of niobium to be temperature dependent. They concluded that this temperature dependence was due to a mechanism independent of impurities, such as the Peierls-Nabarro barriers. They determined the impurity dependence of the yield stress to be less than that found by Lawley et al.[21] in molybdenum. This result seems in agreement with the findings of Adams et al.,[22] that the dislocation locking term in niobium is about one-twentieth the value found in molybdenum.

Masters and Christian[5] measured the flow parameters $(\Delta\sigma/\Delta \ln \dot{\epsilon})_T$ and $(\Delta\sigma/\Delta T)_{\dot{\epsilon}}$ for polycrystalline specimens of niobium, vanadium, tantalum, iron and single crystals of niobium. They concluded that the temperature dependence of the flow stress was due almost entirely to thermal activation over the Peierls-Nabarro energy barriers. No differences were detected in the flow parameters due to either impurities or dislocation density and distribution below 90°K; however, some variation of the activation volume with purity for niobium was seen above 90° K. The yield stress variation with temperature for niobium and vanadium was considerably larger than the flow stress variation and was attributed to an influence superimposed on the Peierls-Nabarro barrier.

Kossowsky[13] investigated the anelastic behavior of iron and molybdenum single crystals over the temperature range 5° to 300° K. He determined the effect of temperature, prestrain and impurities on the elastic limit and the anelastic limit. The elastic limit (defined as the stress to produce a damping loop) was found to have a low value at 4.2° K, to have no dependence on prestrain after an initial prestrain and to decrease as the purity increased. The anelastic limit (defined as the stress required to produce an open damping loop) was determined to decrease as the purity increased, to have the same temperature dependence for all purities and to increase with larger prestrains. For molybdenum, impurities enhanced the increase of the anelastic limit with prestrain. Kossowsky attributed the temperature dependence of the elastic and anelastic limits to the inherent resistance of the lattice. It was suggested that the high flow stress at low temperature was not due to an intrinsic mechanism, but rather to a reflection of the rapid work hardening in the microstrain region.

Orava[23] determined the effect of strain rate and temperature on the deformation of single crystals and polycrystalline molybdenum. A plot of the lower yield stress versus logarithm of the strain rate could be divided into a number of linear regions with the number of regions depending on the grain size

and temperature of deformation. For coarse grained and single crystal material only one linear region was obtained. The activation volume increased with strain for the polycrystalline samples, but the activation volume decreased with strain for the single crystals. As indicated previously by Basinski and Christian [3], the positive increase in the activation volume with strain for the polycrystalline samples was considered to be inconsistent with the creation of rate-controlling obstacles during deformation, and an intrinsic lattice resistance mechanism was concluded to be rate controlling. No explanation of the decrease in the activation volume with strain for the single crystals was offered. Close agreement between the strain-rate dependence of both the yield stress and the flow stress was construed as evidence that the two phenomena were controlled by the same mechanism. Orava implied that non-uniform yielding caused the different regions in the curve of lower yield stress versus strain rate and that it was not an indication of different mechanisms being rate controlling.

Stein and Low [24] have shown that the velocity of dislocations in silicon-iron single crystals varied with temperature in the same manner as the yield stress, and hence concluded that it was the intrinsic lattice resistance that controlled the dislocation motion. However, their results also indicated that the temperature had an effect on the strength of dislocation pinning by

impurities. This latter caused an additional temperature dependent term to be superimposed on the intrinsic lattice resistance. Mordike and Haasen [9] found the change in flow stress, due to a change in the strain rate at constant temperature in iron single crystals to increase linearly as the temperature decreased for all values of stress, to increase as the temperature decreased for all values of applied stress and to decrease with increasing purity (the amount of decrease attributed to increased purity was larger at lower temperatures). Because of a minimum in kT/V at -100°C, the possibility of the dispersion of the impurities being a function of both deformation and deformation temperature was considered. It was postulated that at low temperatures the deformation changed the dispersion in a manner which increased the number of obstacles that could be thermally surmounted while at high temperatures, the number of thermally surmountable obstacles decreased with deformation. Mordike and Haasen concluded that the forest and Peierls-Nabarro mechanisms could not explain their results but that the effect of impurities might. Mordike [25] noted that the sensitivity to impurities should be less in metals of large lattice parameter.

Stein, Low and Seybolt [10] suggest that the effect of impurities accounts for the high flow stress at low temperatures in iron single crystals. It was shown that the temperature dependence of the yield strength could be substantially reduced

by purifying. The model proposed by Fleisher[26] and Fleisher and Hibbard[27] was considered to explain their results. Nabarro et al.[28] believe this model will not lead to the observed temperature dependence because it predicts temperature independent hardening below the temperature at which the diffusion of interstitial atoms becomes appreciable.

Koo[11] has shown that impurities affect both the yield and the plastic flow by the same magnitude in tungsten single crystals. Increased purity raised the frequency of twinning but had no effect on the work-hardening rate. Using electrical resistivity measurements at 4.2° K, the differences in purity for the pure and the impure crystals was estimated to be small. For the calculated small differences in purity, the theories of Cracknell and Petch[29], of Schoeck and Seeger[30] and of Fleischer[26] for solid-solution hardening, all of which are based on the elastic interaction of dislocation and interstitial impurities in solid solution, could not account for the observed differences in critical resolved shear stress. Koo concluded that the large amount of strengthening in the less-pure crystals was due to an increase in the amount of minute precipitates.

Fourdeux and Wronski[31] studied the effect of the strain rate on the yield stress in polycrystalline niobium. A plot of the yield stress versus the logarithm of the strain rate was divided

into three linear regions. Previously Sargent et al.[32] obtained similar results exhibiting linear regions. However, their slopes differed from those determined by Fourdeux and Wronski. Since the purity of the samples used by Fourdeux and Wronski was higher than that used by Sargent et al., Fourdeux and Wronski suggested that overcoming impurities could be the mechanism that controlled the deformation.

The influence of impurities was observed to override the grain size effect in polycrystalline niobium by van Torne and Thomas[33]. The flow stress was sensitive to the initial dislocation substructure which, in turn, was determined by the purity of the samples. The distribution and density of the dislocations and their tendency to cell formation in the deformed samples were found to depend on the presence of impurities which formed a precipitate net-work before deformation.

Shaw and Sargent[34] demonstrated that impurity atoms and point defects interact with dislocations by measuring the load relaxation below the upper yield limit in polycrystalline molybdenum and niobium. This was done by loading the samples at constant strain rate to a specified amount and then stopping the machine. Relaxation was determined by measuring the drop in load during a specific time interval. The drop in load was found to grow larger by increasing the initial load, by increasing the

strain rate or by increasing the purity. Repeated tests to the same load level exhibited a decreasing load drop that finally became zero. Radiation damage was found to have the same effect as impurities and to decrease the load drop. The effect of irradiation could be removed by annealing at 170° C for one hour. From this result Shaw and Sargent concluded that the point defects are annealed out in clusters rather than condensed onto the dislocations. Prestrain was found to decrease the relaxation; hence dislocations and point defects that were produced during deformation acted as barriers to the motion of free dislocations.

Lawley, Van den Sype and Maddin [35] found both single and polycrystalline molybdenum to exhibit no significant difference in strain hardening characteristics due to purity. Increasing the purity decreased the yield and flow stresses, improved low temperature ductility, decreased the temperature variation of the flow stress for temperatures above 78° K and produced almost no difference at 4.2° K. They concluded that the concept of a temperature dependent flow stress based on an intrinsic lattice friction would be inconsistent with their results.

The elastic and anelastic limits in polycrystalline iron were measured by Brown and Ekvall [12] as functions of the purity.

No variation of the elastic limit with temperature was found; although the elastic limit was a function of purity. The variation of the anelastic limit with temperature decreased with greater purity. It was postulated that for "pure" iron, the anelastic limit would not be a function of temperature and that the stress required to move dislocations would be independent of the temperature. The temperature dependence of the microscopic yield point was associated with a high rate of work-hardening in the microstrain region.

Recently Stein[50] studied the strain-rate sensitivity of iron single crystals as a function of purity and deformation. He concluded that the results cannot be adequately explained on the basis of a single thermally activated process.

Mitchell, Foxhall and Hirsch[36] reported three-stage stress-strain curves in niobium single crystals. They found that the stages were made more distinct by increasing the purity, decreasing the strain rate or for orientations favoring single slip on one (110) - $[\bar{1}11]$ slip system. Their results indicate that easy glide ends when extensive secondary slip occurs. For a strain rate of 4.5×10^{-5} sec^{-1}, three-stage hardening was found over the temperature range of 201-373 ^{o}K. Increasing the strain rate made the transition from stage I to stage II less distinct, raised the yield stress and decreased sharply the work-hardening rate in stage II. The presence of three-stages appeared to be restricted to a limited range of orientations, temperatures and strain rates.

Testing only at room temperature, Keh[37] and Jaoul and Gonzales[38] found three-stage stress-strain curves in iron single crystals for approximately the same orientation as Mitchell et al.[36] used in niobium. Keh compared his results on iron to the above ones on niobium and concluded that the three-stages are more sharply defined in niobium, that stage I in iron does not increase with deviation from the (001)-(011) symmetry boundary as it does in niobium and that the slope in stage II of iron varies from G/400 to G/900, while this slope remains approximately constant at G/600 in niobium. At higher temperatures, lower strain rates and lower purity, the work hardening behavior of niobium approaches that of iron.

Mitchell and Spitzig[39] determined three-stage stress-strain curves for tantalum single crystals. The effects of purity, orientation and strain rate on the appearance of the stress-strain curves were almost identical to those reported earlier by Mitchell et al.[36] on niobium.

The preceding survey has been concerned with the interaction of impurities and dislocations as determined by mechanical tests. Recently a considerable number of investigators have used transmission electron microscopy to study impurities and dislocations in b.c.c. metals. Some of this work will now be reviewed.

Keh and Weissmann [40] reviewed the general features of the dislocation substructure and the various work-hardening theories which have been proposed for the b.c.c. metals. They concluded that:

1. The deformed substructure in iron and in refractory metals are very similar.
2. Dislocations are kinked and non-uniformly distributed in the early stages of deformation.
3. The development of a cell structure occurs with deformation.
4. The dislocations are more uniformly distributed and exhibit less tendency towards cell formation at lower deformation temperatures.
5. Below the temperature of recovery the density of dislocations as a function of strain is independent of the deformation temperature but dependent upon the grain size.
6. The stacking-fault energy is intrinsically high but may be lowered by impurity segregation to dislocations.
7. The long-range stress fields of dislocation tangles contribute most to the work hardening.

Edington and Smallman [41] noted an absence of a cell structure for vanadium deformed in the temperature range 77° to 673° K.

They considered it possible for the fine dispersion of precipitates found in the annealed material to be responsible for this lack of a well defined cell structure, as was suggested previously by Swann[42]. Over the temperature range Edington and Smallman investigated, the flow stress was found to be proportional to the square of the dislocation density, and the dislocation density was proportional to the strain.

Lawley and Gaigher[43] concluded that the dislocation tangles in deformed single crystals of molybdenum were associated with inclusions or impurity precipitates in the matrix. In areas free from visible perturbations, the dislocations were long, relatively straight, of a predominately screw character and exhibited no tendency towards conventional tangling. This is in agreement with the theory[44] that tangling is a thermally activated process and is expected to stop at low homologous temperatures. Lawley and Gaigher detected no tangling or loop formation due to dislocations cutting the primary slip plane, however, the forest dislocations did appear to pin screw dislocations temporarily along their length.

Stiegler et al.[45] observed an early formation of a cell structure in niobium single crystals. During further deformation, additional dislocations were created which were either

forced or attracted into the cell walls. Dislocations were observed to act as sinks for interstitials with the result that they were quickly surrounded by interstitial atmospheres or precipitates. The pinned dislocations were observed neither to move nor to multiply during deformation.

Berghezan (46) studied the dislocations in polycrystalline niobium by performing two parallel series of tests, examination of foils thinned after deformation and examination during deformation of pre-thinned foils. The dislocations were observed first to form nodules, then skeins, then tangles which joined to form a cell structure, as the strain increased. The dislocations were observed to easily bypass precipitate particles by cross slip. Once the cell structure was formed, no additional work hardening was observed. This lack of work hardening was attributed to the draining of the dislocations into cell walls, thereby leaving the interior of the cells free for dislocation movement. Berghezan concluded that dislocation grouping was a dynamic recovery process governed both by cross slip and by climb, which sooner or later reduces the work-hardening rate and provides additional ductility by reducing the stress field of the uniform dislocation distribution. This conclusion was considered to explain why the shape of the stress-strain curve and the value for the stress and elongation were

strongly dependent on temperature, strain-rate and impurity content, since each parameter could be an influence on the dynamic recovery rate.

Wronski and Fourdeux[47] observed no difference in density or distribution of dislocations due to purity in deformed polycrystalline niobium. However, they did detect a difference in the stress-strain curves due to purity. The strain-rate had a pronounced effect on the dislocation distribution without influencing the total number.

Gilbert, Wilcox and Hahn[48] indicated that a change in the strain rate by a factor of 10^8 was accommodated primarily by an increase in the average dislocation velocity rather than in the number of mobile dislocations. The higher strain rates had less dislocation tangling and a greater density of small loops but about the same overall density as the slow strain rates. Lawley and Gaigher[49] observed similar results in the structure when they lowered the temperature from 300° K to 4.2° K.

From this brief review of results and conclusions, it is observed that considerable disagreement exists concerning the cause of the rapid rise in the yield and flow stresses at low temperatures. In some instances the same experimental results

are interpreted as positive support for different theories. Since all defects and perturbations in the lattice have some effect on the manner in which dislocations produce the required deformation at the applied strain rate, the problem of determining what, and if, one specific mechanism is responsible for controlling the rate of motion is very difficult.

EXPERIMENTAL PROCEDURE

A. General

Tests were conducted on single crystals of molybdenum prepared by the electron-beam melting technique. Before shear testing, the resistance-ratio, $R_{273}/R_{4.2}$, was determined and used as an indication of the purity. Direct shear tests were performed on an Istron Model TT-C-1 testing machine with the (110) - $[\bar{1}11]$slip system oriented for maximum shear stress.

Various levels of purity were determined from the resistance-ratio measurements, and the effect of purity on the stress-strain curve in shear was investigated at two strain rates and five temperatures. Strain rates of approximately $2 \times 10^{-2} sec^{-1}$ and $2 \times 10^{-4} sec^{-1}$ and deformation temperatures of 78°, 200°, 250°, 300°, 350°, and 400° K were used.

The variation of the activation volume with strain and purity for each deformation temperatures was also determined.

B. Crystal Growth

The starting material used in growing the single crystals was obtained in three different lots from the Dover Wire Plant of General Electric Company in the form of one-eighth inch diameter rods. An analysis of each of the lots supplied by the

company is given in Table 1. The electron-beam melting technique described by Lawley [51] was used to grow the single crystals with crystal orientation controlled by seeding. Some of the single crystals were grown in an electron-beam melting apparatus (EBA) built by Youngblood [7], and some were grown in a new EBA built especially for this project and shown in figures 1 and 2. Table 2 gives the starting material, number and speed of the zone passes and other information recorded during the crystal growing process.

In order to produce very high purity single crystals, several parameters in the growing process were varied. It was found that an increased number of zone passes, a higher vacuum, and purer starting material were most effective in increasing the purity of the single crystals. The effects of the number of zone passes and the starting material on the purity are shown in figure 3.

Work by Hay and Scala [52] on tungsten indicated that imposing an electric field along the crystal during the growing process could be either beneficial or detrimental to the overall purity, depending on the direction of the field. Several molybdenum crystals were grown with a relatively low electric field in opposite directions; no difference from the crystals grown with an absence of electric field could be detected.

Table 1

Chemical Analysis of Starting Material as Supplied by General Electric.

Element	Lot 1 ppm	Lot 2 ppm	Lot 3 ppm
Na	2		5
K	1		21
Al	<8		8
Ca	9		5
Si	15	<35	27
Fe	25	<15	19
Cr	<8		8
Ni	7	<10	6
Cu	< 10		8
W	67		97
Mn	< 10		10
Mg	< 10		11
Sn	19		11
Co	< 8		8
Ti	< 10		10
Ag	< 1		1
Pb	< 10		10
Zr	< 10		10
O_2	8 ± 5	10	7 ± 5
N_2	4 ± 4	3	3 ± 3
H_2	1 ± 1	2	1 ± 1
C	20	270	10

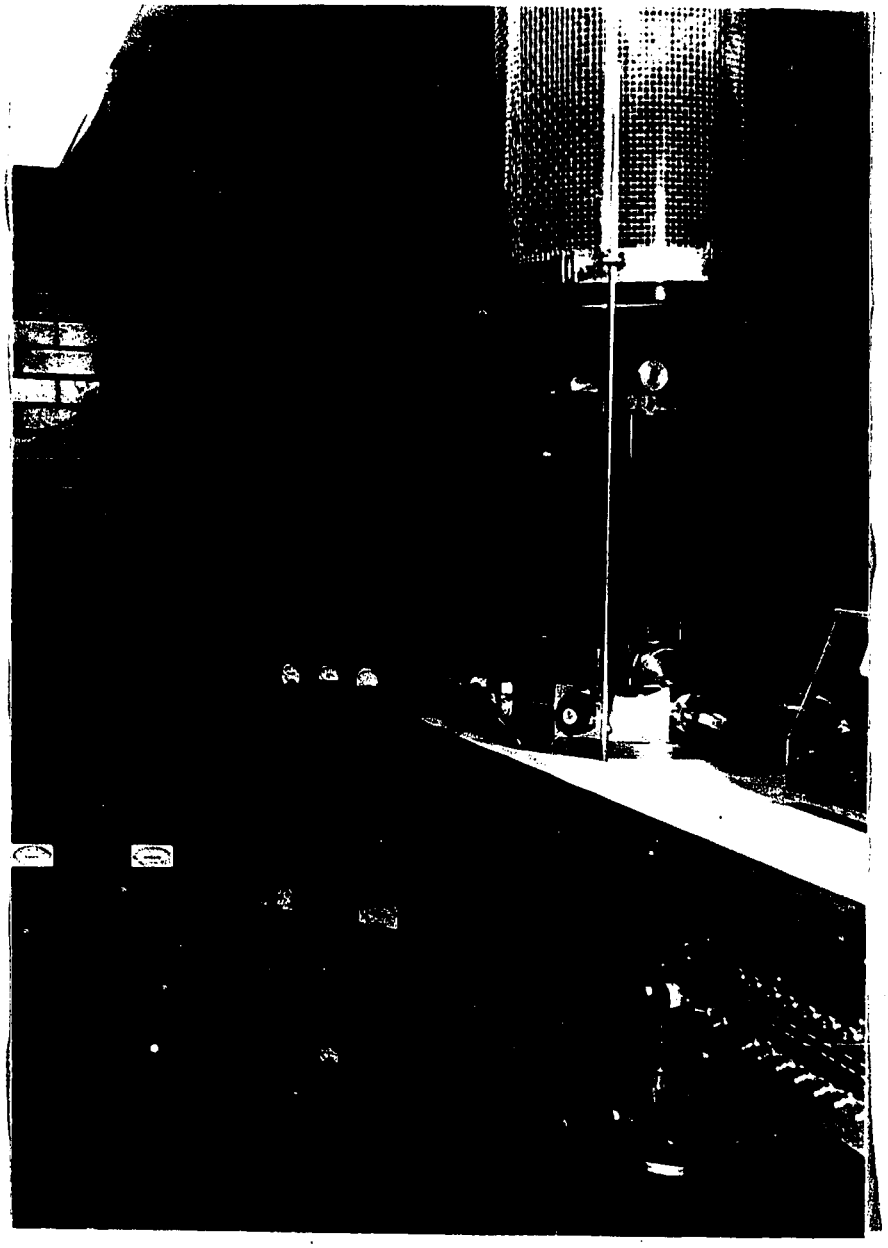

FIGURE 1a. OVER-ALL VIEW OF ELECTRON BEAM ZONE REFINER.

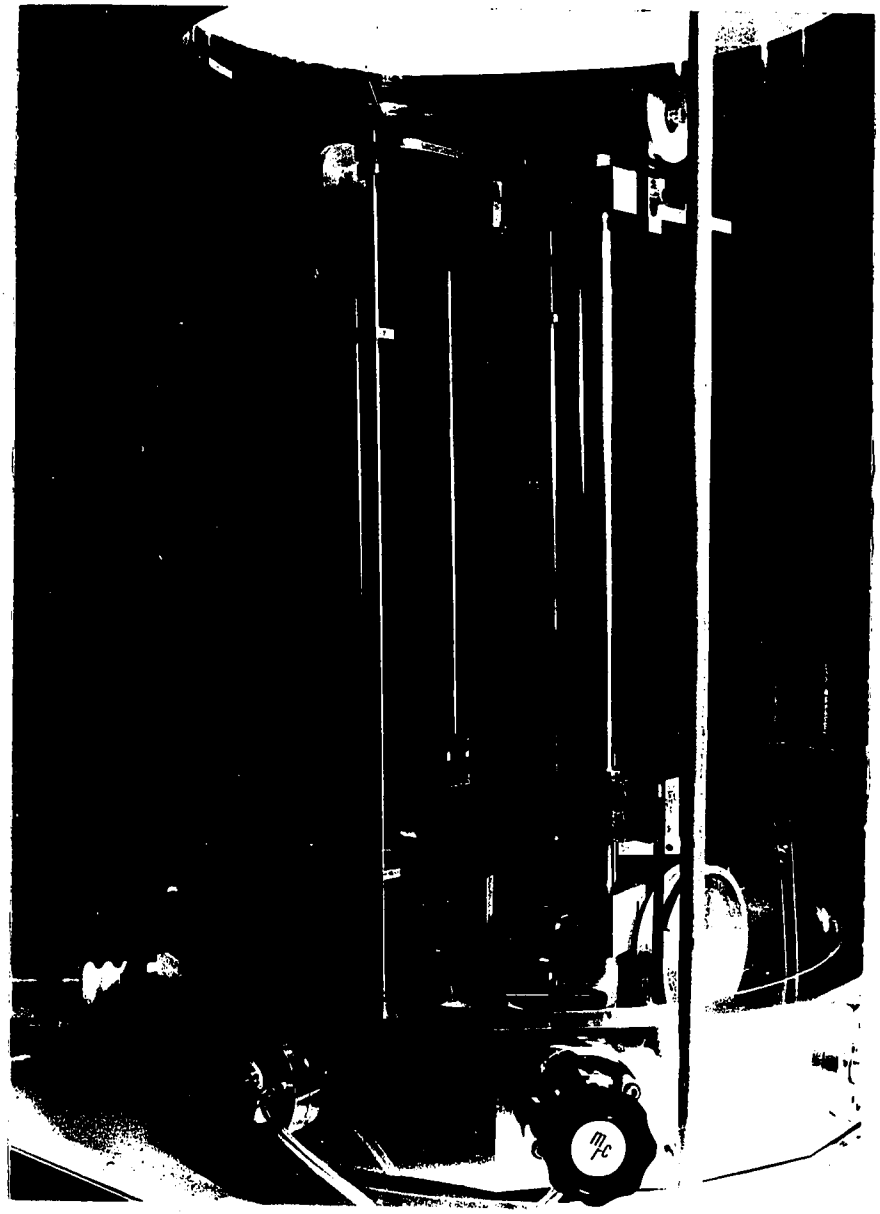

FIGURE 1b. CLOSE-UP VIEW OF ELECTRON BEAM ZONE REFINER.

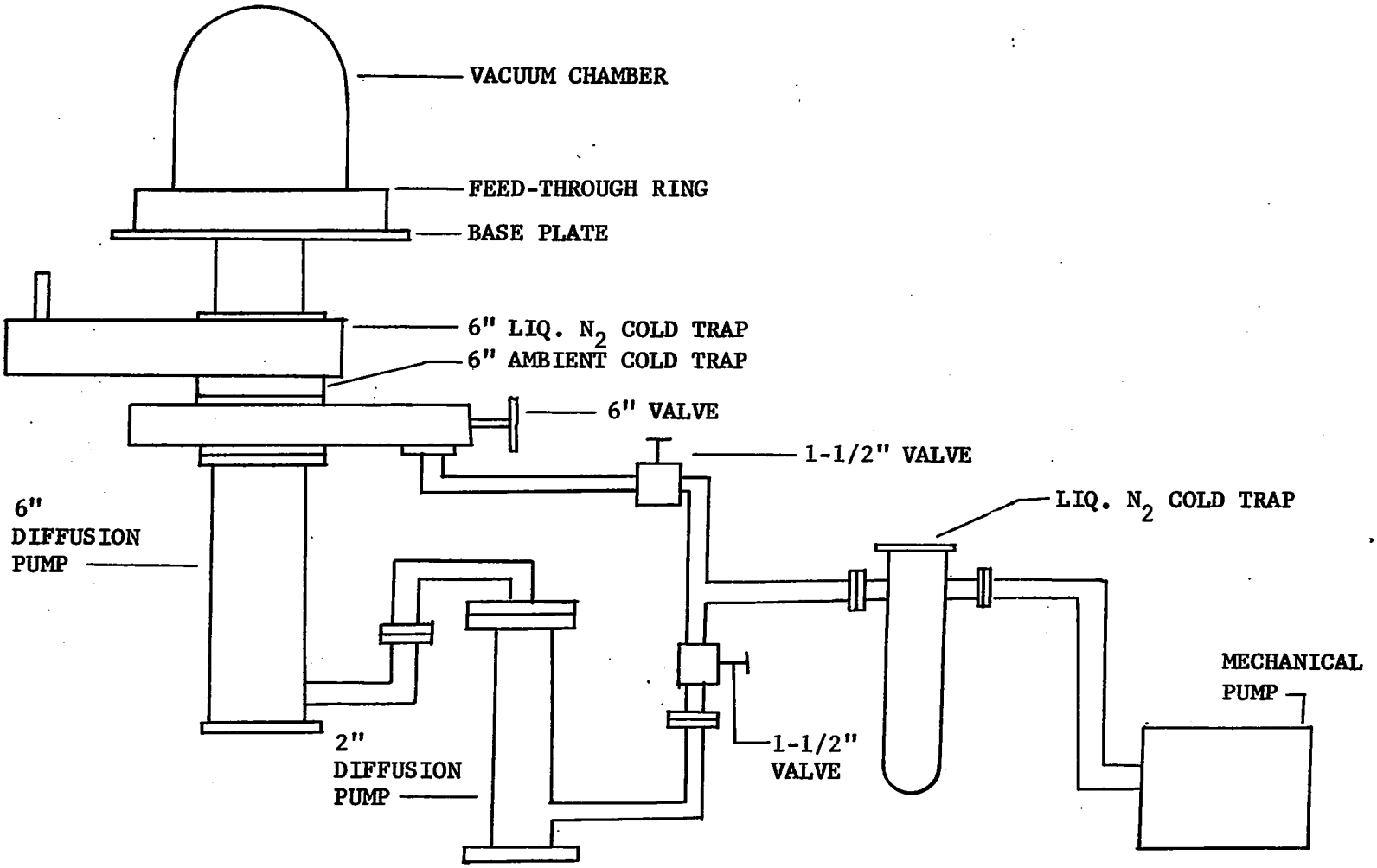

FIGURE 2. SCHEMATIC OF HIGH VACUUM PUMPING SYSTEM.

Table 2

Crystal Number	Starting Material Lot No.	No of Passes	Speed of Passes in/hr	Vacuum on Last Past	Longitudinal current through crystal	$R_{273}/R_{4.2}$ (after annealing)
335	1	4	9.5	$6x10^{-6}$	0	5700
336	1	1	9.5	$1x10^{-5}$	0	460
349	1	4	9.5	$4x10^{-6}$	0	6400
382	1	1	9.5	$1x10^{-5}$	0	1000
383	1	1	9.5	$2x10^{-5}$	0	1000
386	1	1	9.5	$2x10^{-5}$	0	810
387	1	1	9.5	$2x10^{-5}$	0	900
388	1	1	9.5	$2x10^{-5}$	0	1600
390	1	1	9.5	$2x10^{-5}$	0	1800
391	1	1	9.5	$2x10^{-5}$	0	1800
392	1	1	9.5	$2x10^{-5}$	0	1600
393	1	1	9.5	$2x10^{-5}$	0	1600
398	1	1	9.5	$1.5x10^{-5}$	0	1900
400	1	1	9.5	$2x10^{-5}$	0	1500
401	1	1	9.5	$2x10^{-5}$	0	2100
406	1	1	9.5	$1x10^{-5}$	0	1400
407	1	1	9.5	$1x10^{-5}$	0	1500
X-2	1	1	9	$1.5x10^{-6}$	0	700
X-5	2	1	9	$5x10^{-6}$	0	1200
X-7	2	1	9	$2x10^{-6}$	+10	1100
X-8	2	1	3	$1x10^{-6}$	+22	1000

(continued on next page)

Table 2 (continued)

Crystal Number	Starting Material Lot No.	No of Passes	Speed of Passes in/hr	Vacuum on Last Past	Longitudinal current through crystal	$R_{273}/R_{4.2}$ (after annealing)
X-11	2	1	9	$1x10^{-6}$	0	900
X-13	2	2	9	$1x10^{-6}$	0	3600
X-16	2	2	9	$9x10^{-7}$	0	4300
X-17	2	2	9	$9x10^{-7}$	0	4100
X-19	2	3	9	$6x10^{-7}$	0	4800
X-20	3	2	9	$6x10^{-7}$	0	3900
X-21	3	1	3	$1x10^{-6}$	0	1800
X-25	3	1	3	$2x10^{-6}$	-22	1700
X-27	3	3	9/9/3	$5x10^{-7}$	0	7000
X-28	3	1	3	$3x10^{-6}$	0	1500
X-31	3	3	9/9/6	$5x10^{-7}$	0	7200
X-32	3	3	9	$6x10^{-7}$	0	6500
X-33	3	2	9	$8x10^{-7}$	-22	4000
X-34	3	2	9	$8x10^{-7}$	0	5100
X-35	3	1	2	$8x10^{-7}$	0	2500
X-36	3	1	2	$8x10^{-7}$	-22	2600
X-38	3	2	9	$8x10^{-7}$	-22	4600

Foot Notes:

1. x/x/x Indicates speed on each pass.
2. Prefix X indicates crystal was grown in the electron beam melter built especially for this project.

FIGURE 3. THE EFFECTS OF THE NUMBER OF ZONE PASSES AND THE STARTING MATERIAL ON $R_{273/4.2}$.

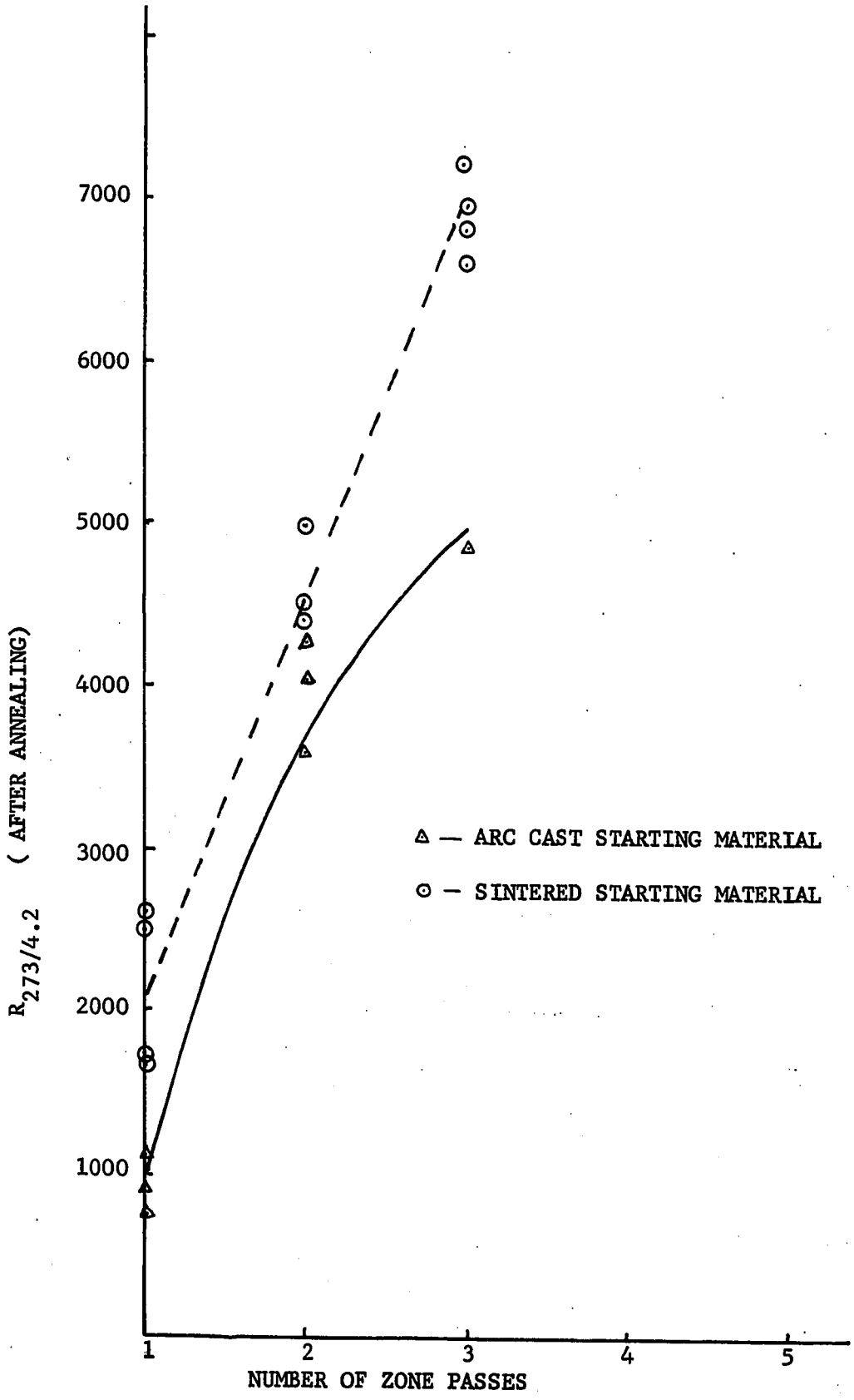

C. Purity Determination

An indication of the purity of the single crystals was assumed to be the ratio of the electrical resistance at 273° K divided by the resistance at 4.2° K; the higher the ratio, the higher the purity. It can be shown that this ratio is inversely proportional to the resistivity at 4.2° K and is independent of the size and shape of the sample.

Because of possible uncertainties, care should be exerted when using this resistance ratio as a measure of the purity. It is well known that the electrical resistivity is most sensitive to impurities in solid solution and much less sensitive to impurities in the form of precipitates. This effect in molybdenum is illustrated quite clearly by the work of Drangel, McMahon and Weinig[53]. They found that the resistance ratio $R_{273}/R_{4.2}$ of a single crystal could be changed by annealing at various temperatures and quenching. Table 3 shows some of their results. Results of a similar nature were encountered in this laboratory while studying the mechanism of purification during the crystal growing process. It is generally believed that the major purification of refractory metals in zone melting is by vaporization of impurities out of the molten zone, but that some purification (zone refining) does occur due to the moving molten zone. This latter mechanism would leave the starting end purer than the rest of the crystal.

Table 3

Resistance Ratios Versus Thermal Histories for Molybdenum

(From Drangel, McMahon and Weinig [53])

Speciman No.		As beamed ⟶	ALL QUENCHED FROM 600°C → 15 hours	400°C → 64 hours	1000°C → 15 hours	600°C → 15 hours	200°C → 24 hours
67B	(10^{-6})	6930	5000	6900	2640	4900	5000
90	(10^{-8})	1335	5000	5000	1520	5350	5000

Several investigators have indicated by resistivity measurements on "as grown" single crystals that zone refining does occur in refractory metals. It is believed by the author that resistivity measurements on single crystals in the "as grown" condition can not be used to study the effectiveness of zone refining. This is due to the vastly different thermal histories of the two ends. When growing single crystals by the electron-beam process, in which only a small zone of the material is molten at one time, there is a significant difference in the rate at which the starting and the stopping ends cool. During the growing process, the molten zone travels very slowly from the starting to the stopping end. As the molten zone proceeds from the starting end, this end begins to cool slowly and by the time the molten zone reaches the stopping point, only about one half of the single crystal remains red hot. At this time the power is turned off and the red hot portion of the crystal is cooled rather quickly. This difference in thermal histories causes more impurities to be in solid solution on the end where the molten zone is solidified.

Figure 4 shows resistivity measurements on a single crystal in the "as grown" state and again after annealing. From these results, there appears to be a small difference in the purity of the ends of the crystals, but considerably less than indicated

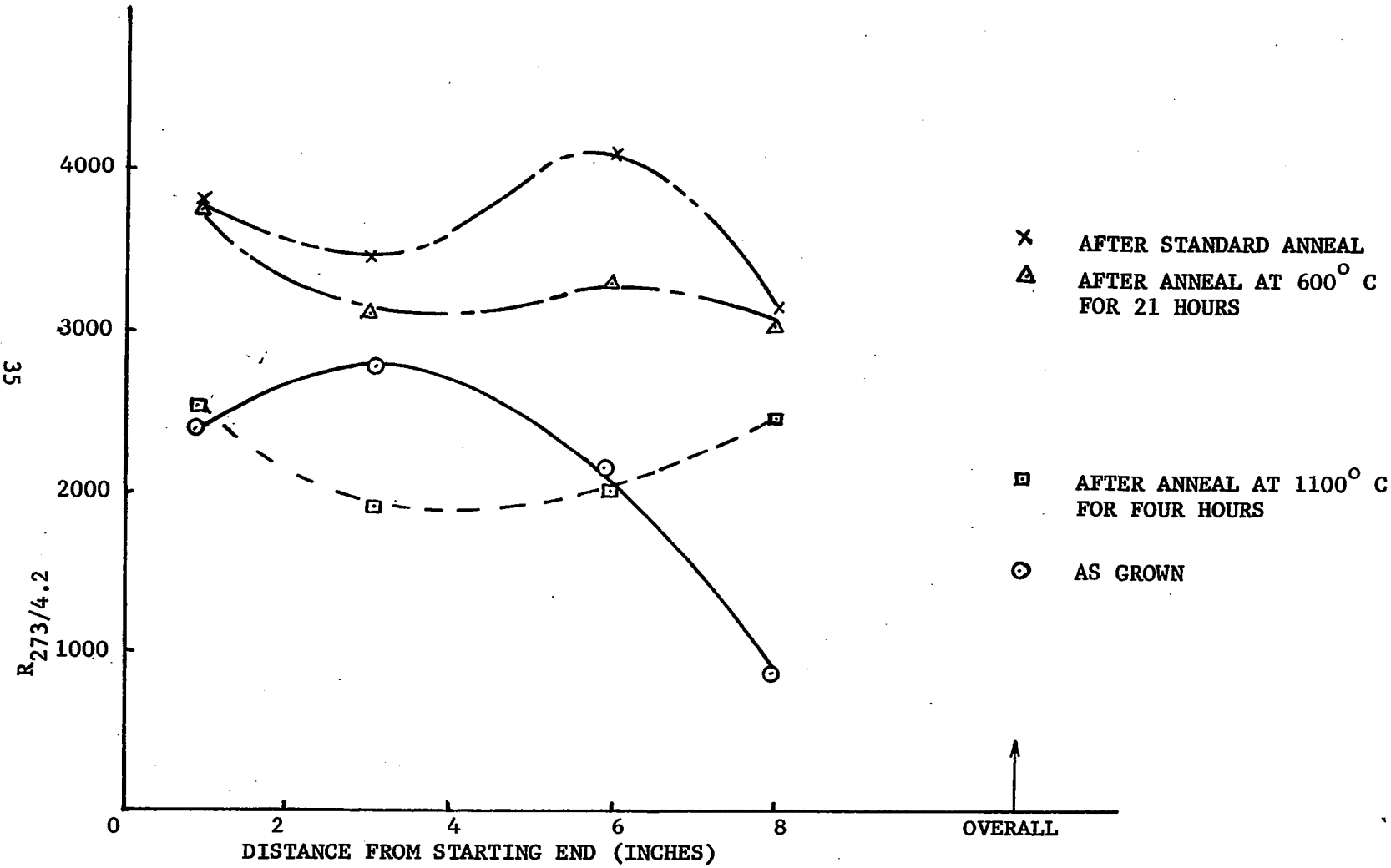

FIGURE 4. RESISTANCE RATIO AFTER VARIOUS THERMAL TREATMENTS.

by the "as grown" tests. An increase in purity is also indicated by the repeated anneals at high temperature.

Even though the relation between purity and the resistance ratio is not without uncertainties, its use can be justified by the fact that no other method is available for the determination of quantitative purity differences. Several previous investigations [7,35] have found that chemical analysis is insensitive to purity differences in zone melted molybdenum; therefore no attempt was made to use this method.

In order to minimize the ambiguities in the resistance-ratios, all crystals were given the same thermal treatment prior to the measurement of the resistance. This thermal treatment consisted of heating at 1000°C for 21 hours, followed by 21 hours at 600°C, and furnace cooling to room temperature. A dynamic vacuum between 1×10^{-6} torr and 1×10^{-7} torr was maintained during the annealing treatment.

Resistance measurements were made by spot welding potential and current leads to the crystals and using them as four terminal resistors in the circuit shown in figure 5. The distance between potential leads was approximately 1.5 inches, and the current leads were placed at least one eighth inch outside the potential leads. Resistance values were determined by measuring values

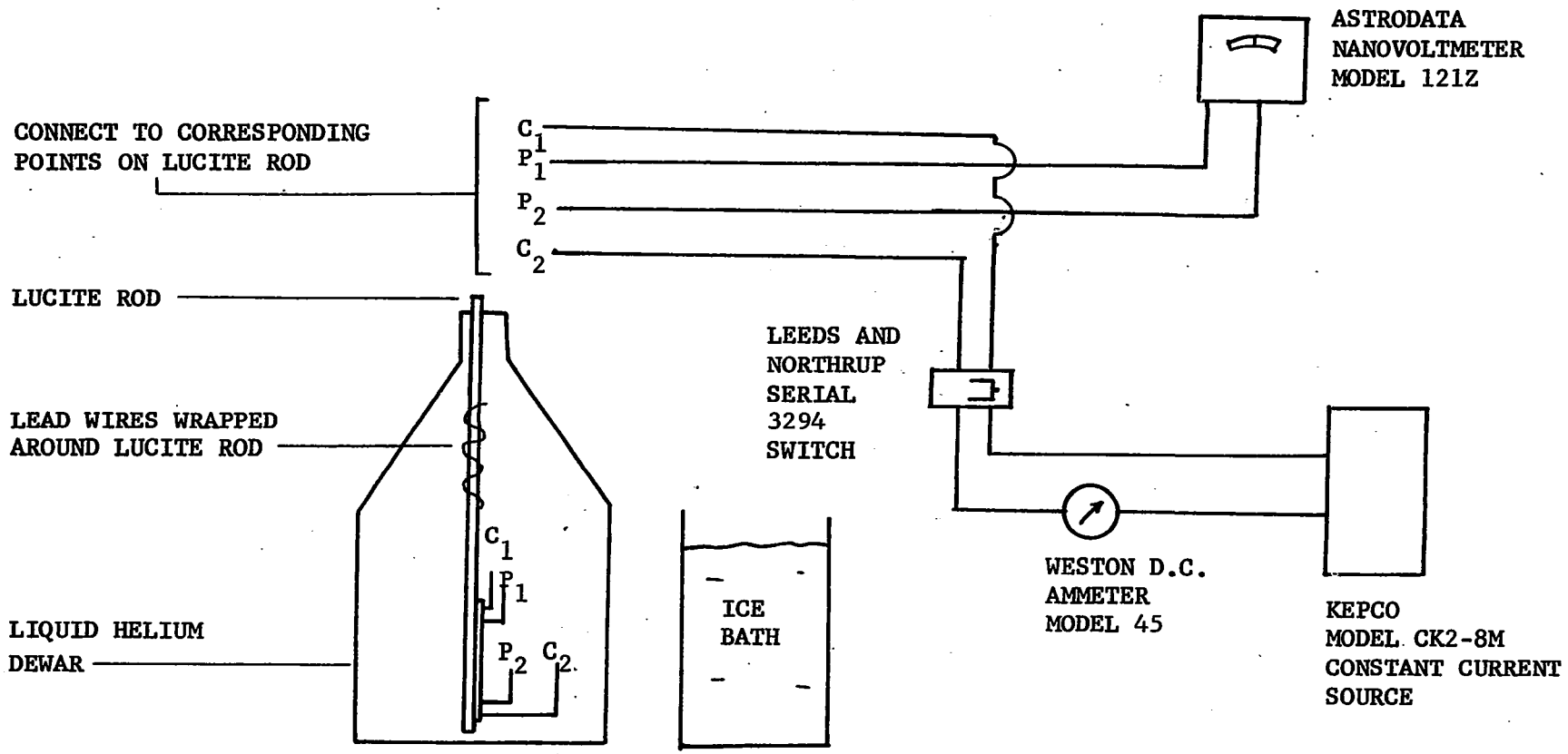

FIGURE 5. SCHEMATIC OF RESISTANCE MEASURING EQUIPMENT.

of E and I. In order to compensate for thermal emf's, the current direction was reversed, and an average of the voltage drop through the specimen was used in calculating the resistance. Current values of 1 and 2 amperes were used at 273°K and 4.2°K , respectively. The resistance ratio could be determined with an accuracy of ±5%.

D. Orientation

Crystal orientation was determined by the Laue back-reflection method. Only single crystals with the [110] direction within 3° of the cylindrical axis of the crystal were used for these tests. All crystals were measured several times until the incident beam was along the $[1\bar{1}1]$ direction, then the point of incidence on the surface of the crystal marked. This mark was used to orient the $[\bar{1}11]$ direction along the direction of loading in the Instron machine.

E. Strain

The single crystals were deformed in a manner which placed maximum shear stress on the (110) plane and in the $[\bar{1}11]$ direction. This was accomplished by holding the crystals in two sets of split grips which were moved relative to one another; this is illustrated schematically in figure 6. One set of grips was attached to the cross head of the Instron machine through a set of extension rods and another set of grips was attached to the load

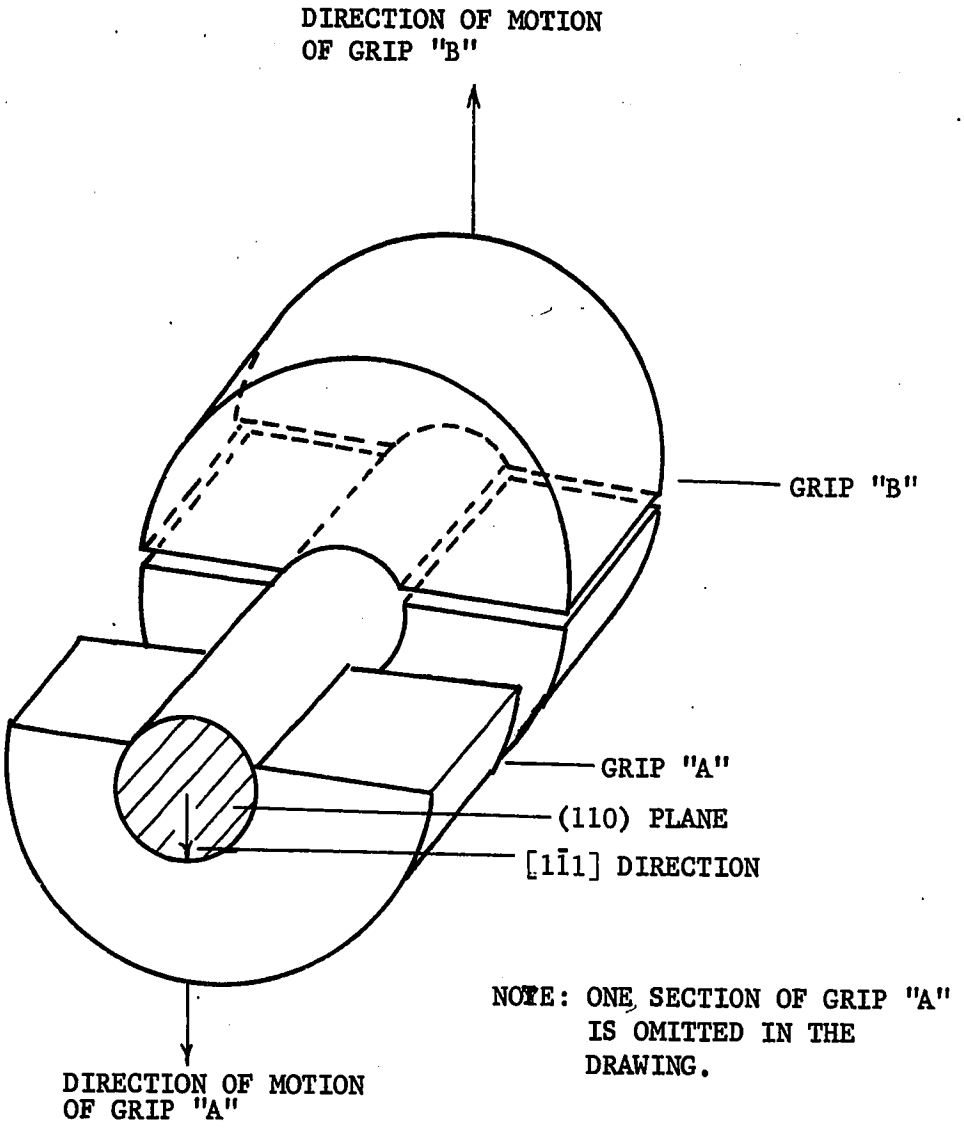

FIGURE 6. SCHEMATIC SHOWING CRYSYAL ORIENTATION DURING SHEAR.

cell of the Instron machine through a pull bar, as shown in figure 7. The extension rods and pull bar were required to permit the lowering of the gripping mechanism into a controlled temperature fluid bath. Several sets of split grips were used to accommodate the slight size differences in the diameters of the single crystals.

Relative displacement of the grips was determined with a Sanborn Model 7 DCDT-050 DC Differential Transformer, also shown in figure 7. The outputs from the transformer and the Instron load cell were impressed on the X and Y scales respectively of a Mosely Autograf, Model 2-D, X-Y recorder. In this way the load-displacement curves could be determined directly. Proper orientation of the $[\bar{1}11]$ direction in the Instron was achieved by first placing the crystal in the center grip and aligning the $[\bar{1}11]$ direction along the center line of the pull rod adapter, as shown in figure 8. With the $[\bar{1}11]$ direction properly aligned, the center grip was tightened around the crystal. This procedure insures that the $[\bar{1}11]$ direction and the direction of application of force are parallel to within 2^{o}. Placement of the crystal in the outer grip was accomplished by first seating it in the upper section as illustrated in figure 9. The lower half of the clamp could then be brought into place and connected to the upper half of the clamp. Before tightening the clamp, the gauge length was set and a spacer

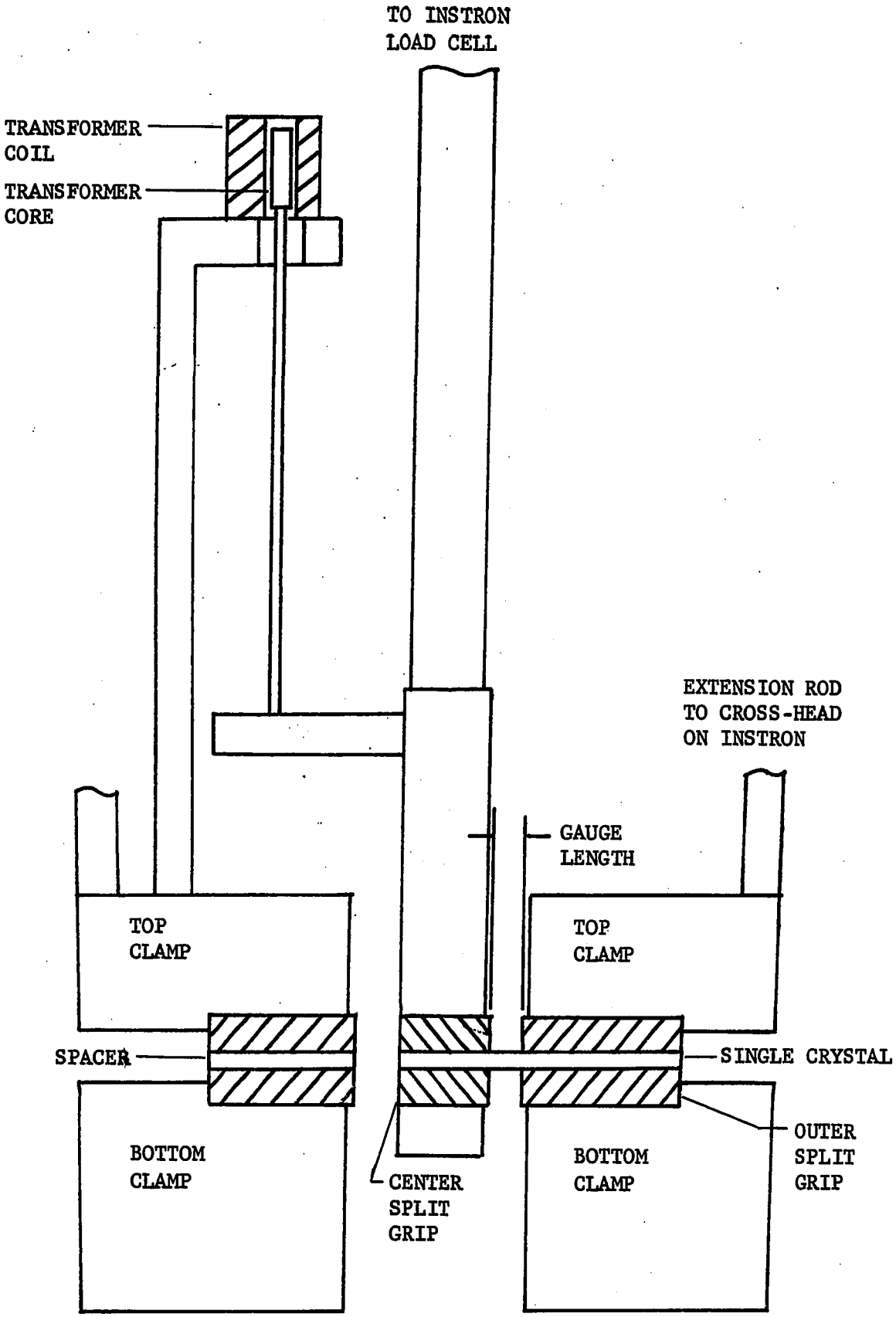

FIGURE 7. SCHEMATIC OF DIRECT SHEAR TESTING APPARATUS.

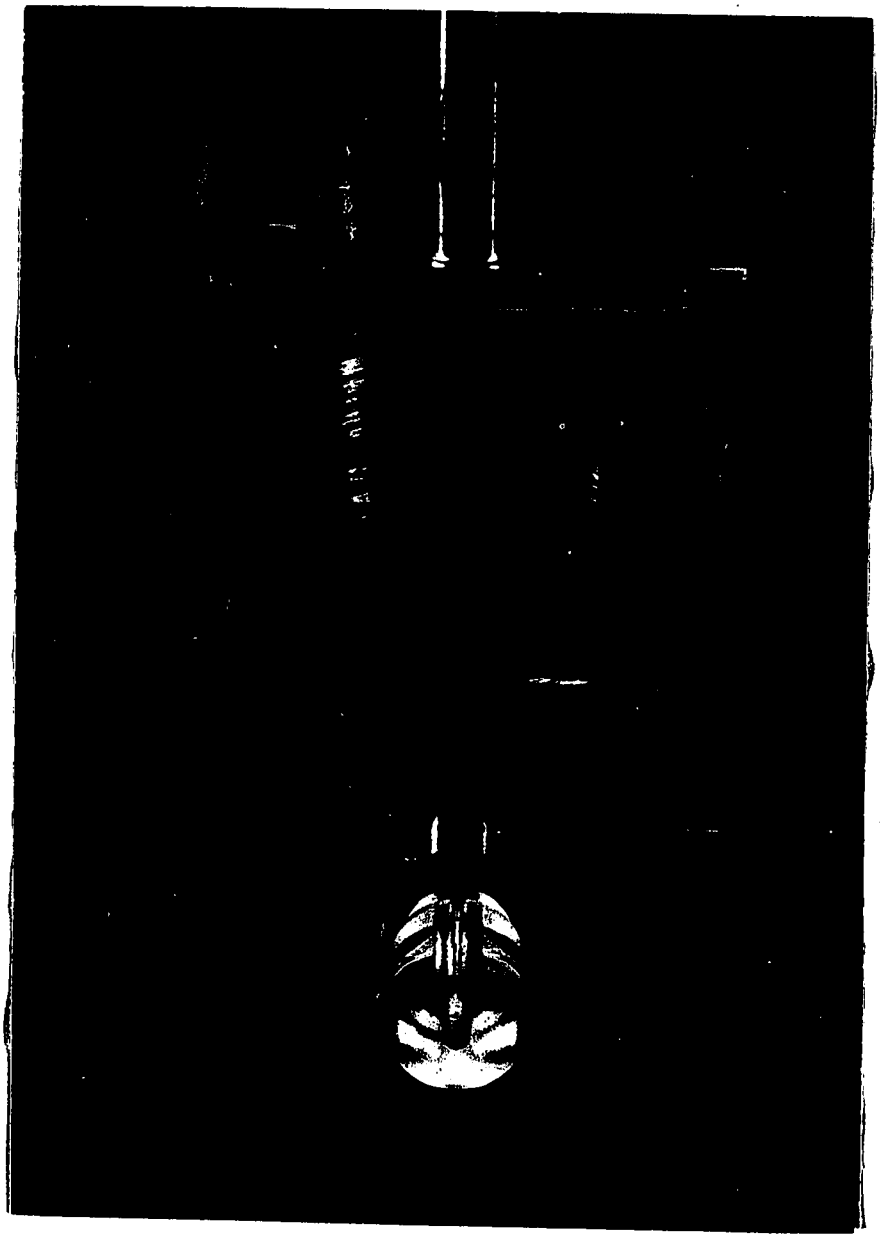

FIGURE 8. SINGLE CRYSTAL ORIENTED IN PULL-ROD ADAPTER.

FIGURE 9. SINGLE CRYSTAL SEATED IN UPPER CLAMP.

placed on the blank side. A gauge length of approximately 1/16 inch was used for all tests, with the exact gauge length being determined optically after deformation.

A typical load-extension curve is shown in figure 10. Since the specimen gripping system was not rigid, the straight line portion of this curve did not correspond to the shear modulus of molybdenum. Plastic strains were measured as the deviation from the extension of the straight line portion of the curve.

F. Temperature Control

A special container was designed in which the specimen was immersed in a fluid bath during the deformation. This bath could be controlled to within $\pm .2^{\circ}$ C using a Halikainen Thermotrol, Model 1053A. Figure 11 is a schematic drawing, and figure 12 shows the container ready to be raised into position. Below room temperature, the bath fluid was commercial grade isohexane, except for the 78 K bath were liquid nitrogen was employed. A silicone oil bath was used above room temperature. Temperature measurements were made with an iron-constantan thermocouple and a Leeds and Northrup, Model 8686, potentiometer.

G. Activation Volume-V

This test consisted of loading the crystal at a constant strain rate and then suddenly changing the strain rate by a factor

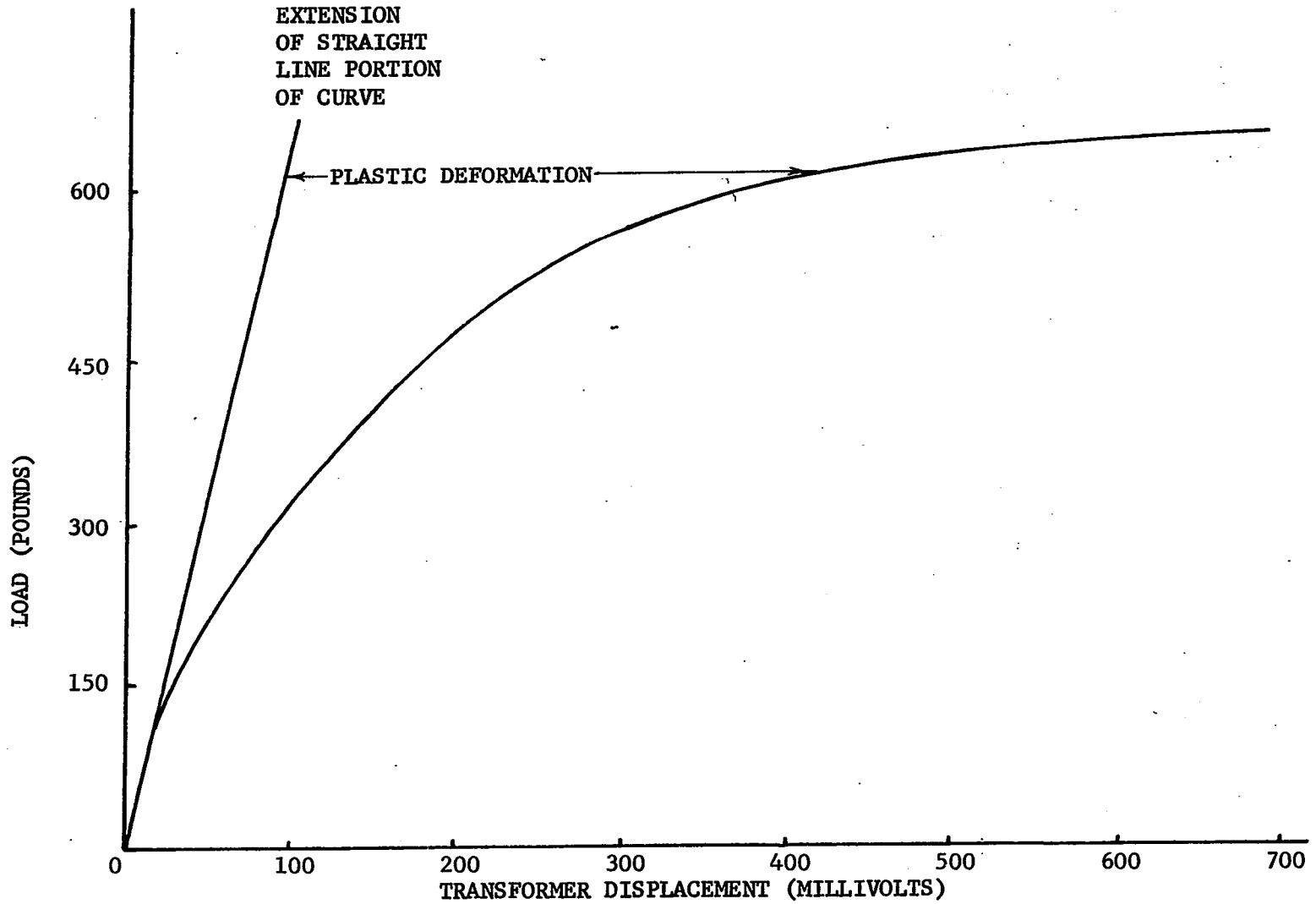

FIGURE 10. SCHEMATIC SHOWING TYPICAL LOAD-DISPLACEMENT CURVE FROM X-Y RECORDER.

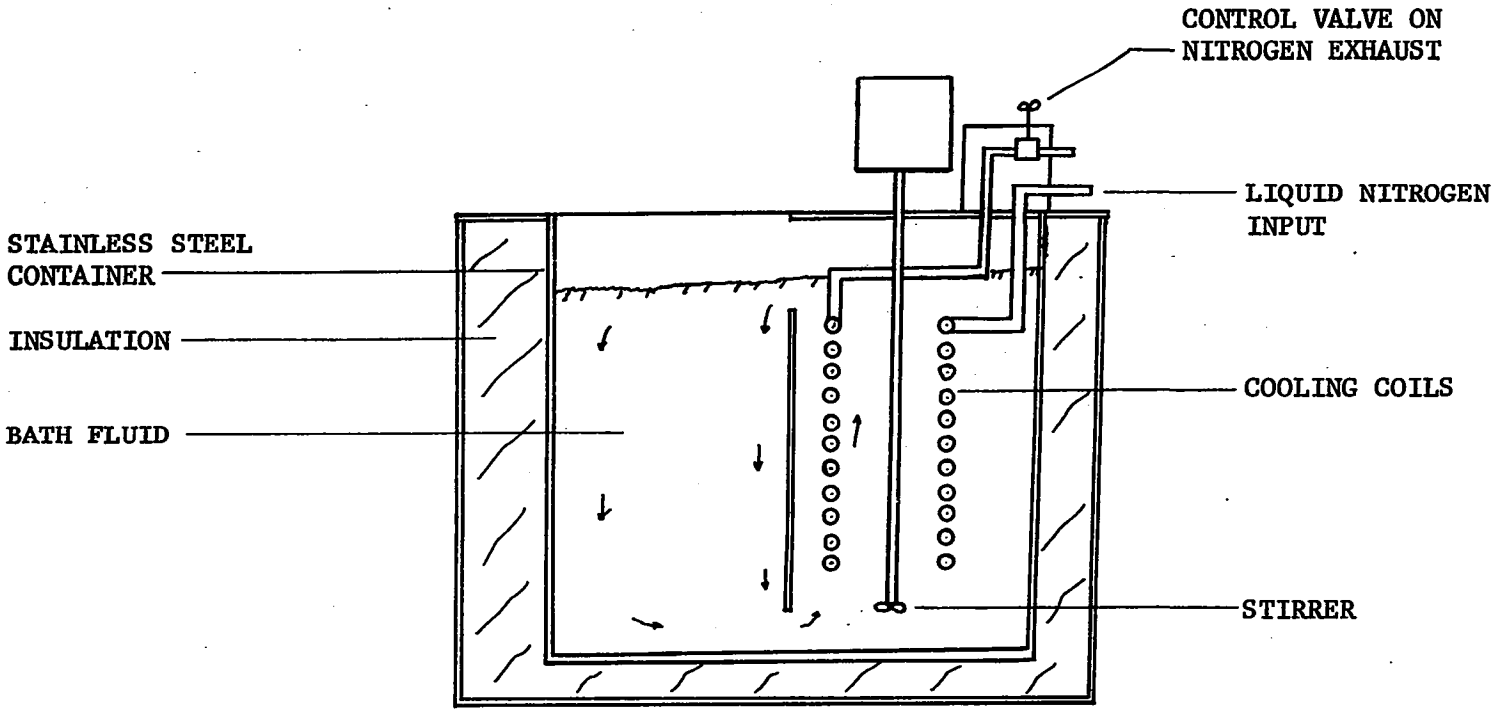

FIGURE 11. SCHEMATIC OF CONTROLLED-TEMPERATURE BATH.

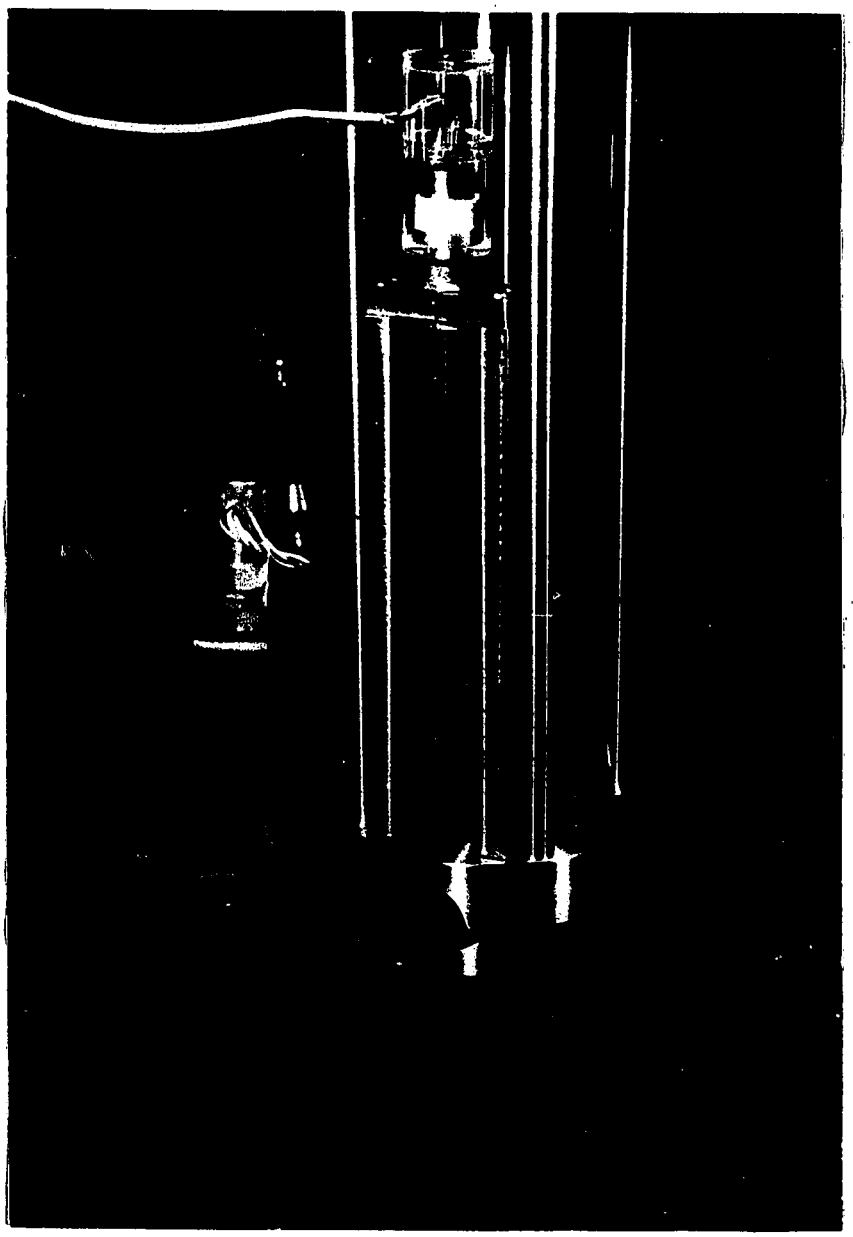

FIGURE 12. SHEAR APPARATUS READY TO BE IMMERSED IN CONTROLLED TEMPERATURE BATH.

of 5. Figure 13 is reproduced from a typical load versus—displacement curve of the X-Y recorder to illustrate the technique used to obtain V. The specimen was strained at the higher rate to point A, where the cross-head movement was reversed and the specimen was unloaded in an approximately elastic manner. After a short time, the cross-head movement was reversed again (point B) and the speed changed to the new (lower) rate. The curve was then allowed to stabilize itself at the new strain rate. At point C the cross-head rate was suddenly returned to the higher speed and the curve allowed to stabilize itself again at this rate. The high speed portions of the curves were connected, and a line was drawn parallel to the elastic unloading line AB, intersecting the BC portion in its stabilized region, figure 13. The force difference thus obtained was assumed to be at constant plastic strain and therefore at constant dislocation configuration. Conversion of the above force difference to stress allowed the calculation of V from the formula $V = [\Delta \ln \dot{\epsilon}/\Delta\tau_a]_{T,\dot{\epsilon}}$.

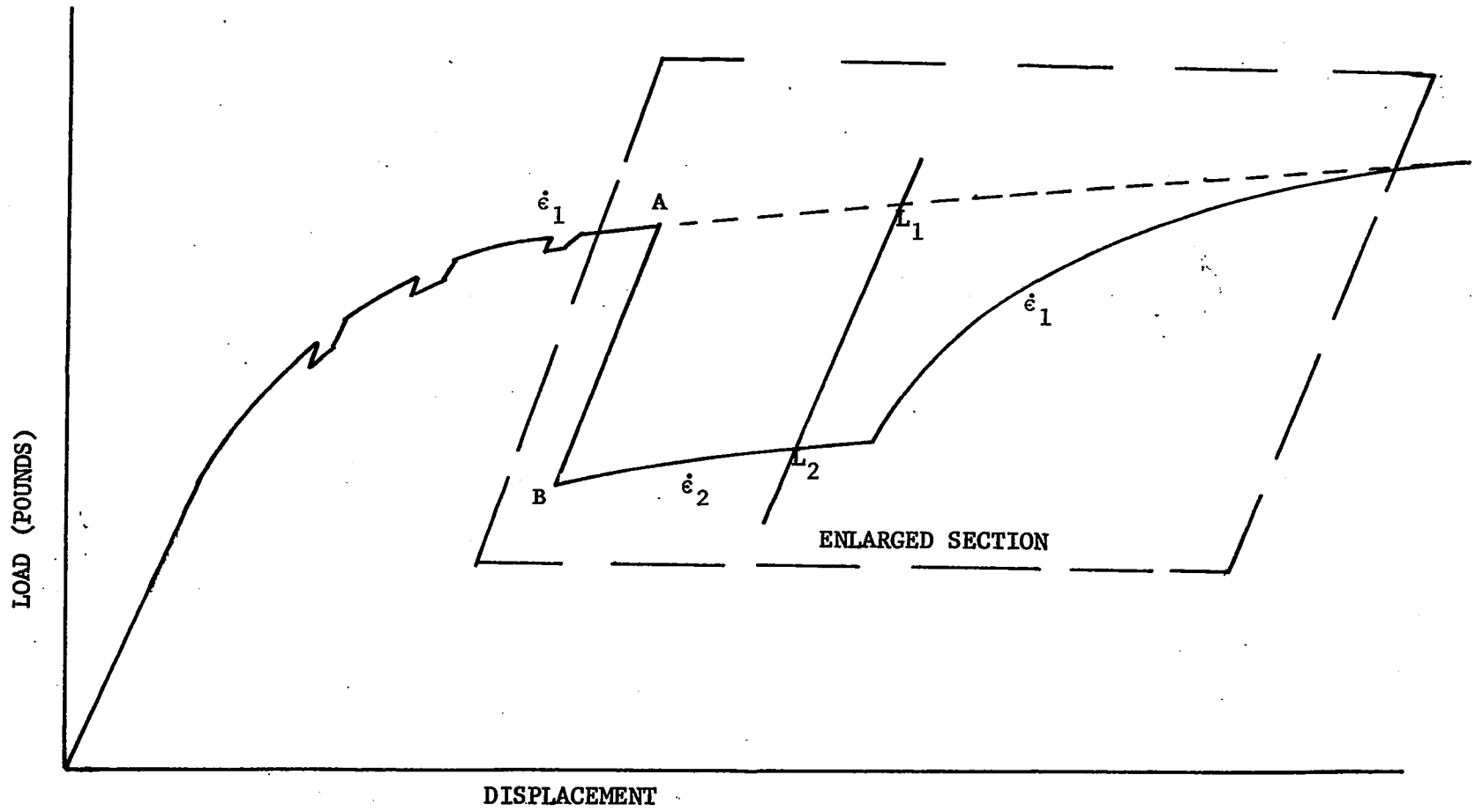

FIGURE 13. PORTION OF LOAD-ELONGATION CURVE OF TYPICAL SPECIMEN.

EXPERIMENTAL RESULTS

I. Stress-Strain Curves

Representative stress-strain curves determined in direct shear for each temperature and strain rate are illustrated in figures 14 through 19. A complete collection of stress-strain curves for all purities and temperatures is presented in the Appendix. The strain indicated in these figures is considered to be the plastic shear strain, determined in the manner explained in the experimental procedure.

Generally the stress-strain curves can be divided into two regions. The first region is characterized by low initial stresses and a very high work-hardening rate. In the second portion of the curve, the stresses are high and the work hardening small. Exceptions to this general two region type behavior are noted at 350° and 400°K and will be discussed later.

The effects of impurities on the stress-strain curves were dependent upon the temperature of deformation. At all test temperatures used the detected difference in the influence of impurities was small and at low temperatures it was limited to the initial portion of the curve. Above 300° K the impurities had little effect on the early stages of deformation but altered the curvature of the stress-strain curves outside the initial region.

FIGURE 14. STRESS-STRAIN CURVES FOR MOLYBDENUM SINGLE CRYSTALS DEFORMED AT 78° K IN DIRECT SHEAR.

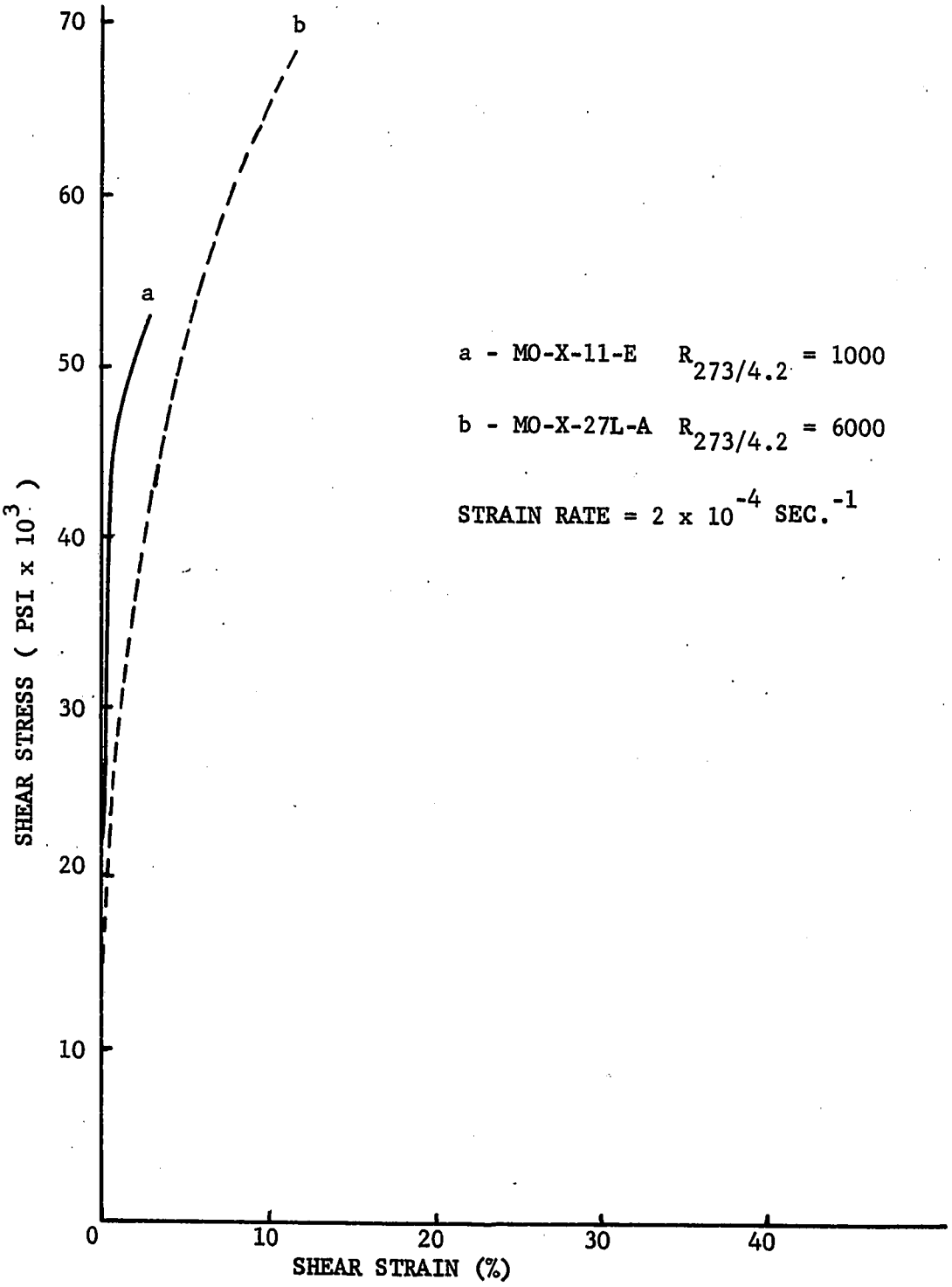

FIGURE 15. STRESS-STRAIN CURVES FOR DEFORMATION AT 200° K IN DIRECT SHEAR.

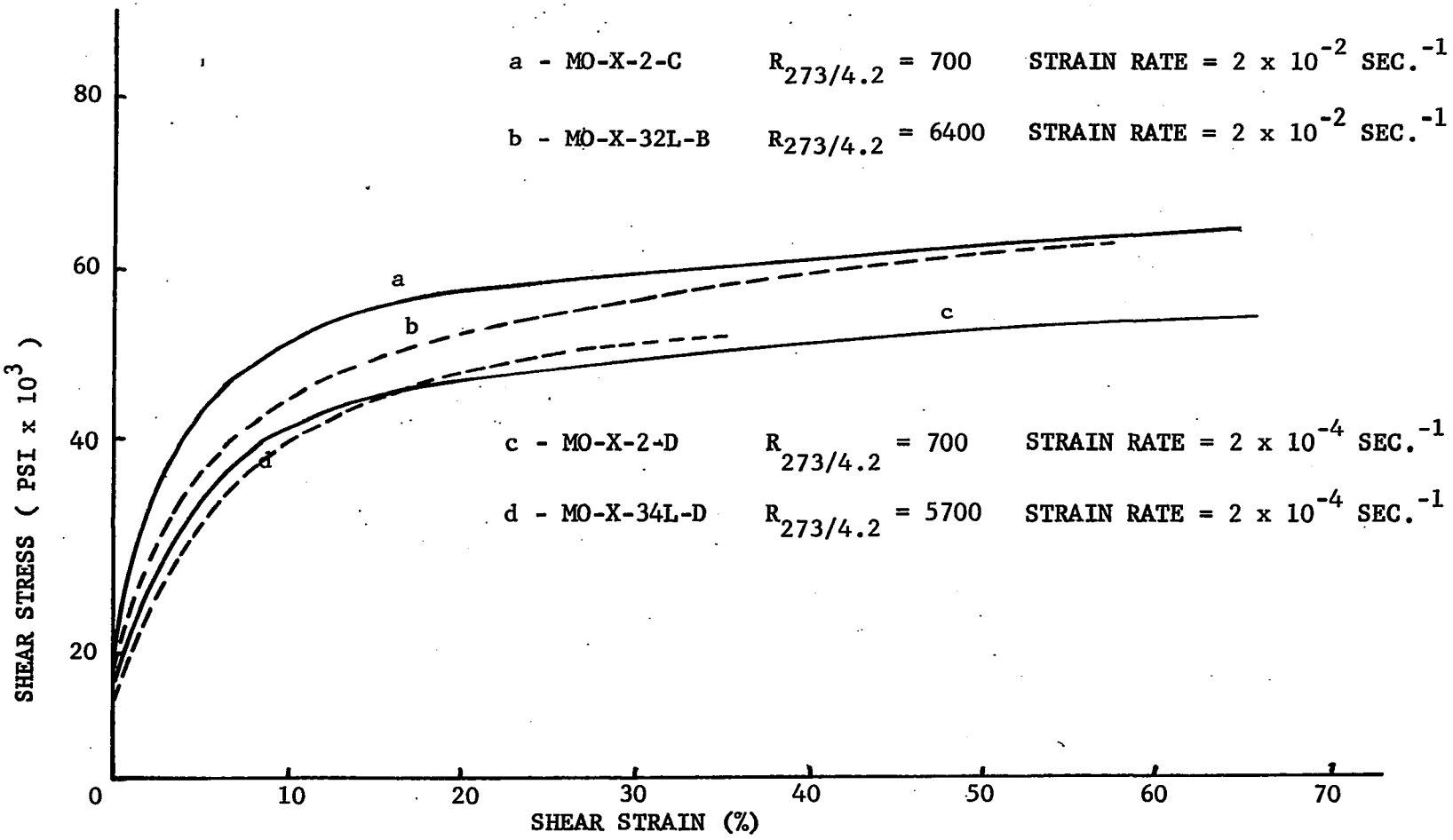

FIGURE 16. STRESS-STRAIN CURVES FOR DEFORMATION AT 250° K IN DIRECT SHEAR.

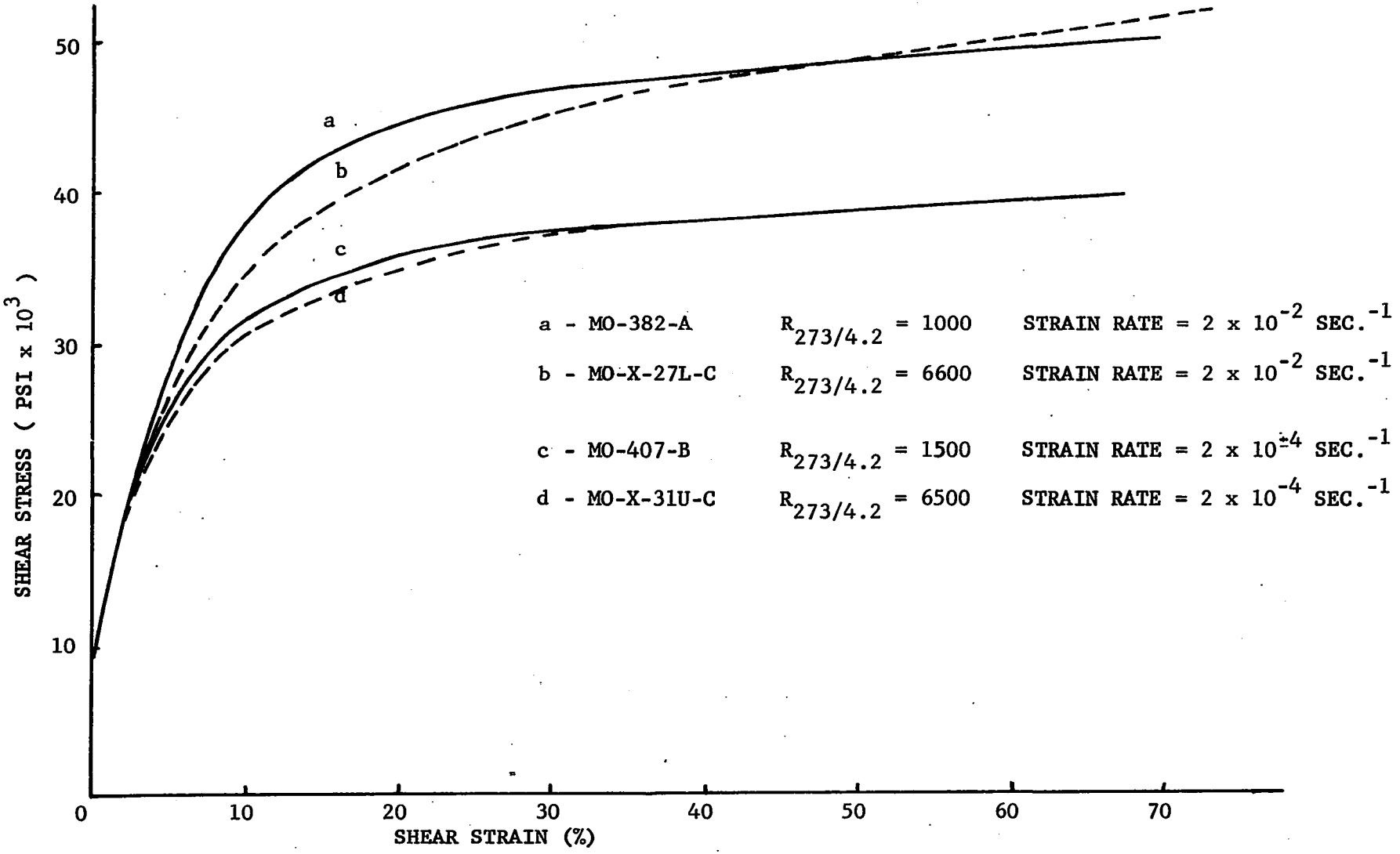

FIGURE 17. STRESS-STRAIN CURVES FOR DEFORMATION AT 300° K IN DIRECT SHEAR.

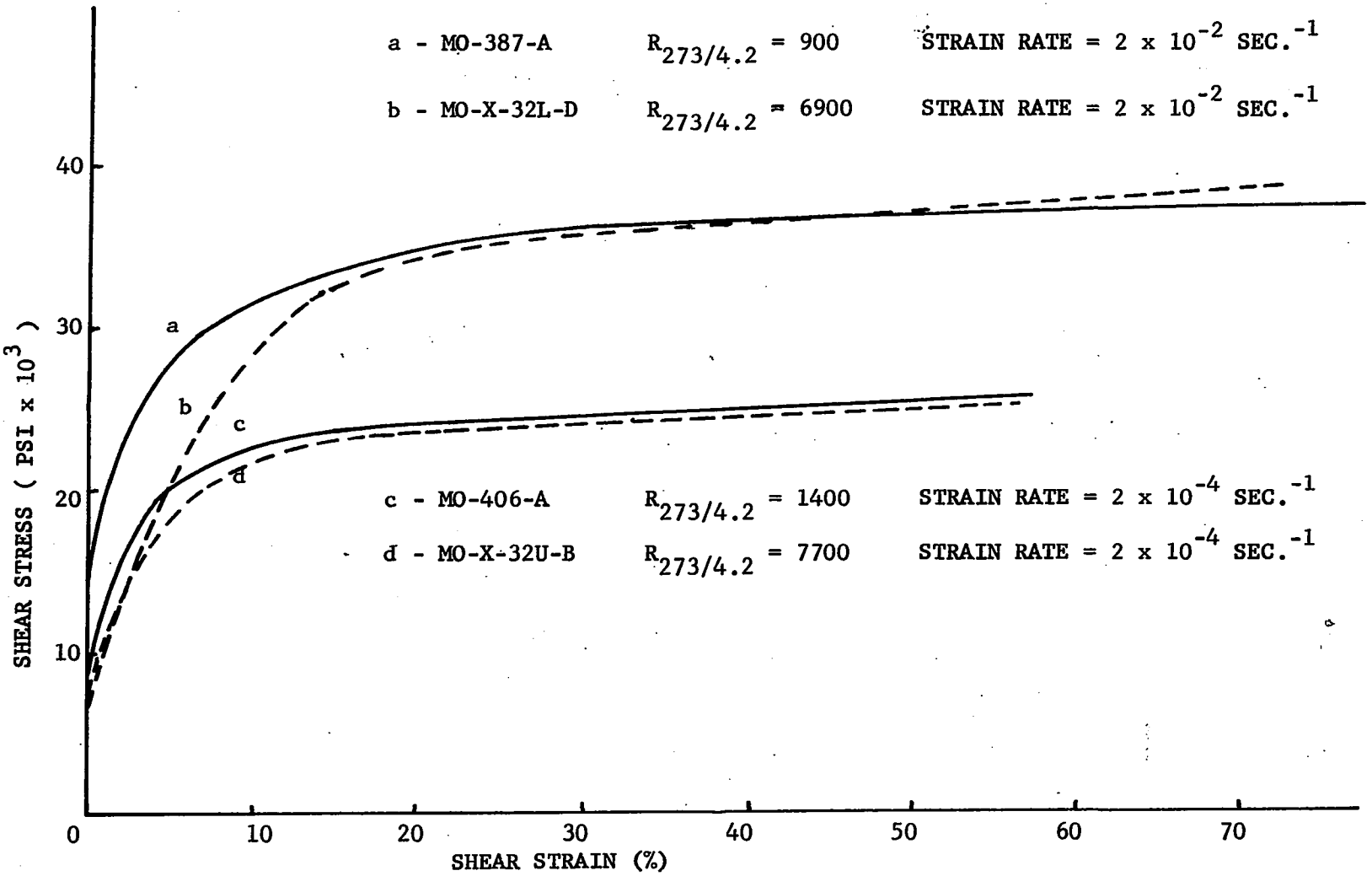

FIGURE 18. STRESS-STRAIN CURVES FOR DEFORMATION AT 350° K IN DIRECT SHEAR.

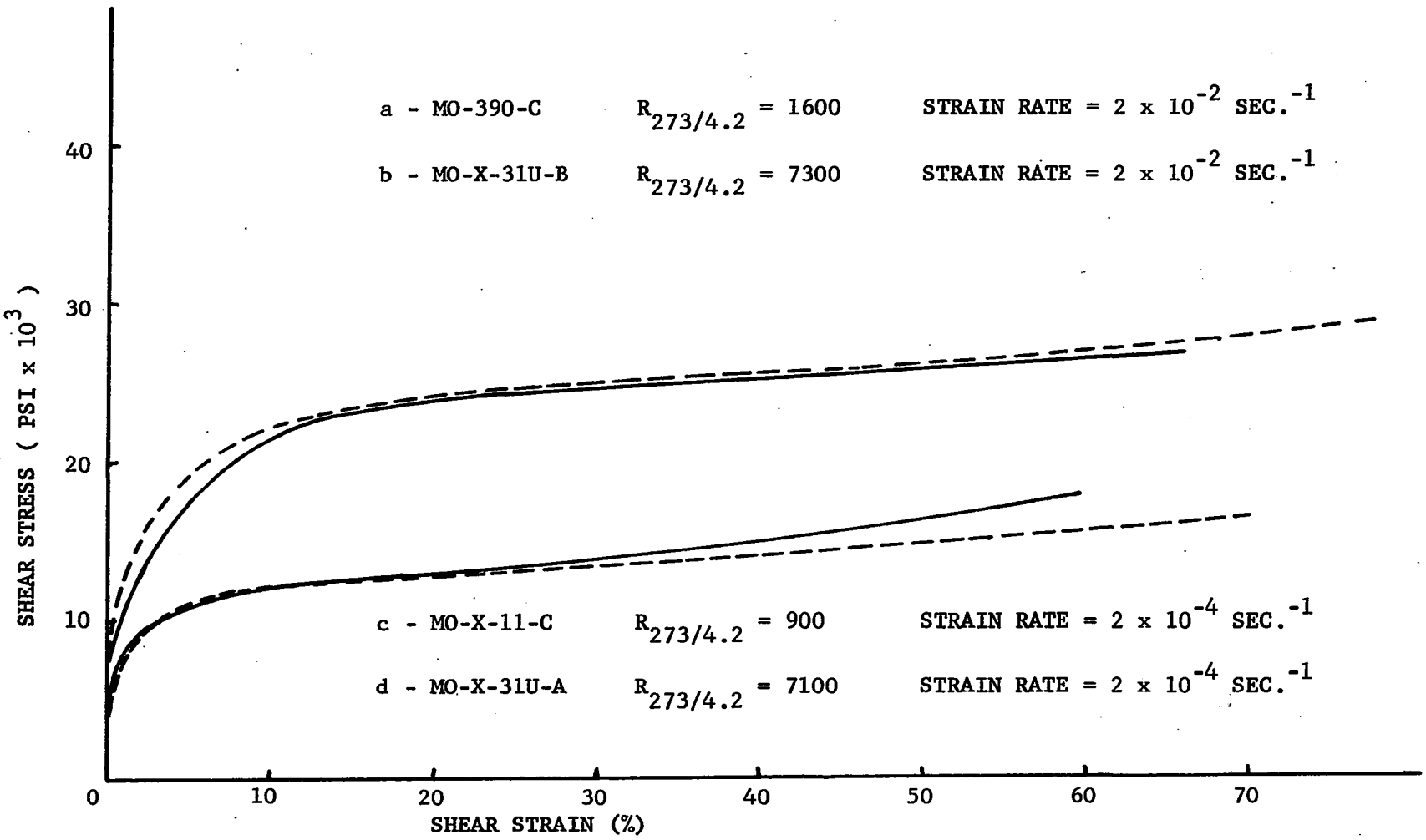

FIGURE 19. STRESS-STRAIN CURVES FOR DEFORMATION AT 400° K IN DIRECT SHEAR.

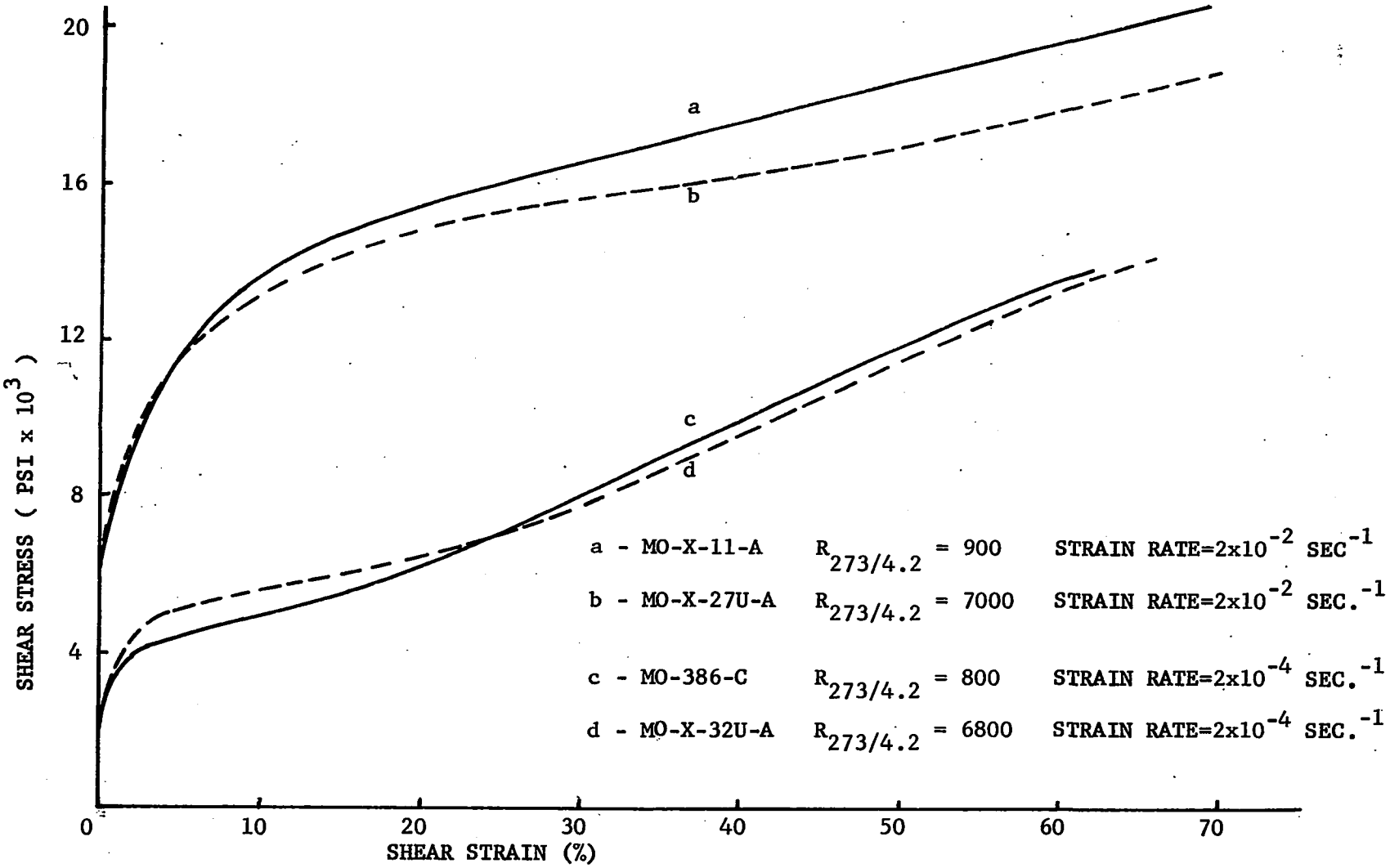

Increasing the strain rate or decreasing the deformation temperature has similar effects on the stress-strain curves. Either change increases the flow stress and the extent of the initial rapid work-hardening region.

Loss of ductility is the property most strongly influenced by impurities at 78° K. Initially the flow stress of the purer material is lower, but this difference is reduced with increasing strain, as revealed in figure 14. It appears that both impurity levels would be along a common curve beyond about 10% strain if the impure crystal had had more ductility. No loss of ductility due to impurities is present above 78°K.

Figure 15 illustrates typical stress-strain curves obtained at 200°K. This figure indicates that impurities cause a difference in the initial region of these curves, but the difference is reduced as the deformation proceeds. It is also evident from figure 15 that:

(1) The impurities influence the flow stress more at the higher strain-rate.

(2) The work-hardening rate decreases continuously with strain for both strain rates.

Typical stress-strain curves determined at 250 °K are displayed in figure 16. It is seen in this figure that the curves for the lower strain rate are linear after about 30% strain.

A linear portion is found at the high strain rate only for the purer crystal after about 40% strain. The impurity effect is again greater for the higher strain rate.

Figure 17 is representative of the stress-strain curves obtained at 300°K. Linear work-hardening is again present at high strains for both purities at the low strain rate and for only the purer crystal at the higher strain rate.

A deviation from the general two-region stress-strain curve becomes evident at 350°K. Figure 18 indicates that the presence of the third region is a function of both the impurity content and the strain rate. Increasing either of these has the tendency to obliterate the third region. The region commences where the curvature of the stress-strain curve changes from negative to positive, as illustrated schematically in figure 20.

The per cent strain at which region 3 starts, becomes larger with increasing purity. Also evident from figure 18 is the fact that impurities have no effect on the initial portion of the stress-strain curves at 350°. This is also true at 400°K.

At 400°K the presence of a fourth region is detected. Figure 20 illustrates schematically what is considered to be region 4; its existence at 400°K is evident in figure 19.

FIGURE 20. SCHEMATIC DRAWING SHOWING HOW STRESS-STRAIN CURVES COULD BE DIVIDED INTO REGIONS.

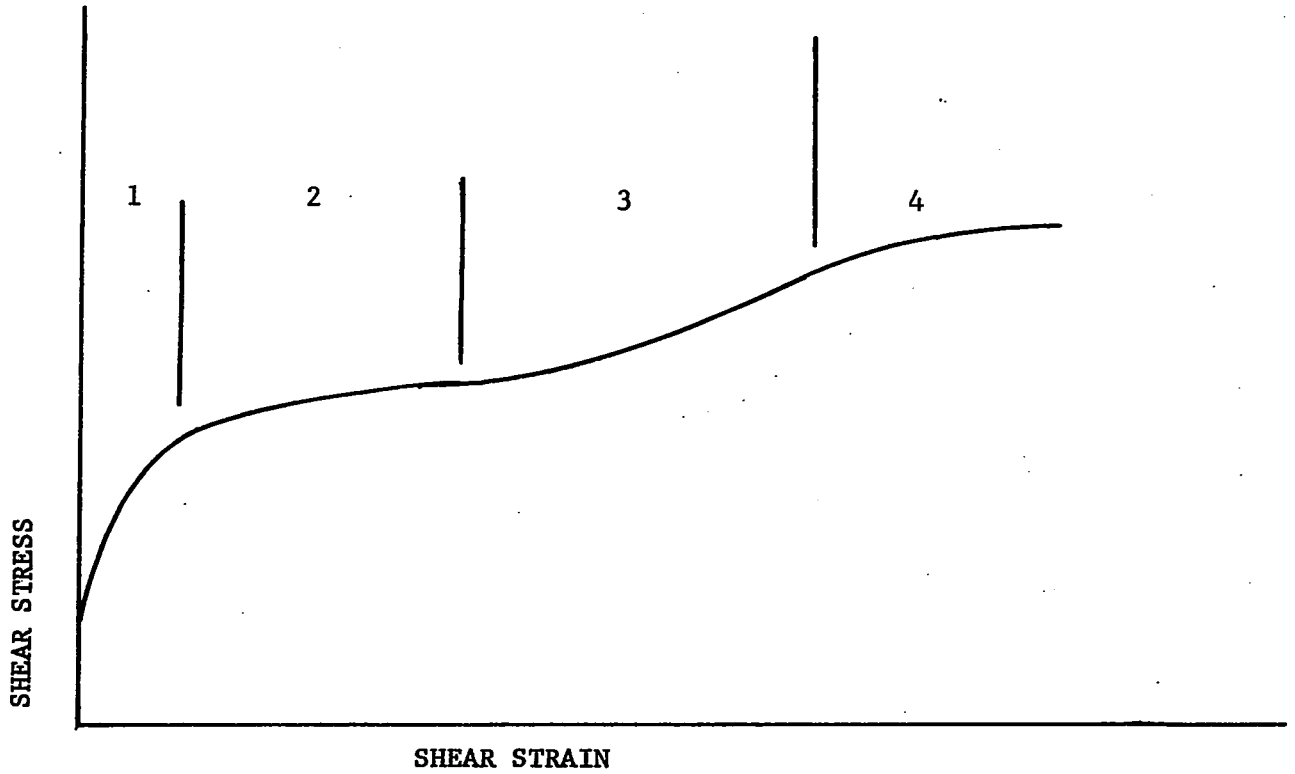

Impurities seem to have no effect on this fourth region; however, an increase in the strain rate is found to eliminate it.

The effect of temperature on the stress-strain curves is shown in figures 21 and 22 for the low and high strain rates, respectively. Except for an abnormality between 250° and 300°K at the high strain rate, an increase in the temperature causes a decrease in the flow stress at all strains. The exception noted at 250° - 300° may be due to experimental error.

Temperature changes do not have a monotonic effect on the work-hardening rate in the high strain regions of the curves. The variation of the work-hardening rate at 60% strain with deformation temperature is given in figure 23. This figure indicates that increasing the temperature above 200°K first decreases the work-hardening rate and then causes it to increase once again.

The temperature dependence of the flow stress at 60% strain is almost identical for both the low and high strain rates. This temperature dependence of the flow stress is illustrated in figure 24. Figures 25 and 26 illustrate the temperature dependence of the yield point for the low and high strain rates, respectively.

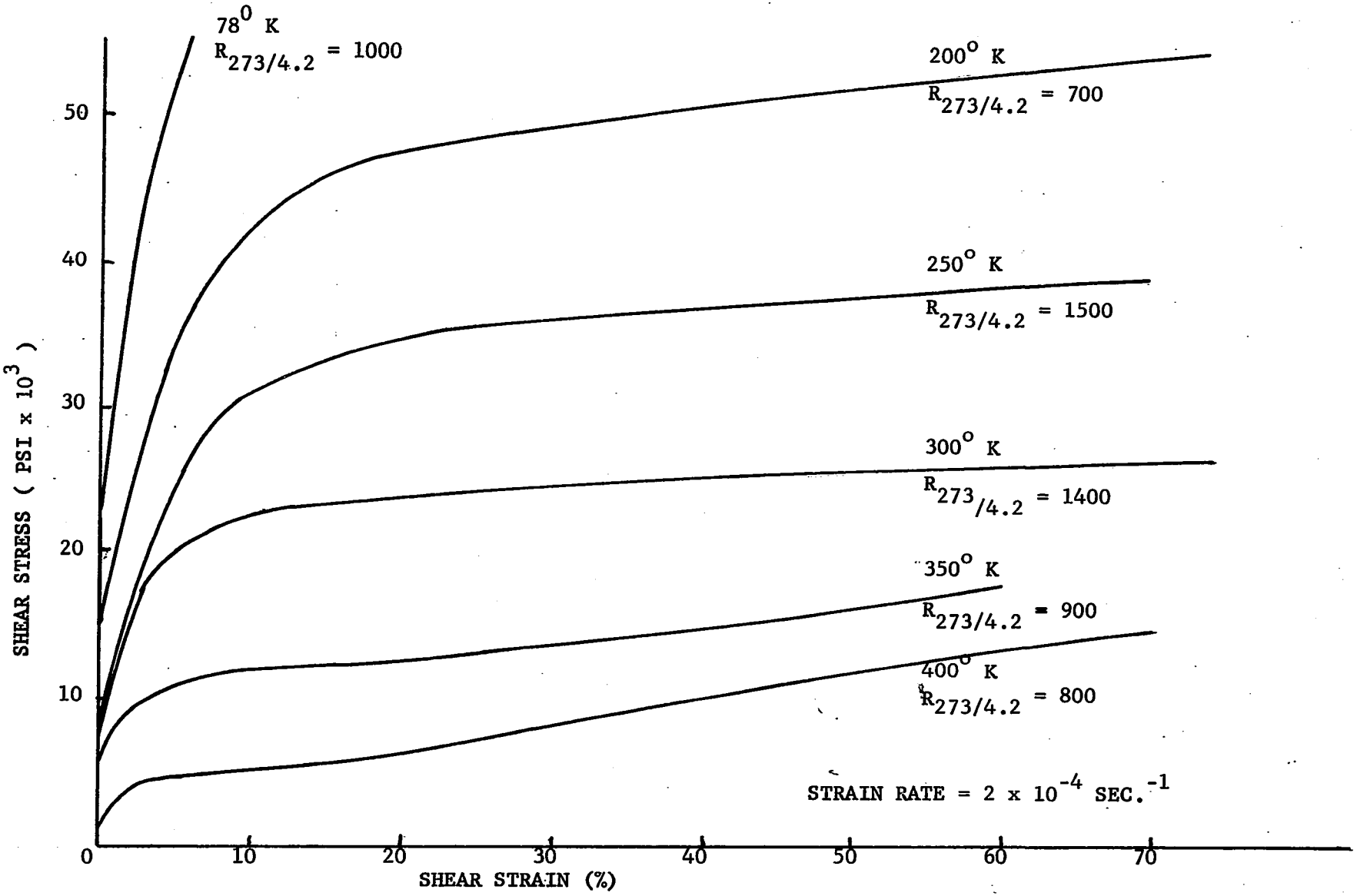

FIGURE 21. EFFECT OF TEMPERATURE ON THE STRESS-STRAIN CURVES IN DIRECT SHEAR.

FIGURE 22. EFFECT OF TEMPERATURE ON THE STRESS-STRAIN CURVES IN DIRECT SHEAR.

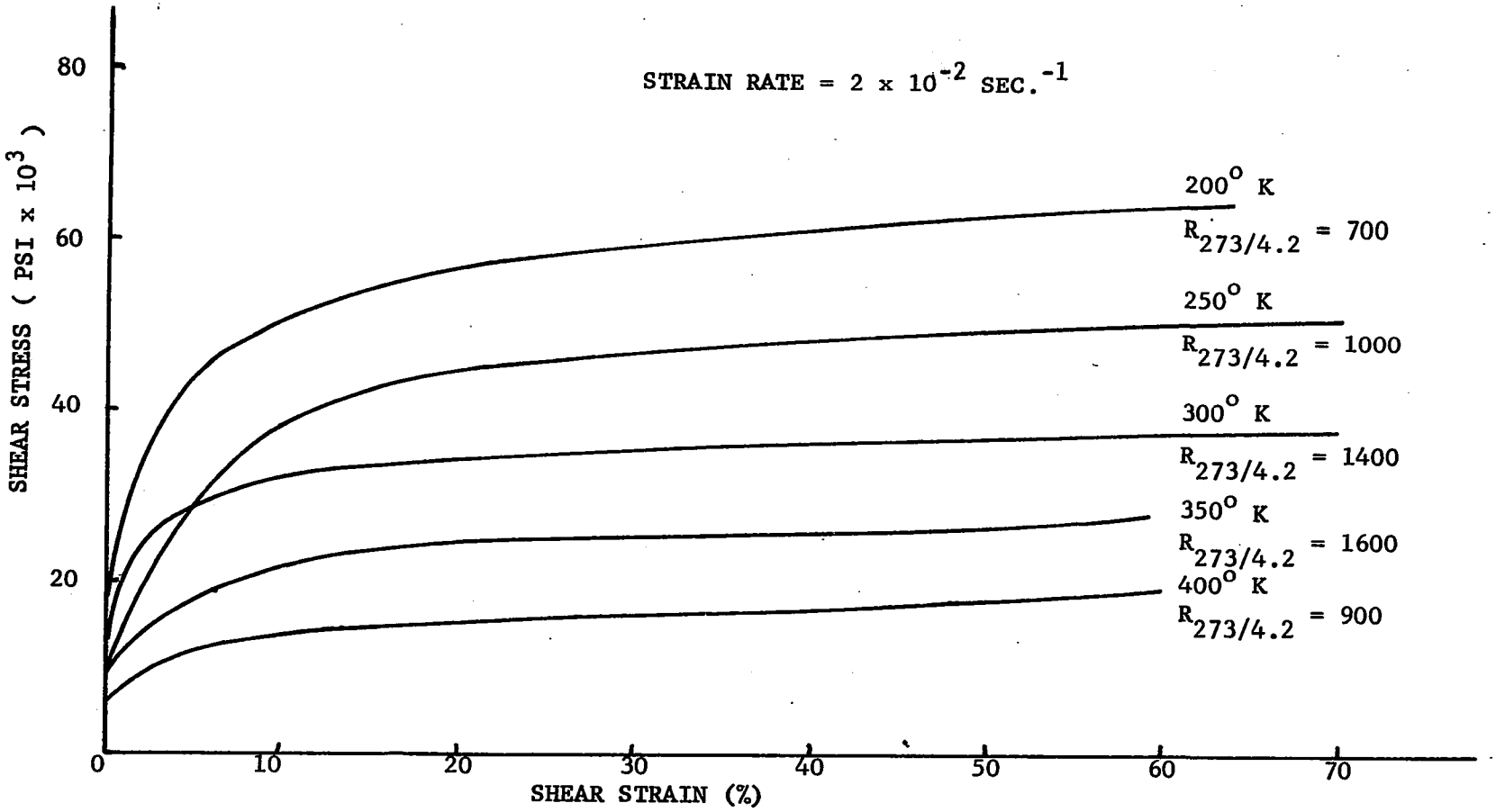

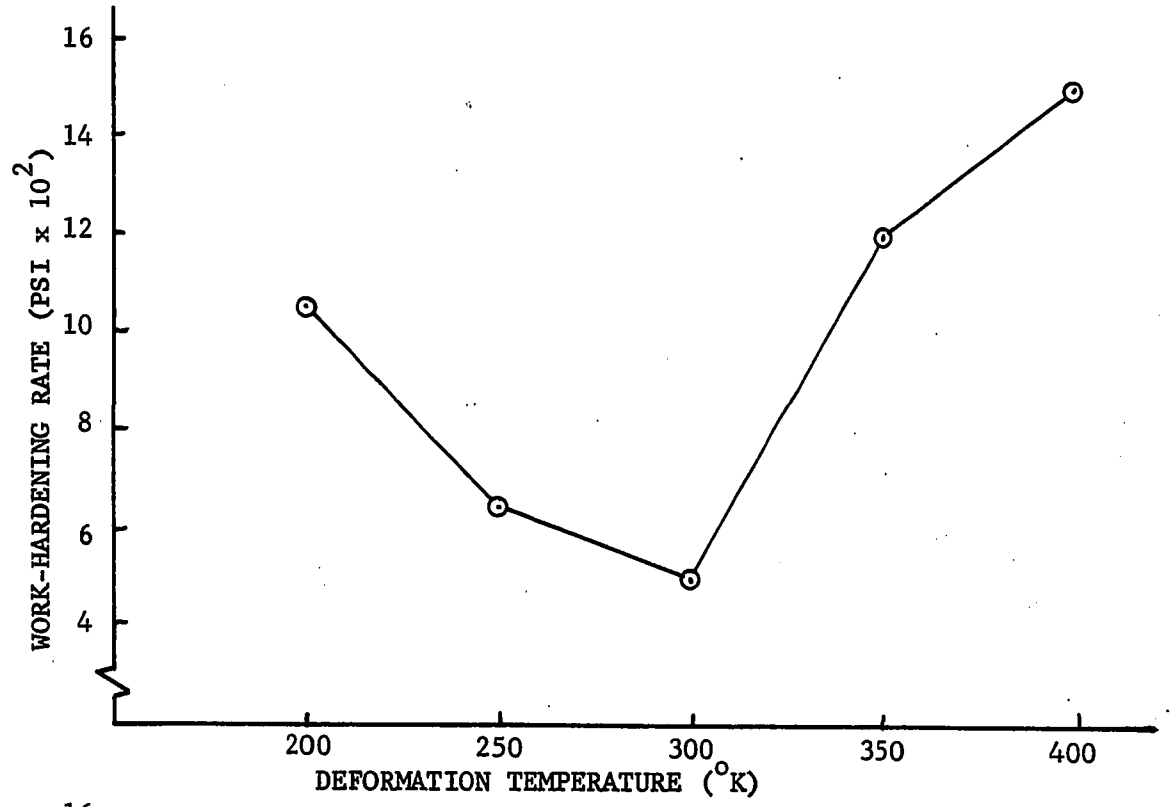

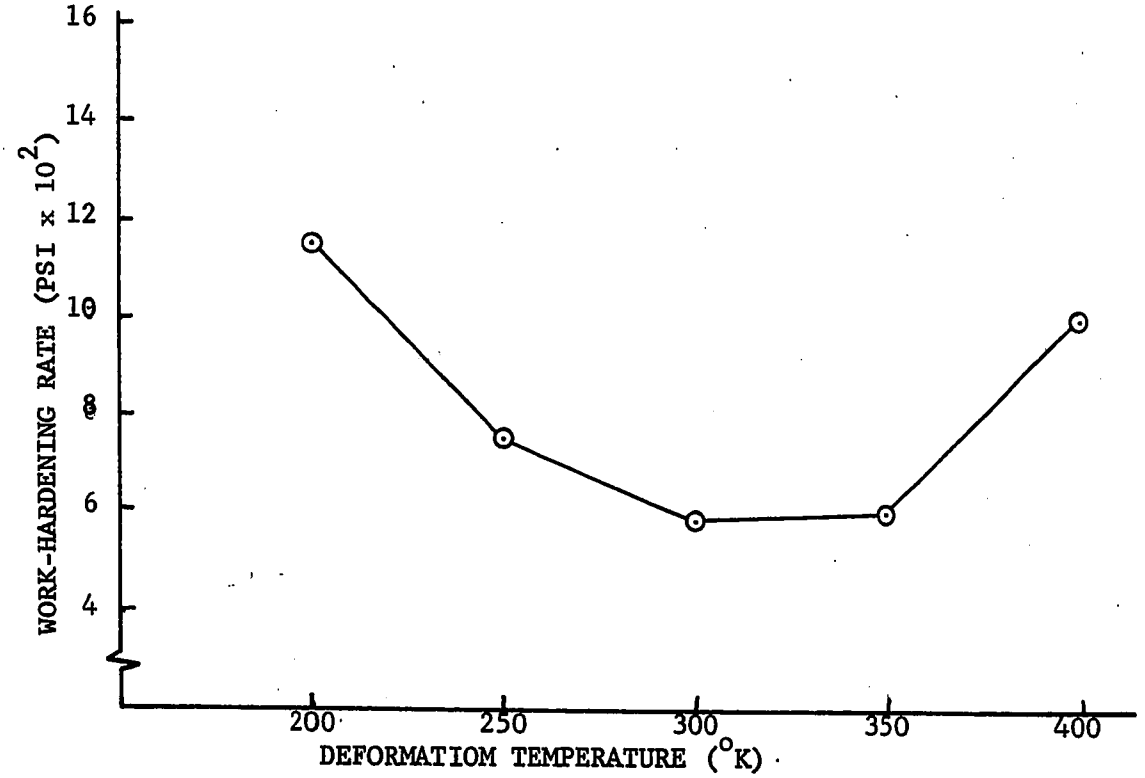

FIGURE 23. WORK-HARDENING RATE AT 60% SHEAR STRAIN.

FIGURE 24. TEMPERATURE VARIATION OF FLOW STRESS AT 60% STRAIN.

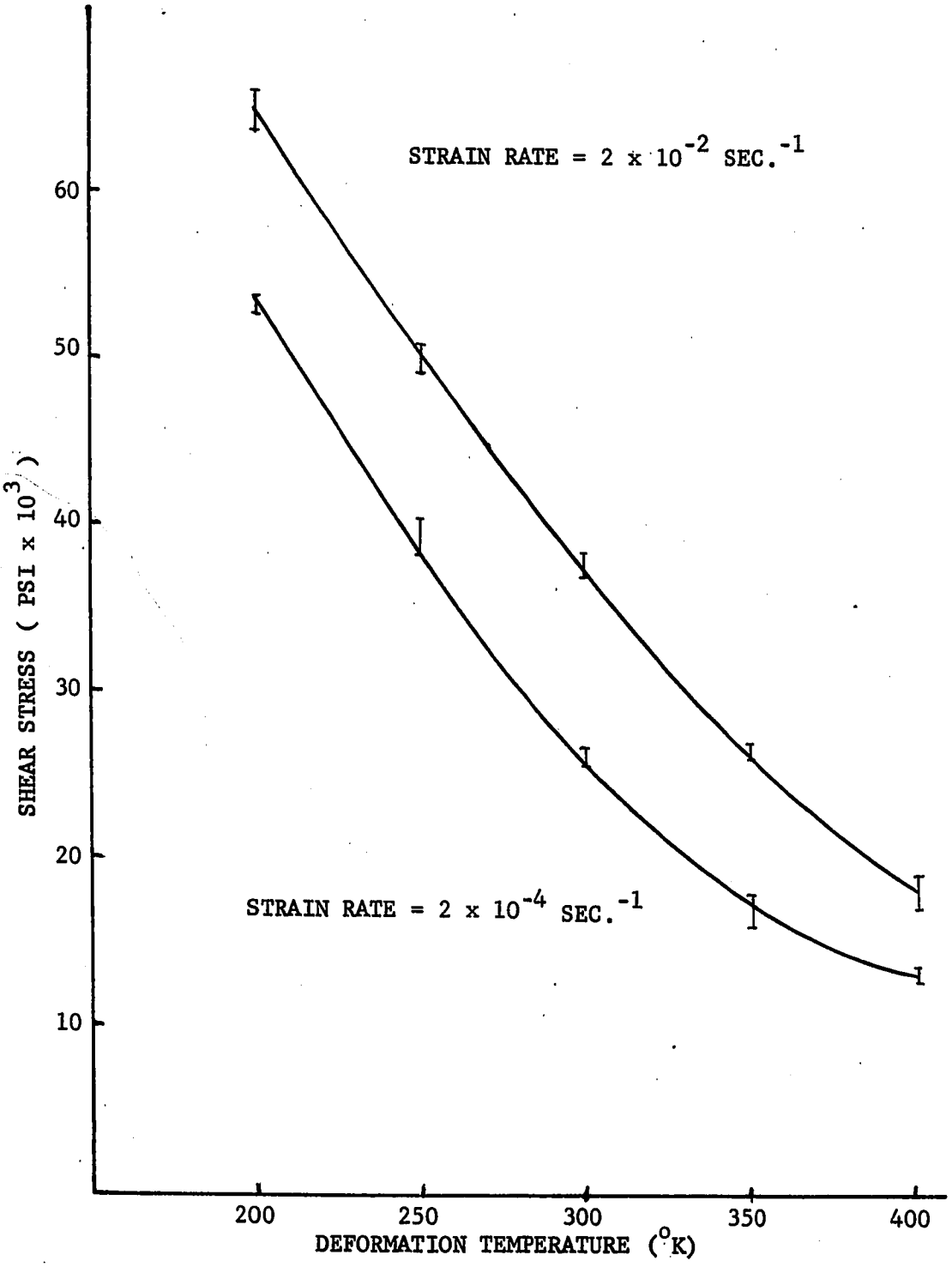

FIGURE 25. VARIATION OF YIELD STRESS WITH TEMPERATURE.

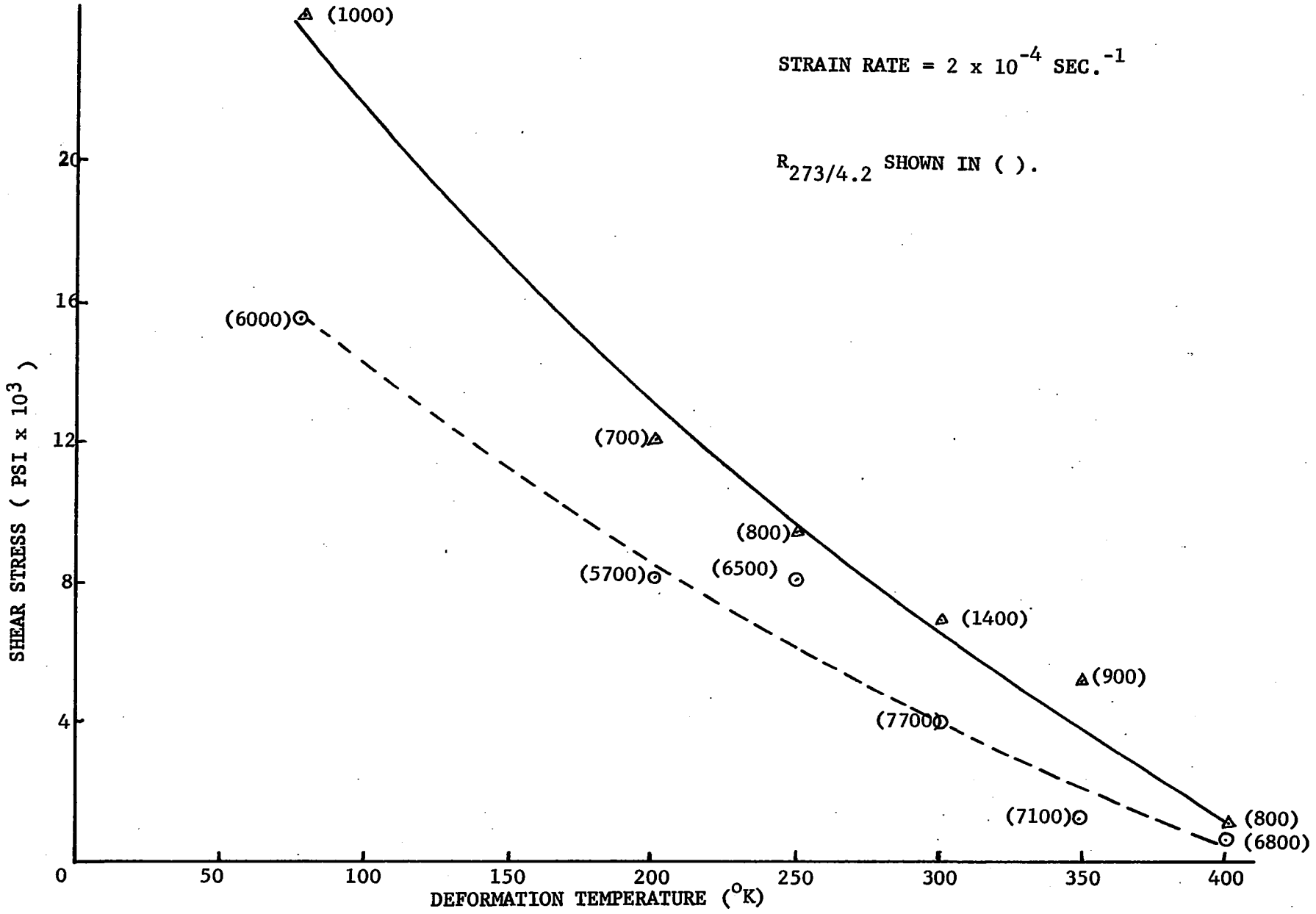

FIGURE 26. VARIATION OF YIELD STRESS WITH TEMPERATURE.

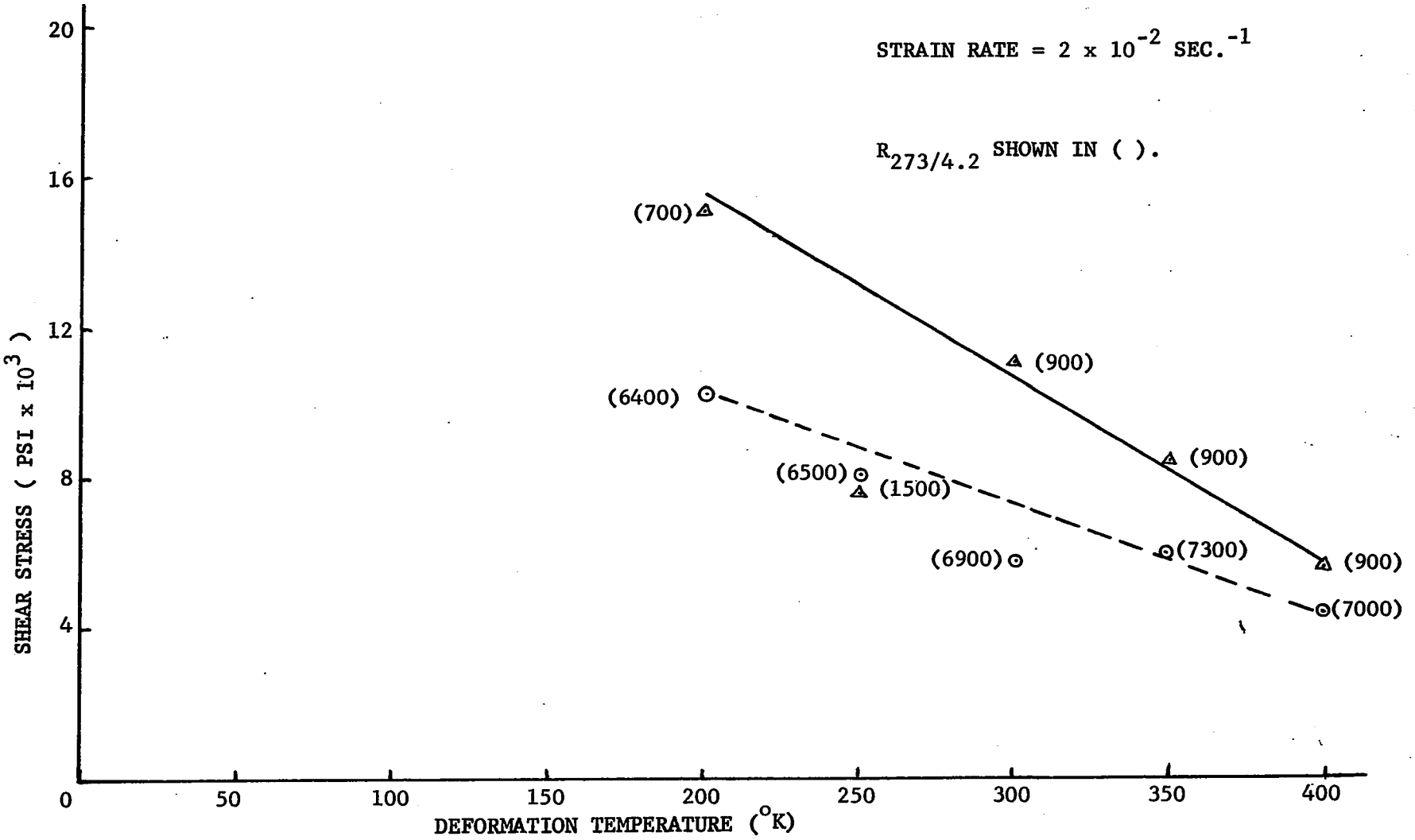

II. Activation Volume

Below 300°K the activation volume appears to be a function of the purity of the crystals. As the deformation temperature increases above 300°K, the effect of impurities decreases, and at 400°K no change due to impurities is detectable.

Figures 27 through 31 exhibit the typical effects of impurities and strain on the activation volume for deformation temperatures of 200°, 250°, 300°, 350° and 400° K, respectively. All of the data obtained in this series of tests are presented in the appendix.

Inspection of Figure 27 reveals the activation volume at 200°K is reduced considerably in the low strain region by the impurities. Deformation continuously reduces any difference in V attributable to impurities, and the curves finally converge at high strains. With increasing deformation temperature, the initial difference due to impurities is reduced and the deformation required to completely remove this difference is decreased.

The variation of the activation volume with strain can be divided into regions equivalent to those used in the stress-strain curves. Whenever the stress increases rapidly with strain, the activation volume deceases rapidly with strain, and if the stress varies slowly with strain, the activation volume varies slowly with

FIGURE 27. ACTIVATION VOLUME VERSUS SHEAR STRAIN FOR DEFORMATION AT 200° K.

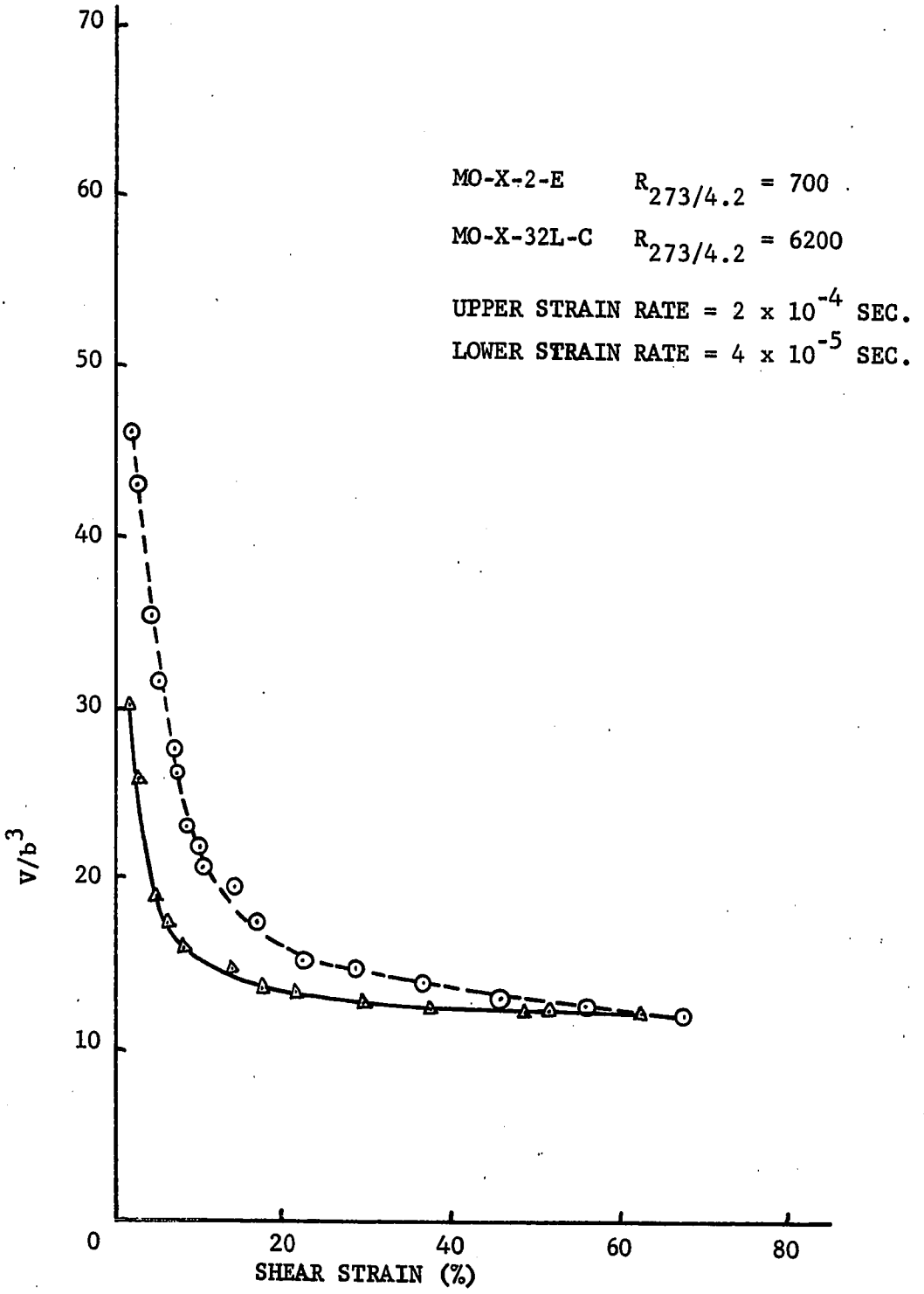

FIGURE 28. ACTIVATION VOLUME VERSUS SHEAR STRAIN FOR DEFORMATION AT 250° K.

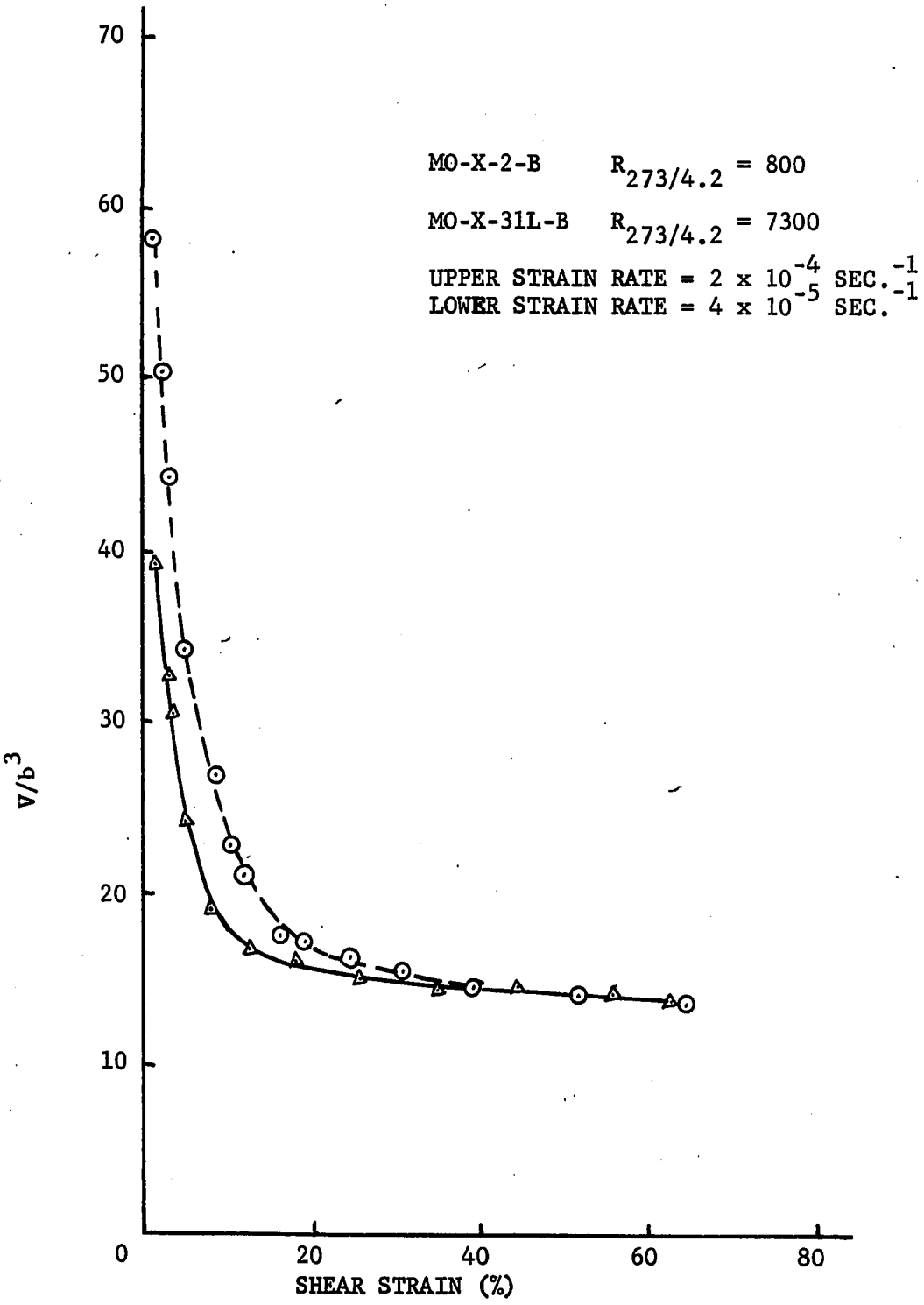

FIGURE 29. ACTIVATION VOLUME VERSUS SHEAR STRAIN FOR DEFORMATION AT 300° K.

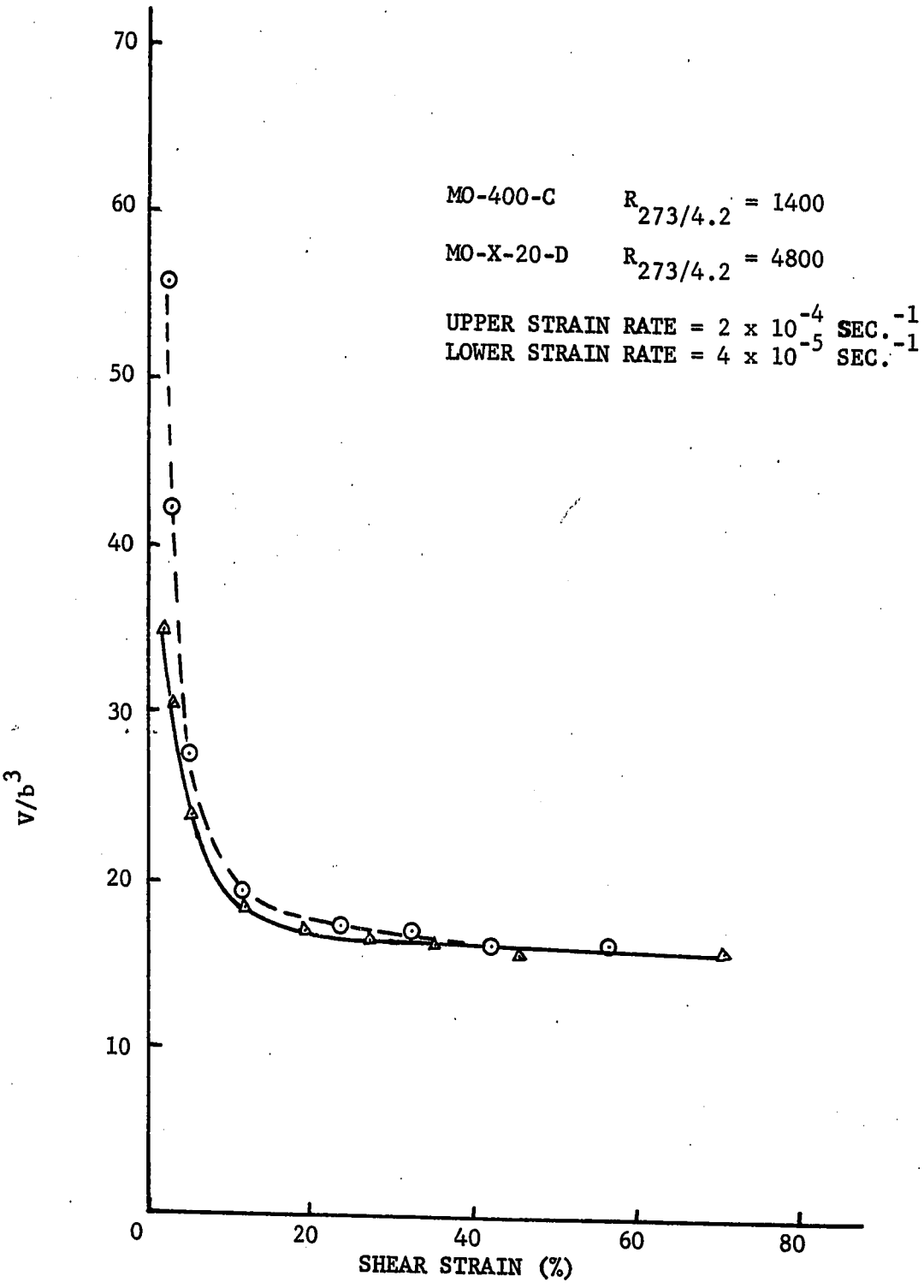

FIGURE 30. ACTIVATION VOLUME VERSUS SHEAR STRAIN FOR DEFORMATION AT 350° K.

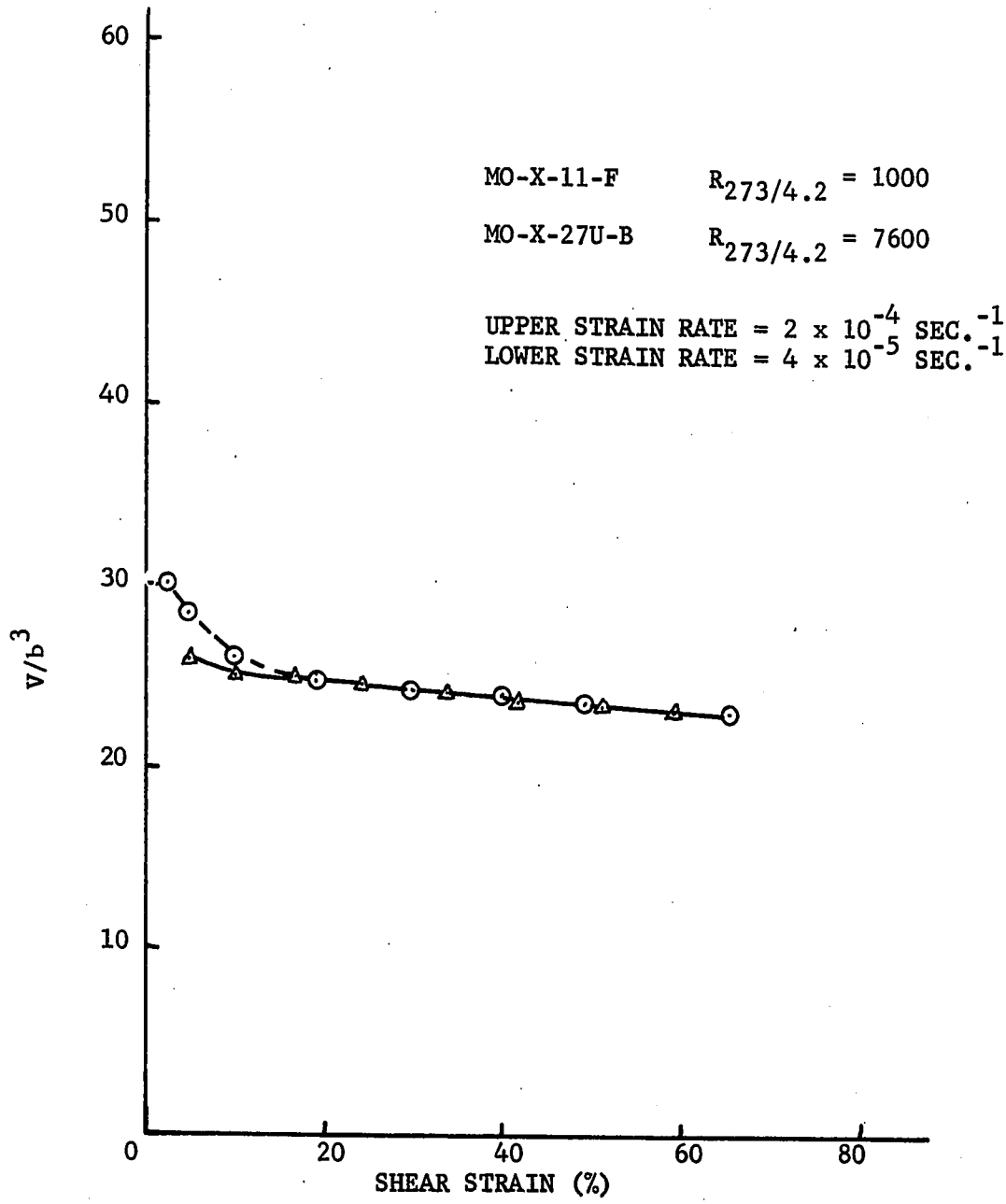

FIGURE 31. ACTIVATION VOLUME VERSUS SHEAR STRAIN FOR DEFORMATION AT 400° K.

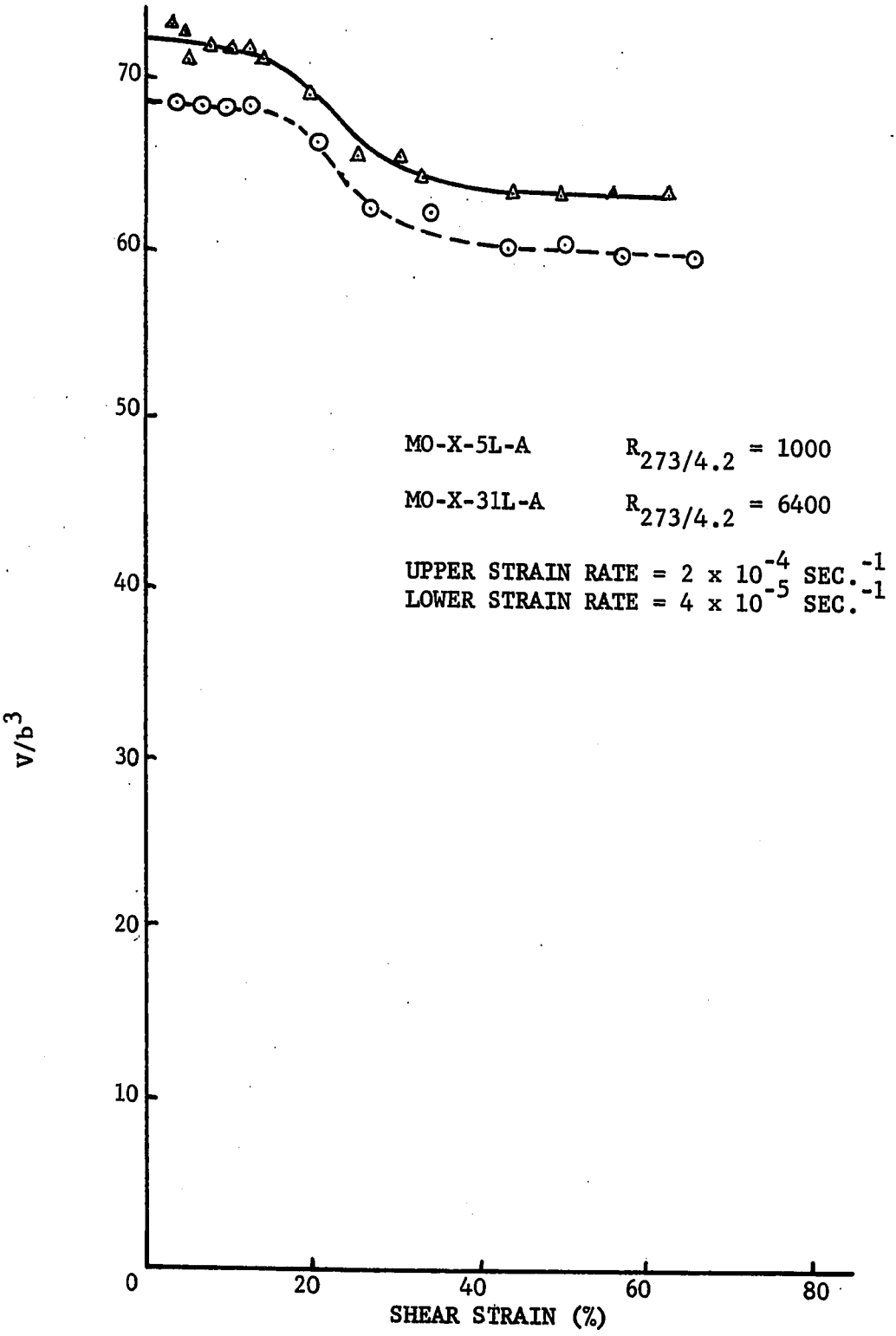

strain. This type of related behavior is found at all temperatures and purities. To illustrate the close relationship, the variation of both stress and activation volume with strain are illustrated in figures 32 and 33 for 200° and 400° K, respectively. It is seen in figure 33 that in the region tentatively identified as easy-glide, the activation volume remains constant.

Figures 34 and 35 illustrate the variation of the activation volume with temperature at 5%, 10%, 20%, 40% and 60% strain for the high and low resistance ratio crystals. Figure 34 reveals that the activation volume does not increase monotonically with temperature at all strains for the purer specimens.

FIGURE 32. STRESS AND ACTIVATION VOLUME VERSUS STRAIN FOR DEFORMATION AT 200° K.

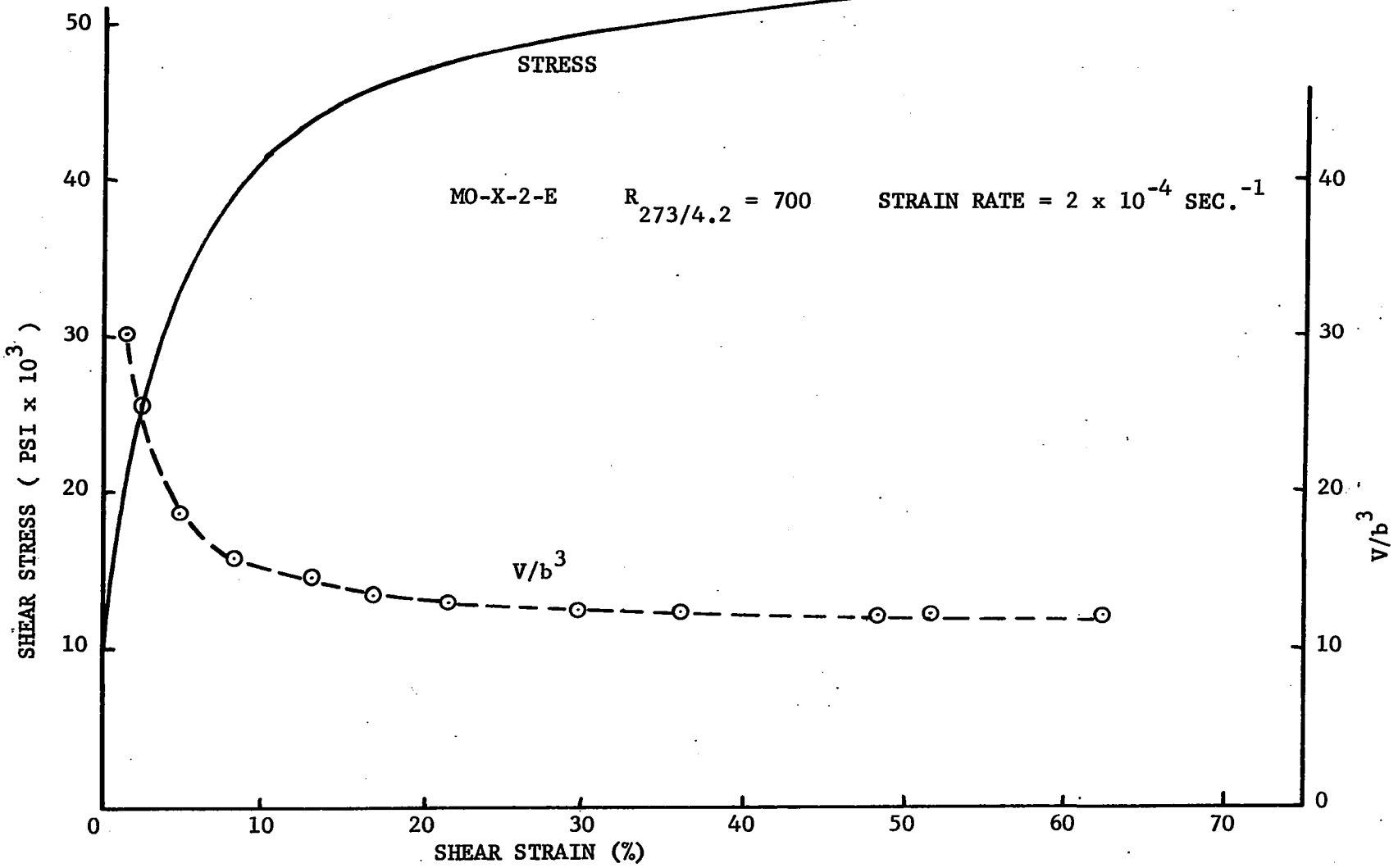

FIGURE 33. STRESS AND ACTIVATION VOLUME VERSUS SHEAR STRAIN FOR DEFORMATION AT 400° K.

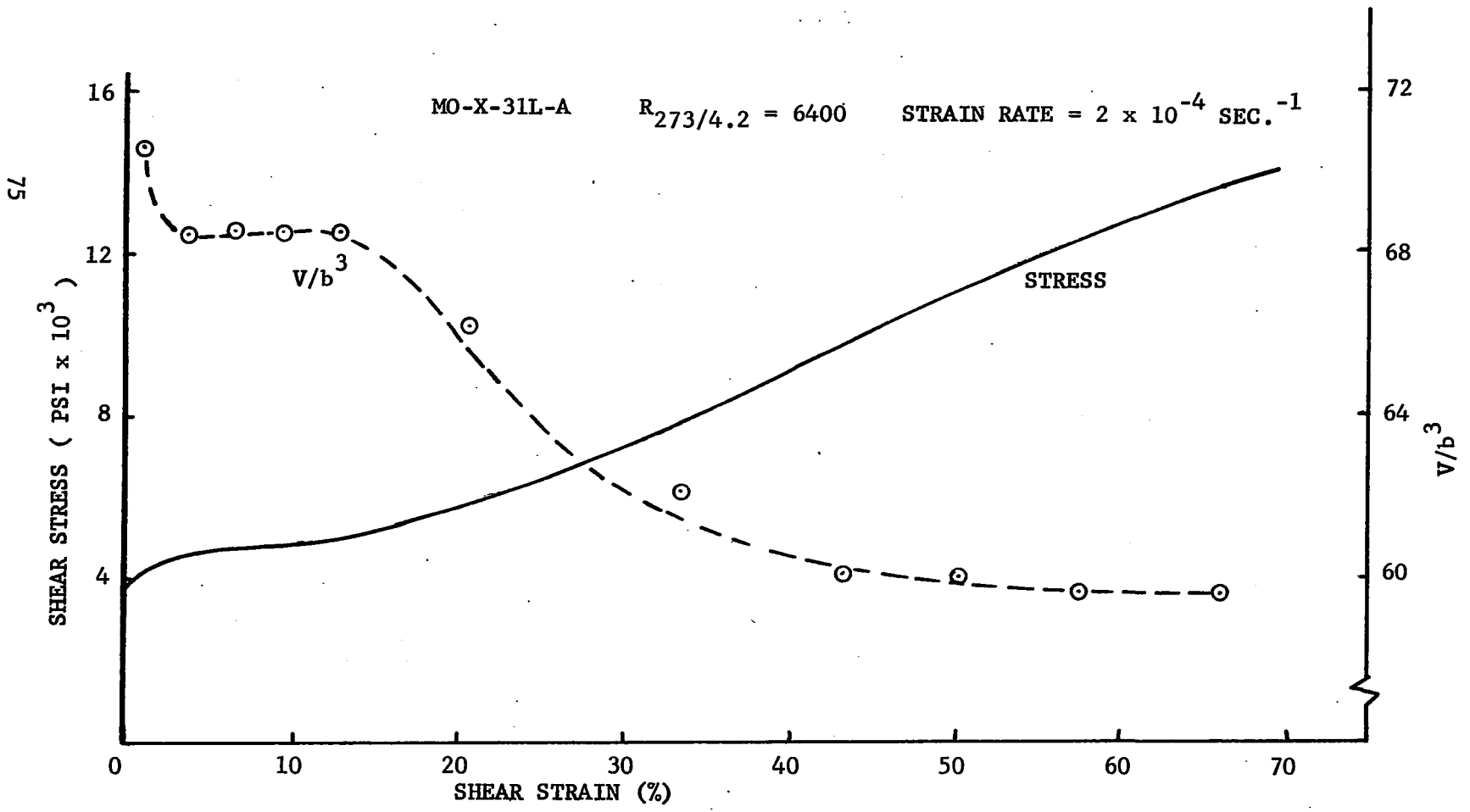

FIGURE 34. ACTIVATION VOLUME VERSUS DEFORMATION TEMPERATURE FOR VARIOUS AMOUNTS OF SHEAR STRAIN.

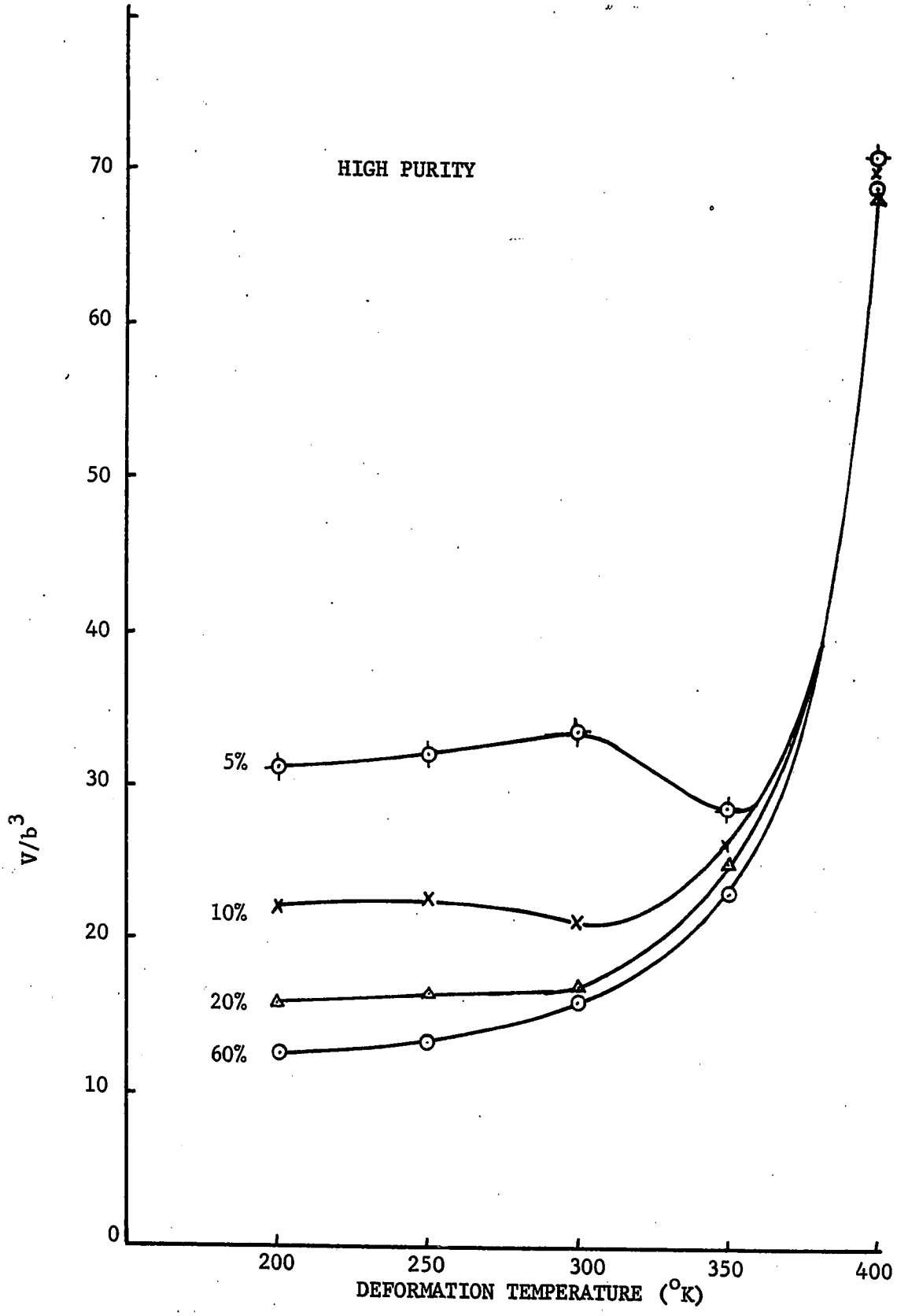

FIGURE 35. ACTIVATION VOLUME VERSUS DEFORMATION TEMPERATURE FOR VARIOUS AMOUNTS OF SHEAR STRAIN.

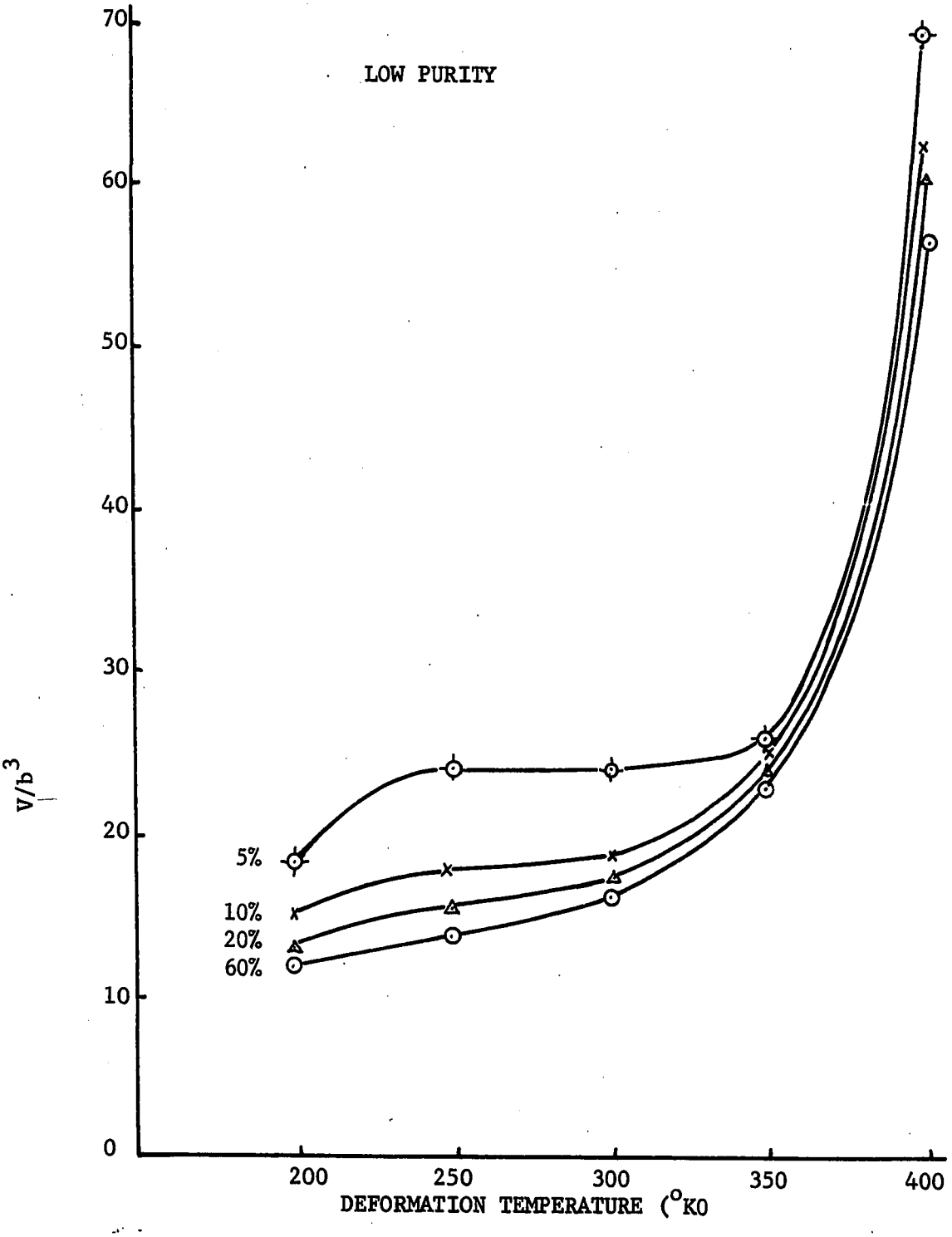

DISCUSSION OF RESULTS

The statement, "impurities affect the mechanical properties of metals and especially the b.c.c. metals," is generally accepted. However, there is conflict concerning the way in which the impurities bring about this change. As is evident from the background material presented earlier, many tests have been made and with a variety of methods for the purpose of ascertaining the influence of impurities. The results have not always been in agreement, and several possible reasons exist, namely:

(1) Impurities affect different b.c.c. metals in various ways.

(2) Grain boundaries may mask impurity effects.

(3) The change in mechanical properties produced by a unit change in purity varies with the total impurity level.

(4) The effects of impurities are temperature dependent.

(5) The effects of impurities vary with the dislocation structure.

(6) The effects of impurities vary with the presence of other defects of atomic size.

(7) The effects of impurities are dependent upon the velocity of the dislocations.

Perhaps all of these influences can be correlated by stating that the effects of impurities are dependent upon the "stress state" existing at the time measurements are made.

I. Stress-Strain Curves

The stress-strain curves obtained at 400°K, figure 19, are not the parabolic-type curves which result so frequently for the b.c.c. metals. Close examination of the curves reveal the existence of features which are similar to the three-stage hardening stress-strain curves often observed for f.c.c. metals. Recent results on niobium,[36,54] iron[37,38] and tantalum[39] single crystals have indicated the occurrence of three-stage hardening in other b.c.c. metals under restricted conditions of purity, orientation, temperature and strain rate. However, to the author's knowledge, no one has previously reported three-stage hardening in molybdenum or any of the other Group VIA (Cr,Mo, W) metals. The detection of three-stage hardening in molybdenum, coupled with the previous results on iron and the Group VA metals, raises the definite possibility that the b.c.c. and f.c.c. metals are not as dissimilar in their fundamental behavior during plastic deformation as has been previously thought. At this time it might be advisable to review the three-stage hardening in the f.c.c. metals and to consider those factors which enhance its appearance. Afterwards the expected effects of these same factors in the b.c.c. structure may explain some of the variations in the stress-strain curves of the f.c.c. and b.c.c. metals.

Stage I, or the easy-glide region, is characterized by a low

rate of work hardening; the existence and length of this region depends on orientation, purity and the size of the crystals. During easy-glide, the slip distance is considered to be large, and many dislocations are assumed to slip out of the crystal. Naturally this makes the extent of easy-glide sensitive to sample size and surface conditions. Most investigators[55] assume that only one slip system is operating and that easy-glide ends when secondary slip systems are activated. Hence, orientations which favor single slip enhance the extent of the easy-glide region.

Stage II, or the linear hardening region, has a slope which is approximately independent of the applied stress, temperature, orientation or impurity content. The ratio $(d\tau/d\epsilon)/G$ in this second stage is of the same order of magnitude for all f.c.c. metals, 200 - 600. Several mechanisms have been proposed to explain the linear work hardening in Stage II, the pile-up theory[55], the forest theory[56] and the jog theory[57]. Of these three theories, the oldest is the pile-up theory proposed by Seeger[55]. He has assumed the transition from Stage I to Stage II to being with the onset of glide on secondary slip systems. Interaction of the secondary and primary dislocations produces obstacles usually considered to be sessile dislocations of the Lomer-Cottrell type, which block the primary dislocations in order to produce pile-ups. Stage II continues as long as dislocations pile up behind the obstacles and ends when the dislocations begin bypassing the obstacles.

Stage III, or the parabolic hardening region, the onset of which is highly temperature dependent, exhibits a decreasing rate of work hardening. This stage is usually associated with gross cross-slip, and the point of initiation of Stage III usually increases with decreasing temperature. Stage III indicates that dislocations held up in Stage II are now able to move under a sufficiently high stress by a process that was suppressed at lower stresses.

Some differences which exist in the stress-strain curves of the f.c.c. metals are attributed to variations in the stacking-fault energy. Metals with a high stacking-fault energy exhibit all three stages under more restricted conditions than the metals with a low stacking-fault energy. Quite often in the high stacking-fault energy metals, Stage III begins before Stage II become predominant. The widely split dislocations in the low stacking-fault energy metals prevent the easy cross slip of the screw dislocations, and the initiation of Stage III is thereby delayed. In the high stacking-fault energy metals, the screw dislocations are not widely split and cross slip becomes much easier; hence, Stage III starts at lower stresses.

Temperature changes mainly affect the onset of Stage III; the lower the temperature of deformation, the higher is the stress

corresponding to the onset of Stage III. Thermally activated cross slip is considered to explain the temperature dependence of Stage III. With the aid of thermal energy, cross slip can be initiated at much lower stresses than that which is required in the absence of thermal energy.

Impurities also affect the ease of cross slip and thereby the initiation of Stage III. Ahlers[58] has shown that the energy of cross slip in silver single crystals is lowered by a factor of two by the presence of 4 ppm of oxygen over that for a crystal containing only 2 ppm oxygen. Due to the differences in elastic constant, the effects of impurities is expected to be considerably larger in the b.c.c. metals.

It has been recognized that impurities in the f.c.c. metals affect the easy-glide region in a manner dependent upon the solubility of the impurities. Impurities with high solubilities tend to raise the critical shear stress, but tend to make the extent of easy-glide larger and of lower slope. Low-solubility impurities increase the slope in the easy-glide region and sometimes suppress it completely. Low solubility is usually connected with stress fields around atoms, a tendency to cluster, and similar phenomena which are all capable of interfering with the dislocation movement.

Although three-stage hardening is considered characteristic of the f.c.c. metals, apparently there are parameters which can influence the presence and extent of all three stages. Therefore, the anticipated effects of these same parameters should be resolved before it is assumed that the plastic deformation of the two structures is fundamentally diverse.

Figure 36 illustrates schematically a well defined three-stage stress-strain curve of the type often observed for f.c.c. metals. Also exhibited in figure 36 is a curve of the same shape as observed in the present tests on molybdenum and previous tests on niobium [36] and tantalum [39] at low temperatures. Comparison of the two reveals that the b.c.c. and f.c.c. curves are very similar except for the absence of Stage I in the b.c.c. curve. Since impurities have suppressed Stage I in the f.c.c. metals, the absence of Stage I in the b.c.c. curves could also be attributed to the presence of impurities without further discussion. However, it might be well to contemplate how the impurities suppress easy-glide in the b.c.c. metals at low temperatures and perhaps why three-stage stress-strain curves are observed for the b.c.c. metals under more restricted conditions than for the f.c.c. metals.

A major difference between the f.c.c. and b.c.c. metals appears to lie in the mobility of the screw dislocations at low temperatures.

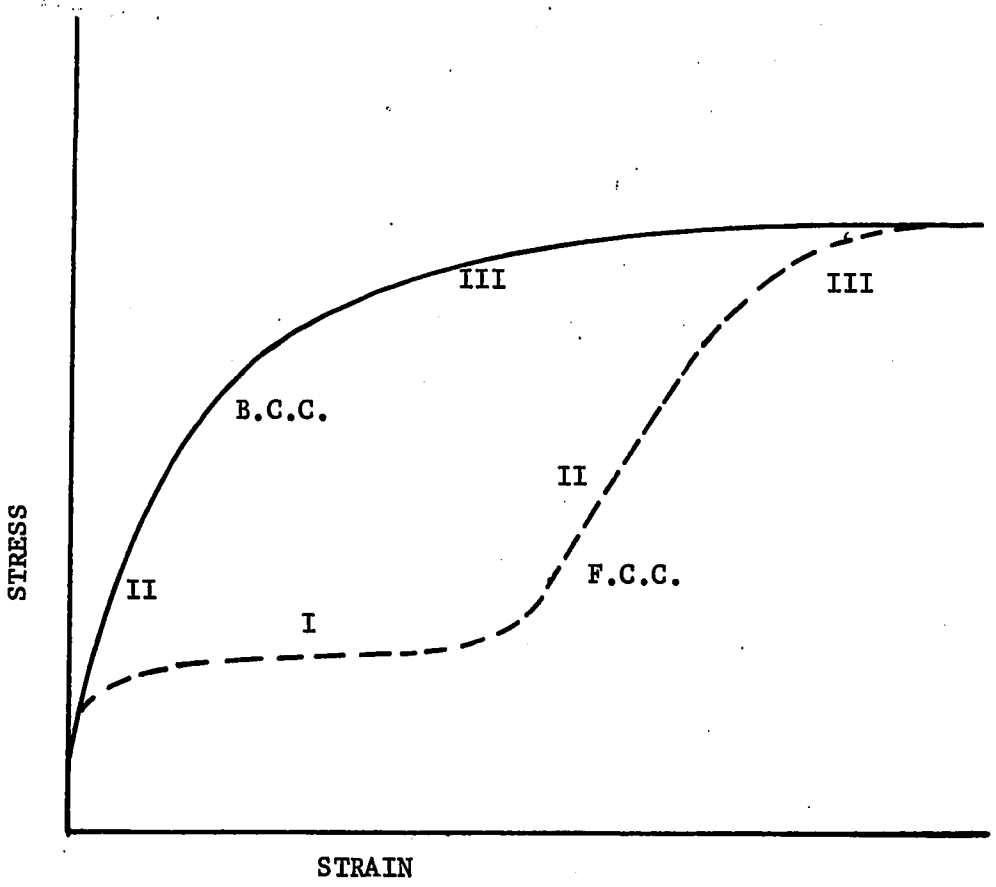

FIGURE 36. TYPICAL STRESS-STRAIN CURVES FOR F.C.C. AND B.C.C. METALS AT LOW TEMPERATURES.

In the f.c.c. metals, both the screw and the edge dislocations are highly mobile and are considered to move over large distances during easy glide. This action permits many dislocations to be emitted by a single source without a stress increase on that source. It has been observed that the screw dislocations in the b.c.c. metals have only limited mobility at low temperature. The difference in the mobility of the screw and the edge dislocations is evident from the elongated loops observed by transmission electron microscopy at low temperatures in the b.c.c. metals[59]. These loops indicate that the edge dislocations can move much farther away from the emitting source than can the screw dislocations. This low mobility of the screw dislocations has been known for some time, and many of the theories for the temperature dependence of the flow stress in the b.c.c. metals are attempts to explain how the mobility of the screw dislocations varies with temperature.

Several authors[60,61,62] have suggested that the low mobility of the screw dislocations is due to the dissociation of the screws into partials which are not in the same plane. The edge dislocations lack the necessary symmetry to dissociate in this manner. Sleeswyk[60] has recently shown that it is energetically more favorable for the screws to dissociate onto two inclined (211) planes rather than in a three fold manner proposed by earlier authors[61,62]. If the screw dislocations are dissociated in

this manner, it will be necessary to produce a constriction or a high-energy fault in order for the screw dislocations to move. When not aided by thermal energy, as for example at low temperatures, a high stress will be required to produce the constriction or high-energy fault. Quite likely the stress required to constrict the screw dislocations will be high enough to induce some cross slip and thereby account for the appearance of wavy slip lines observed even at low temperatures in b.c.c. metals.

The dissociation of the screw dislocations will also offer an explanation for other experimental results. Quite often the screw dislocations are observed lying along close-packed directions in the b.c.c. metals. This preferred orientation of the screws has been taken by some investigators to be proof that a high Peierls-Nabarro energy barrier controls the movement of the dislocations at low temperatures. However, if the screw dislocations are dissociated, they will tend to align themselves along low-energy directions regardless of whether activation over the Peierls-Nabarro barriers is rate controlling.

Although it is not their only effect, impurities are considered to influence the dissociation of the screw dislocations. The b.c.c. metals are known to have intrinsically high stacking-fault energies. In fact, the stacking-fault energy is so high that dissociation of

dislocations cannot be detected in the "pure" b.c.c. metals by electron microscopy. Naturally very small amounts of impurities are considered to be increasing the dissociation of the dislocations, but the amount of dissociation is below the limit of resolution in the electron microscope.

It is proposed that the difference in the appearance of the f.c.c. and b.c.c. stress-strain curves at low temperatures is related to the way the screw dislocations dissociate in the two lattices. In the f.c.c. metals, the dislocations are dissociated into partials which are on the same plane, and no recombination of partials or production of a high energy fault is required for movement of the dislocations. Under an applied stress, both edge and screw dislocations can move away from an emitting source, unless obstructed by impurity atoms. The exertion of very little back-stress on the source permits a considerable number of dislocations to be emitted by the same source without an additional increment of stress being applied to the source. Because the stress remains low, very little dislocation movement on secondary slip systems is produced and the easy-glide region is quite extensive at low temperatures. Impurities are thought to suppress the easy-glide region in the f.c.c. metals by creating obstacles in the lattice, thereby restricting movement of the dislocations away from the sources.

The easy-glide in b.c.c. metals is considered to be due only to the movement of edge dislocations. The screw dislocations are believed to be dissociated as proposed by Sleeswyk[60]. In order to move the screw dislocations, a high stress is required to cause recombination or creation of a high-energy fault. Hence, easy-glide in the b.c.c. metals is assumed to continue as long as there are edge dislocations which can move easily under an applied stress. Impurities are thought to suppress the easy-glide by locking the edge dislocations and preventing their free movement through the lattice at low temperatures. As the temperature is raised, the effectiveness of impurities as pinning points decreases until a temperature is reached whereby the impurities are no longer effective obstacles. The edge dislocations are then thought to be able to move through the lattice easily, thereby producing an easy-glide region. Some support for the effectiveness of impurities as obstacles that decrease with rising temperature is obtained from the results of Stein *et al.*[3,10]. They state that the pinning points in iron become weaker with increasing temperature. The present results also indicate that the effectiveness of impurities as obstacles decreases as the temperature is increased.

The effect of impurities in suppressing the stages in the b.c.c. metals is also apparent from the work of Mitchell, Foxall and Hirsch[36]. They found that the three stages in niobium

became more distinct with increasing purity, decreasing strain rate or orienting the crystals so that single slip on one (110)-[$\bar{1}11$]slip system was favored. By examining figure 19 it can be seen that the strain rate had similar results in molybdenum. In fact, for the impure crystal, only Stage III can be detected at the high strain rate.

The solubility data presented by Hahn, Gilbert and Jaffee[63] indicate that impurities will effect molybdenum even more than niobium. They show that the solubility for interstitials in the Group VA (V, Nb, Ta) is 3 or 4 orders of magnitude larger than in the Group VIA (Cr, Mo, W) metals. As mentioned earlier, a low solubility is associated with a large stress field around the solute atoms, a tendency to cluster and a general tendency to obstruct the motion of dislocations.

Probably the most characteristic feature of the three-stage hardening curves in the f.c.c. metals is the slope of Stage II, Most of the f.c.c. metals have approximately the same θ_{II}/G regardless of the orientation, purity or temperature. For the b.c.c. metals, the slope of Stage II has not been quite as constant and has had about half the value found in the f.c.c. metals. The following representative values for θ_{II}/G have been determined: niobium[36], G/600; tantalum[39], G/600; iron[37], G/400 to G/900.

The present results indicate θ_{II}/G in molybdenum is G/900. Mitchell et al.[36] have suggested that the reduced value of θ_{II}/G is due to the varying dislocation interactions in the two structures, while the basic hardening mechanism are the same. Another explanation for the lower slope in Stage II may be because the high stacking-fault energy of the b.c.c. metals permits some cross slip to occur during Stage II. Perhaps this cross slip lowers the work-hardening rate, and Stage III represents the start of extensive cross slip. However, no further discussion of the hardening mechanism in molybdenum is justified without extensive electron microscopy and slip band studies.

II. Activation Volume

The activation volume was determined from equation (9) by neglecting the second term on the R.H.S. of this equation. The neglected term, $[\partial \ln \dot{\epsilon}_o / \partial \tau_a]_{T,\epsilon}$, should be small if the number of mobile dislocations stays approximately constant and only their velocity increases with increased strain rate. The basis of this assumption is the work of Gilbert, Wilcox and Hahn[48]. They measured the dislocation densities as a function of plastic strain in recrystallized polycrystalline molybdenum at two greatly different strain-rates (2×10^{-5} and 2×10^{3} sec^{-1}). Their results indicated only a small difference in the total dislocation density, and they concluded that an enlargement in the strain rate by 10^8 was accommodated mainly by an increase in the average dislocation velocity rather than in the number of mobile dislocations. It is felt that only in the very early stages of deformation will the error introduced by neglecting $[\partial \ln \dot{\epsilon}_o / \partial \tau_a]_{T,\epsilon}$ be appreciable. Even in this initial region, the same error should be introduced in both the pure and the impure samples, and any difference in activation volume could be attributed to impurities.

The activation volume decreased with increasing strain at all deformation temperatures tested. Except at 400° K, the rate of decrease was initially very rapid and continously changed to a lower value as deformation proceeded. Similar results were obtained

previously by Youngblood[7] for molybdenum single crystals in direct shear. Orava[64] also found the activation volume to decrease with strain for molybdenum single crystals tested in tension.

Consideration of figure 27 reveals the activation volume to be higher for the purer crystals, especially in the early stages of deformation. At this temperature, 200°K, the impurities definitely seem to have created obstacles to the movement of the dislocations. However, to explain the convergence of the activation volumes for the pure and the impure crystals at higher strains, it is necessary to postulate that other obstacles which have the same effect as impurities are created during deformation. The postulate that obstacles are created during deformation which oppose the movement of dislocations is in agreement with other experimental data. Keh and Weissmann[40] and Lawley and Gaigher[43] have observed the obstruction of gliding dislocations by the "forest" dislocations.

That obstacles are created during deformation which are equivalent to the obstacles of impurities can also be inferred from the work of Shaw and Sargent[34]. They investigated the load relaxation below the upper yield limit on polycrystalline molybdenum and niobium. The load drop was found to be less for

both decreasing purity and repeated tests to the same specific load. This indicates that the obstacles created by impurities are equivalent to the obstacles created by the movement of dislocations. The effect of radiation damage and prestrain was to decrease the load drop, and hence, to produce further proof that the dislocations which move are sensitive to barriers created by other dislocations and point defects. Reid, Gilbert and Rosenfield [65] have also indicated that grown-in dislocations hold an important role as obstacles.

Increasing the deformation temperature above 200°K reduced the effect of impurities on the activation volume. Similar results have been found by Mordike and Haasen [9] and Stein and Low [24] for the effect of impurities in iron single crystals.

If the intrinsic lattice resistance or cross slip controls the movement of dislocations at low temperatures, the activation volume is not a function of the structure (strain) or the purity. The apparent variation of the activation volume with strain and purity obtained in the present tests would be explained in one of two ways:

(1) The activation volume decreases with strain because the effective stress increases with strain.

(2) The impurities and strain both change the $\dot{\varepsilon}_o$ term in equation (9) which has been neglected in calculating the activation volume.

The results of Herring[14] and Michalak[66] refute argument number one, since they show the effective stress to be essentially constant. Michalak's[66] results also indicate that the number of mobile dislocations remains approximately constant, with the increase gained by multiplication, offset by the decrease due to obstacles. Most of the results which indicate a variation in the mobile dislocation density do so only for the small strain region. Since the variation of activation volume with strain and purity persists outside this region, it seems likely that the activation volume is a function of the purity and structure of the samples.

Additional evidence that the activation volume is a function of the structure is exhibited in figure 33. This figure makes apparent the fact that in the region tentatively identified as easy-glide, the activation volume remains constant. During this portion of the curve, the dislocation configuration is considered to remain approximately the same. At the end of easy-glide, the dislocation structure changes with strain, and it is here that the activation volume begins to decrease with increasing strain. When Stage III is reached and "dynamic recovery" begins, the activation

volume once again becomes almost independent of the strain. This type of behavior is to be expected if the activation volume is actually a function of the dislocation structure. During Stage III, the dislocation structure is beginning to recover about as fast as it is changed.

CONCLUSIONS

The influence of impurities is dependent upon the temperature of deformation. At low temperatures the effects of impurities is limited to the initial stages of deformation and is rapidly obliterated by work hardening. Increasing temperatures cause a decrease in the influence of impurities and permit detection of features characteristic of the f.c.c. metals. By considering the effects of impurities, stacking-fault energies and temperature on the movement of dislocations in the f.c.c. and b.c.c. metals, the stress-strain curves of the two types of metals are not as different as previously thought.

Although impurities create obstacles which can be overcome with aid of thermal energy, equivalent obstacles are also created during plastic deformation. Therefore, the correct model for the mechanism which controls the movement of dislocations must account for both impurities and other obstacles.

BIBLIOGRAPHY

1. H. Conrad: J. Iron and Steel Inst., 198, 1961, 364.

2. J. Heslop and N. J. Petch: Phil. Mag., 1, 1956, 866.

3. Z. S. Basinski and J. W. Christian: Aust. J. Phys., 13, 1960, 299.

4. H. Conrad and S. Fredrick: Acta Met., 10, 1962, 1013.

5. B. C. Masters and J. W. Christian: The Relation Between the Structure and Mechanical Properties of Metals, Teddington Conf., 1963, 559.

6. G. Schoeck: Acta Met., 9, 1961, 382.

7. J. L. Youngblood: Ph. D. Thesis, Rice University, 1963.

8. D. P. Gregory, A. N. Stroh and G.H. Rowe: Trans. Met. Soc. AIME, 227, 1963, 678.

9. B. L. Mordike and P. Haasen: Phil Mag., 7, 1962, 459.

10. D. F. Stein, J. R. Low and A. V. Seybolt: Acta Met., 11, 1963, 1253.

11. R. C. Koo: Acta Met., 11, 1963, 1083.

12. N. Brown and R. Ekvall: Acta Met., 10, 1962, 1101.

13. R. Kossowsky: Ph. D. Thesis, University of Pennsylvania, 1963.

14. R. B. Herring: M. S. Thesis, Rice University, 1965.

15. N. F. Mott: Phil. Mag., 44, 1953, 742.

16. G. Schoeck: Phys. Stat. Sol., 8, 1965, 499.

17. H. Conrad and W. Hayes: Trans. ASM, 56, 1963, 249.

18. G. Alefeld: Z Naturf., 172, 1962, 899.

19. E. R. Parker and J. Washburn: ASM Seminar, Modern Research Techniques in Physical Metallurgy, 1953, 186.

20. J. F. Wellings and R. Maddin: Technical Report No. A. D. 278051, 1962.

21. A. Lawley, J. Van den Sype and R. Maddin: J. Inst. Metals, 91, 1962, 23.

22. M. A. Adams, A. C. Roberts and R. E. Smallman: Acta Met., 8, 1960, 328.

23. E. Votava: "Effect of Purity on the Mechanical Properties of Niobium," Plansee Proceedings, 1964.

24. D. F. Stein and J. R. Low: J. Appl. Phys., 31, 1960, 362.

25. B. L. Mordike: Z Metalk., 53, 1962, 586.

26. R. L. Fleisher: Acta Met., 10, 1962, 835.

27. R. L. Fleisher and W. R. Hibbard: The Relation Between Structure and Mechanical Properties of Metals, Teddington Conf., 1963, 262.

28. F. R. N. Nabarro, Z. S. Basinski and D. B. Holt: Adv. in Phys., 13, 1964, 193.

29. A. Cracknell and N. J. Petch: Acta Met., 3, 1955, 186.

30. G. Schoeck and A. Seeger: Acta Met., 7, 1959, 469.

31. A. Fourdeux and A. Wronski: Acta Met., 11, 1963, 1271.

32. G. A. Sargent, P. J. Sherwood and A. A. Johnson: Nature, 195, 1962, 374.

33. L. I. Van Torne and G. Thomas: Acta Met., 11, 1963, 881.

34. B. J. Shaw and G. A. Sargent: Acta Met., 12, 1964, 1215.

35. A. Lawley and H. L. Gaigher: J. Appl. Phys., 33, 1962, 3594.

36. T. E. Mitchell, R. A. Foxall and P. B. Hirsch: Phil. Mag., 8, 1963, 1895.

37. A. S. Keh: Phil.Mag., 12, 1965, 9.

38. D. Jaoul and D. Gonzalez: J. Mech. Phys. Solids, 12, 1961, 16.

39. T. E. Mitchell and W. A. Spitzig: Acta Met., 13, 1965, 1169.

40. A. S. Keh and S. Weissmann: Electron Microscopy and Strength of Crystals, ed. G. Thomas and J. Washburn, New York, Interscience, 1963, 231.

41. J. W. Edington and R. E. Smallman: J. Aust. Inst. Met., 8, 1963, 8.

42. P. R. Swann: Electron Microscopy and Strength of Crystals, ed. G. Thomas and J. Washburn, New York, Interscience, 1963, 131.

43. A. Lawley and H. L. Gaigher: Appl. Phys. Letters, 2, 1963, 123.

44. D. Kuhlmann-Wilsdorf and H. G. F. Wilsdorf: Acta Met., 10, 1962, 584.

45. J. O. Stiegler, C. K. H. Dubose, R. E. Reed, Sr. and C. J. McHargue: Acta Met., 11, 1963, 851.

46. A. Berghezan: "Deformation Properties of Niobium," Plansee Proceedings, 1964.

47. A. Wronski and A. Fourdeux: J. Less-Common Metals, 7, 1964, 205.

48. A. Gilbert, B. A. Wilcox and G. T. Hahn: Phil. Mag., 12, 1965, 649.

49. A. Lawley and H. L. Gaigher: Phil. Mag., 10, 1964, 15.

50. D. F. Stein: Acta Met., 14, 1966, 99.

51. A. Lawley: Electron Beams, Ed. R. Bakish, John Wiley & Sons, New York, 1962.

52. D. R. Hay and E. Scala: Report No. 250, The Materials Science Center, Cornell University, Ithaca, New York.

53. I. Drangel, P. McMahon and S. Weinig: "Sixth Alloyd Electron Symposium", 1964.

54. E. Voltava: Phys. Stat. Sol., 5, 1964, 427.

55. A. Seeger: Dislocations and Mechanical Properties of Crystals, John Wiley and Sons, New York, 1956, 243.

56. Z. S. Basinski: Phil Mag., 4, 1959, 393.

57. P. B. Hirsch: The Relation Between Structure and Mechanical Properties of Metals, Teddington Conf., 1963, 39.

58. M. Ahlers: Z. Metallkde., 55, 1965, 741.

59. A. Lawley and H. L. Gaigher: Phil. Mag., 8, 1963, 1713.

60. S. W. Sleeswyk: Phil. Mag., 8, 1963, 1467.

61. P. B. Hirsch: Fifth International Congress of Crystallograph, Cambridge, 1960.

62. T. E. Mitchell, R.A. Foxall and P. B. Hirsch: W.A.D.D. Technical Report Contract No. AF 33(616)-6838, 1963.

63. G. T. Hahn, A. Gilbert and R. I. Jaffee: DMIC Memorandum 155, Battelle Memorial Inst., Columbus, Ohio, 1962.

64. R. N. Orava: Trans. Met. Soc. AIME, 230, 1964, 1614.

65. C. N. Reid, A. Gilbert and A. R. Rosenfield: Phil. Mag., 12, 1965, 649.

66. J. T. Michalak: Acta Met., 13, 1965, 213.

ACKNOWLEDGEMENTS

The author wishes to gratefully acknowledge and thank Dr. Franz R. Brotzen, Dean of Engineering, Rice University, for his advice, assistance and encouragement throughout the course of this project. The author also desires to thank the following who contributed substantially to this project:

Dr. M. L. Rudee and Dr. J. M. Roberts of the Mechanical and Aerospace Engineering and Material Science Department, Rice University, for their numerous suggestions and stimulating discussions.

Dr. H. E. Rorschach, Physics Department, Rice University, for his help and advice on certain experimental procedures.

Mr. W. Ruska, Chemical Engineering Department, Rice University, for designing the electron-beam zone refiner which was used to grow some of the single crystals.

Messrs. R. G. Guidry, J. A. Ehlert, H. L. Hales, J. M. Chappell, C. R. Martin, D. F. James and R. Martin for their efforts in the construction of certain portions of the apparatus.

Messrs. J. Hansberry, R. Eanes and G. Forristall for helpful assistance in growing and orienting single crystals and in fabricating apparatus.

Miss Leona Hoop, Mechanical and Aerospace Engineering and Material Science Department, and Mrs. C. Lopez, secretary to the Dean of Engineering, Rice University, for their aid in administrative procedures.

The National Aeronautics and Space Administration for its grant, #NsG-6-59, under which a majority of this work was performed.

Mrs. W. Goldston for financial assistance in the form of a two year fellowship.

Mr. and Mrs. J. D. Richardson and Mr. and Mrs. E. R. Whitmire for their countinued encouragement and financial assistance.

My wife, Rilda Whitmire, for her encouragement and assistance throughout the course of this project.

APPENDIX

All of the results obtained in the present tests are catalogued in this appendix according to the following system:

I. Stress-Strain Curves

A. Curves determined at the slow strain-rate.

1. 78 ^{o}K
2. 200 ^{o}K
3. 250 ^{o}K
4. 300 ^{o}K
5. 350 ^{o}K
6. 400 ^{o}K

(By increasing $R_{273/4.2}$ ratio at each temperature)

B. Curves determined at the high strain-rate.

1. 200 ^{o}K
2. 250 ^{o}K
3. 300 ^{o}K
4. 350 ^{o}K
5. 400 ^{o}K

(By increasing $R_{273/4.2}$ ratio at each temperature)

II. Activation Volume Curves

1. 200 ^{o}K
2. 250 ^{o}K
3. 300 ^{o}K
4. 350 ^{o}K
5. 400 ^{o}K

(By increasing $R_{273/4.2}$ ratio at each temperature)

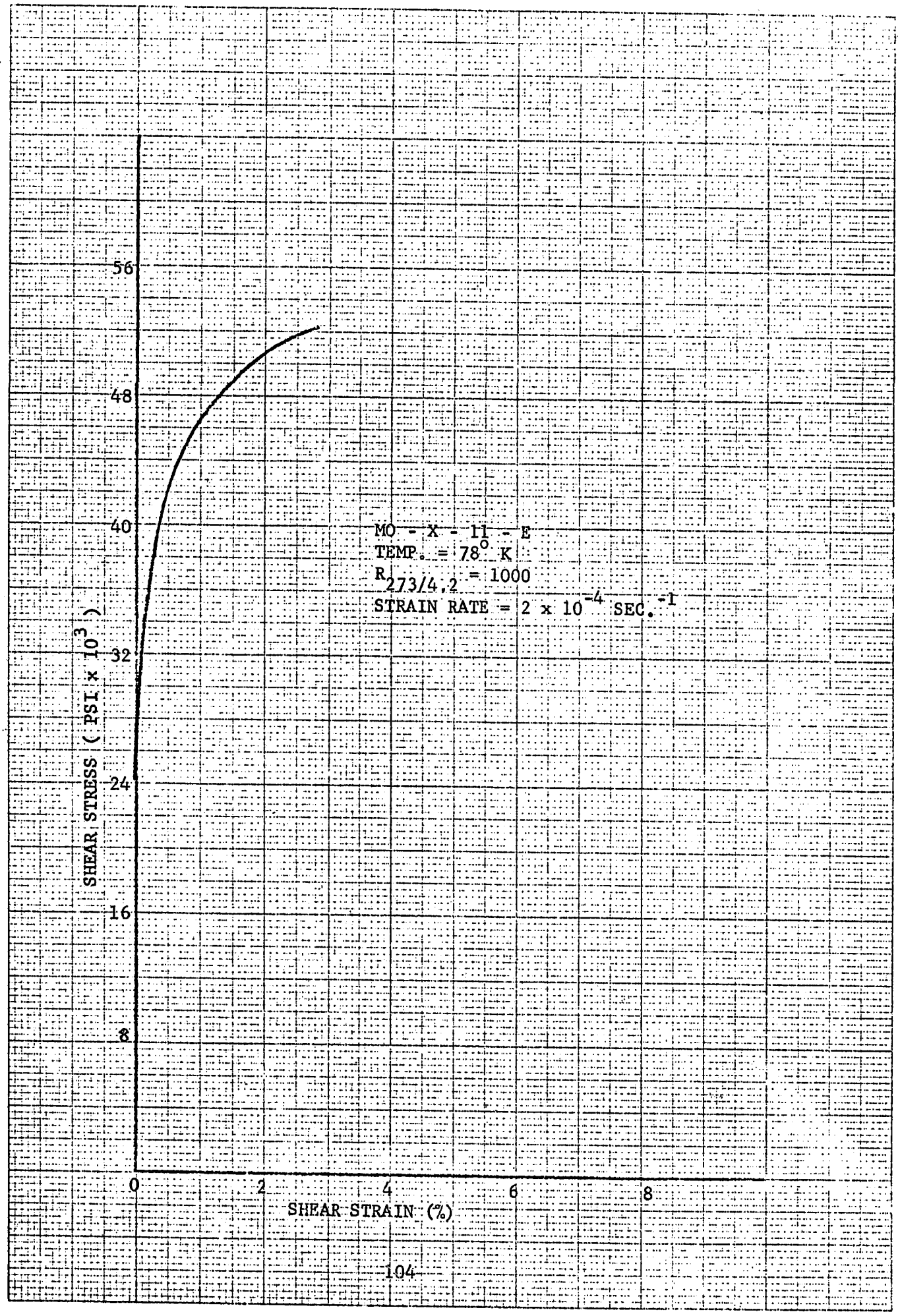

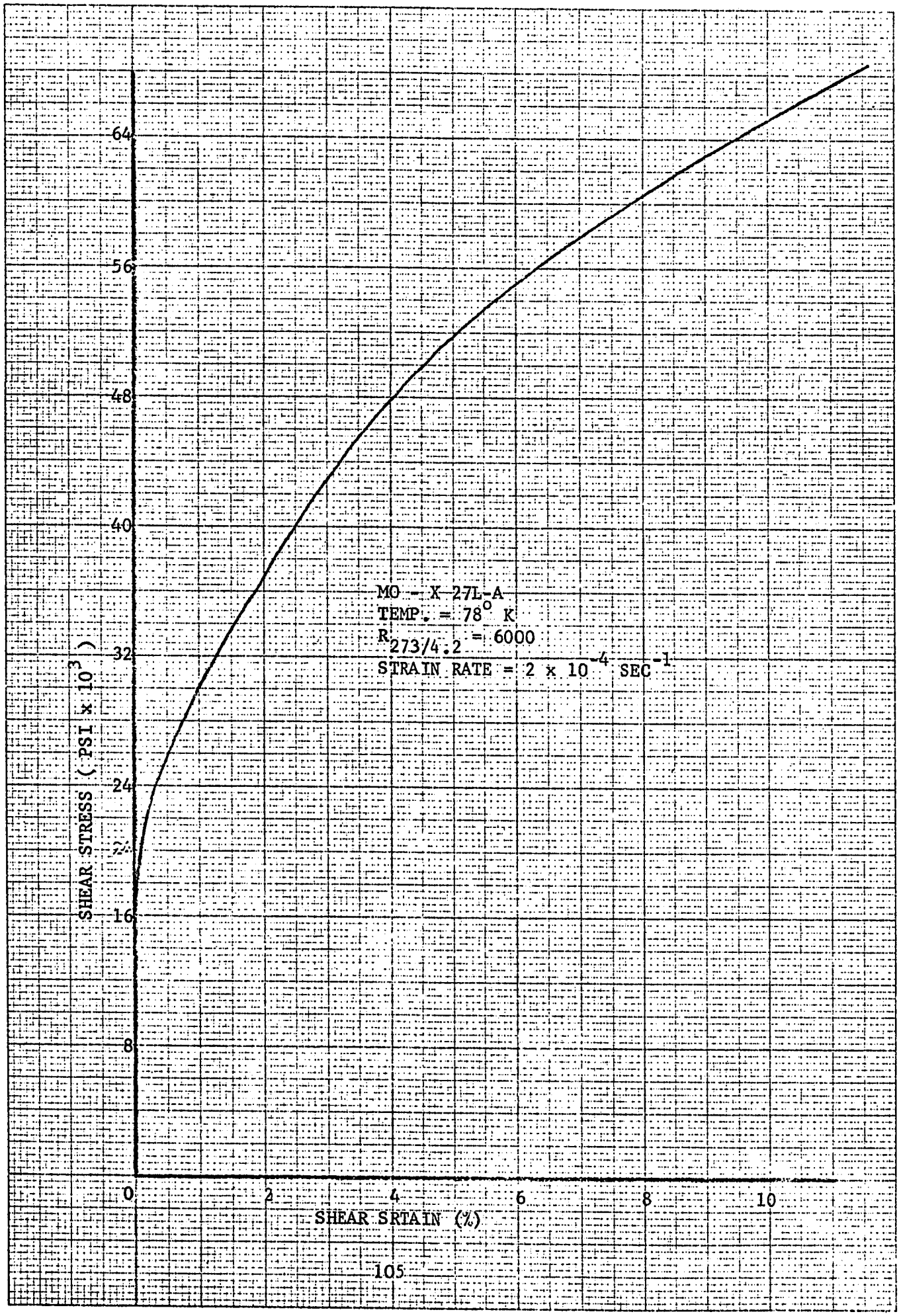

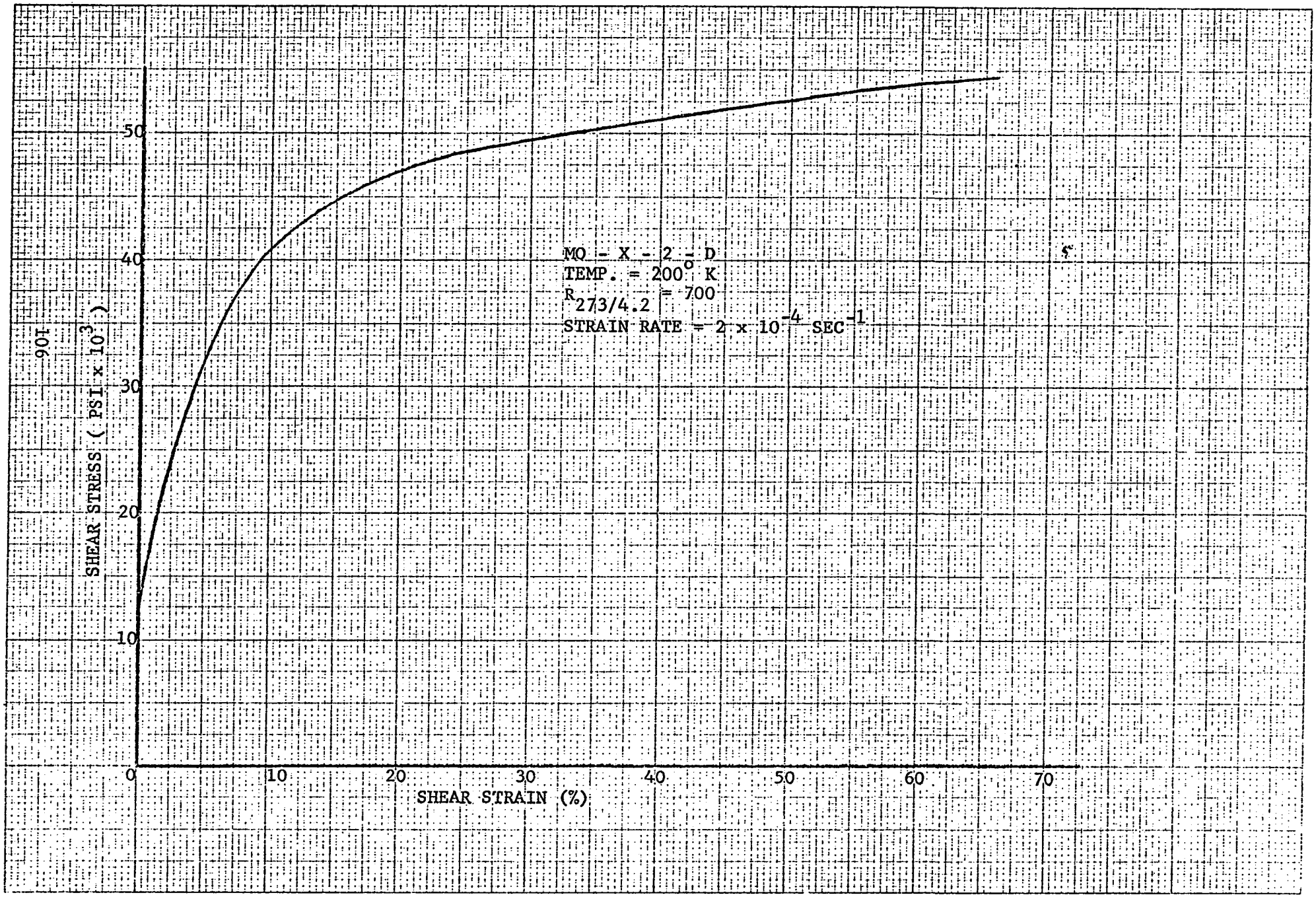

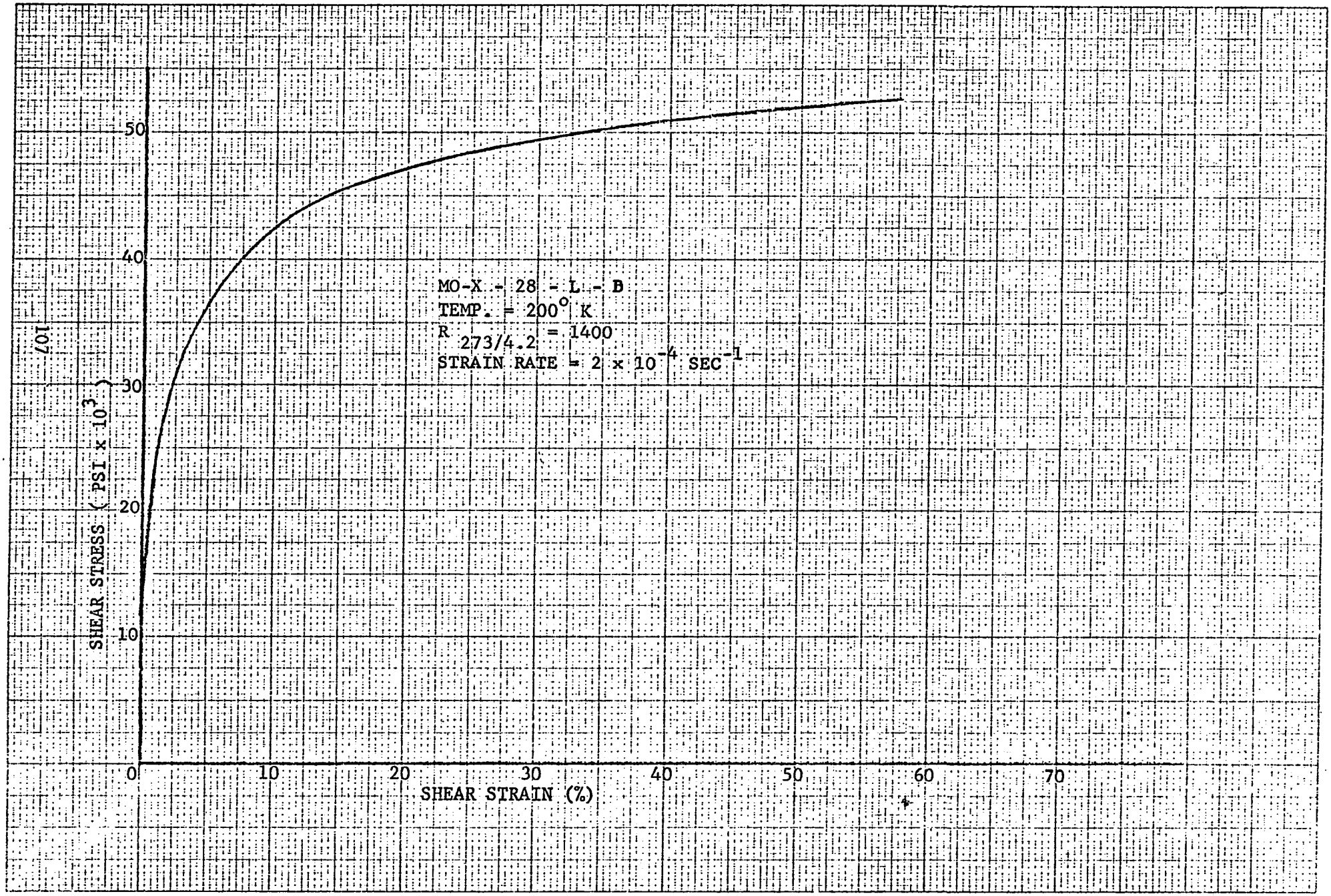

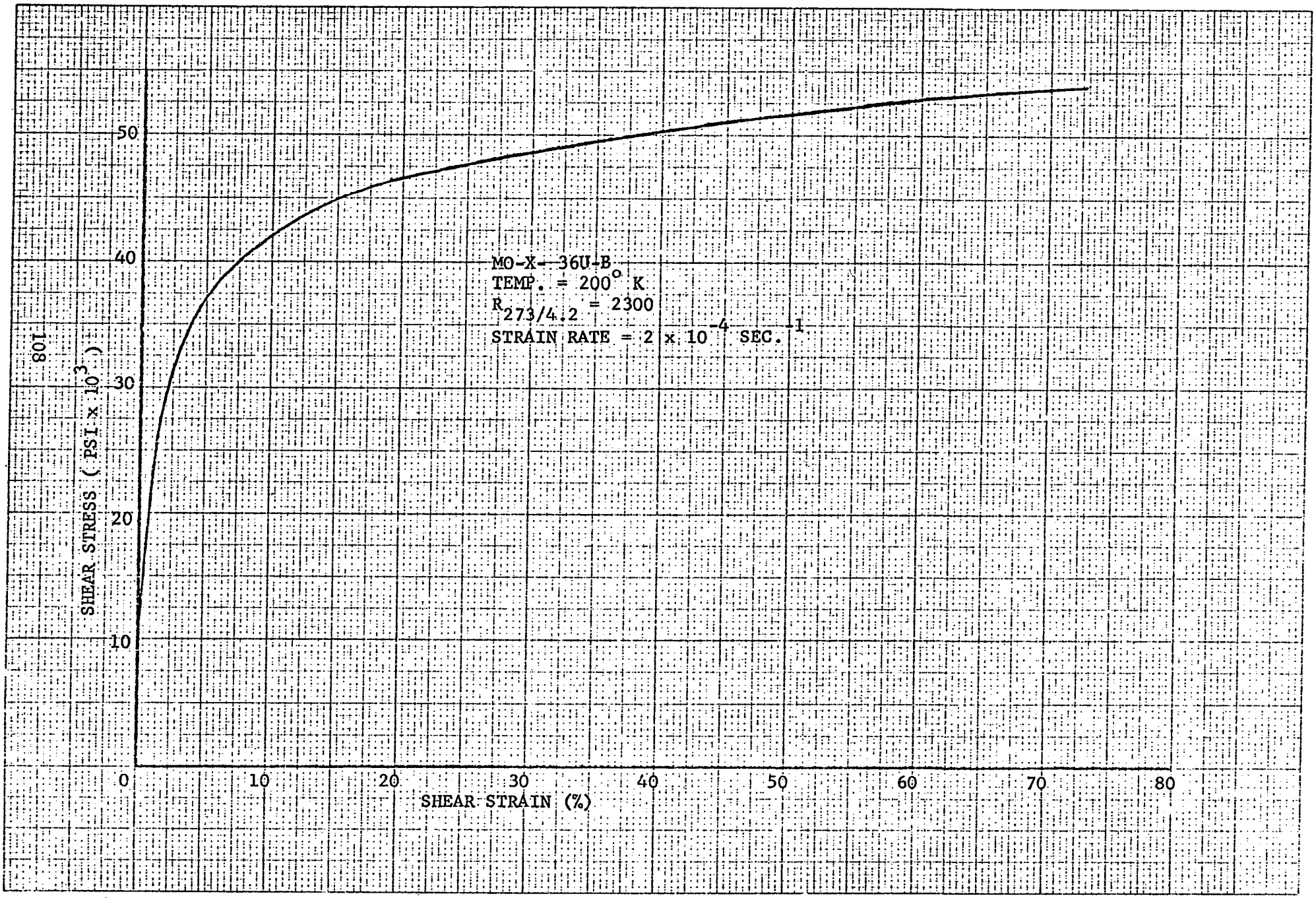

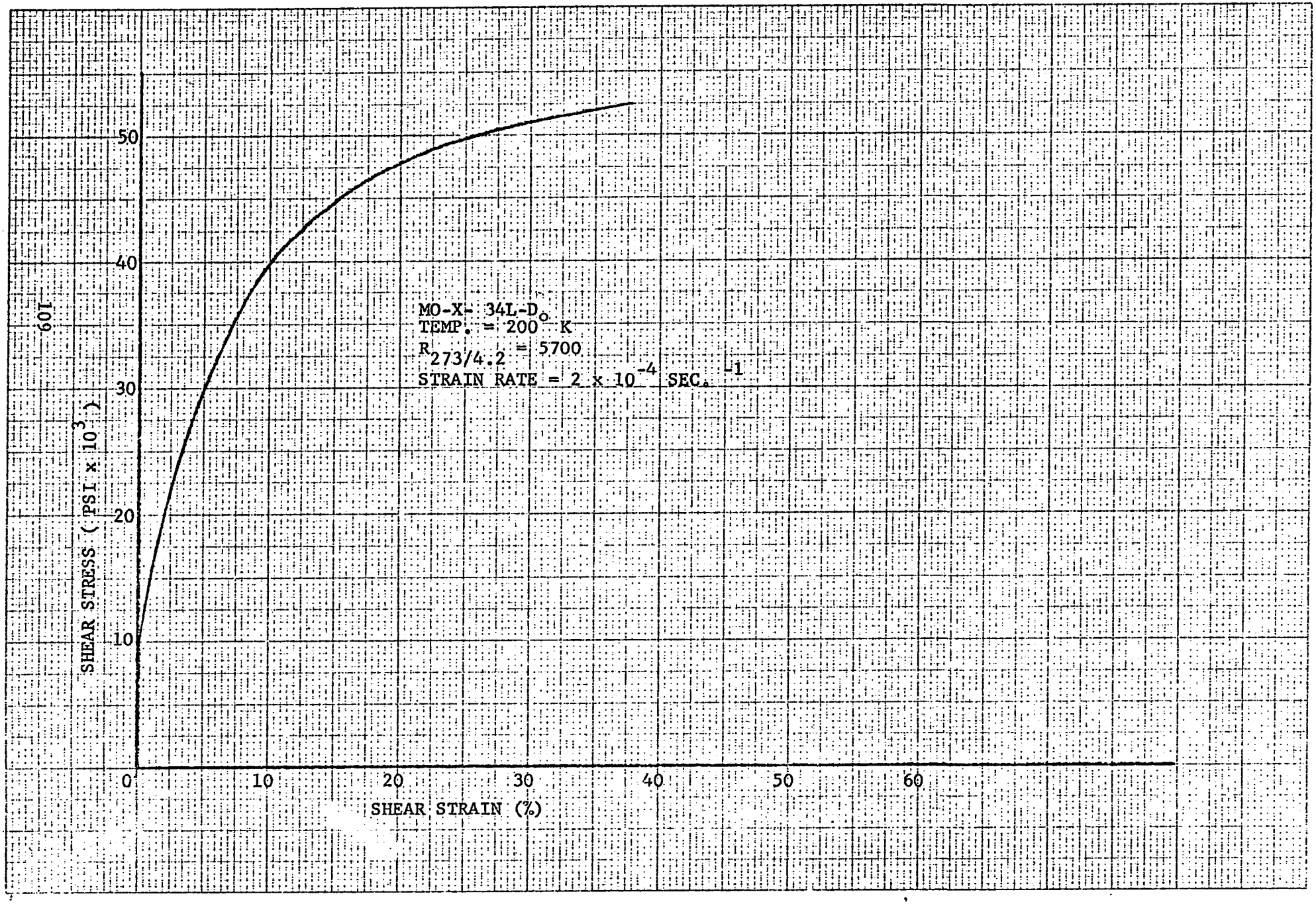

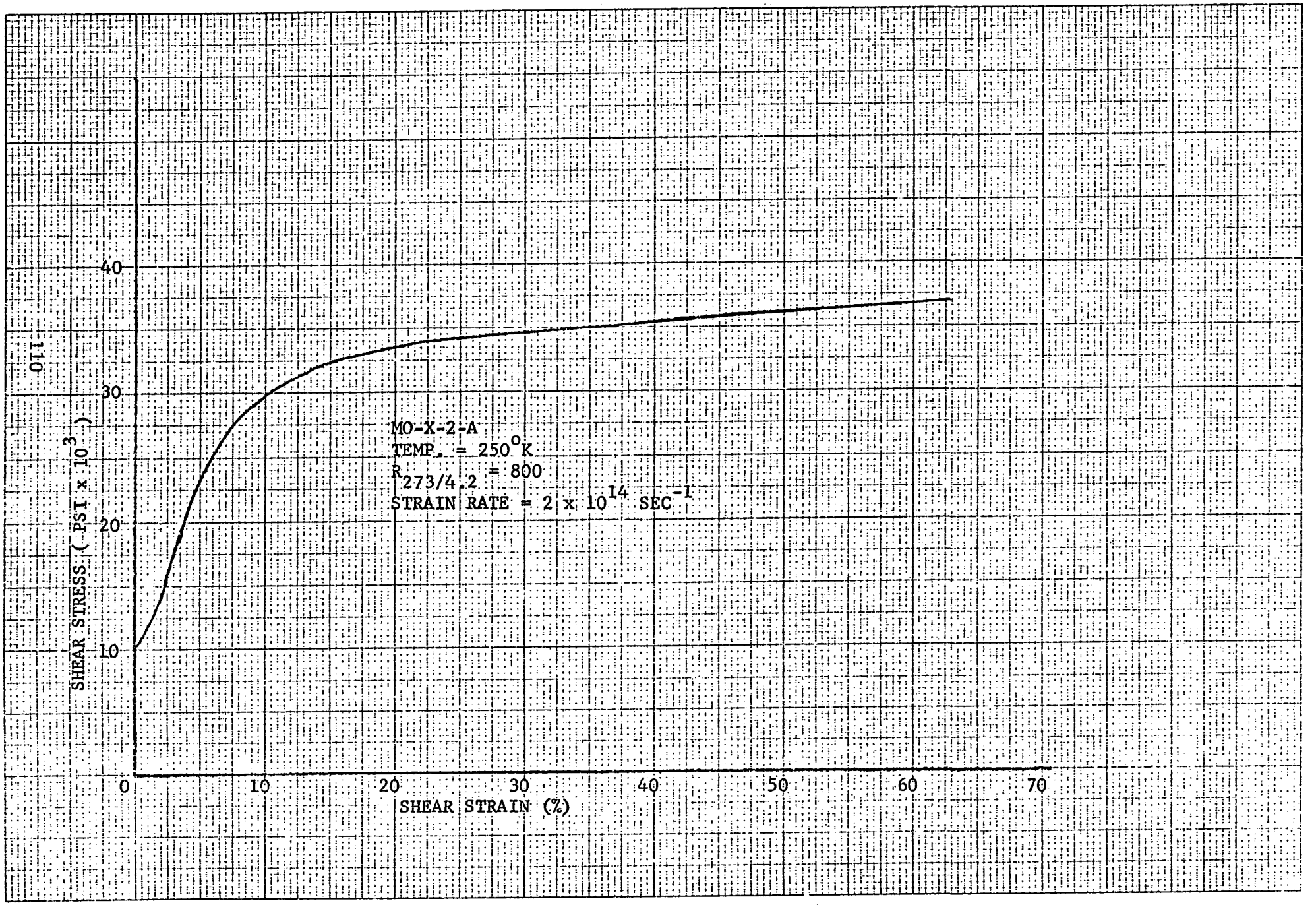

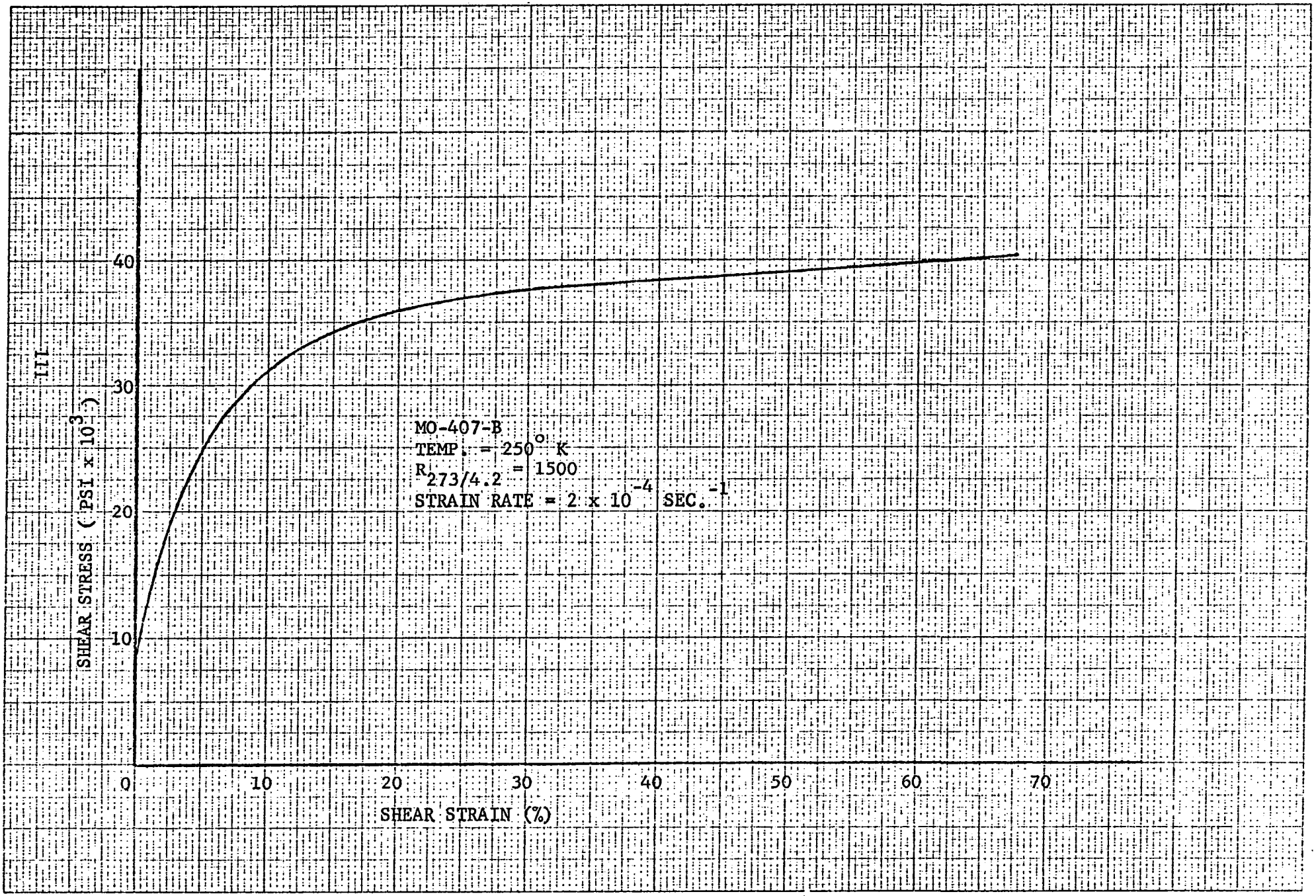

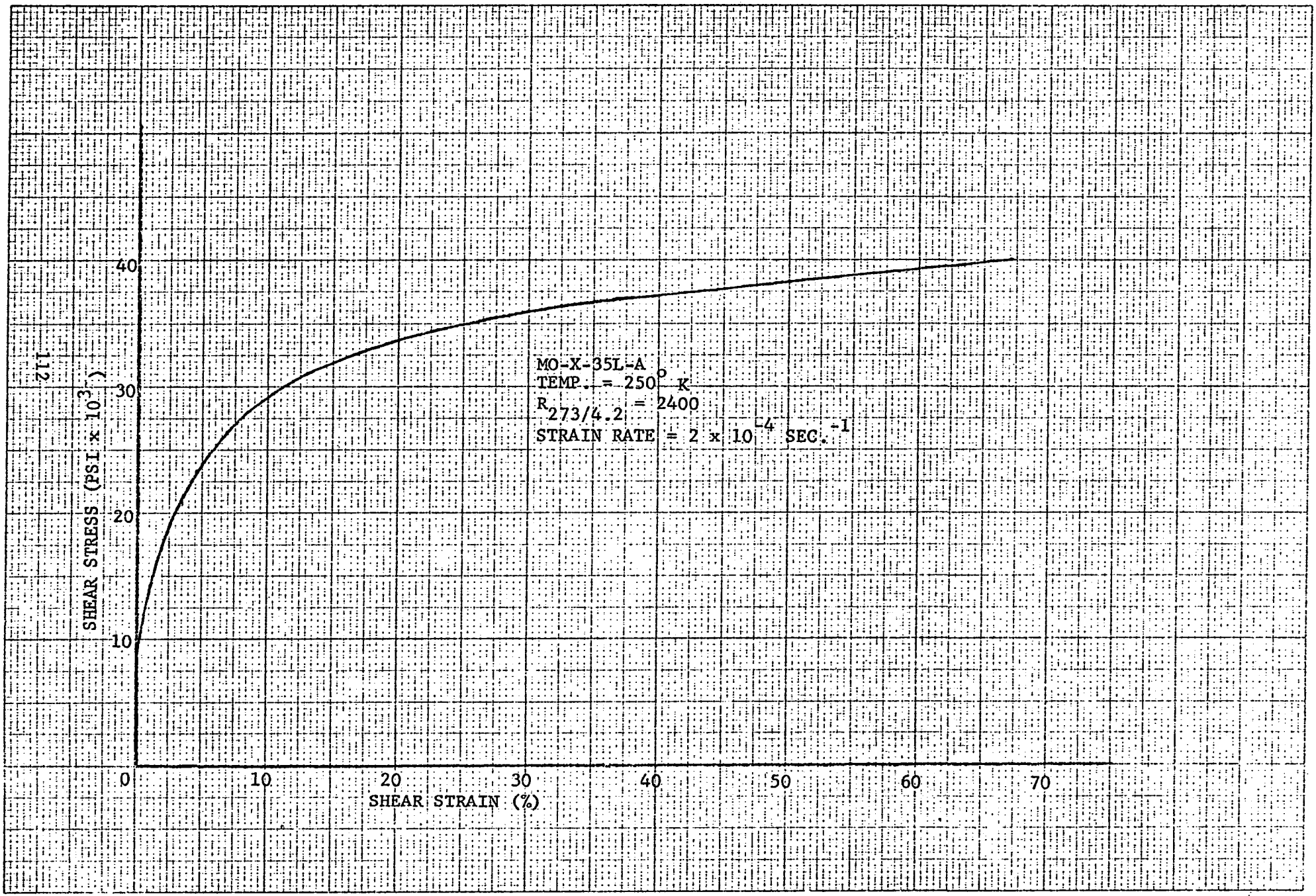

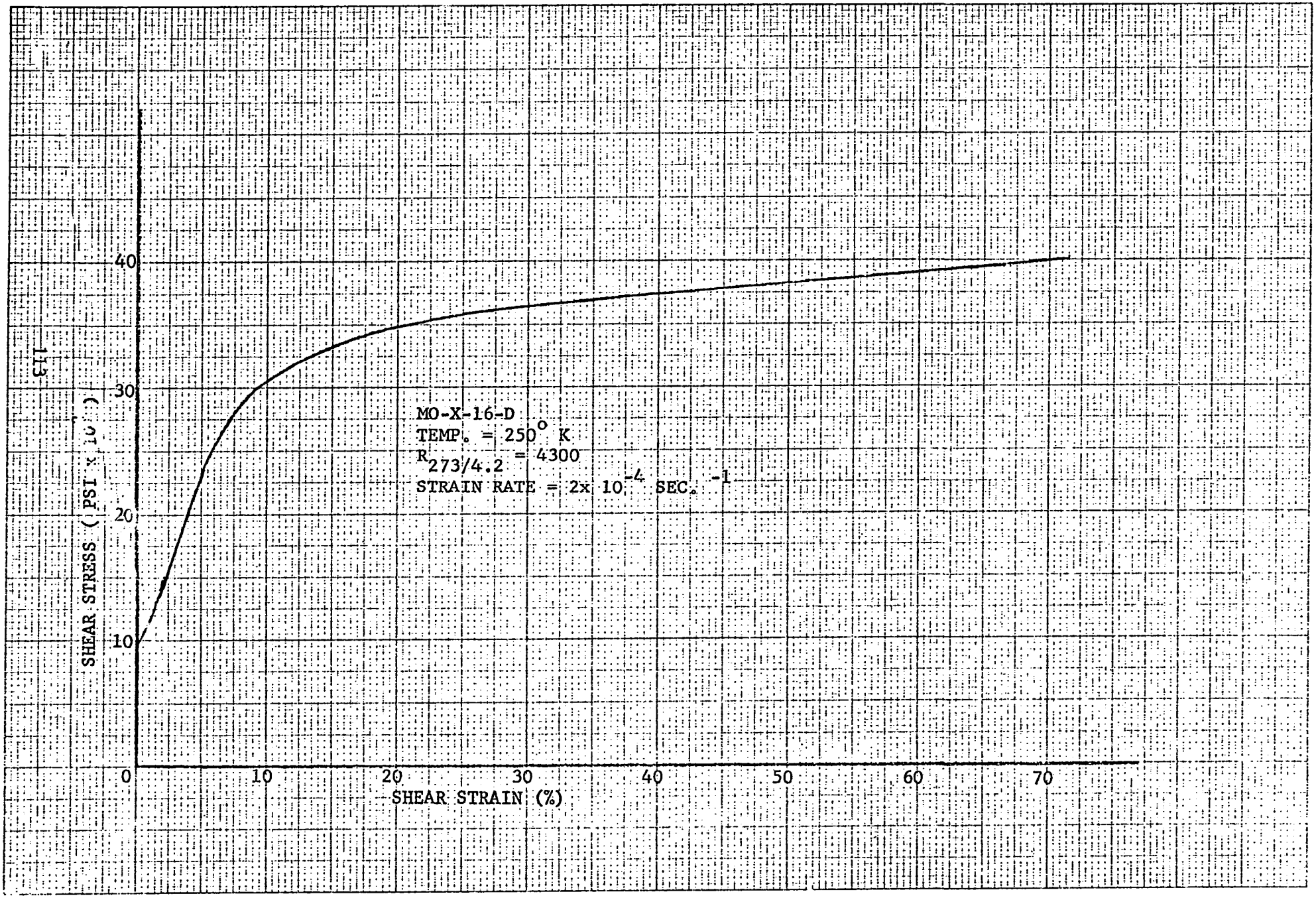

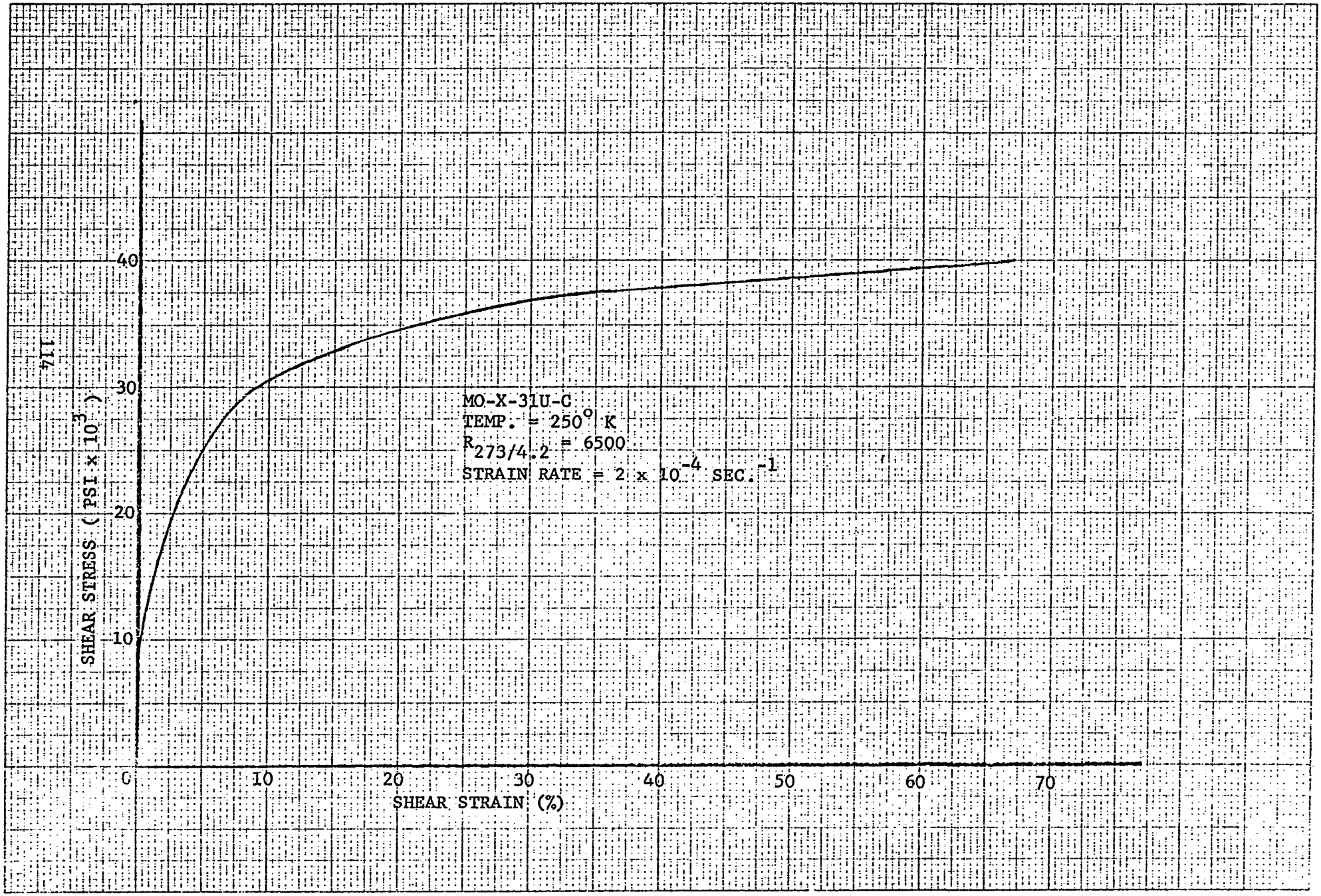

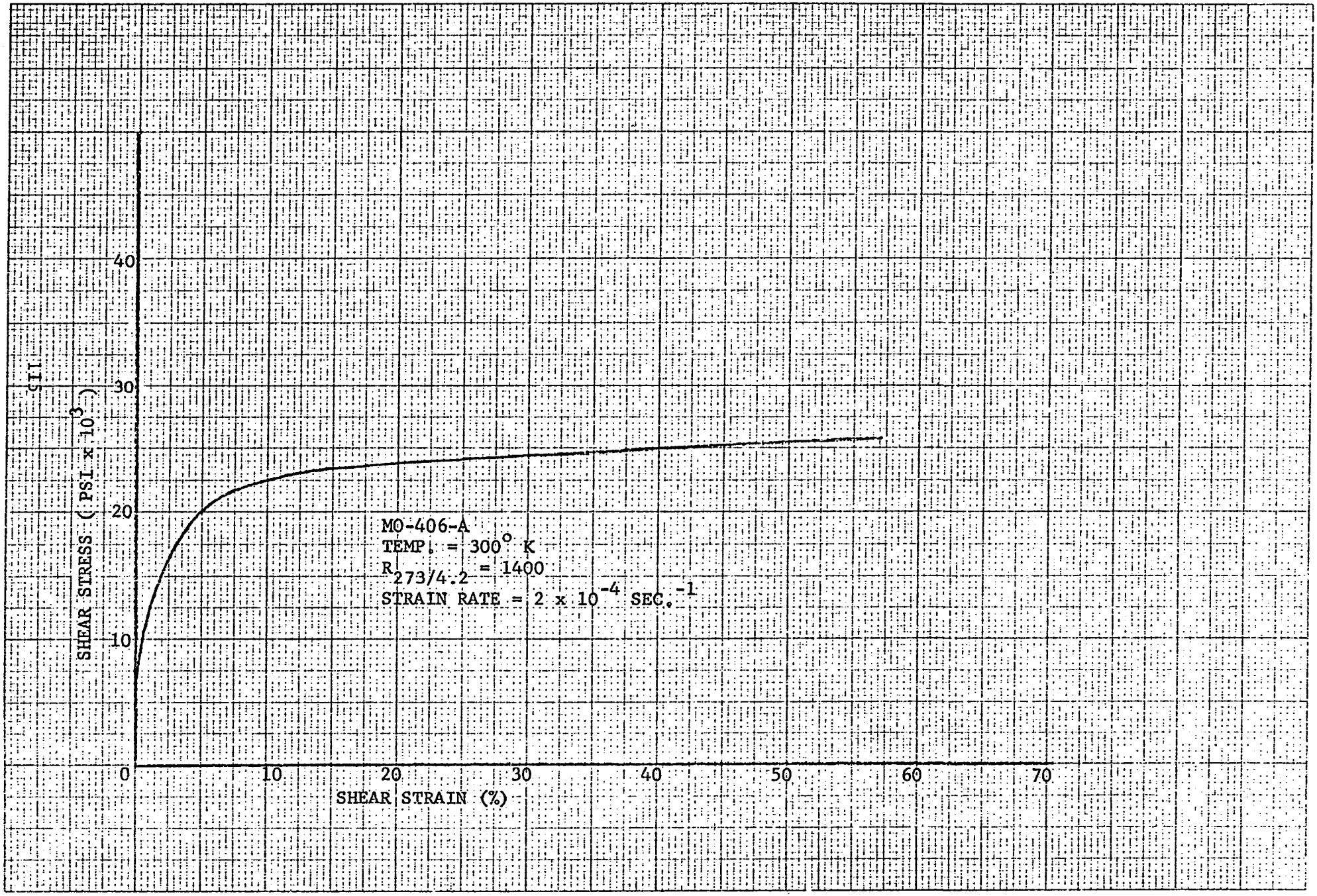

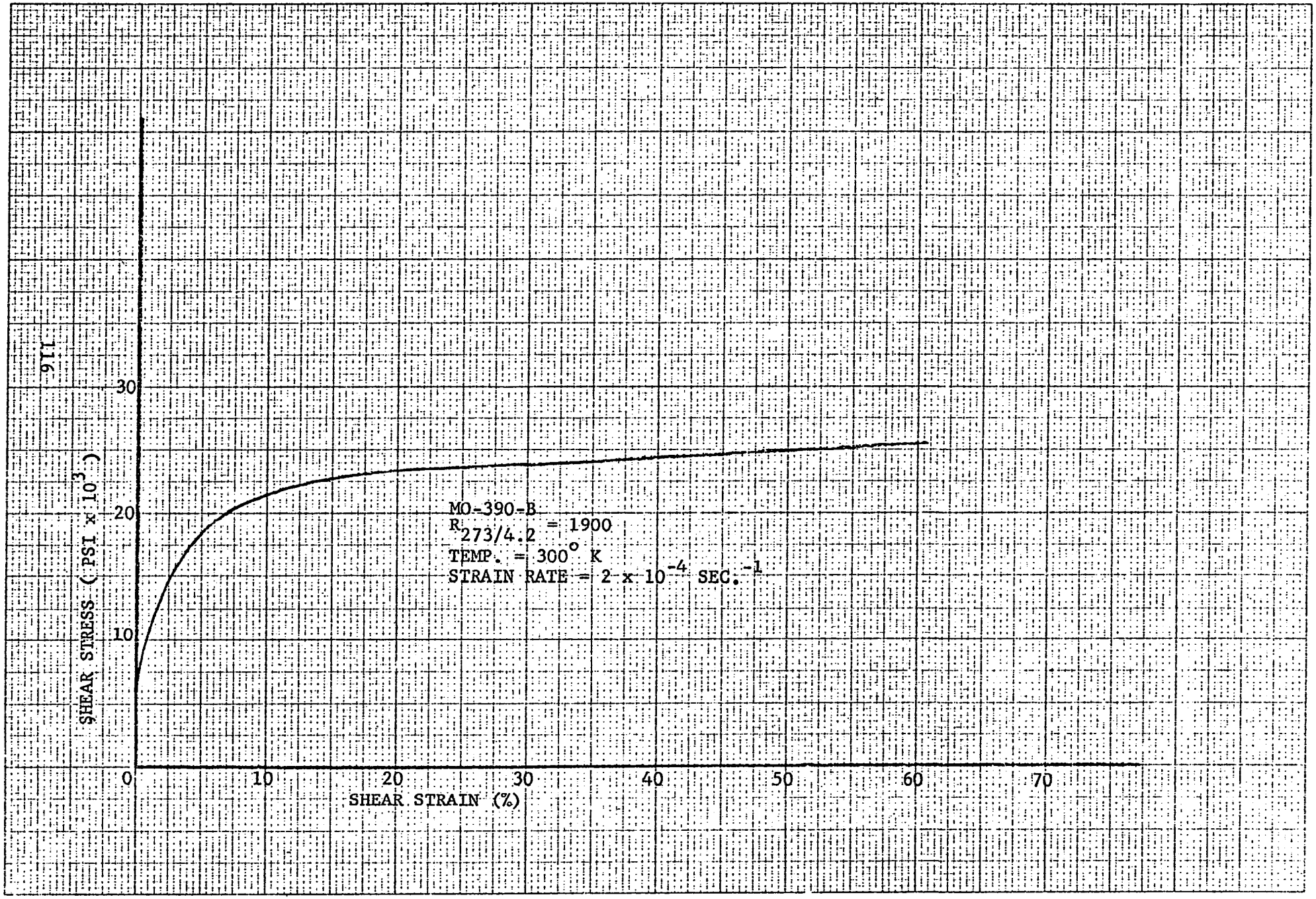

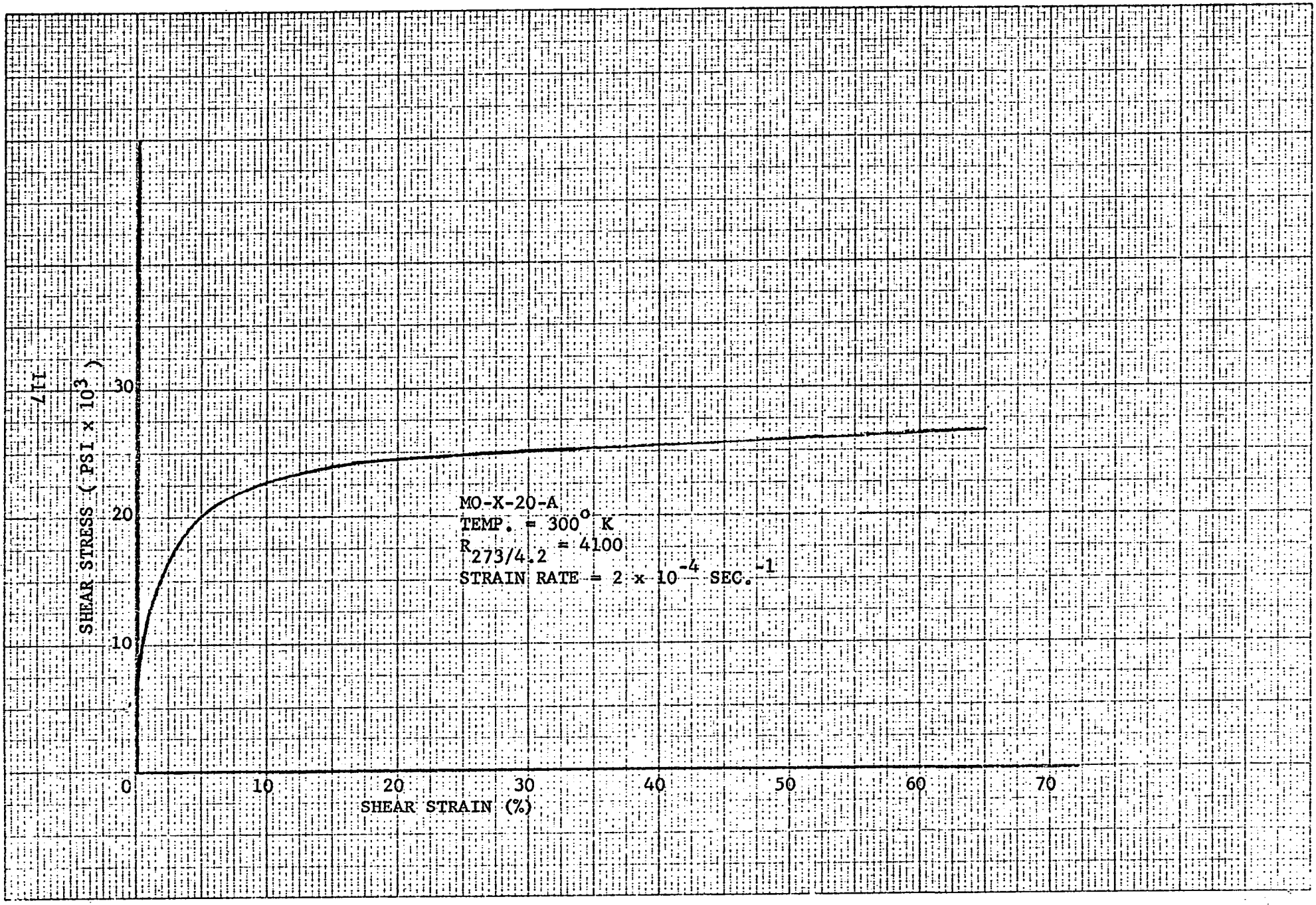

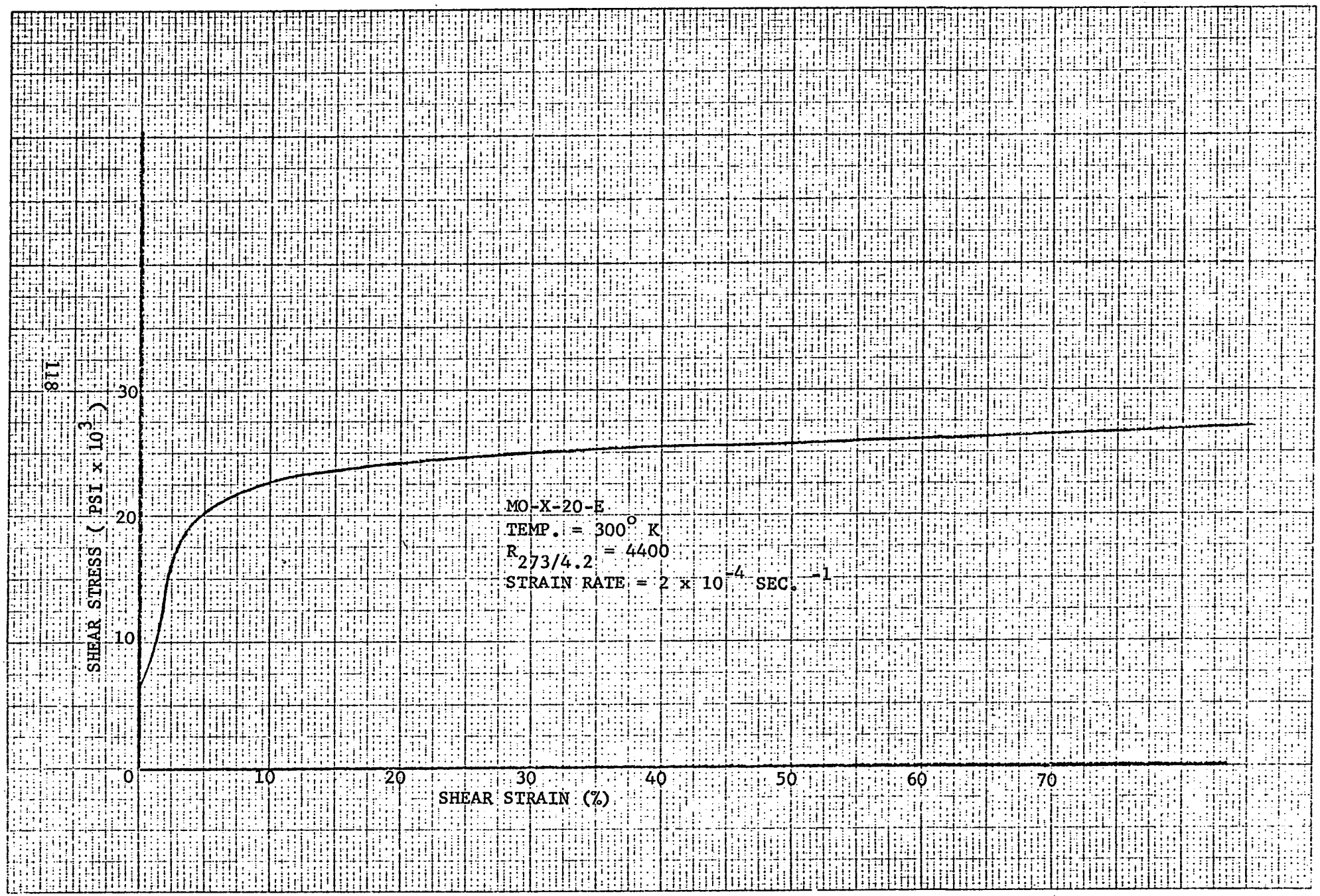

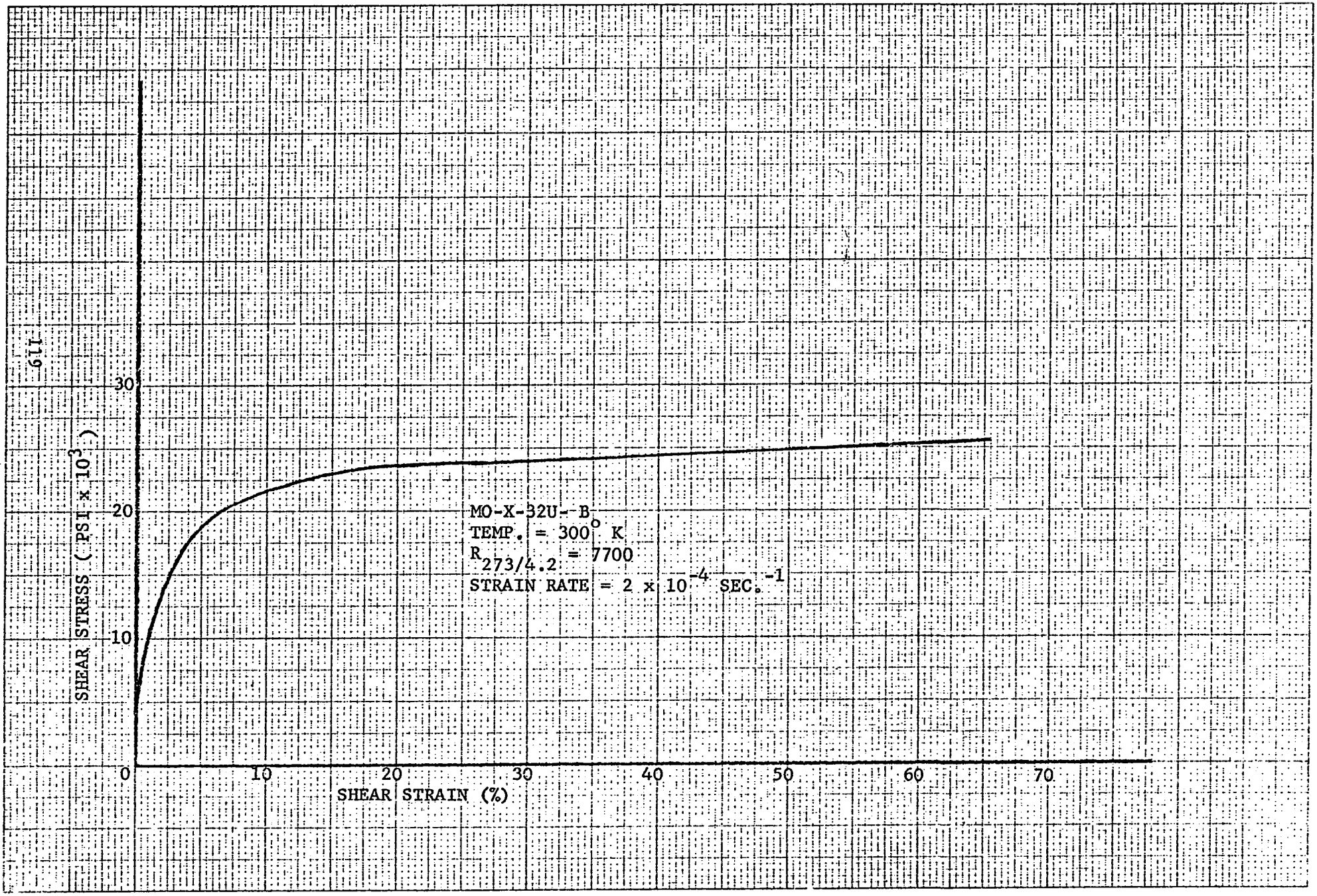

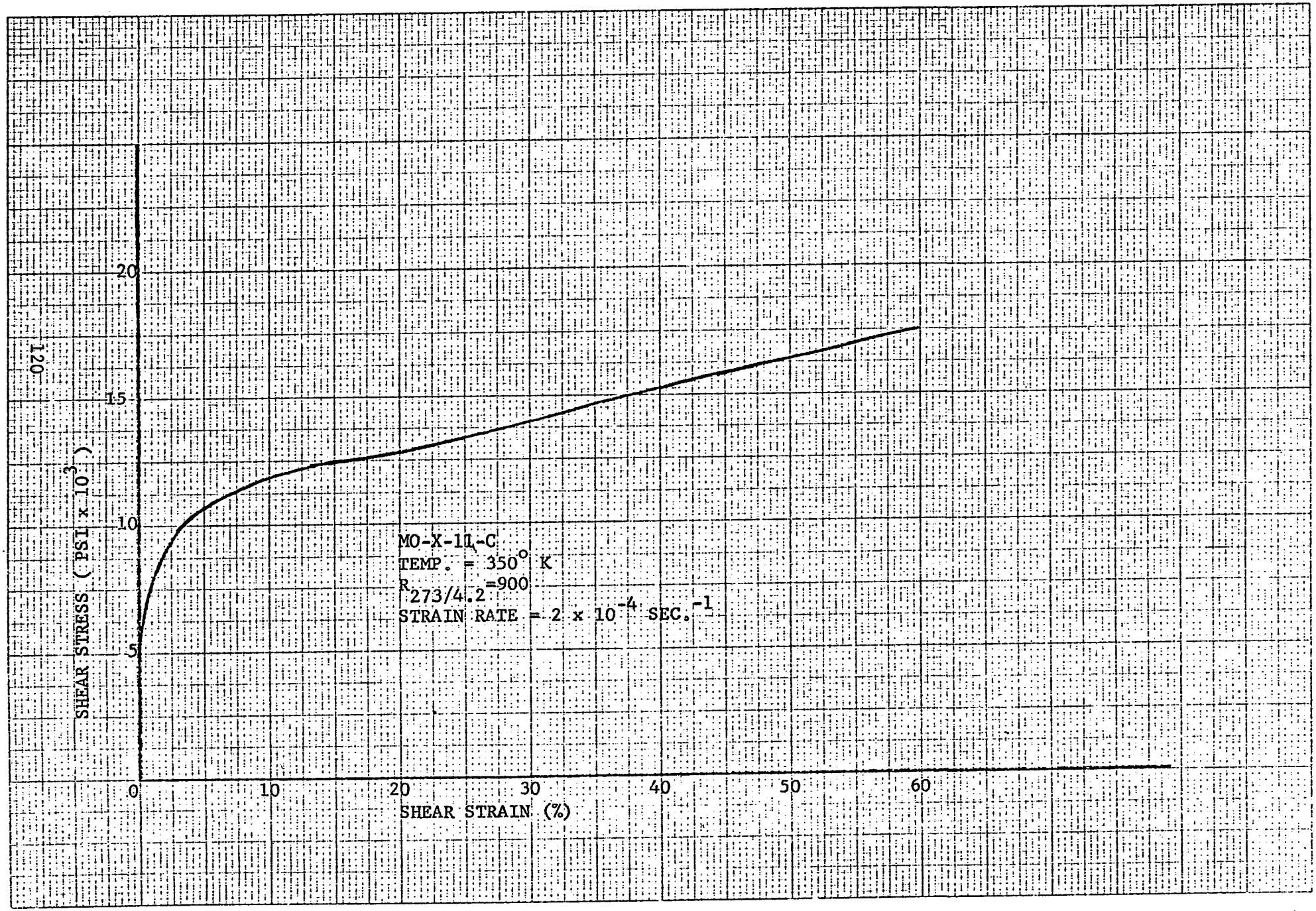

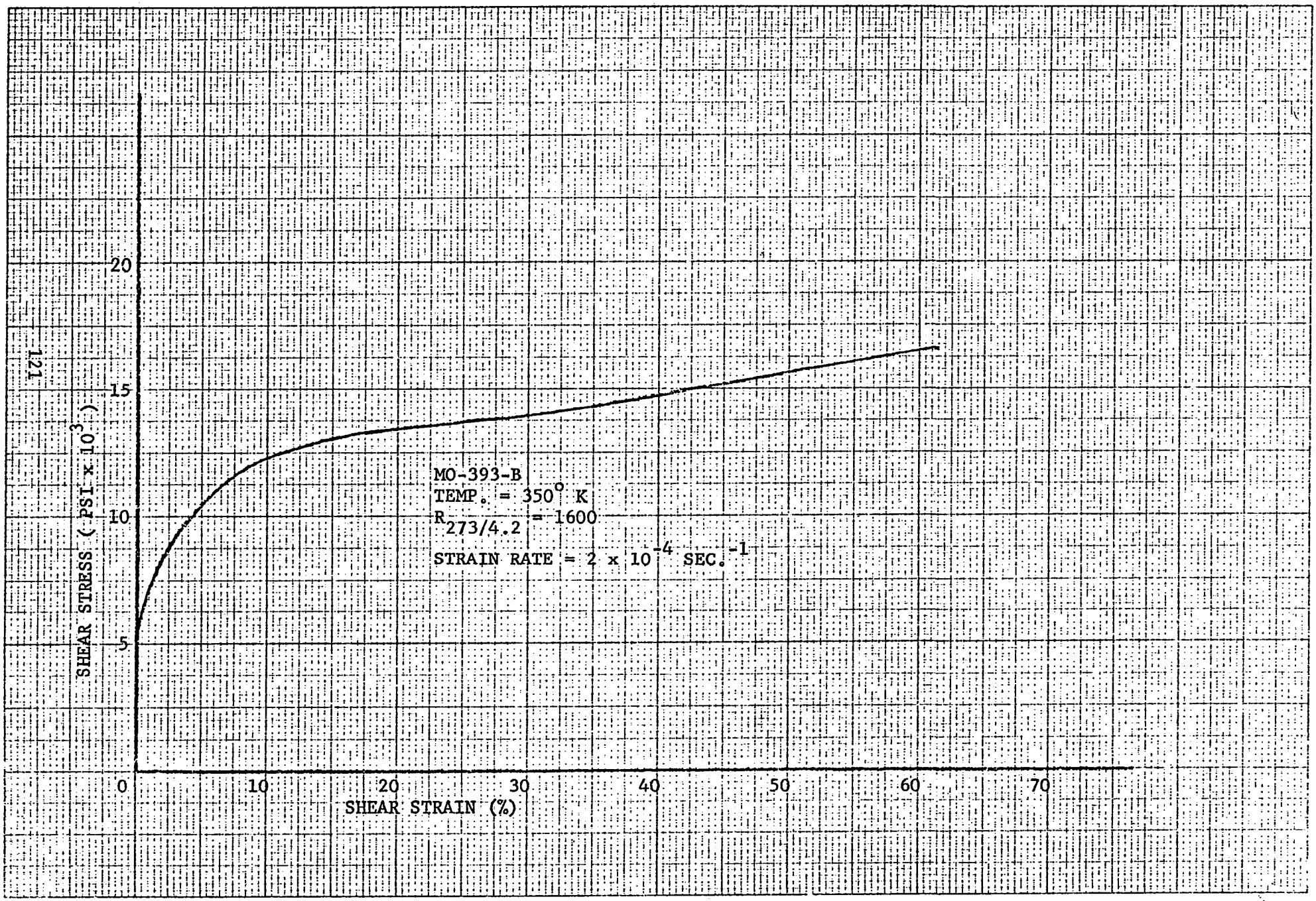

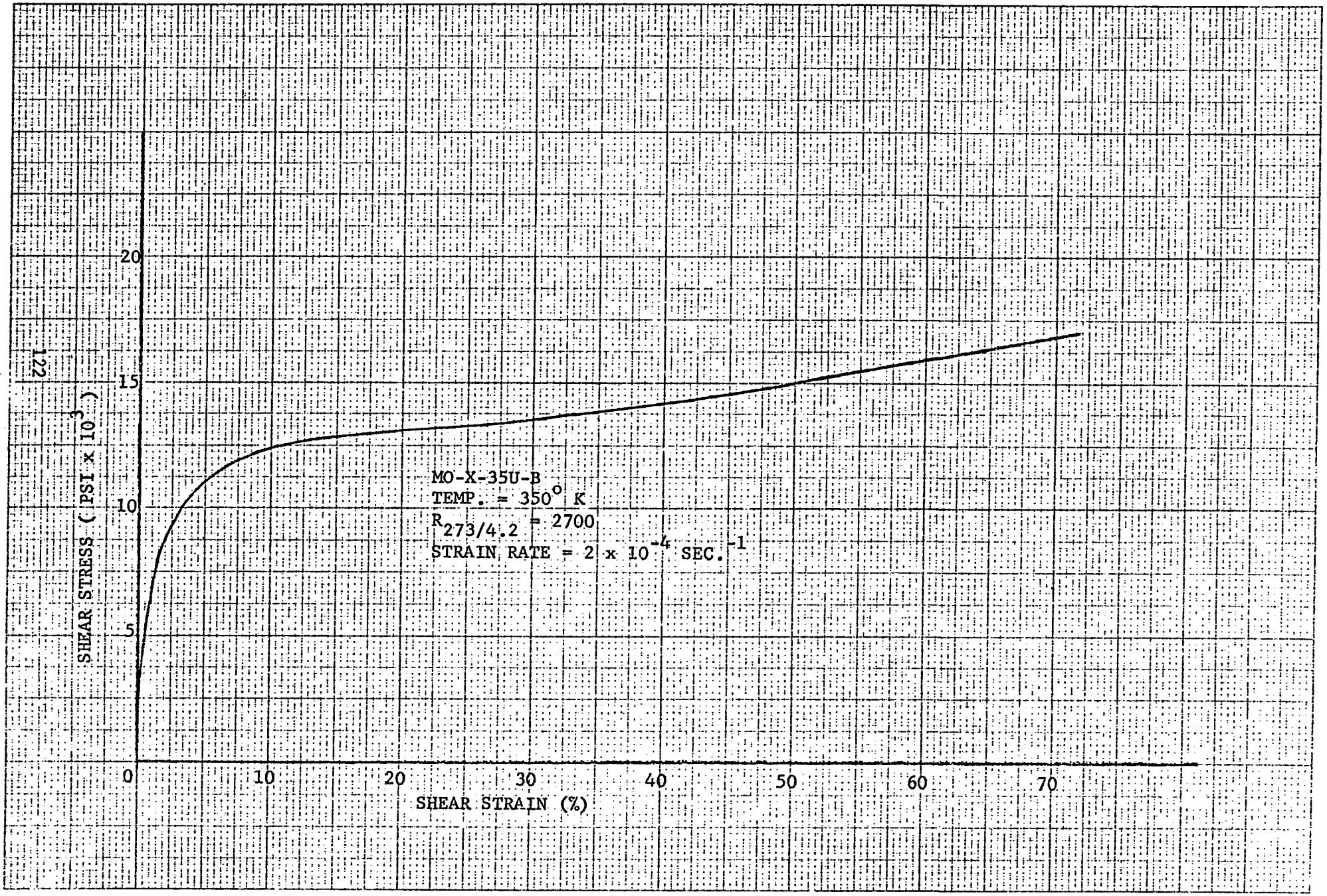

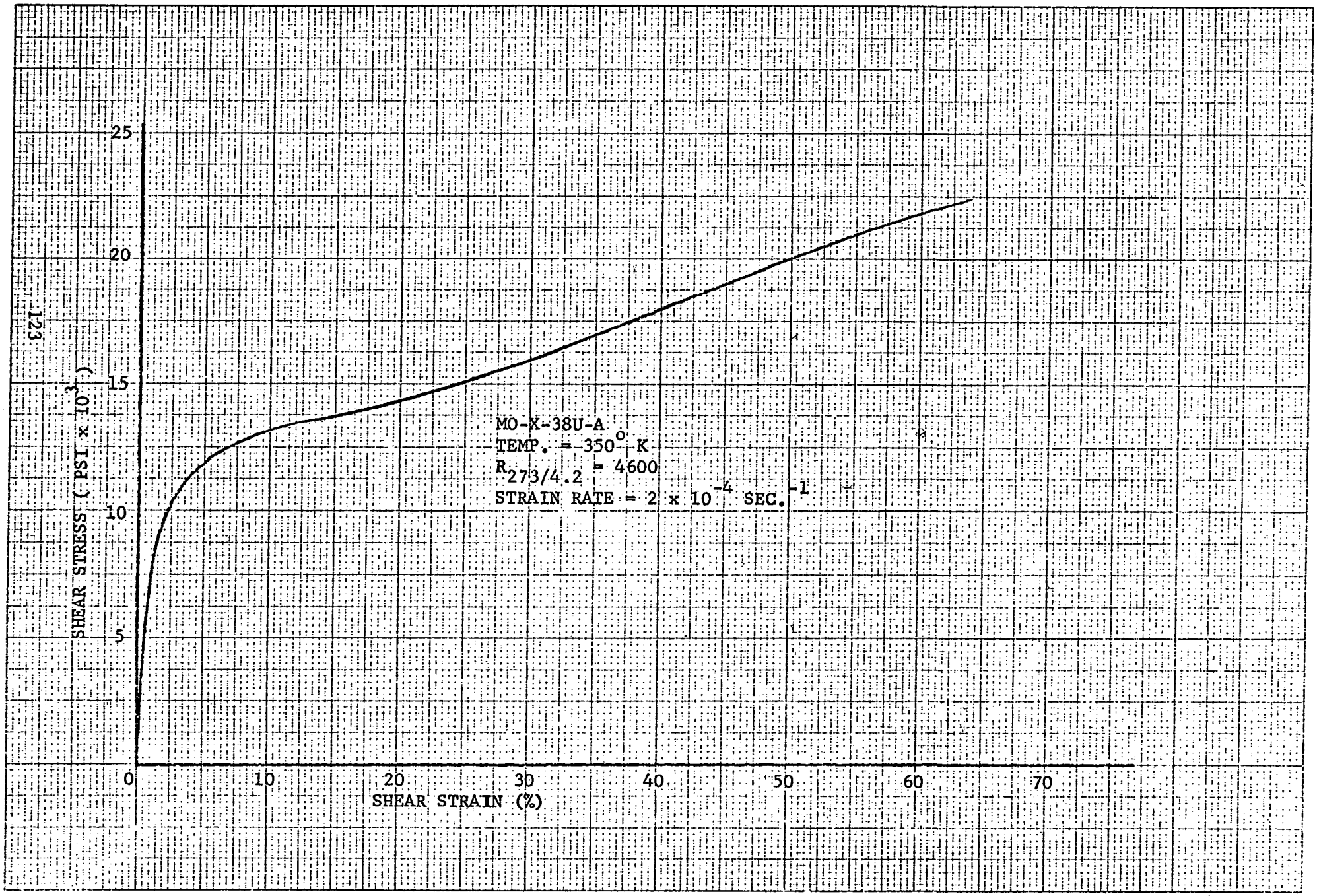

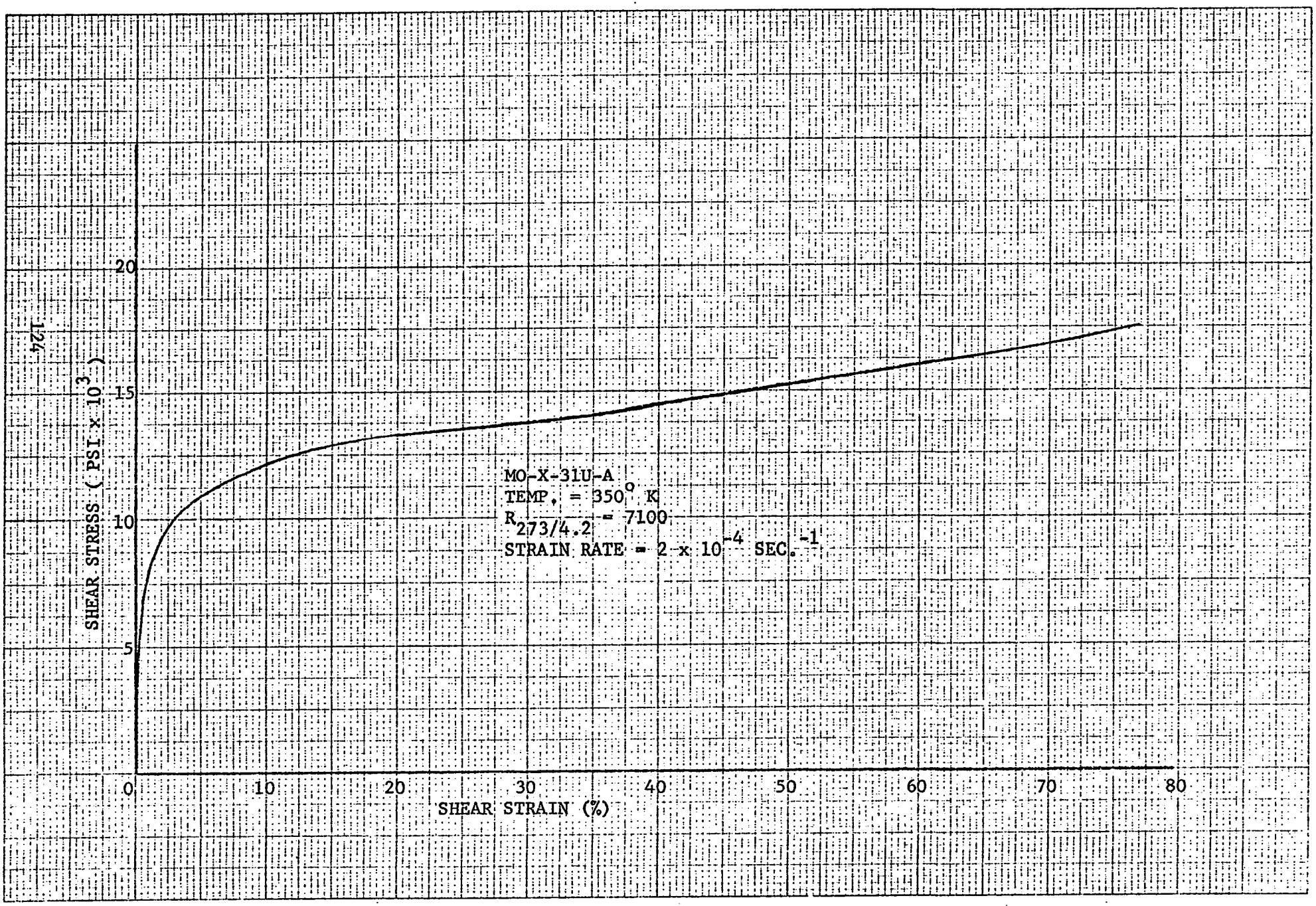

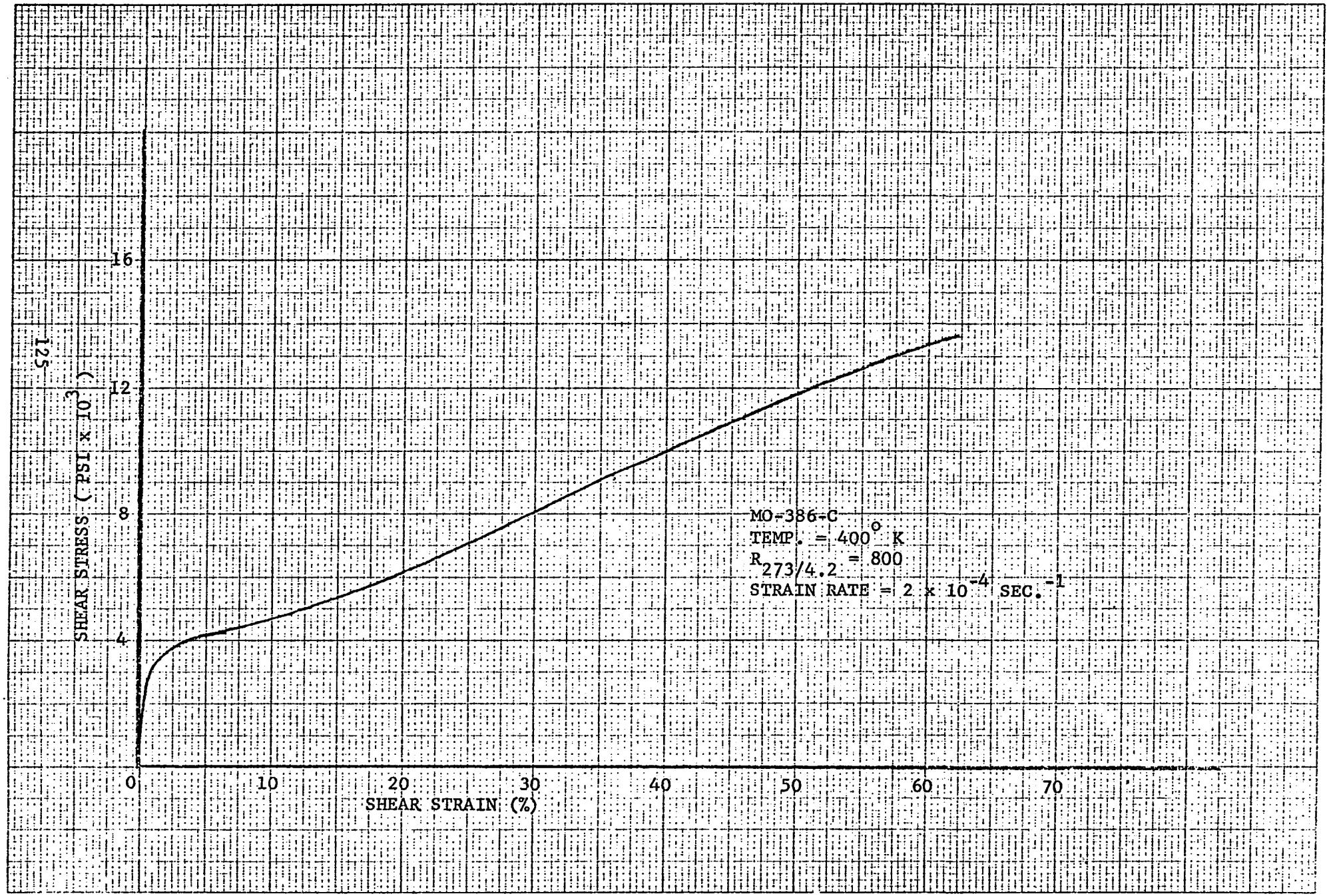

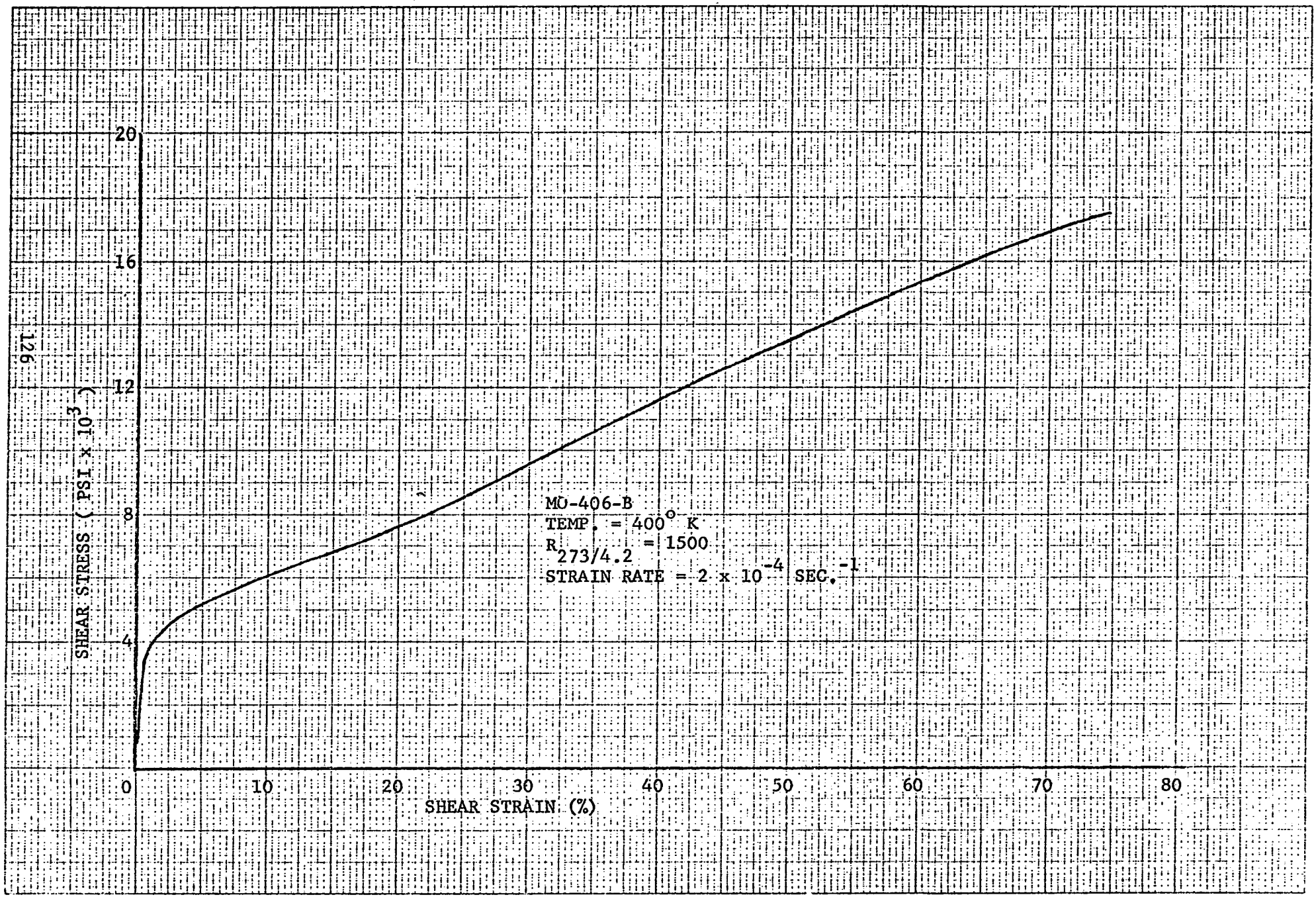

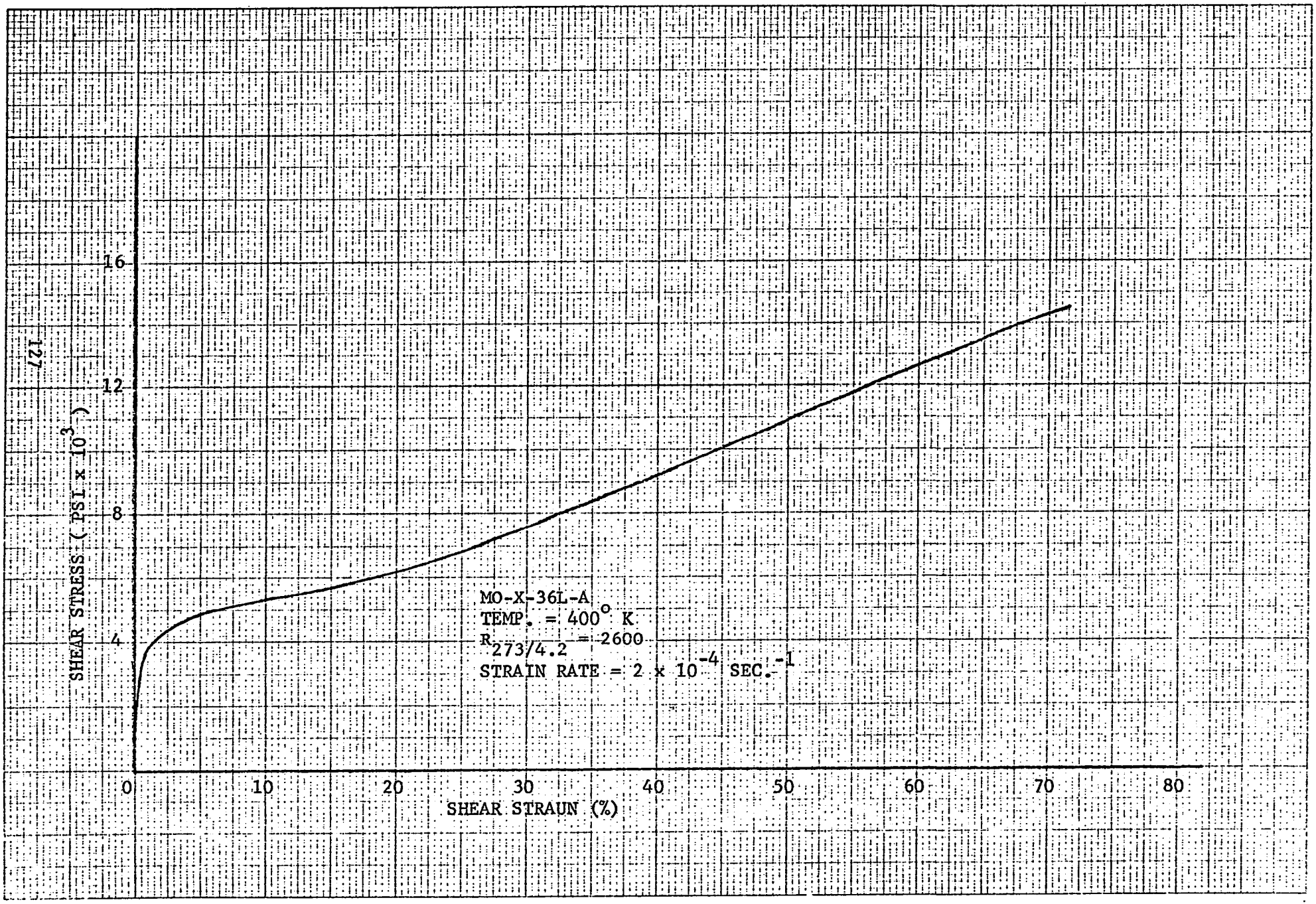

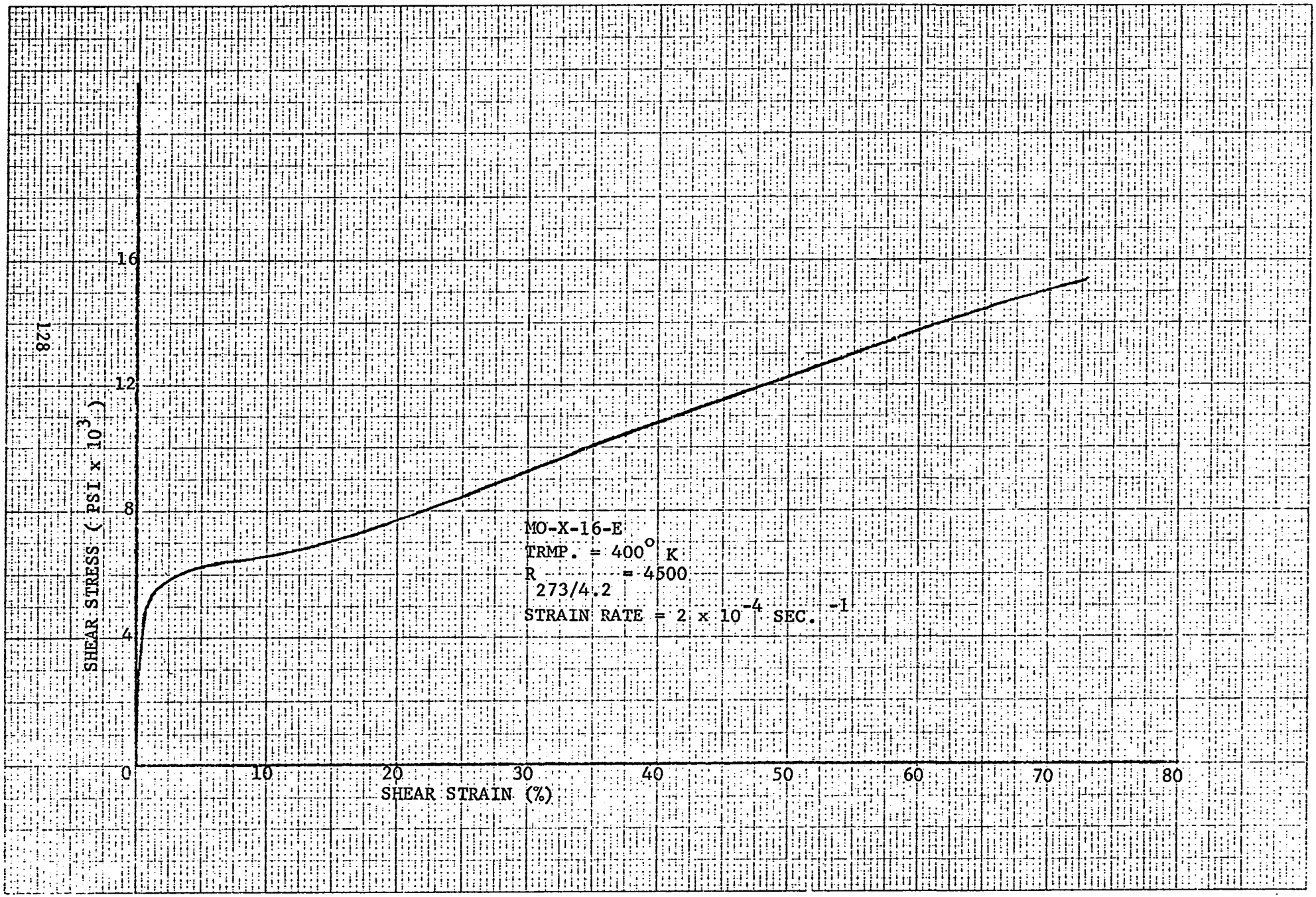

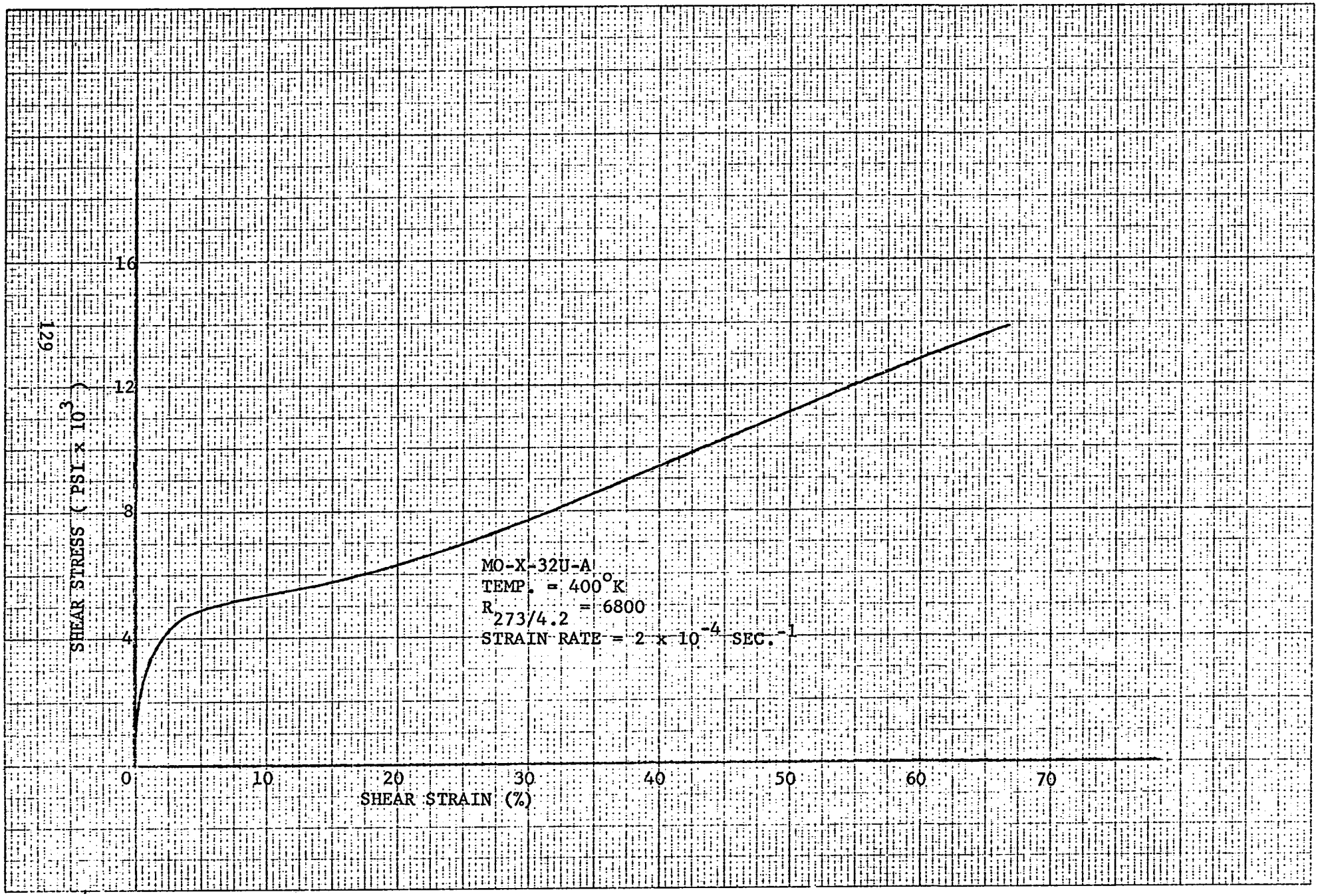

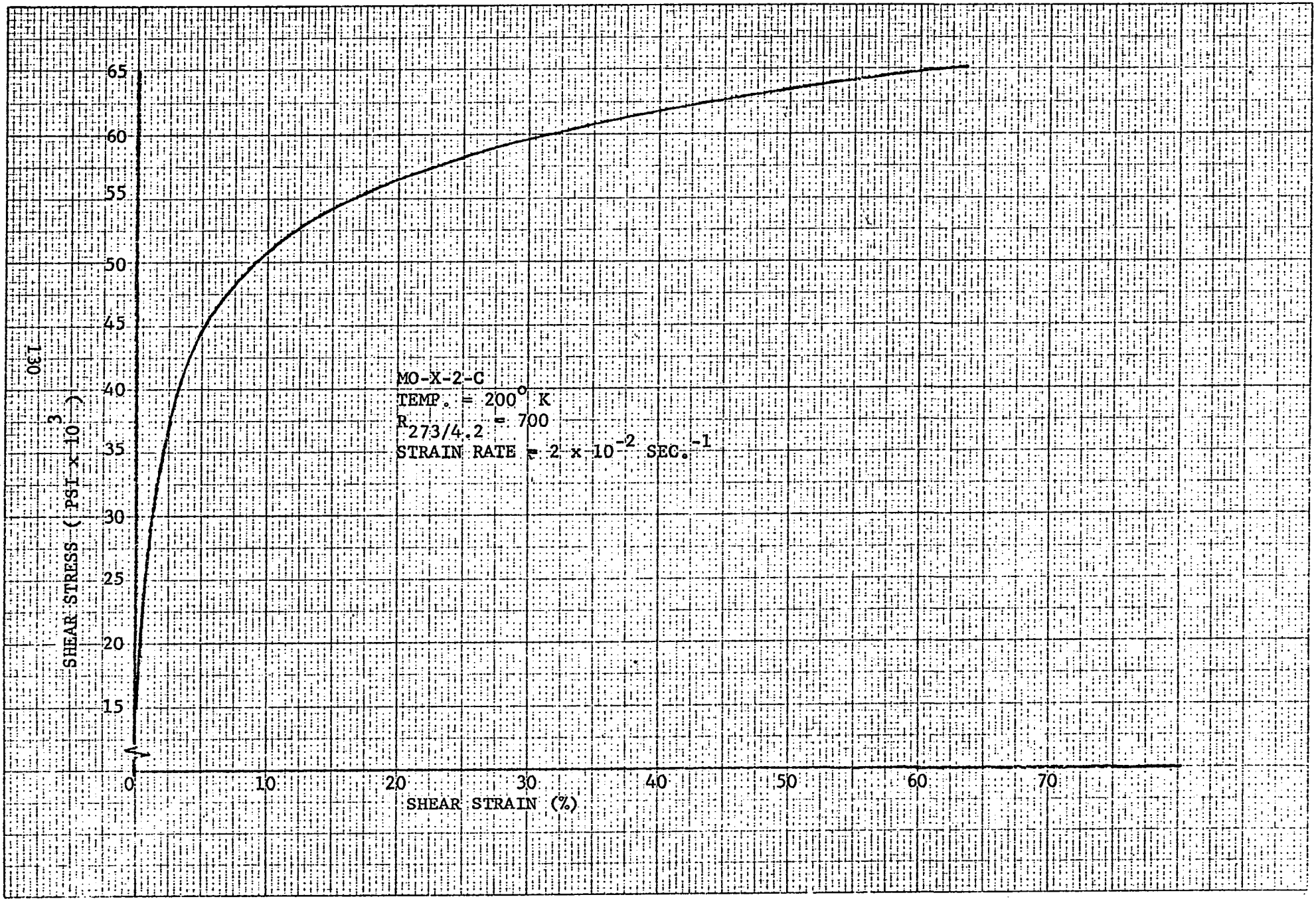

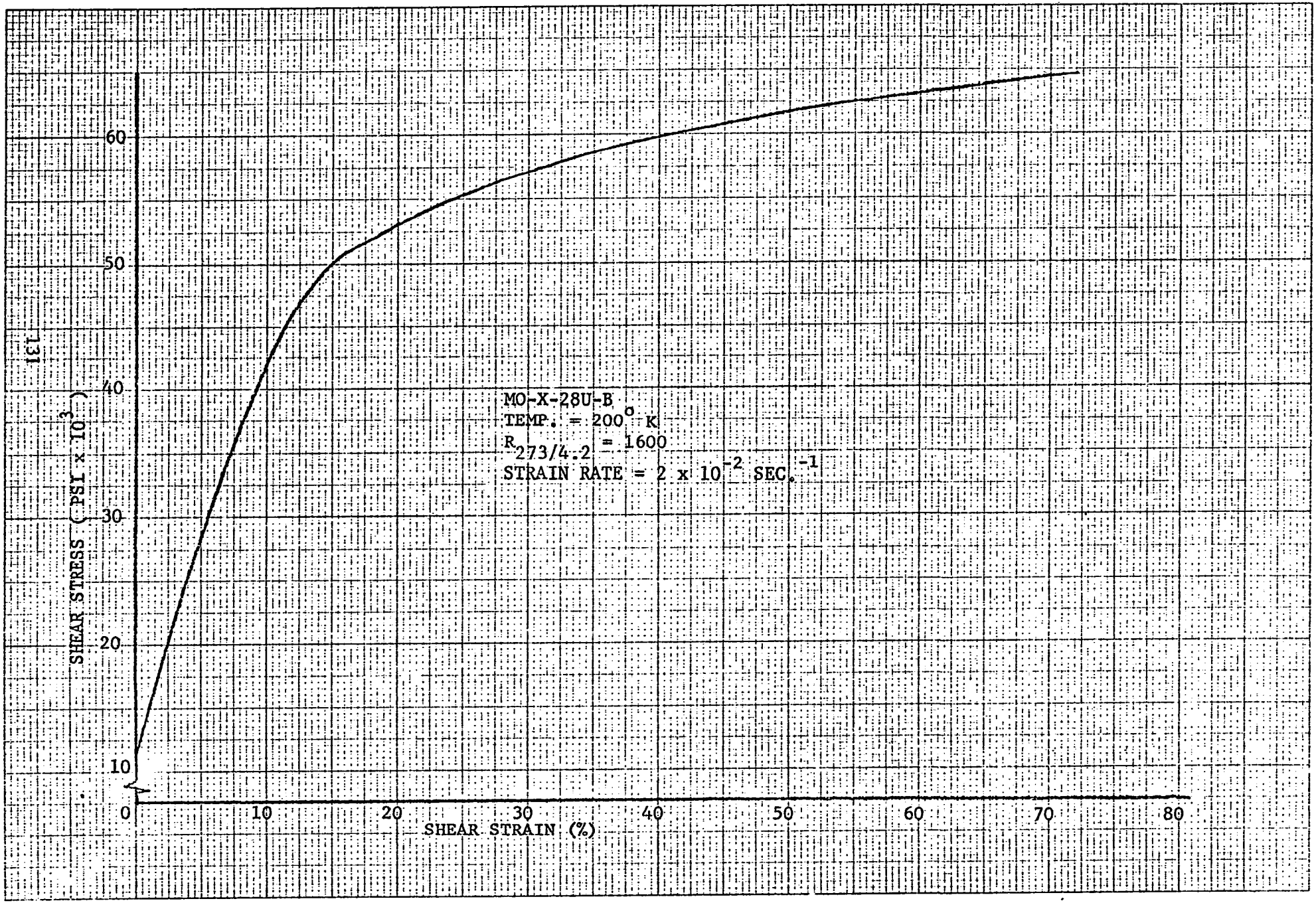

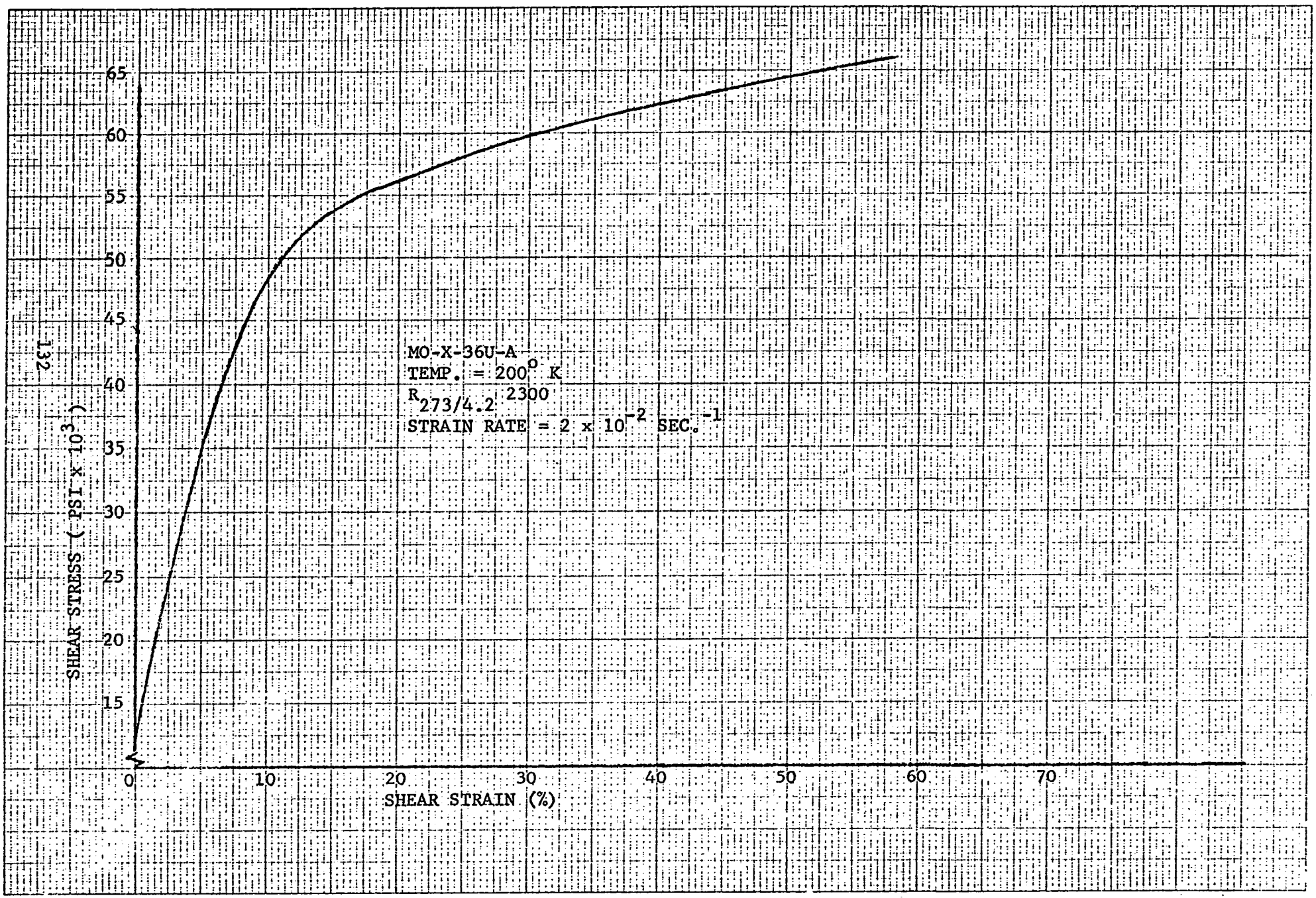

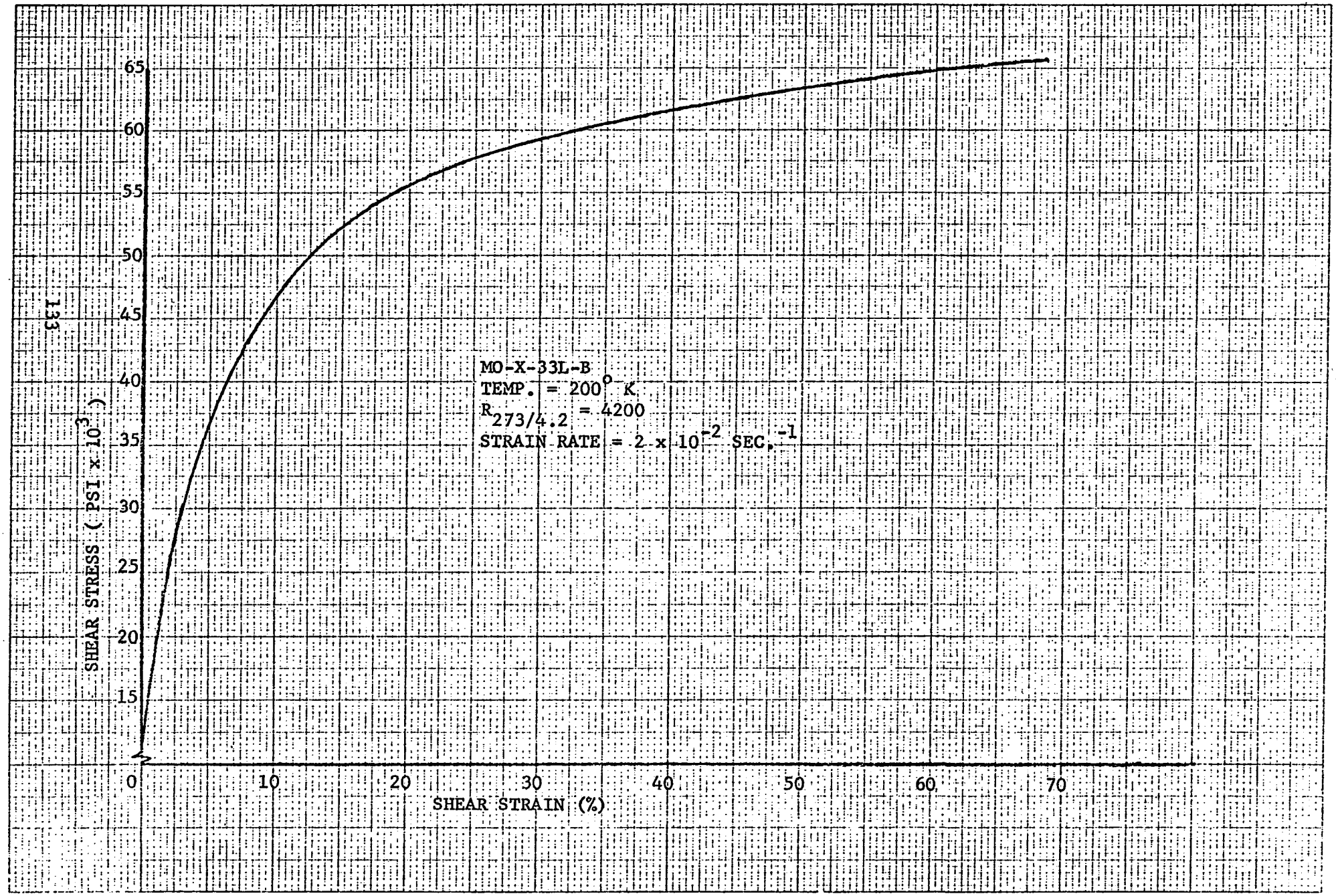

133

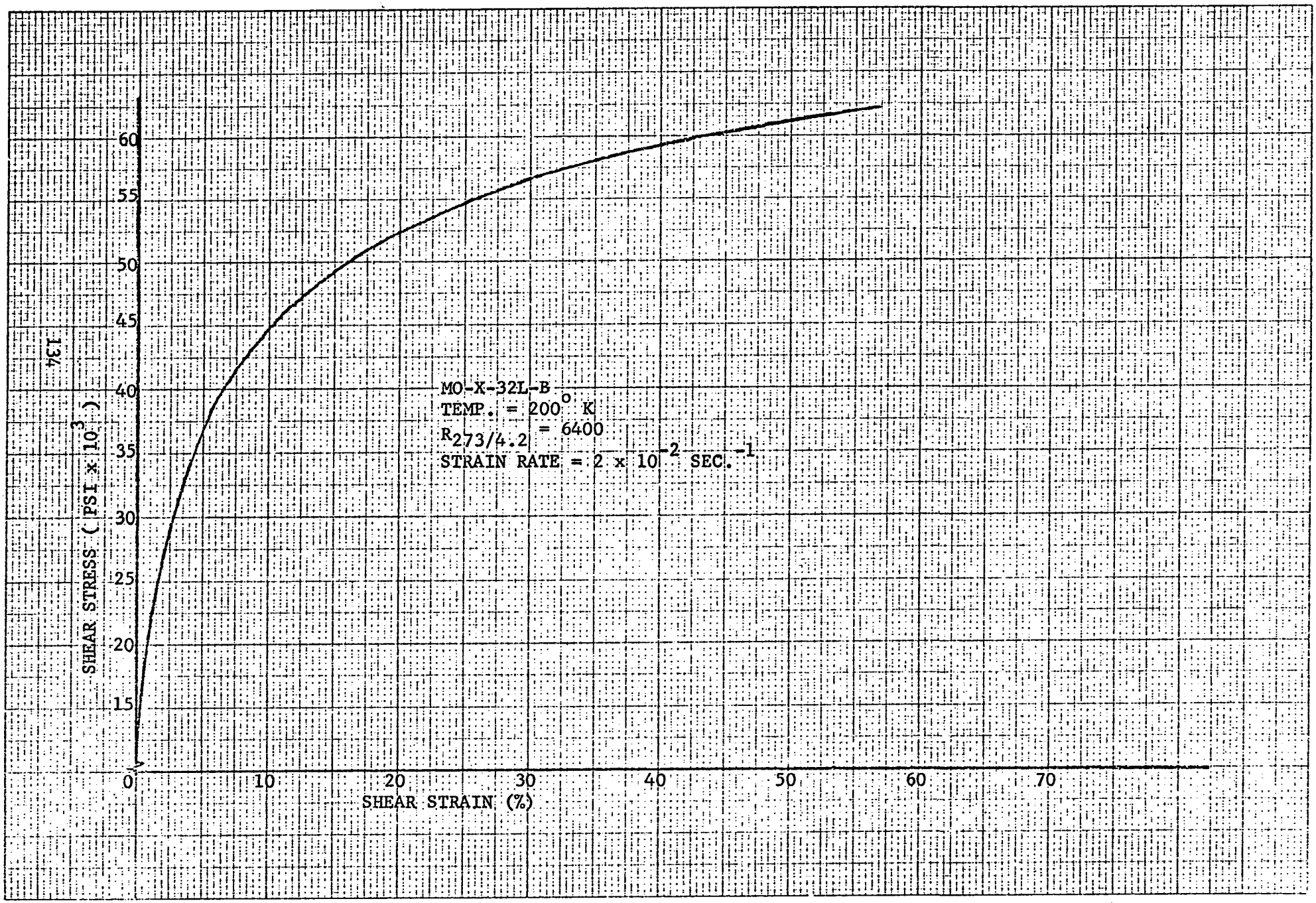

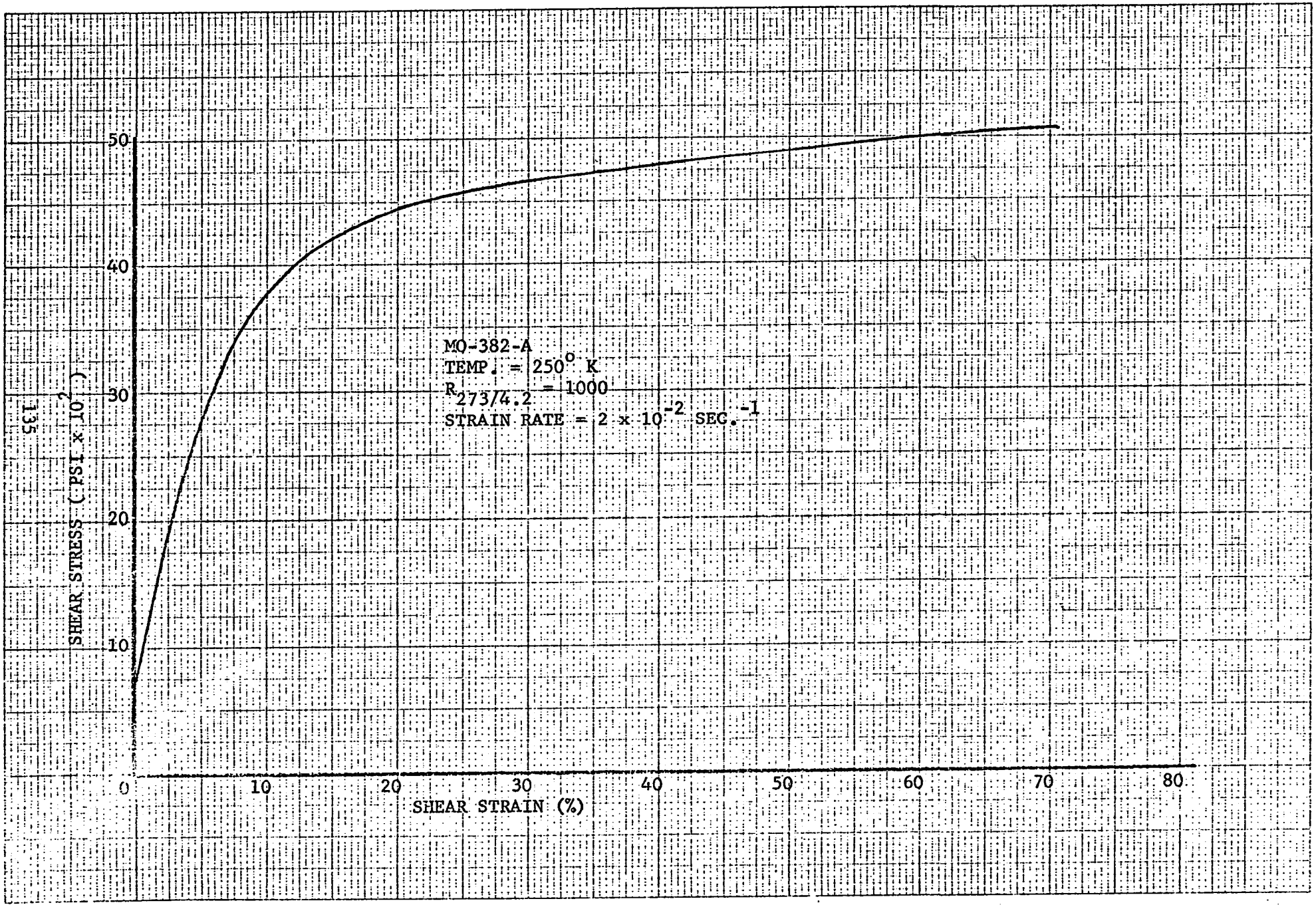

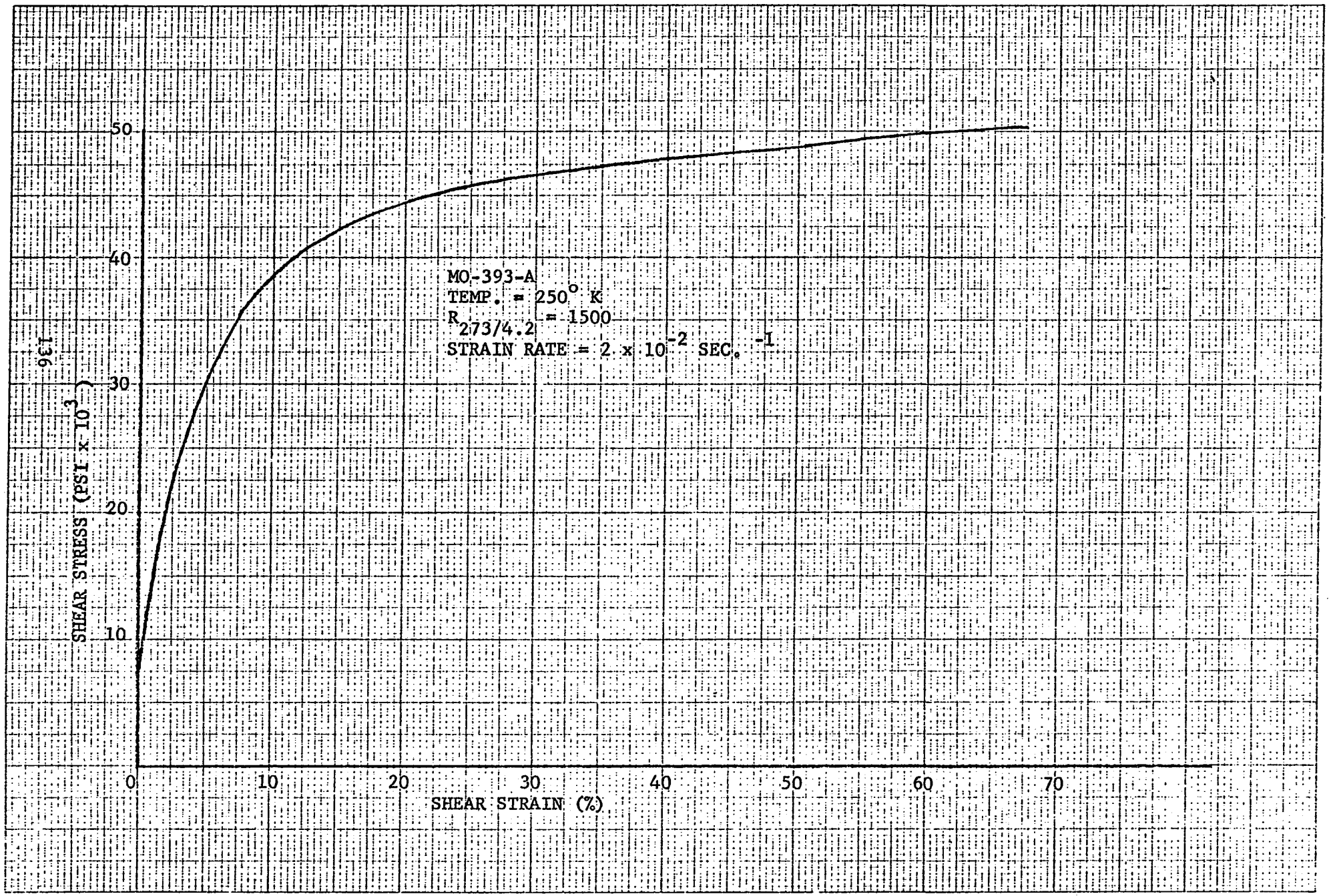

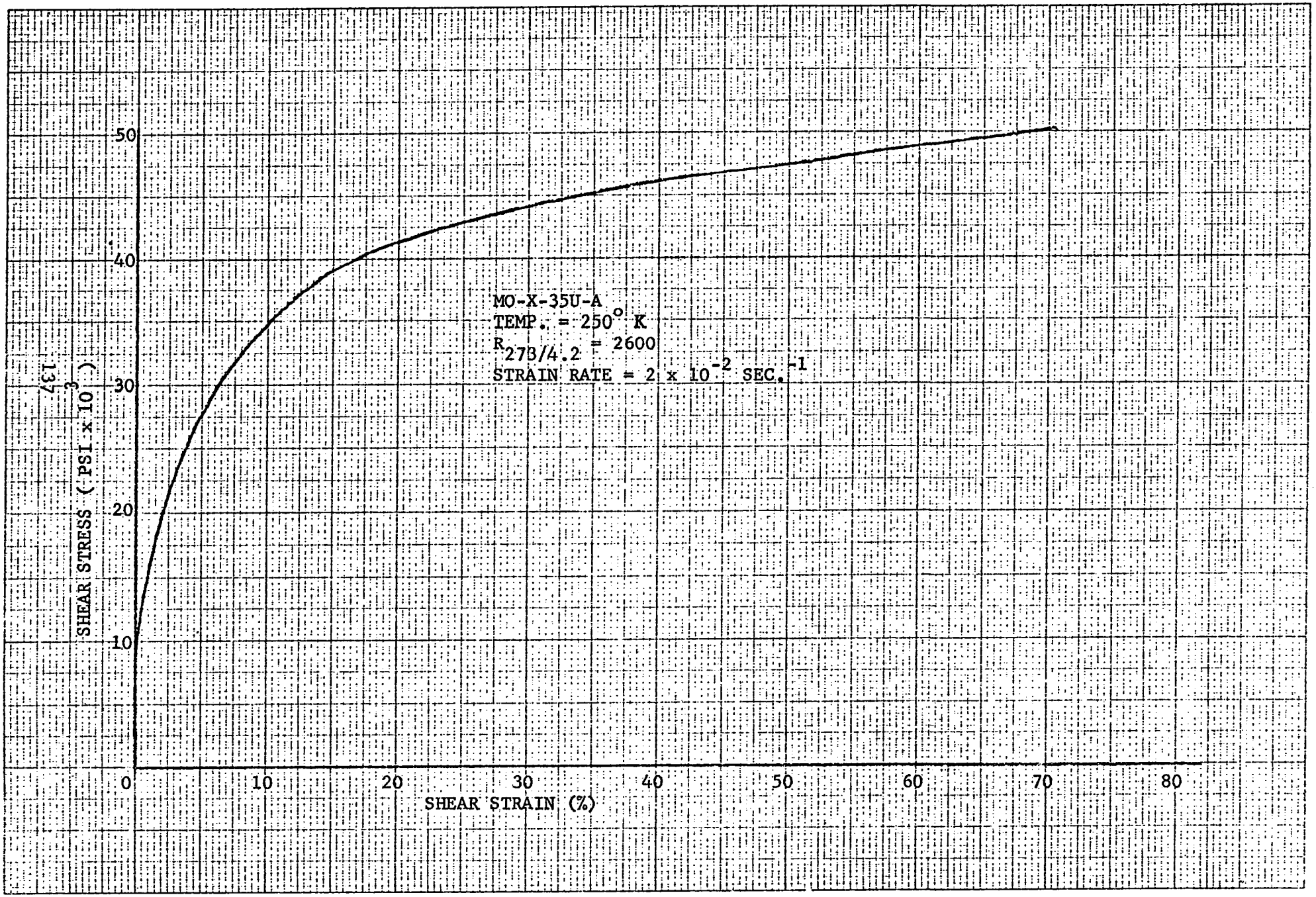

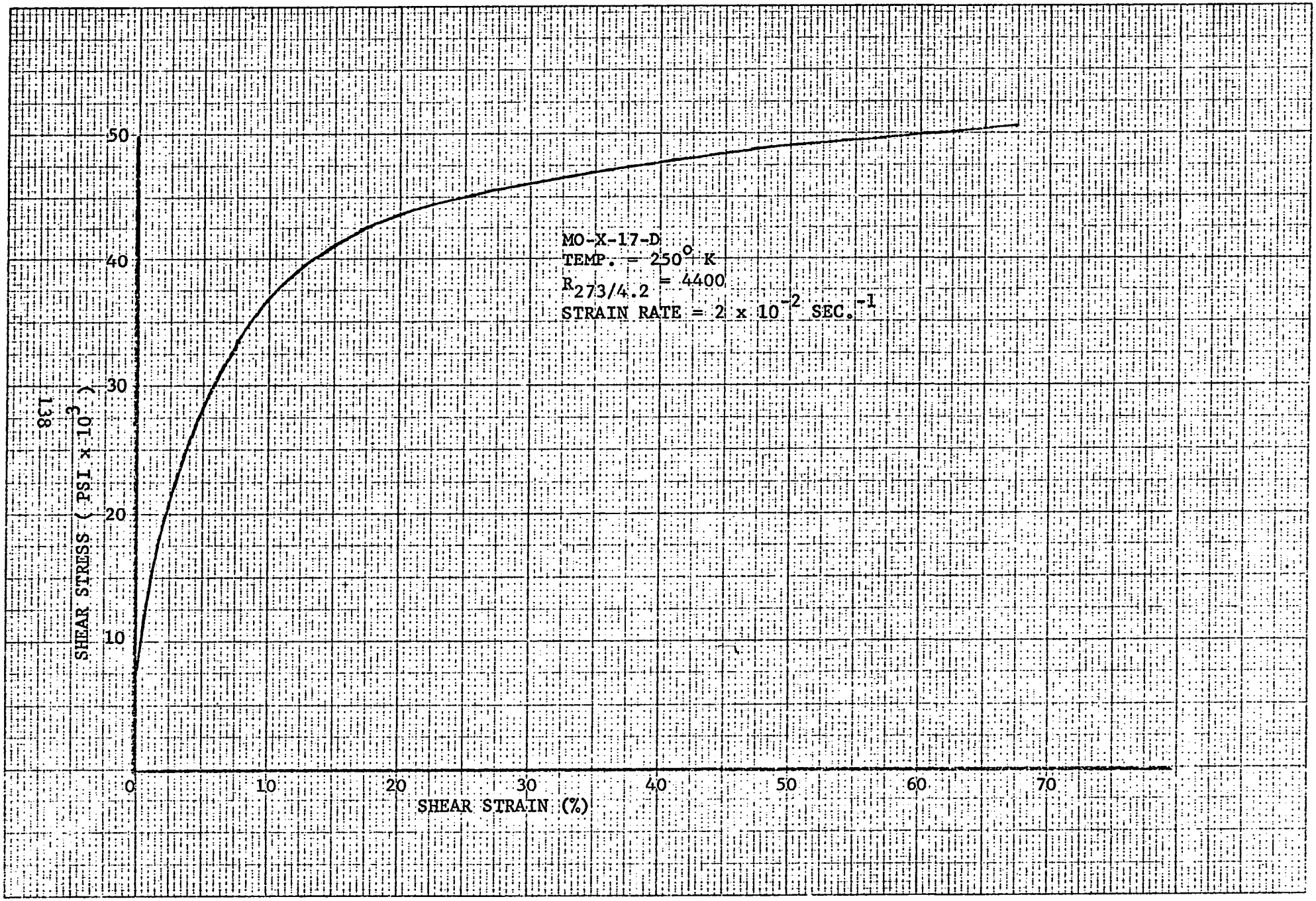

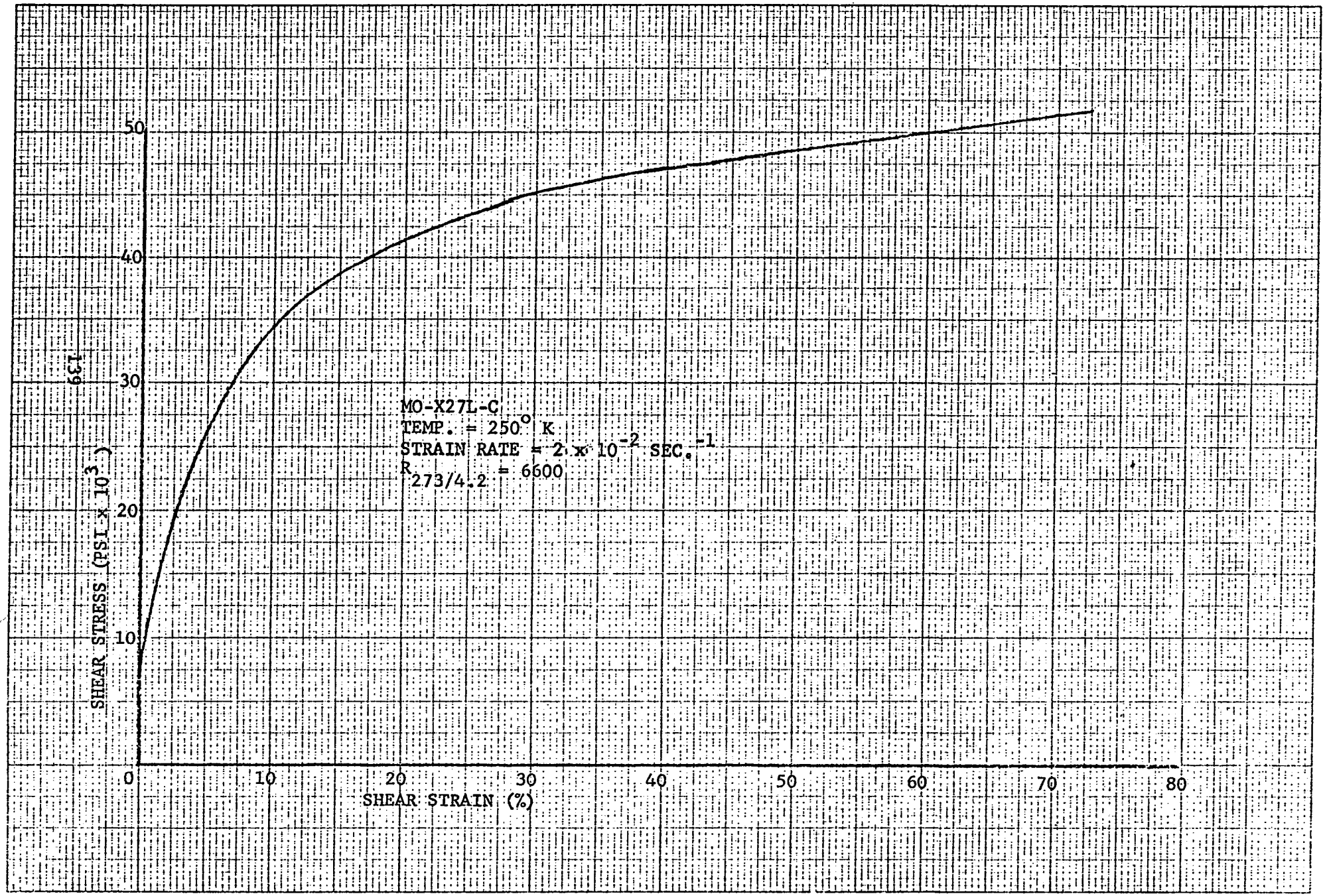

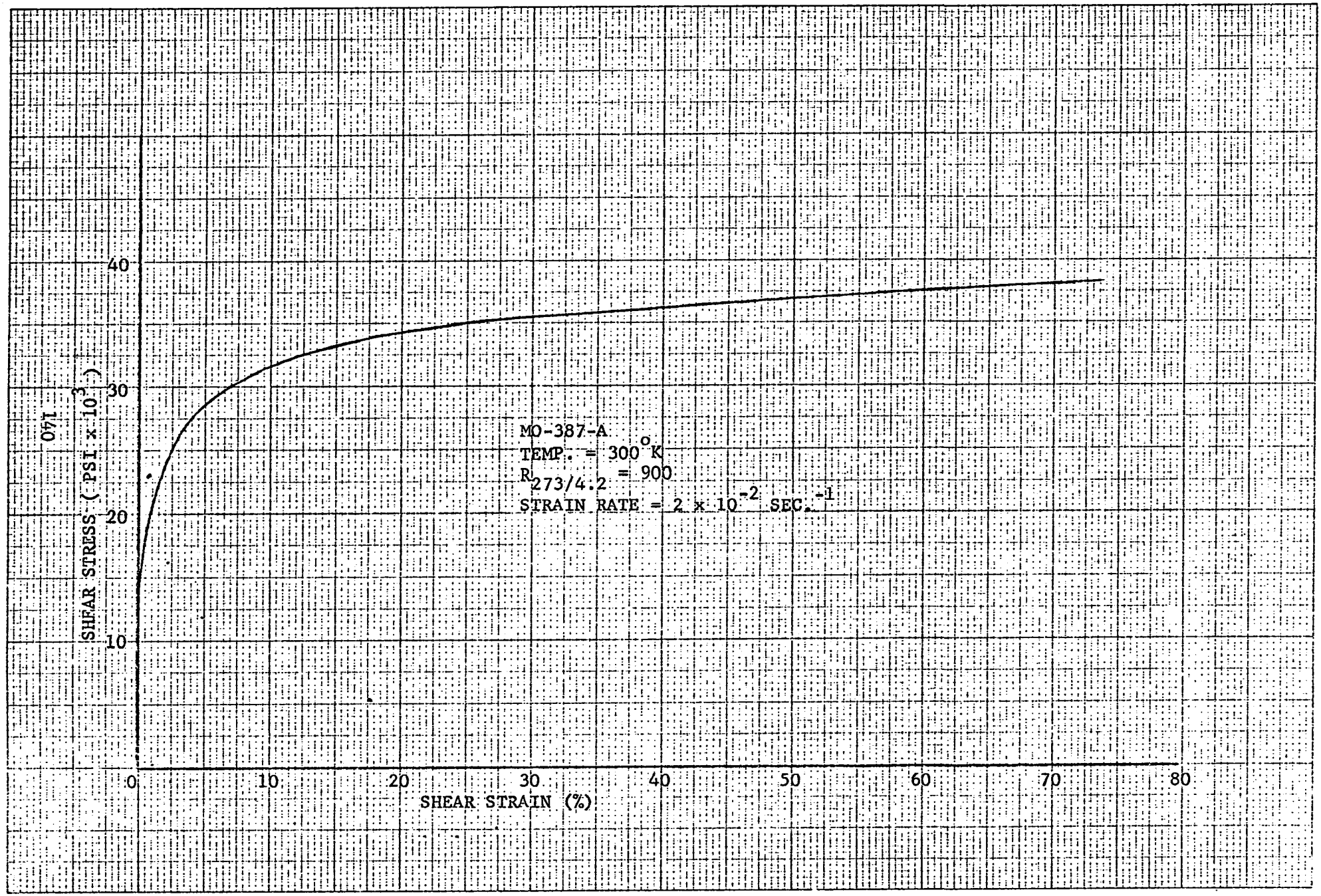

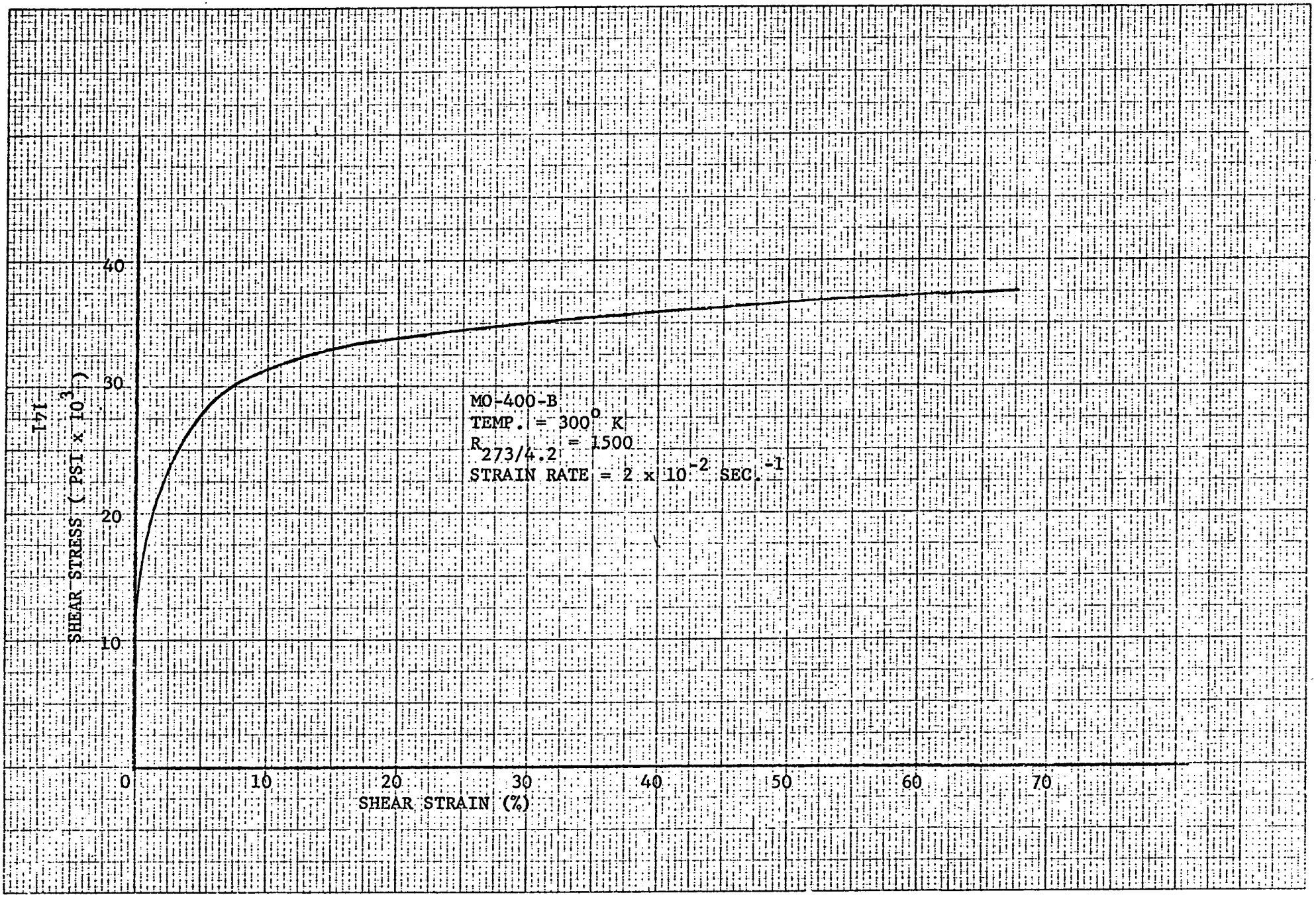

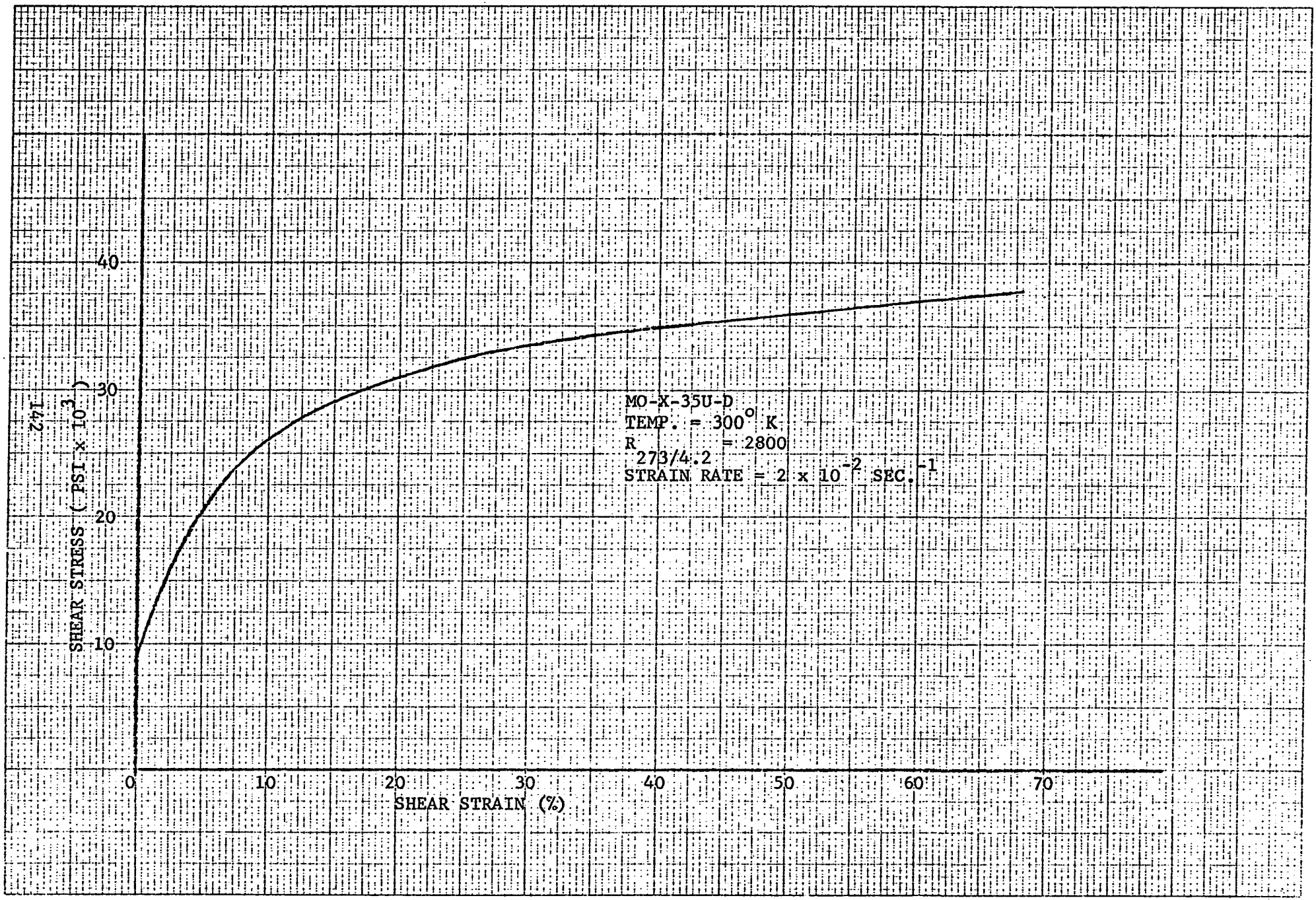

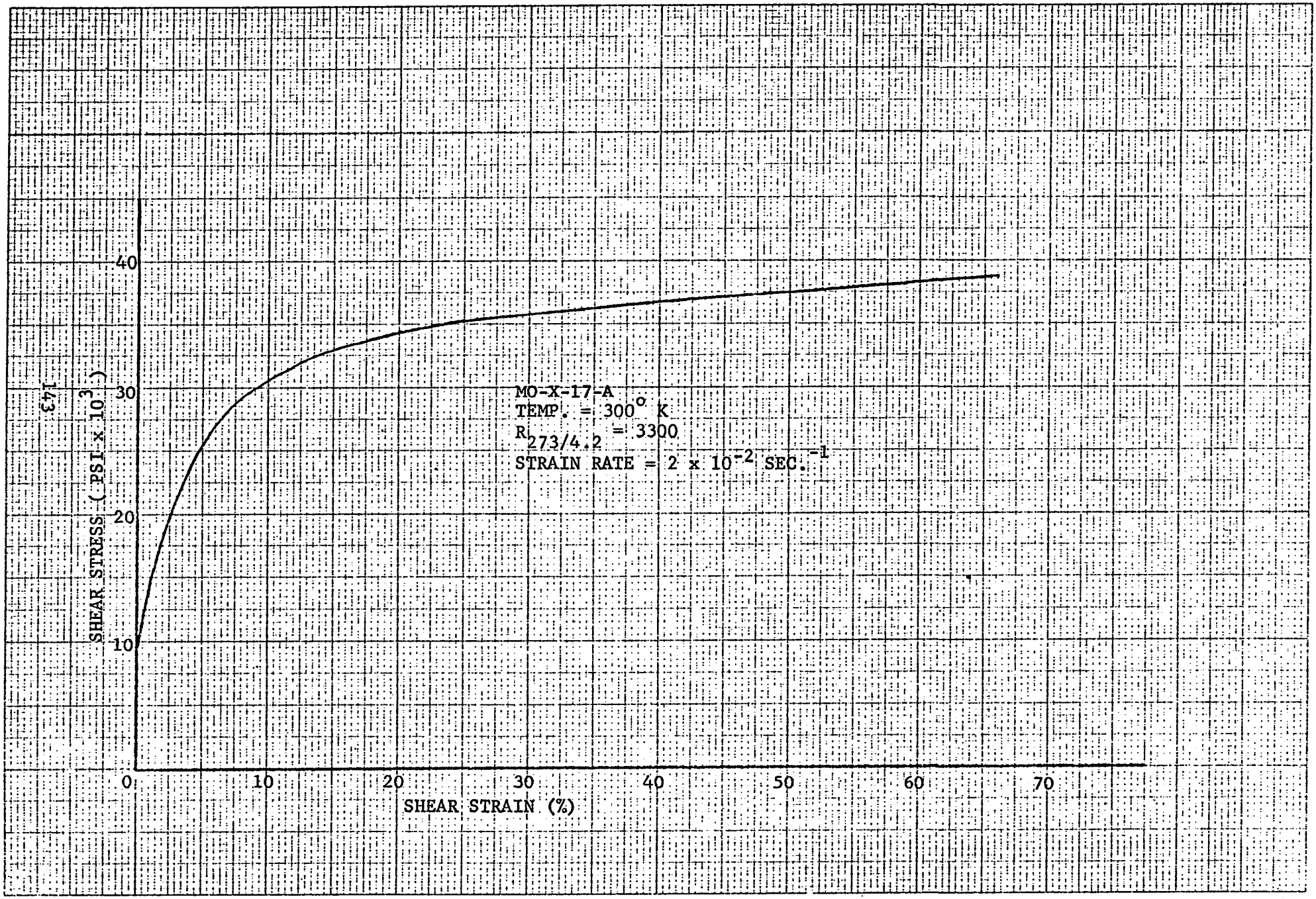

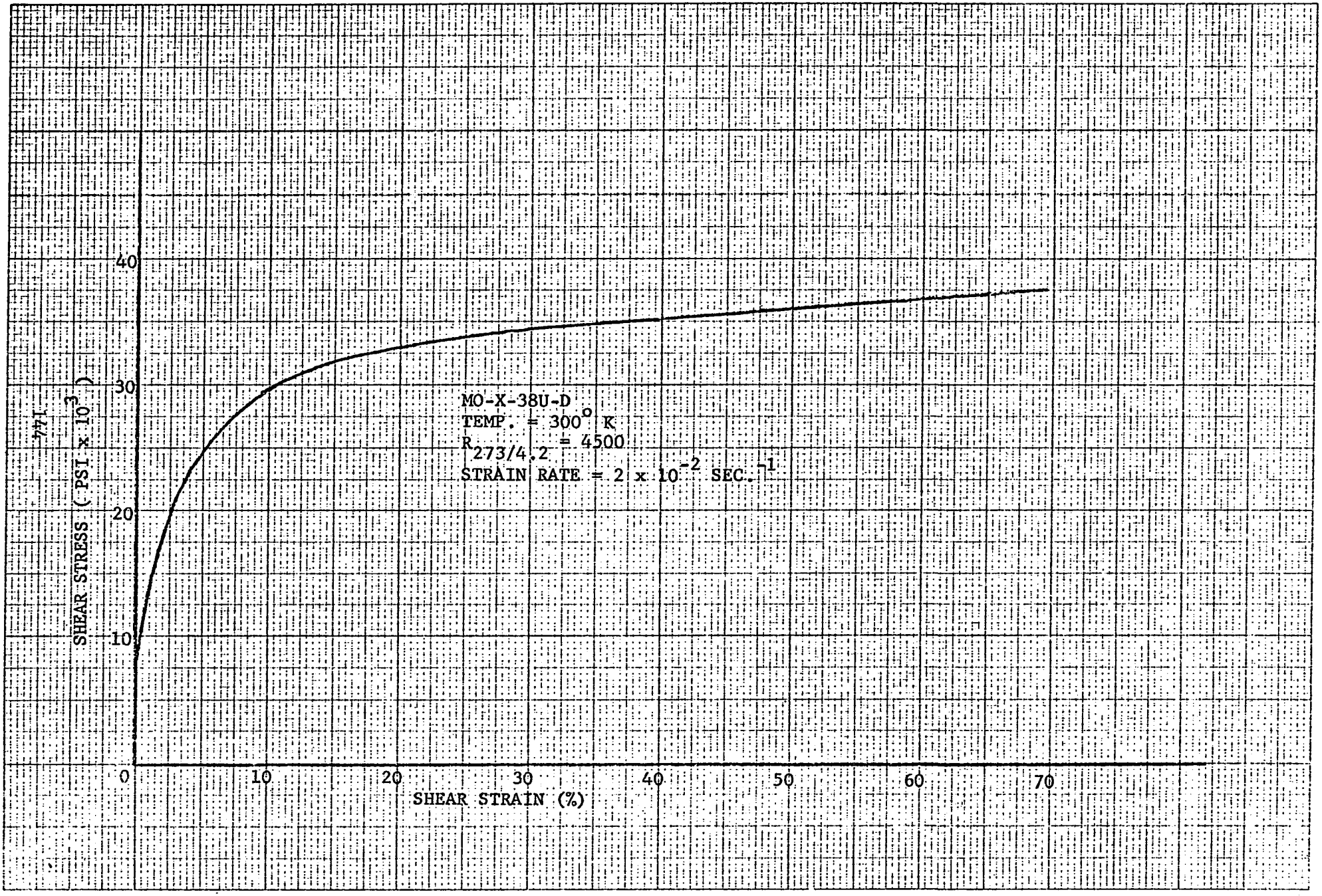

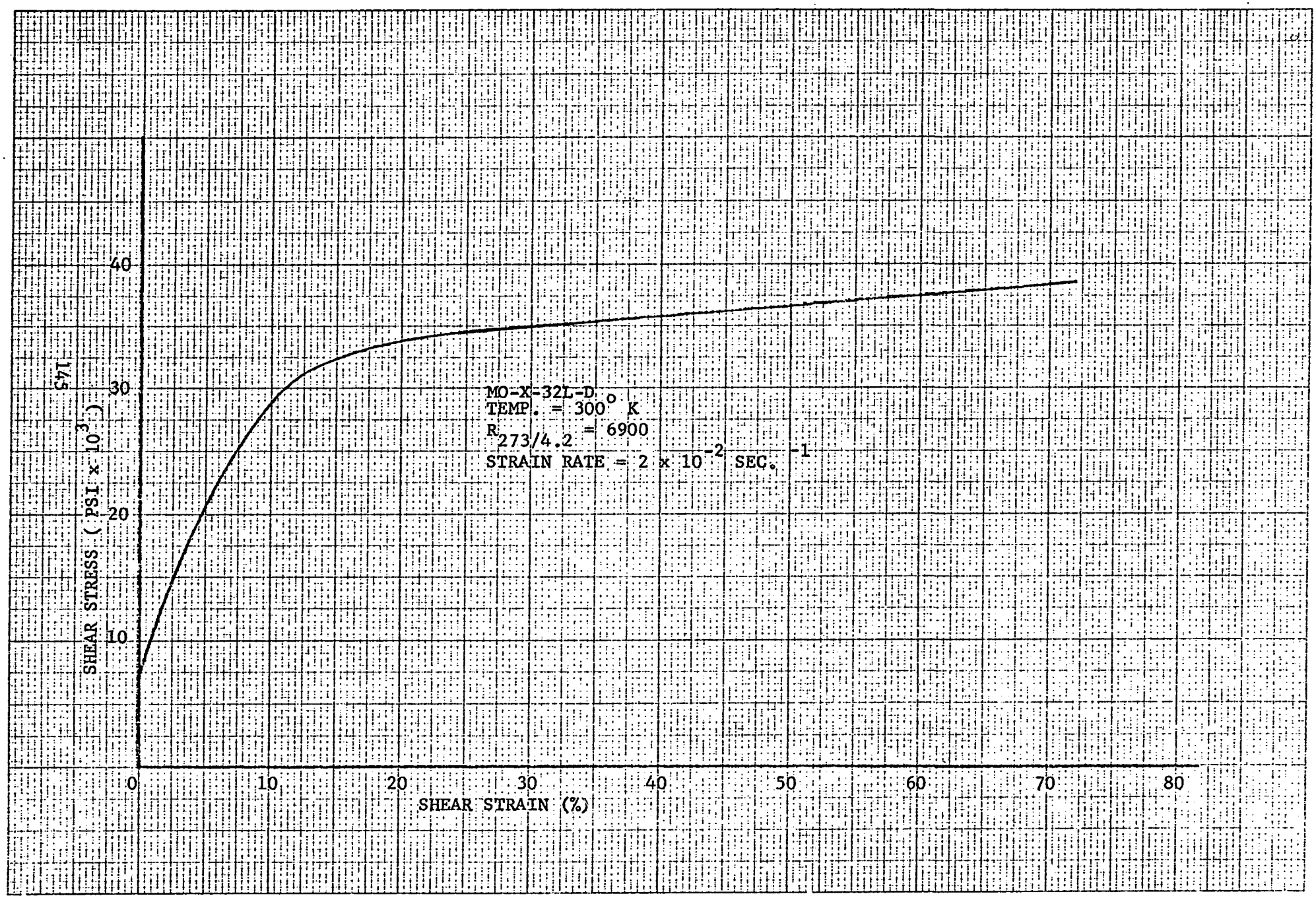

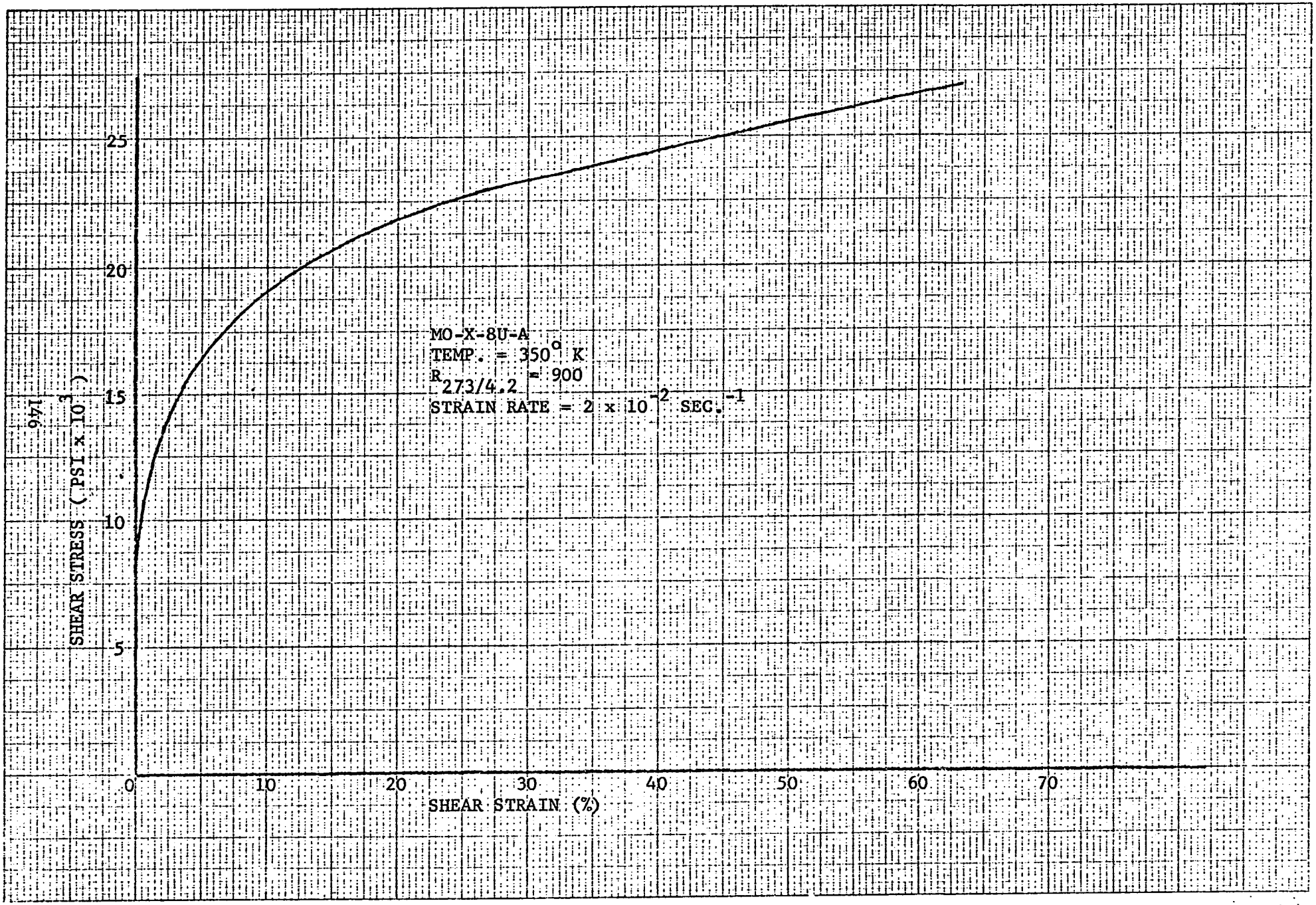

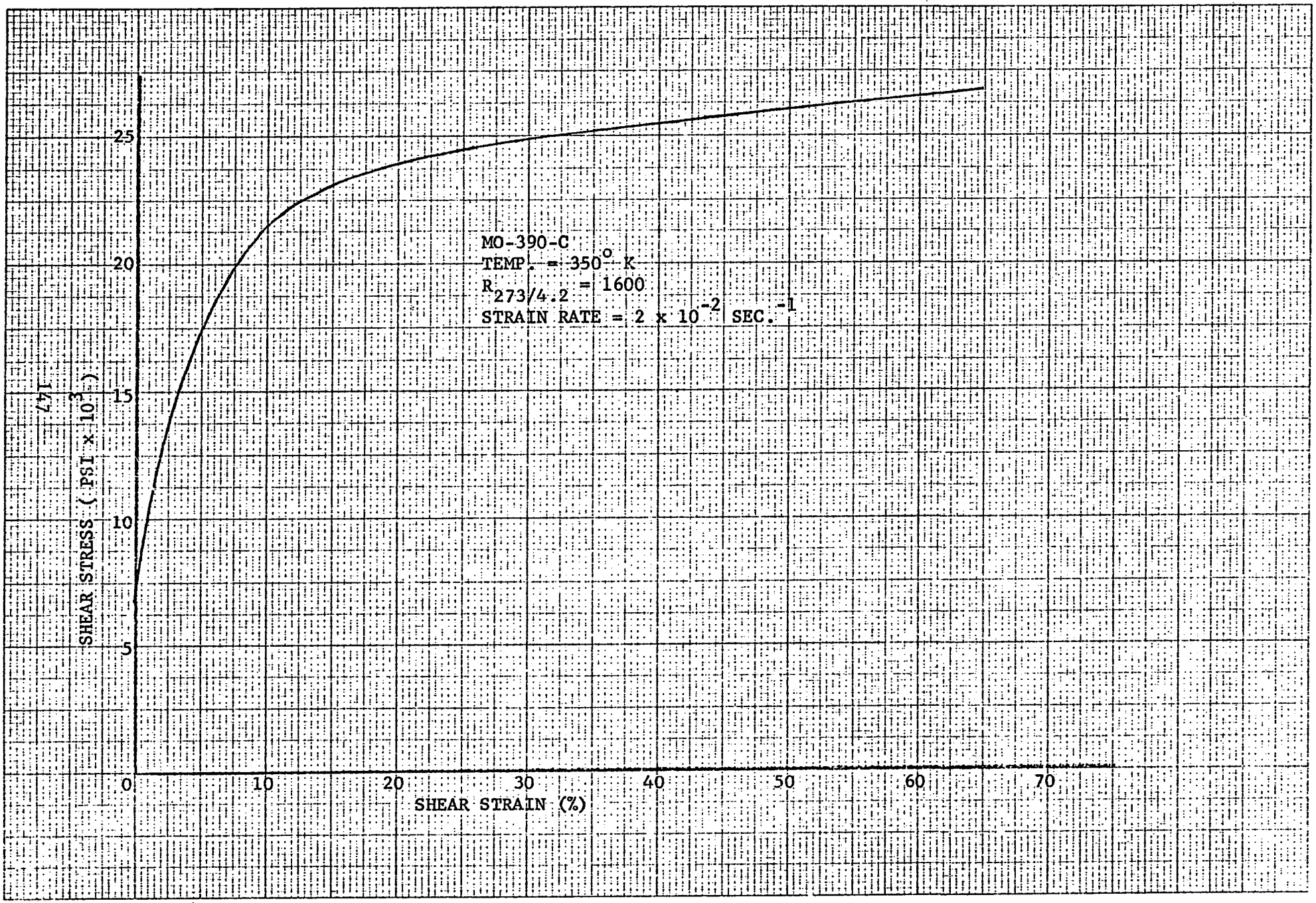

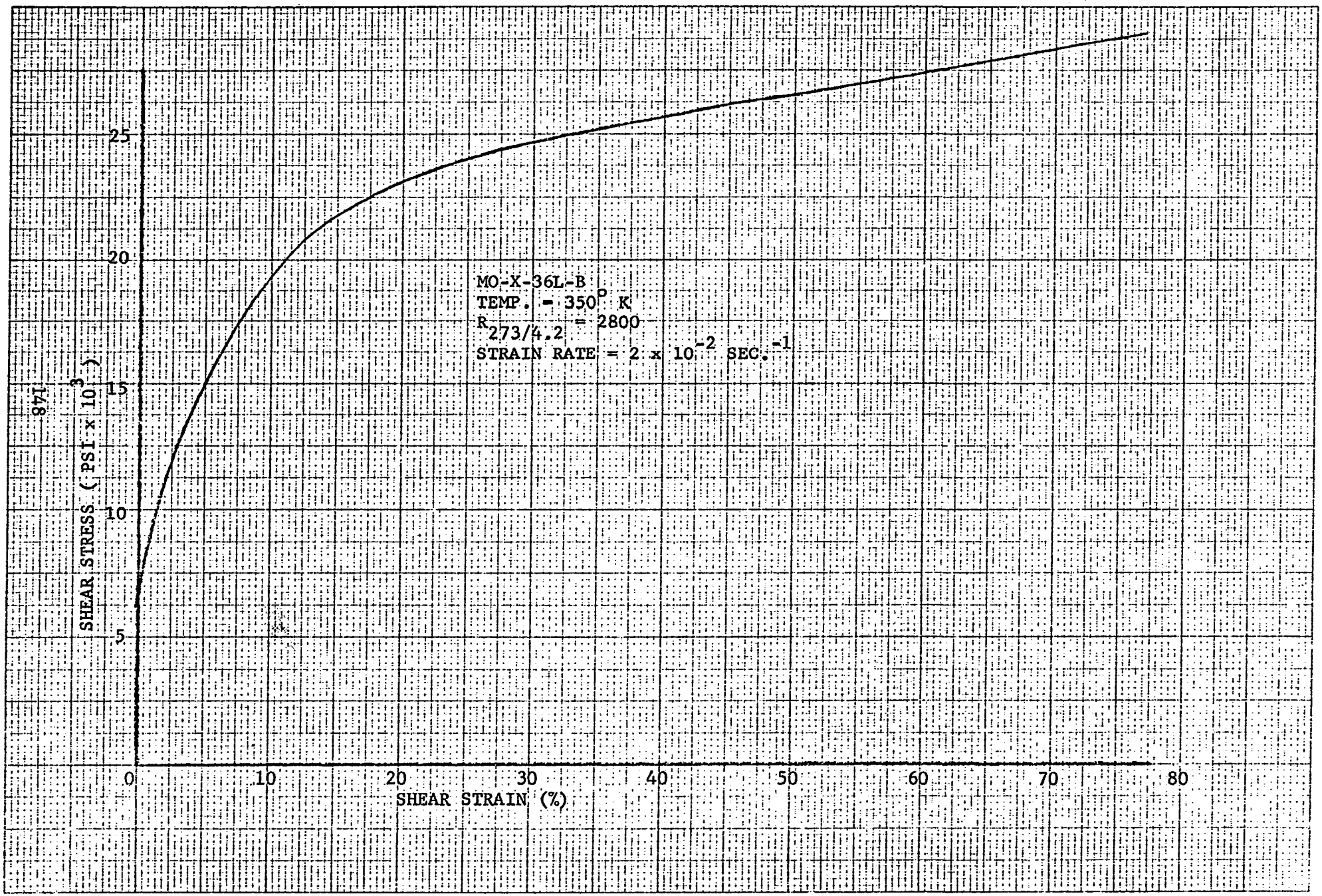

148

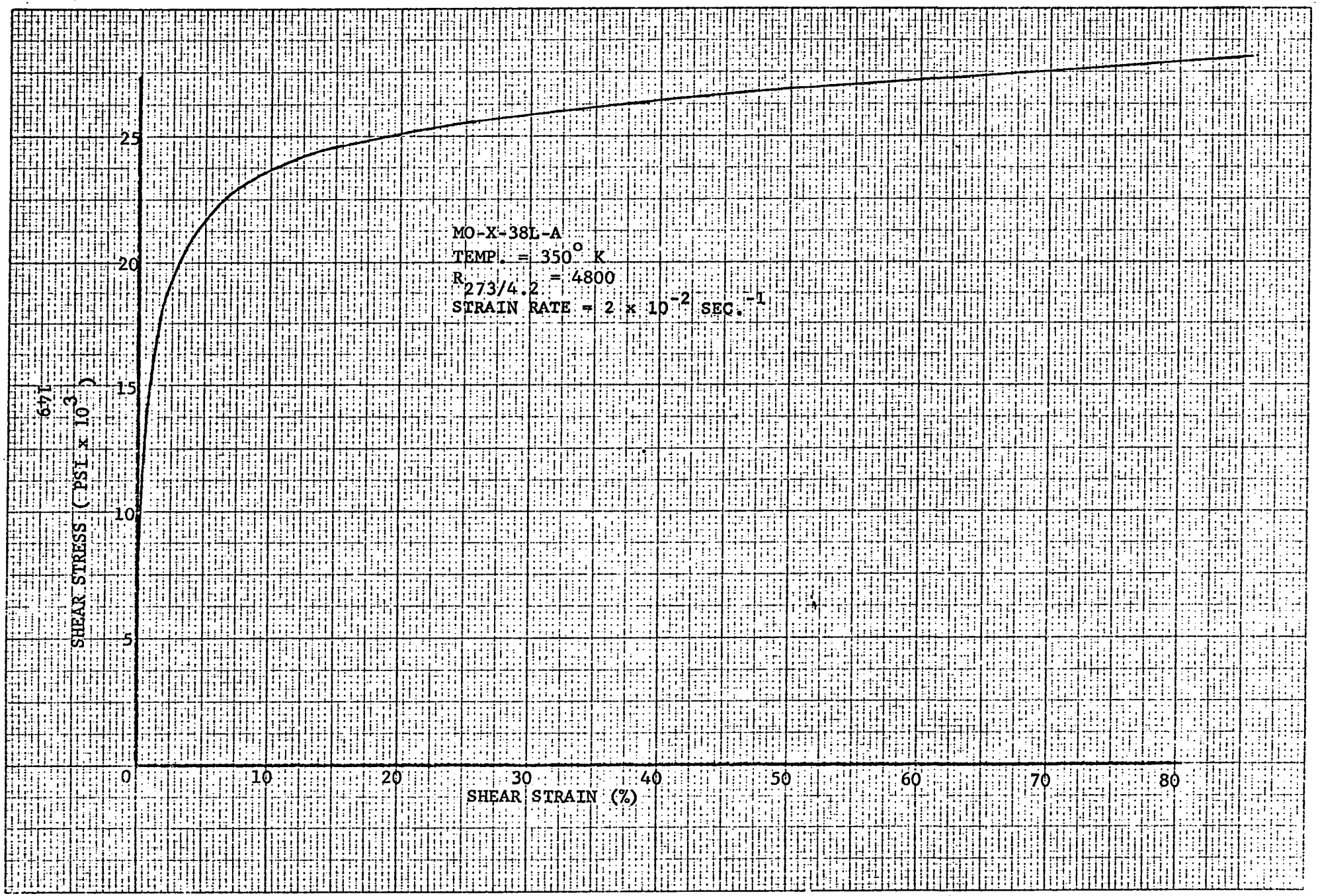

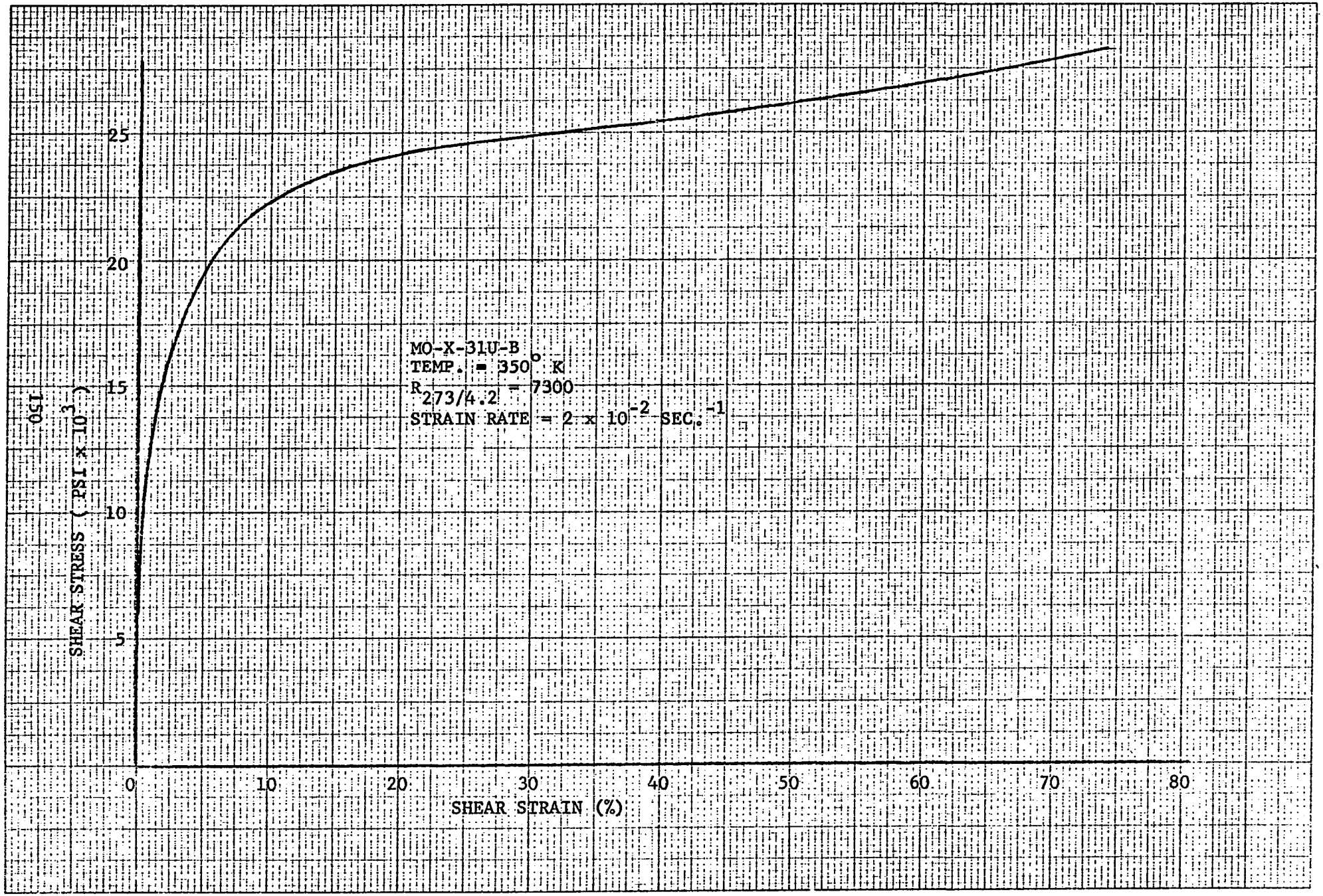

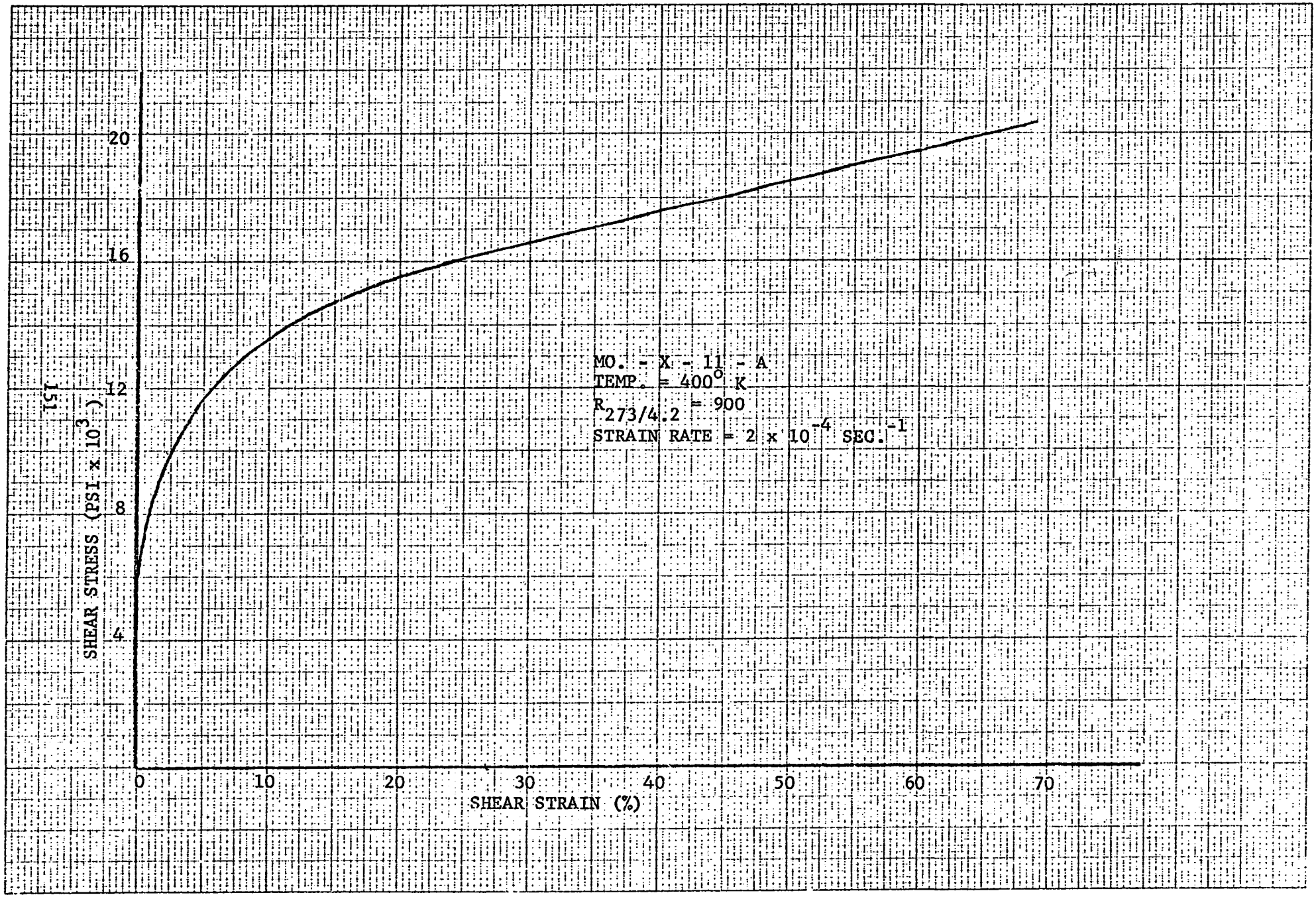

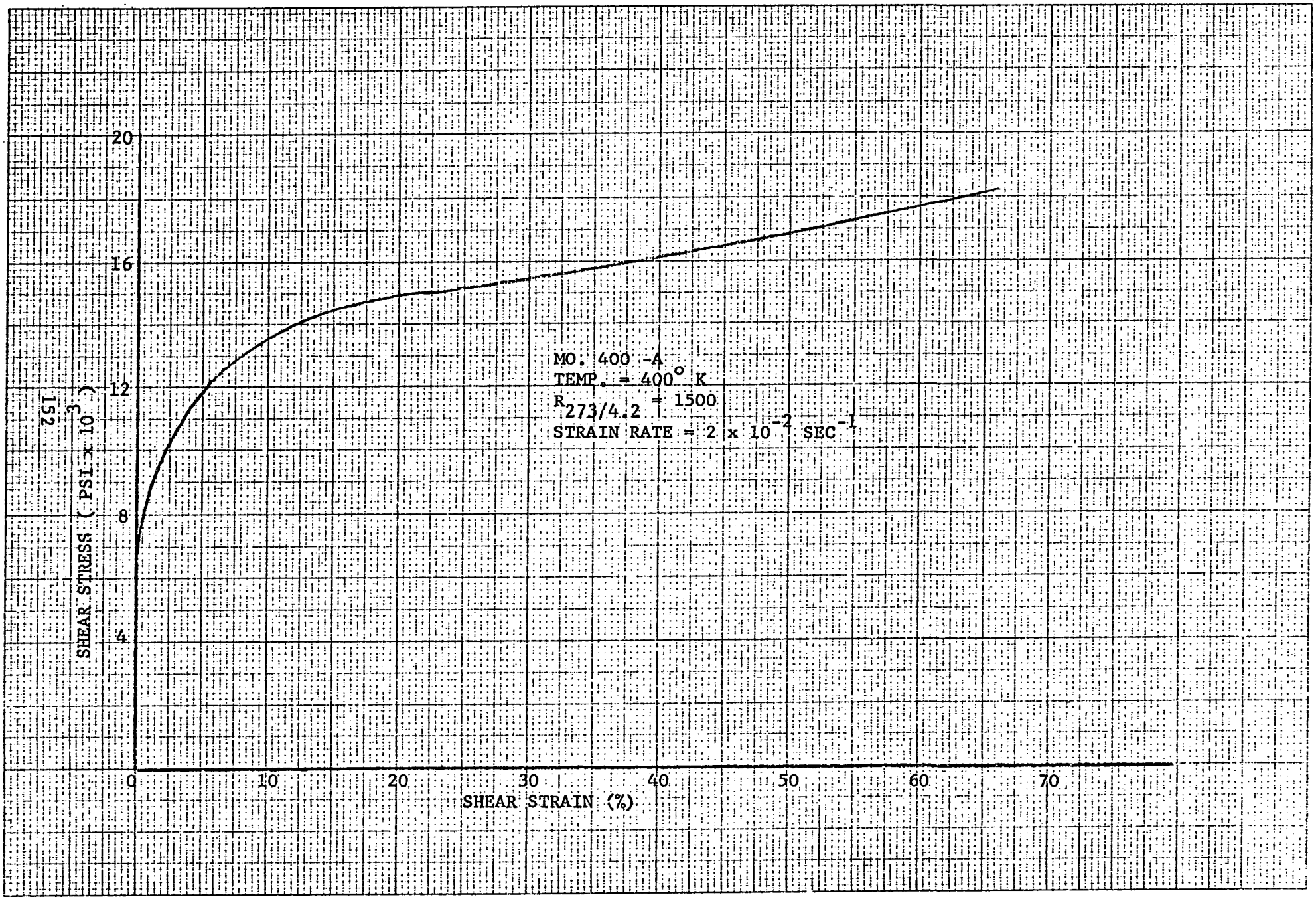

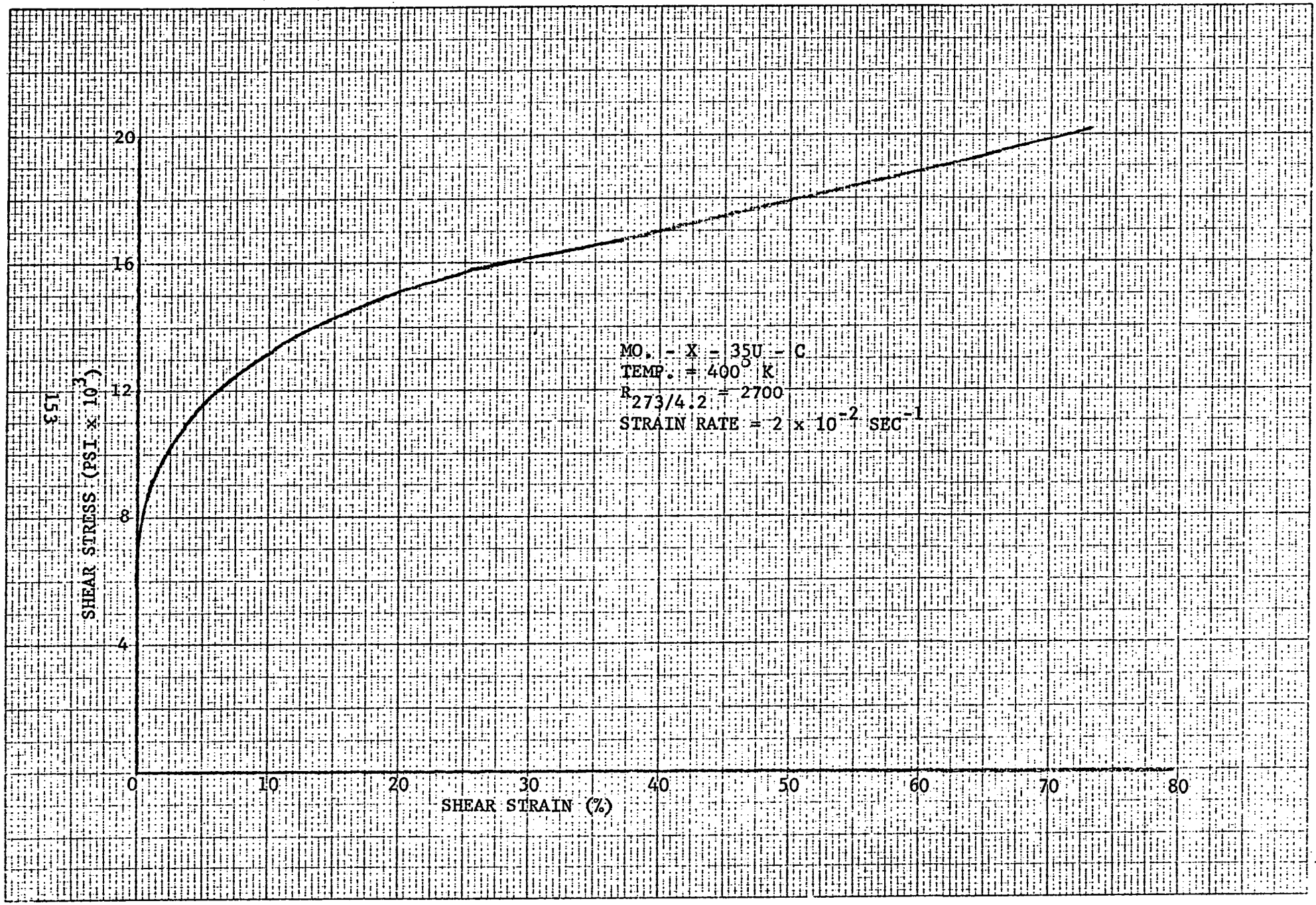

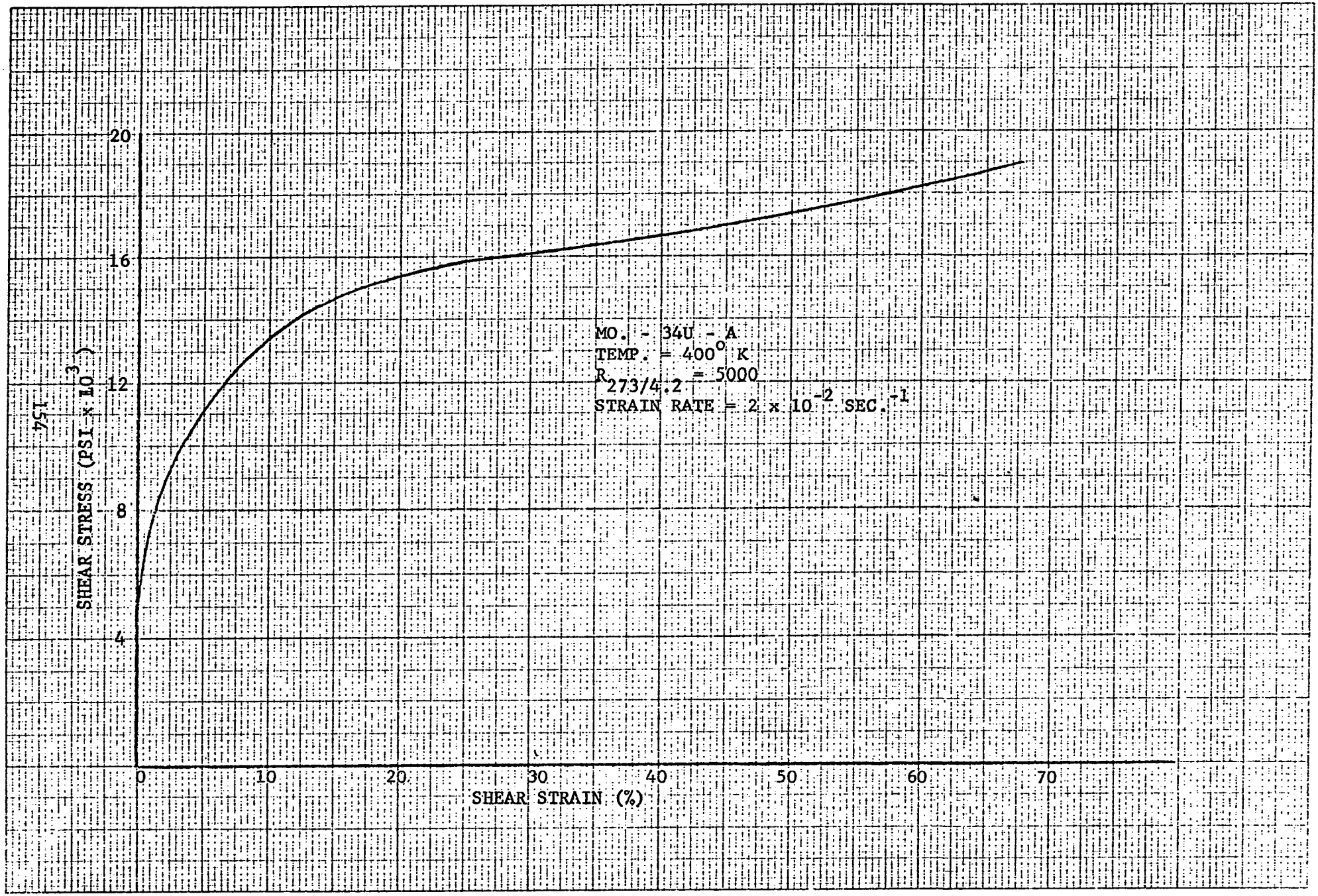

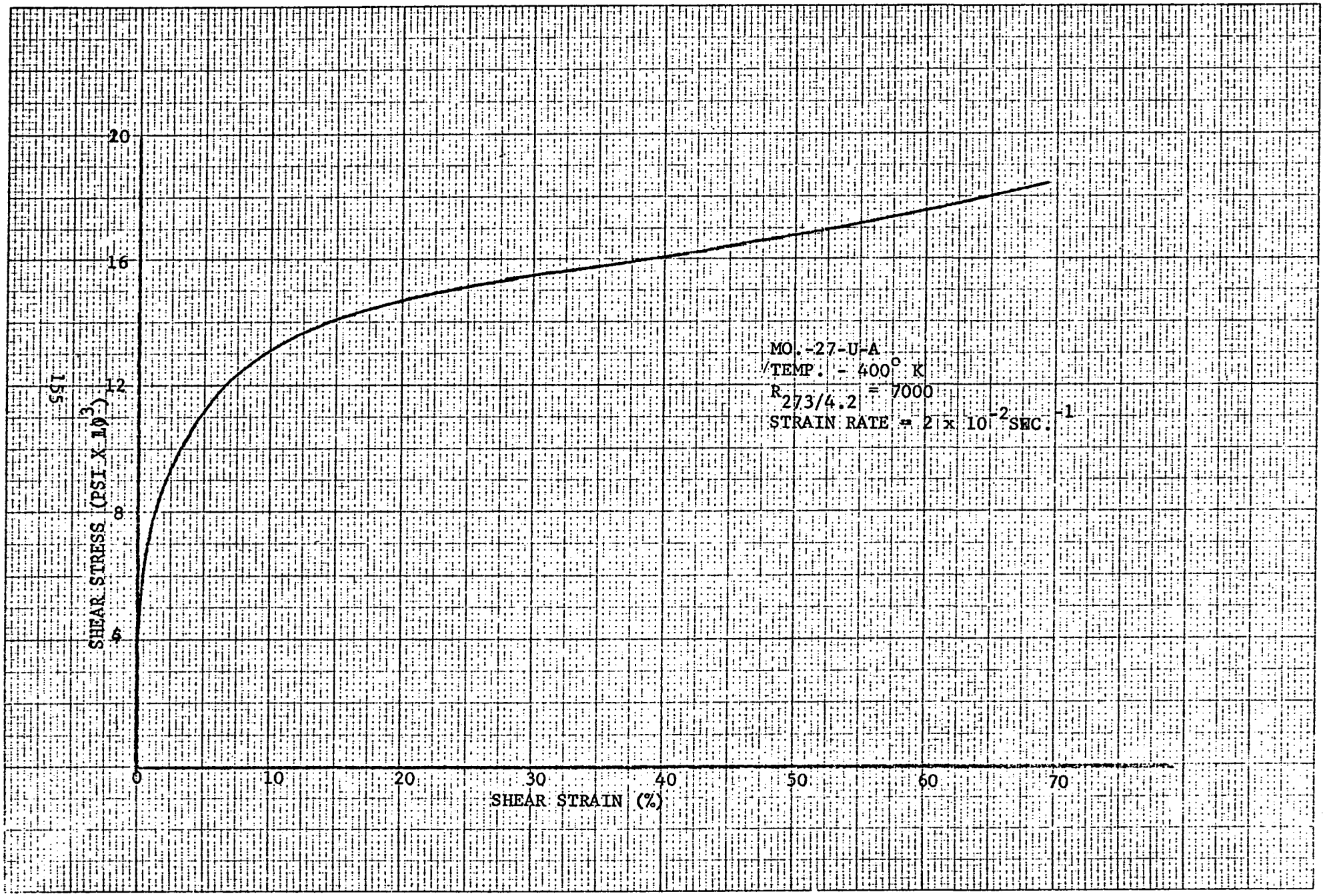

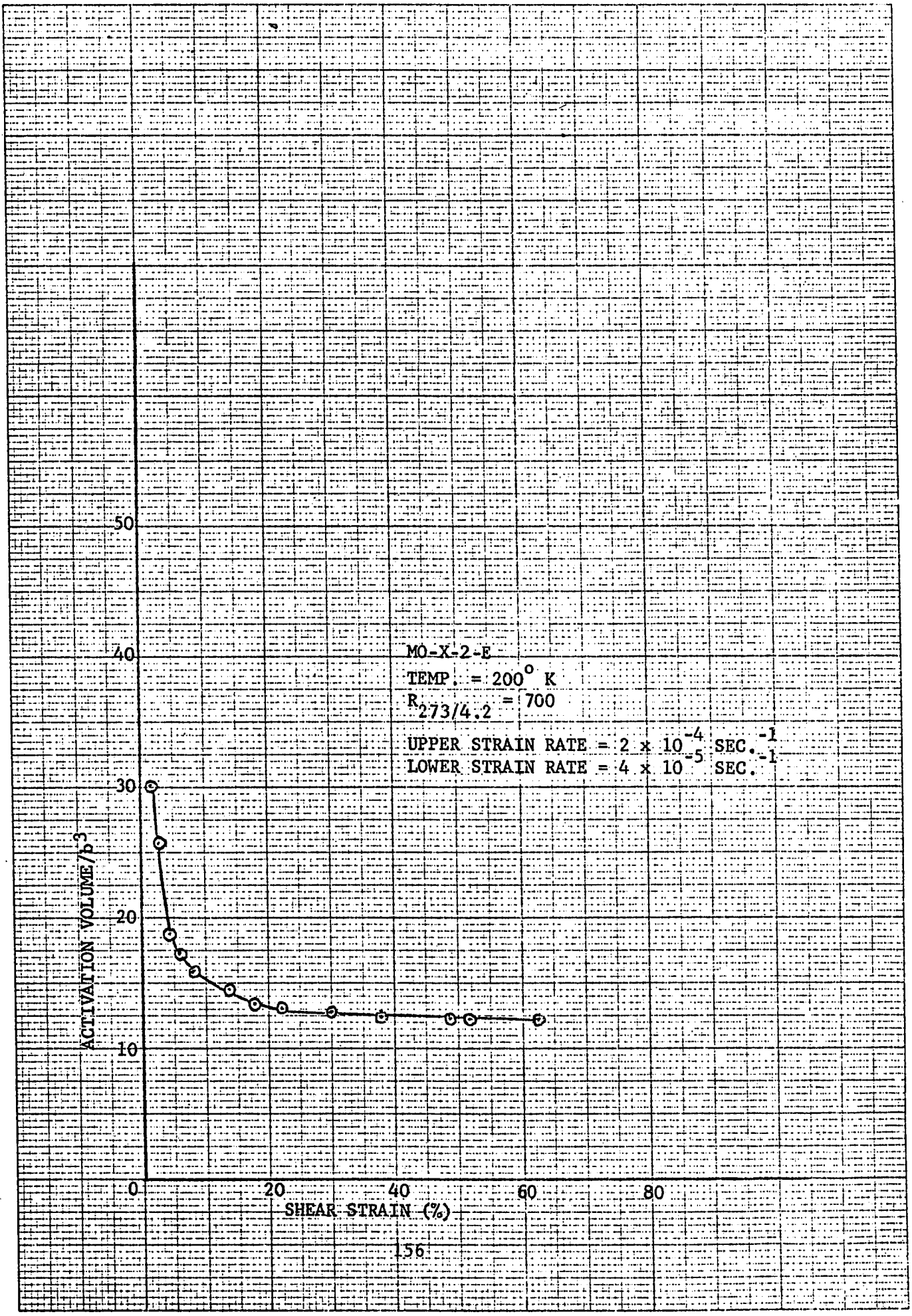

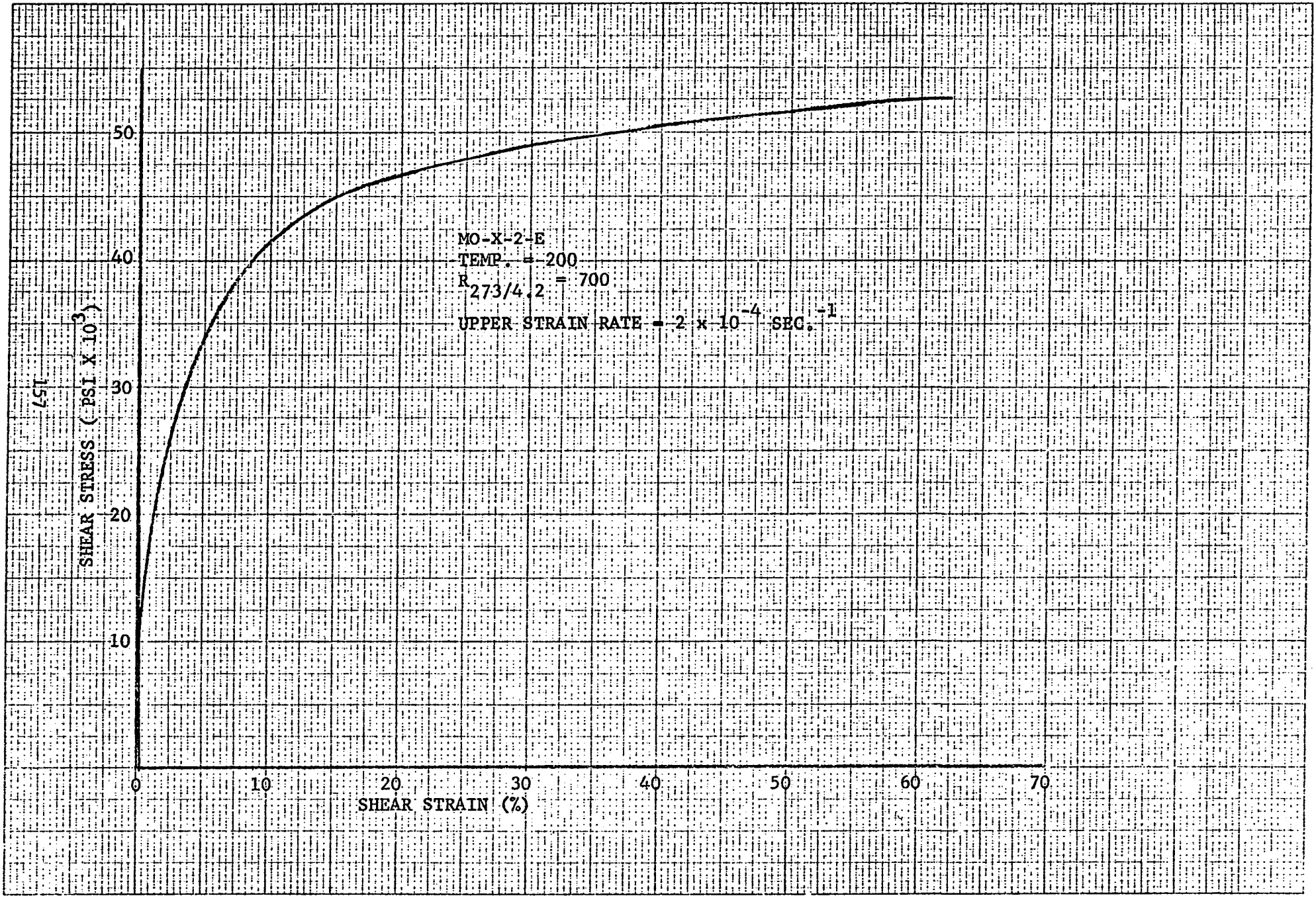

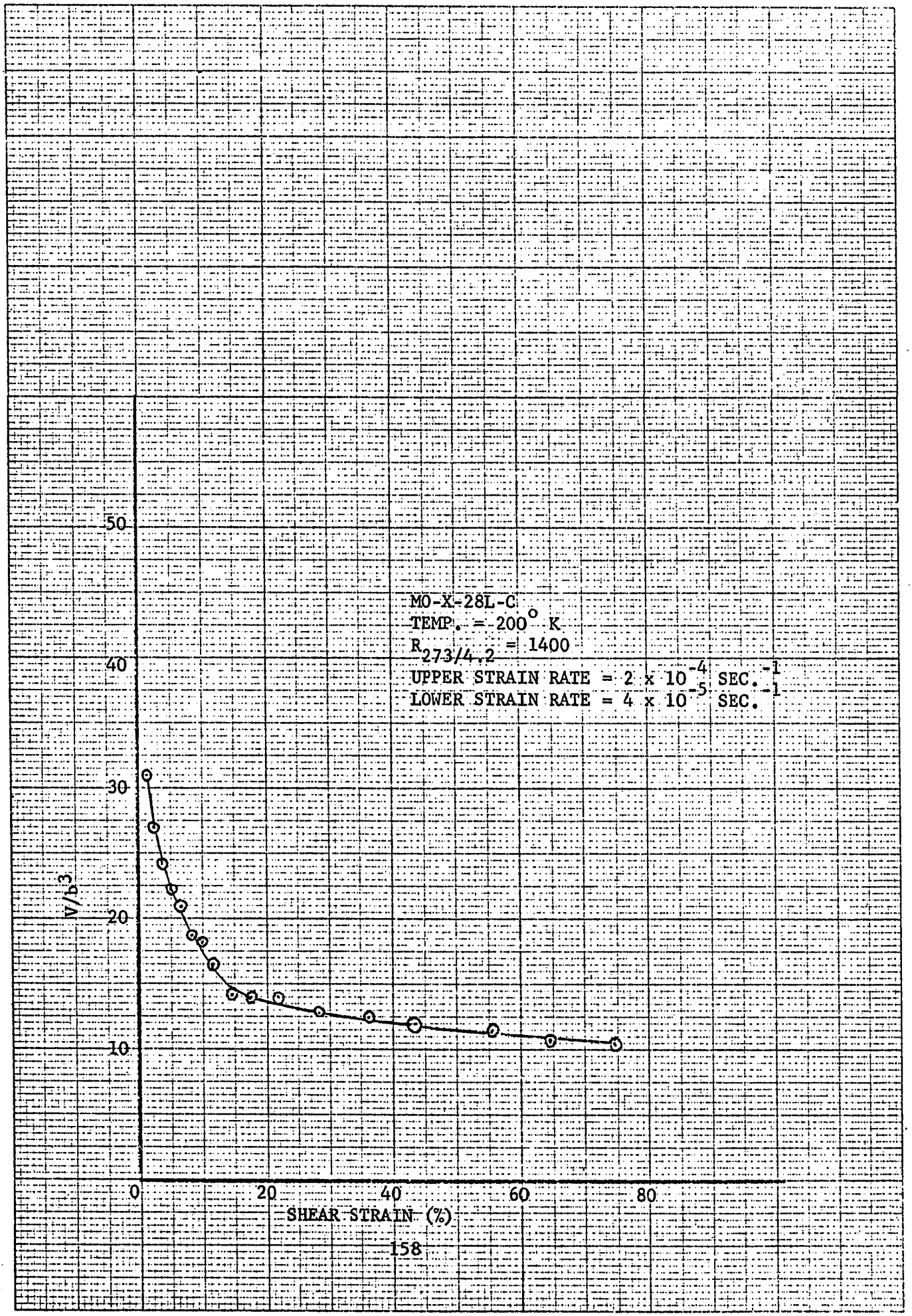

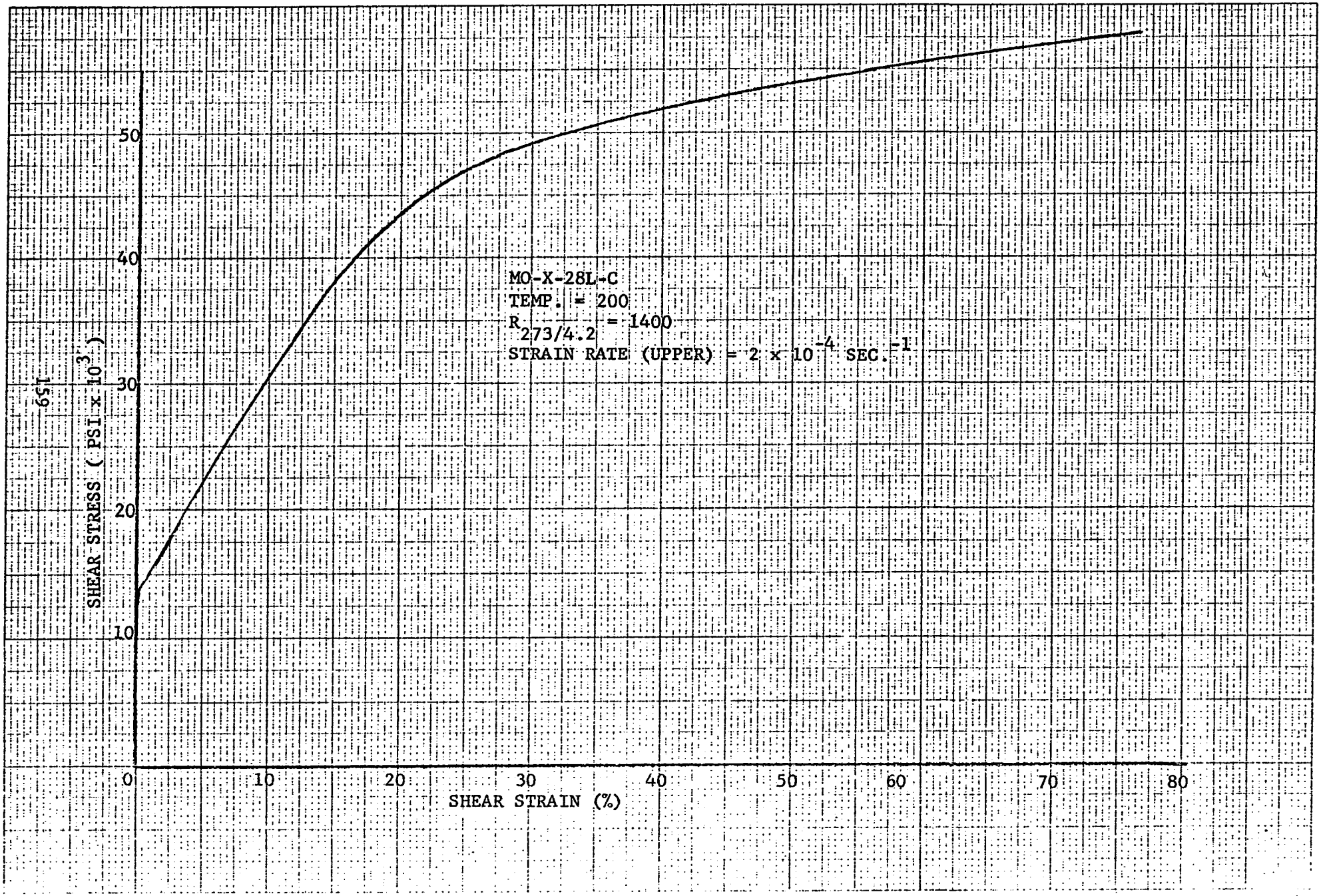

159

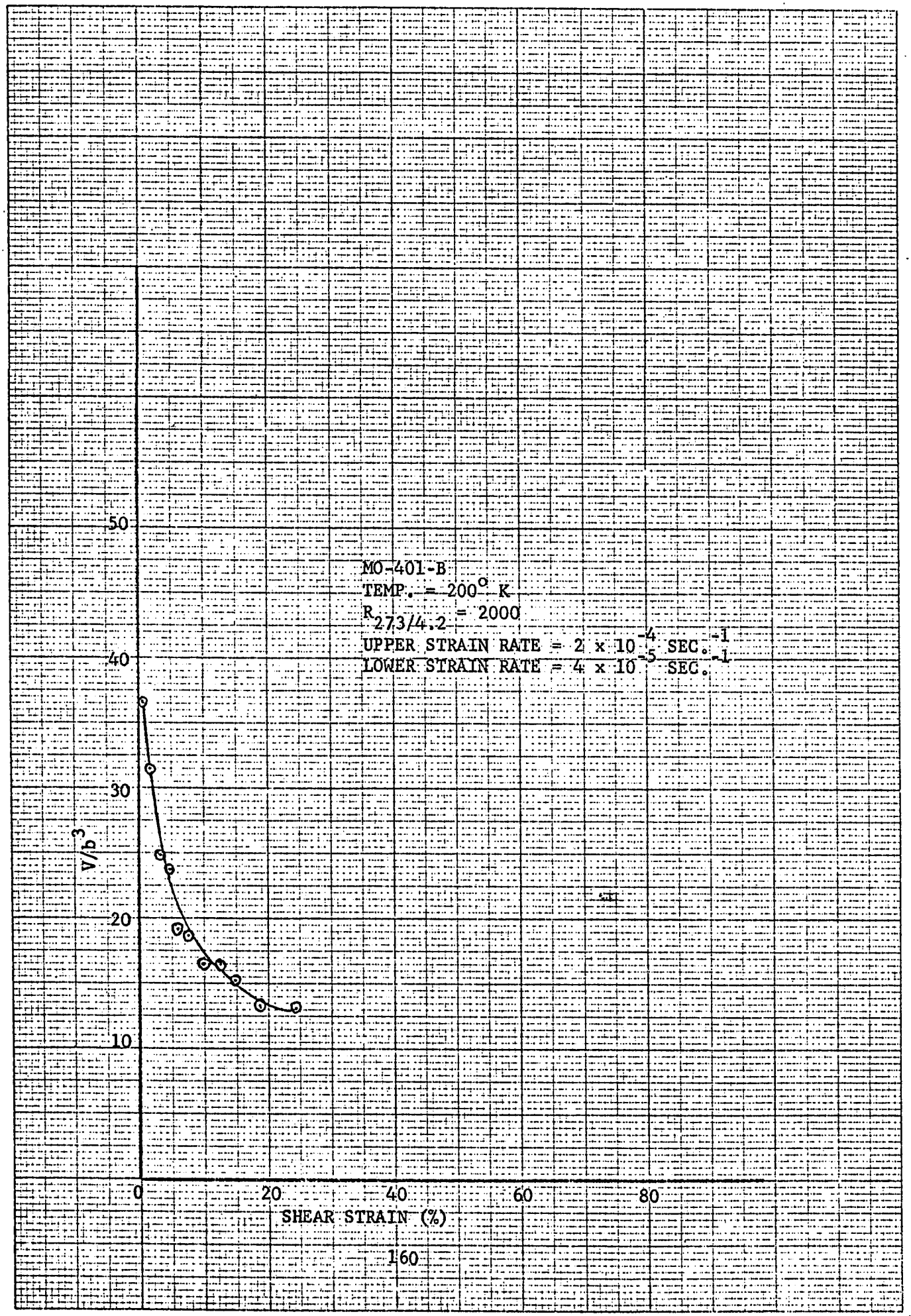

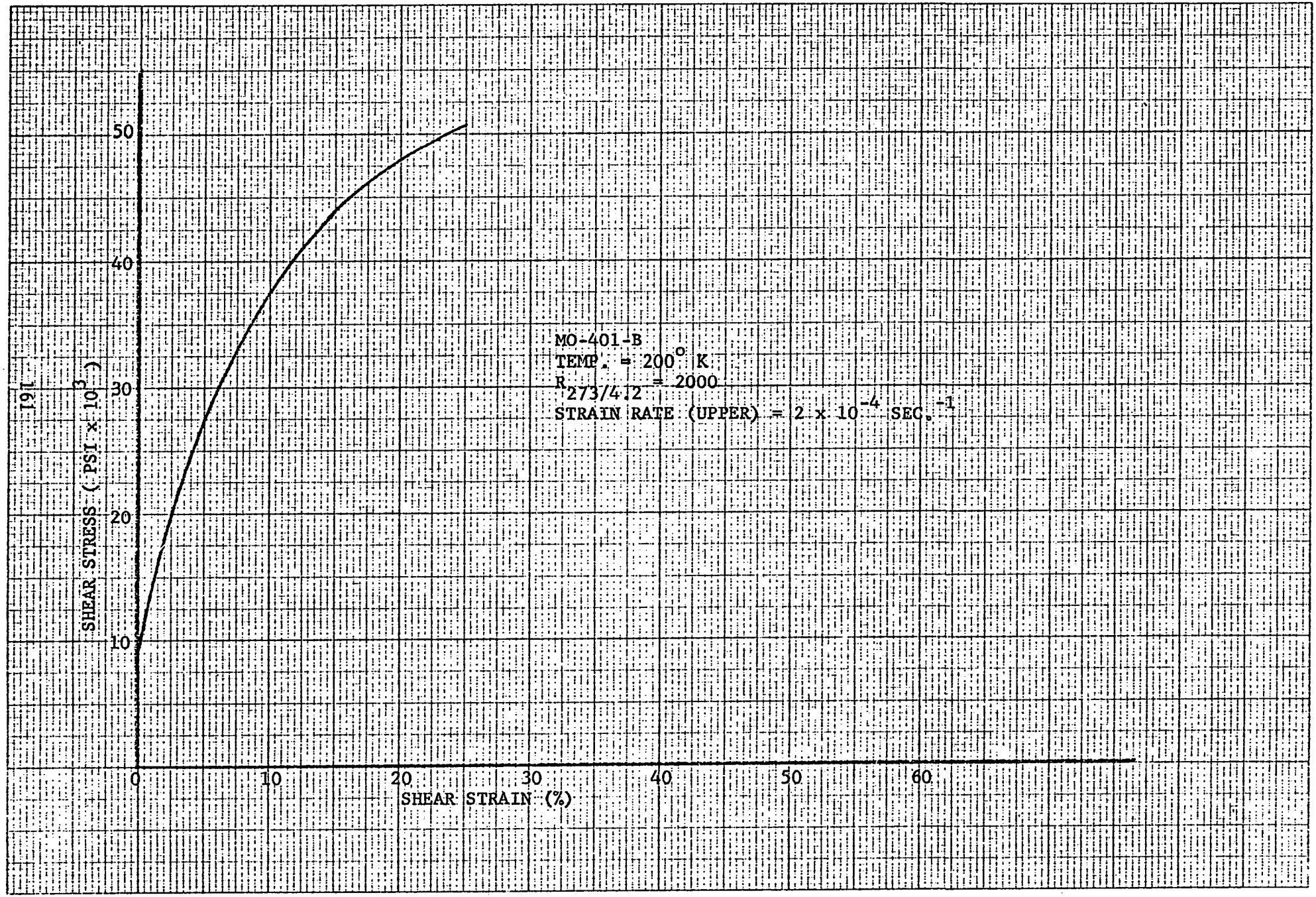

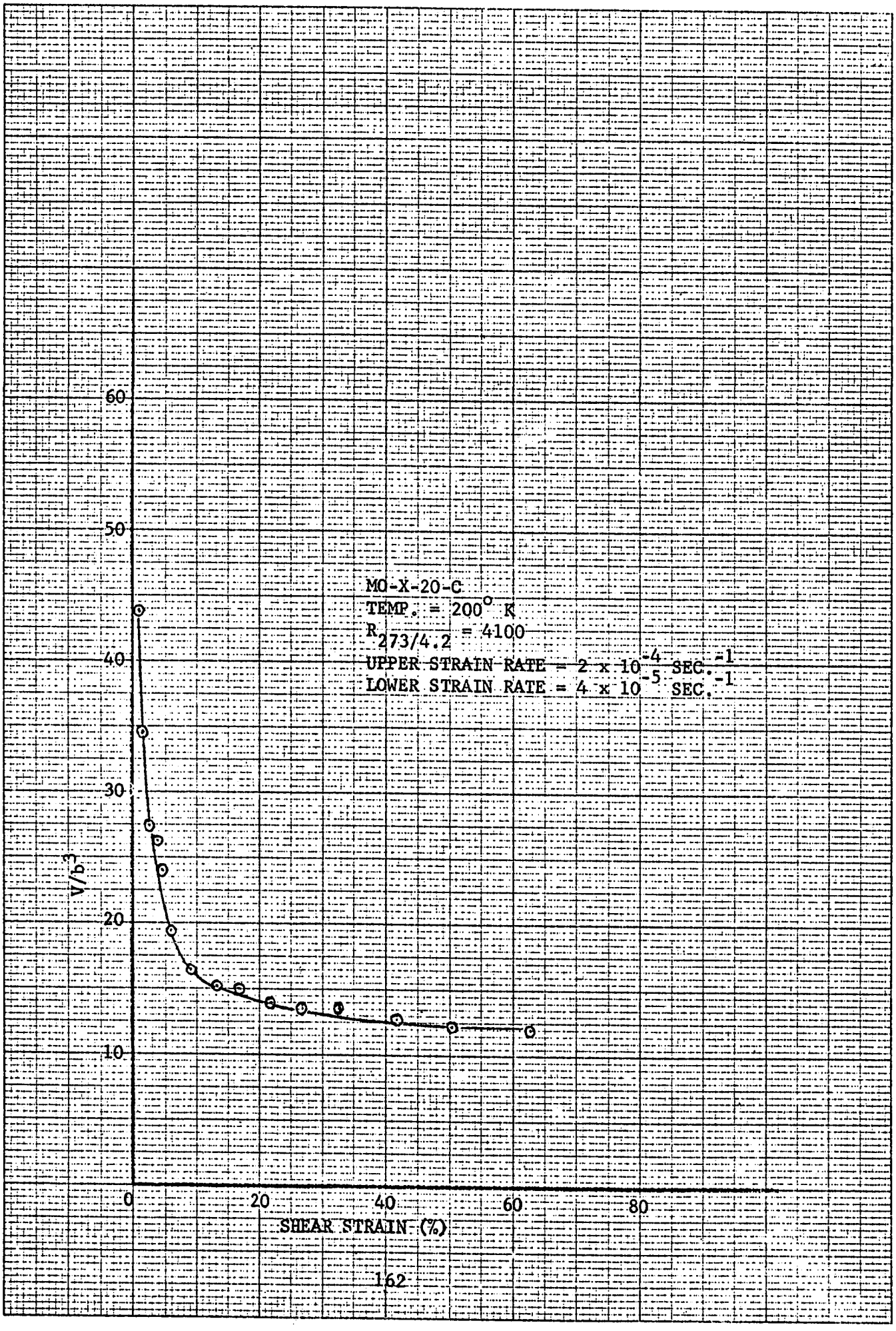

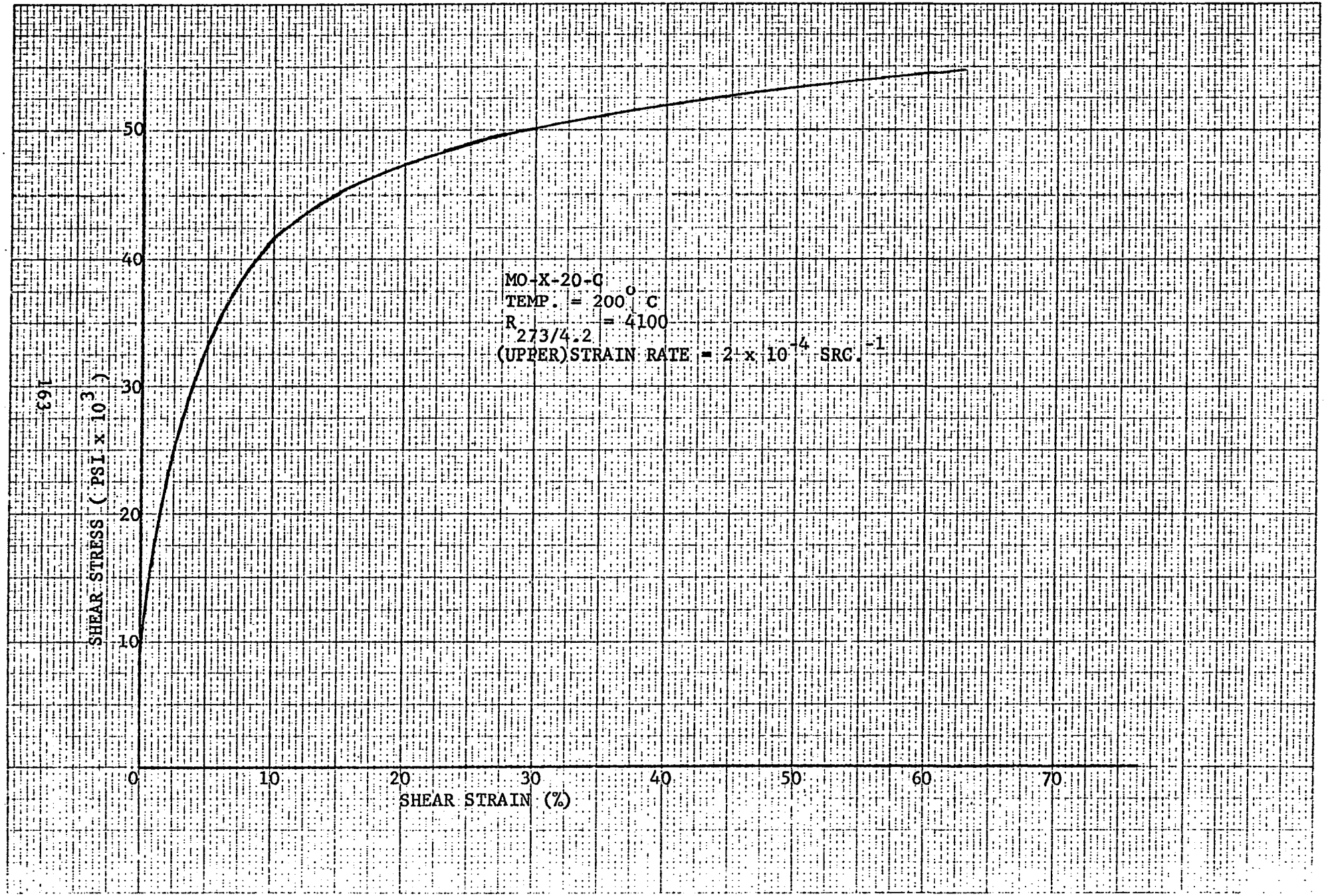

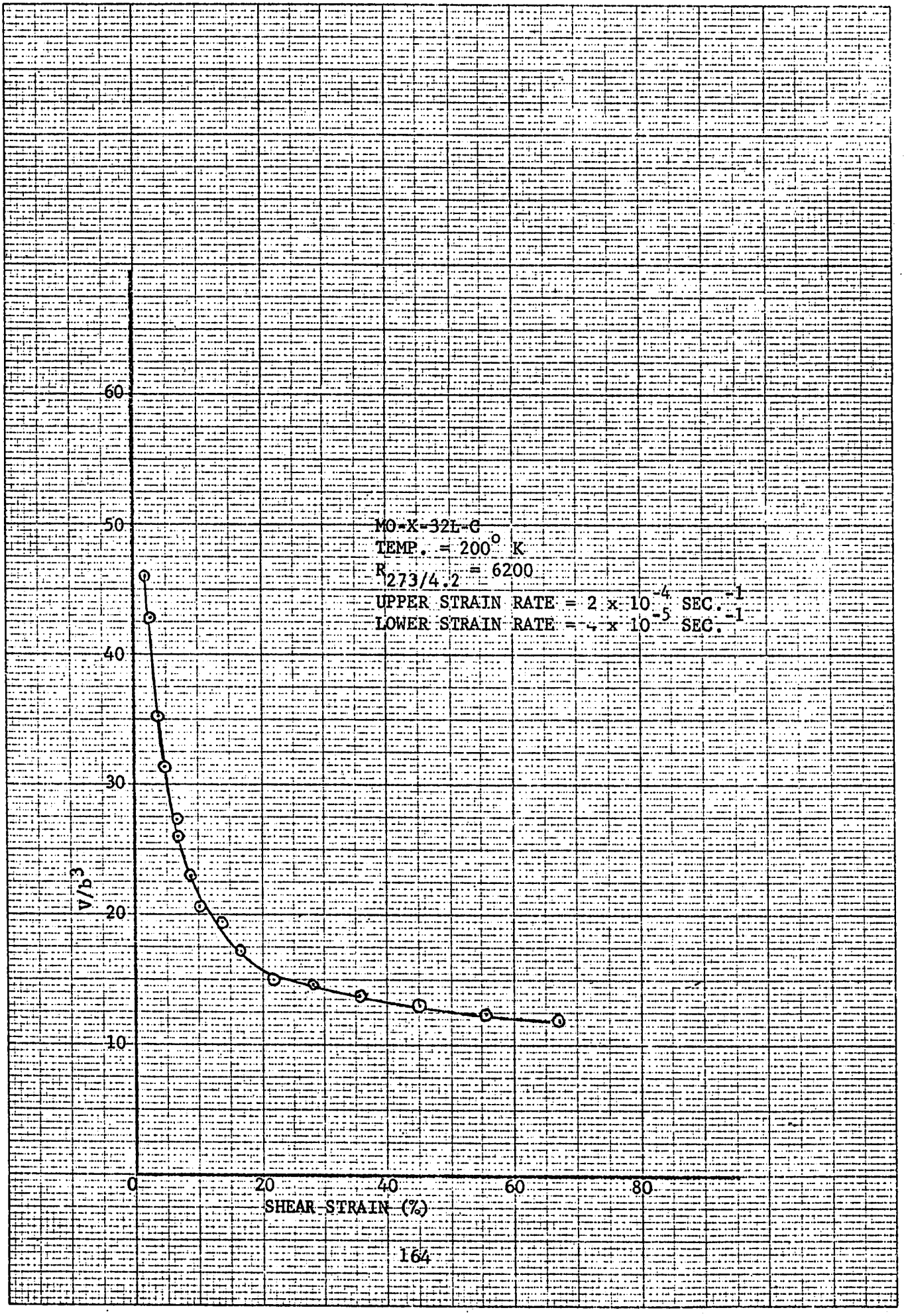

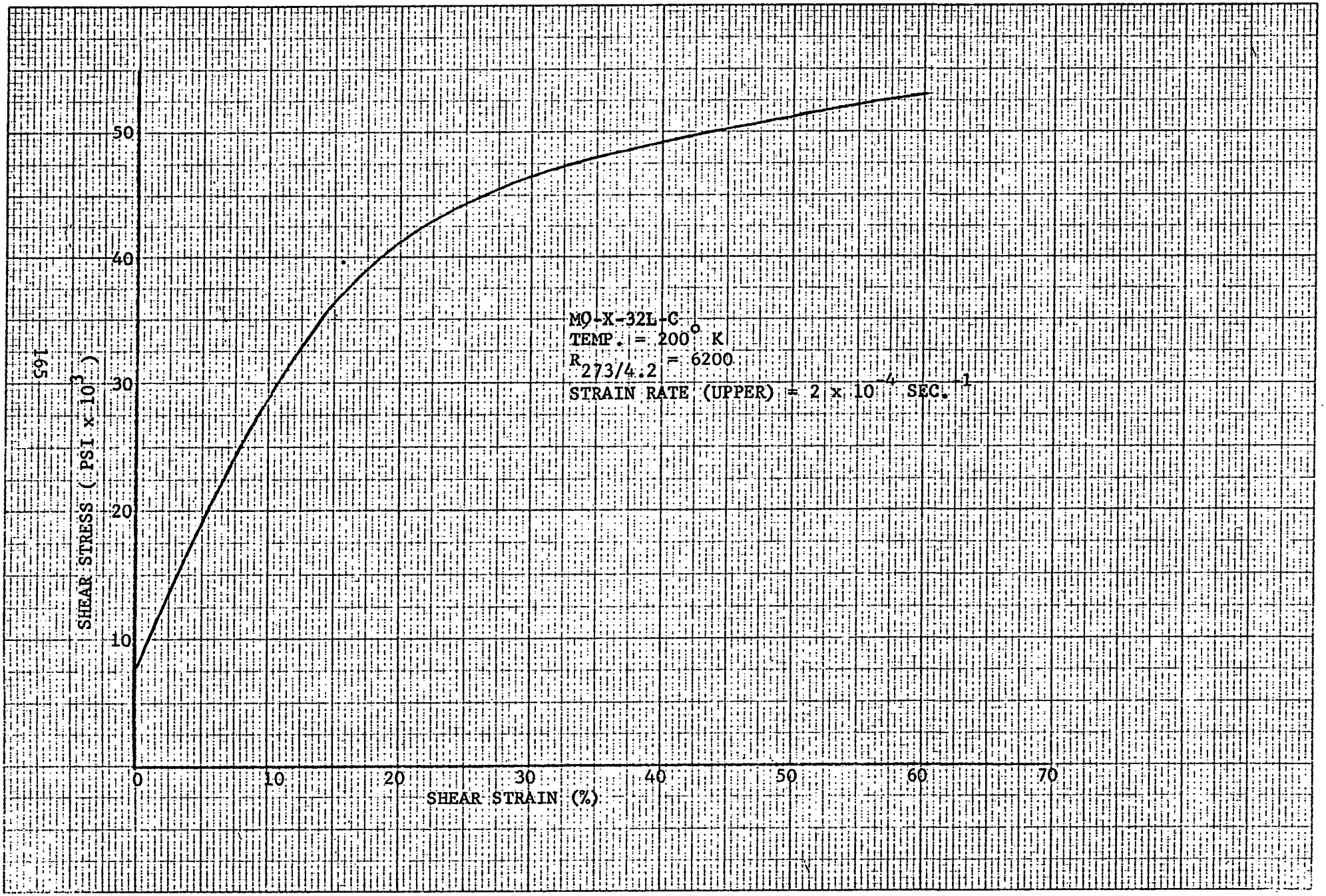

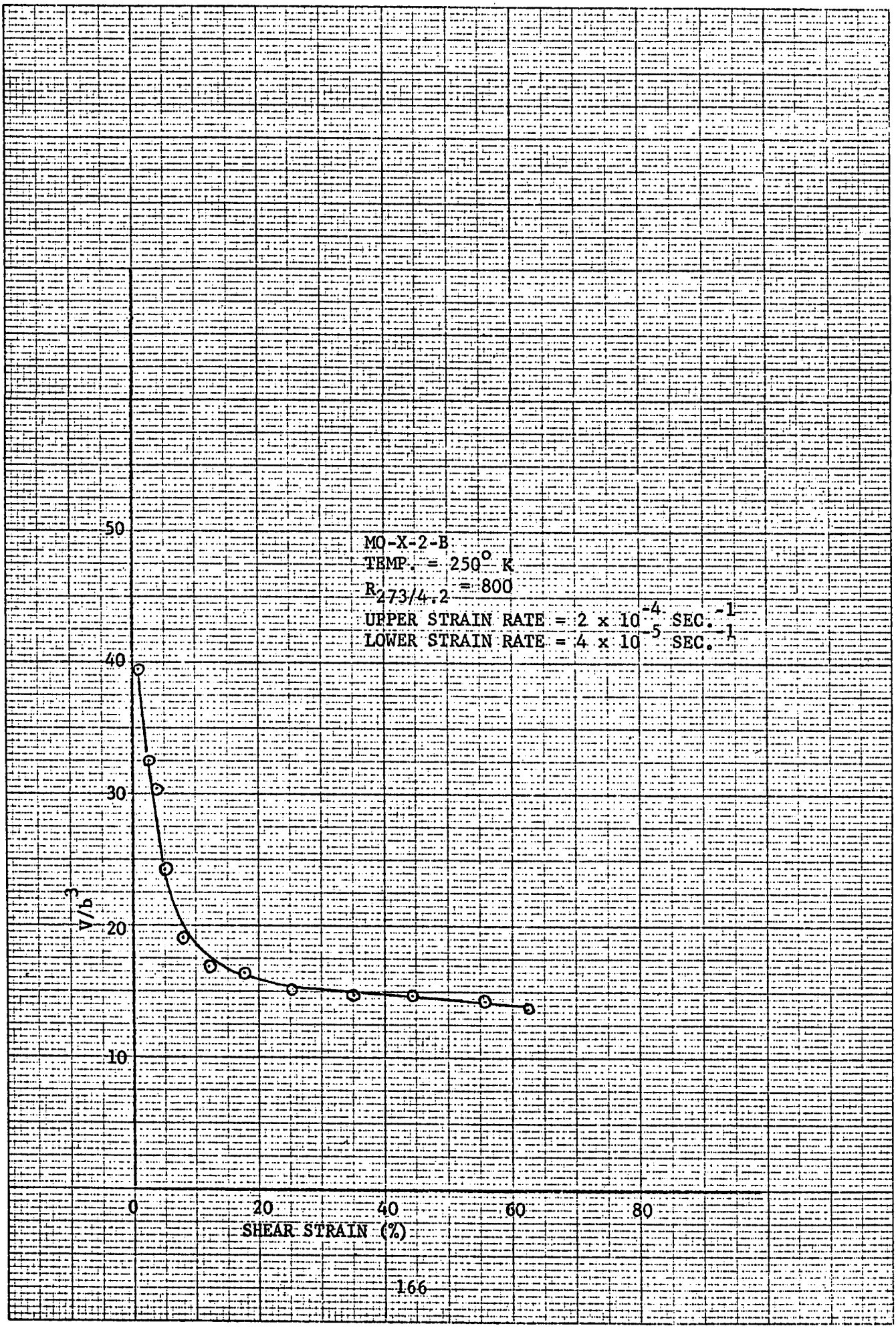

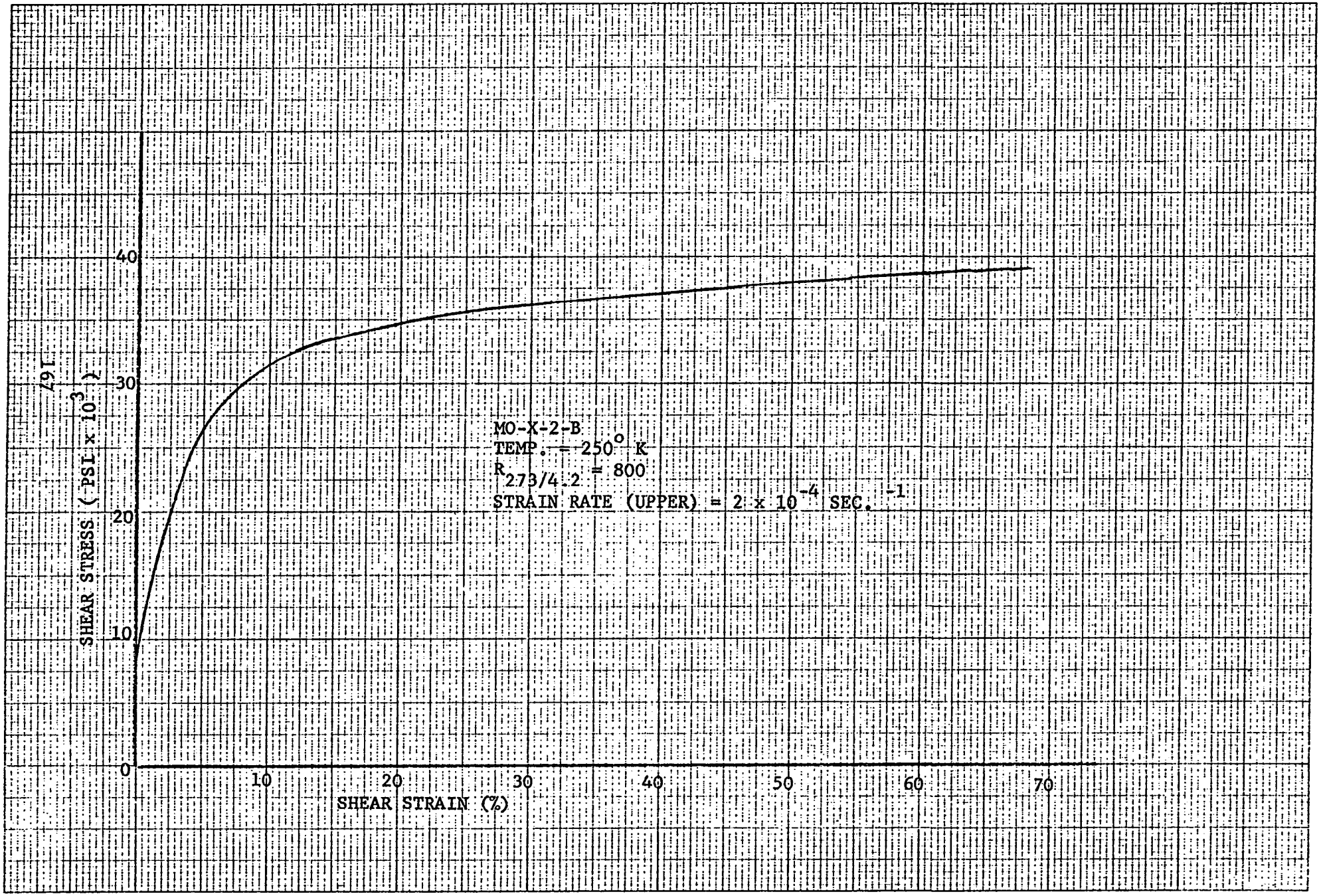

167

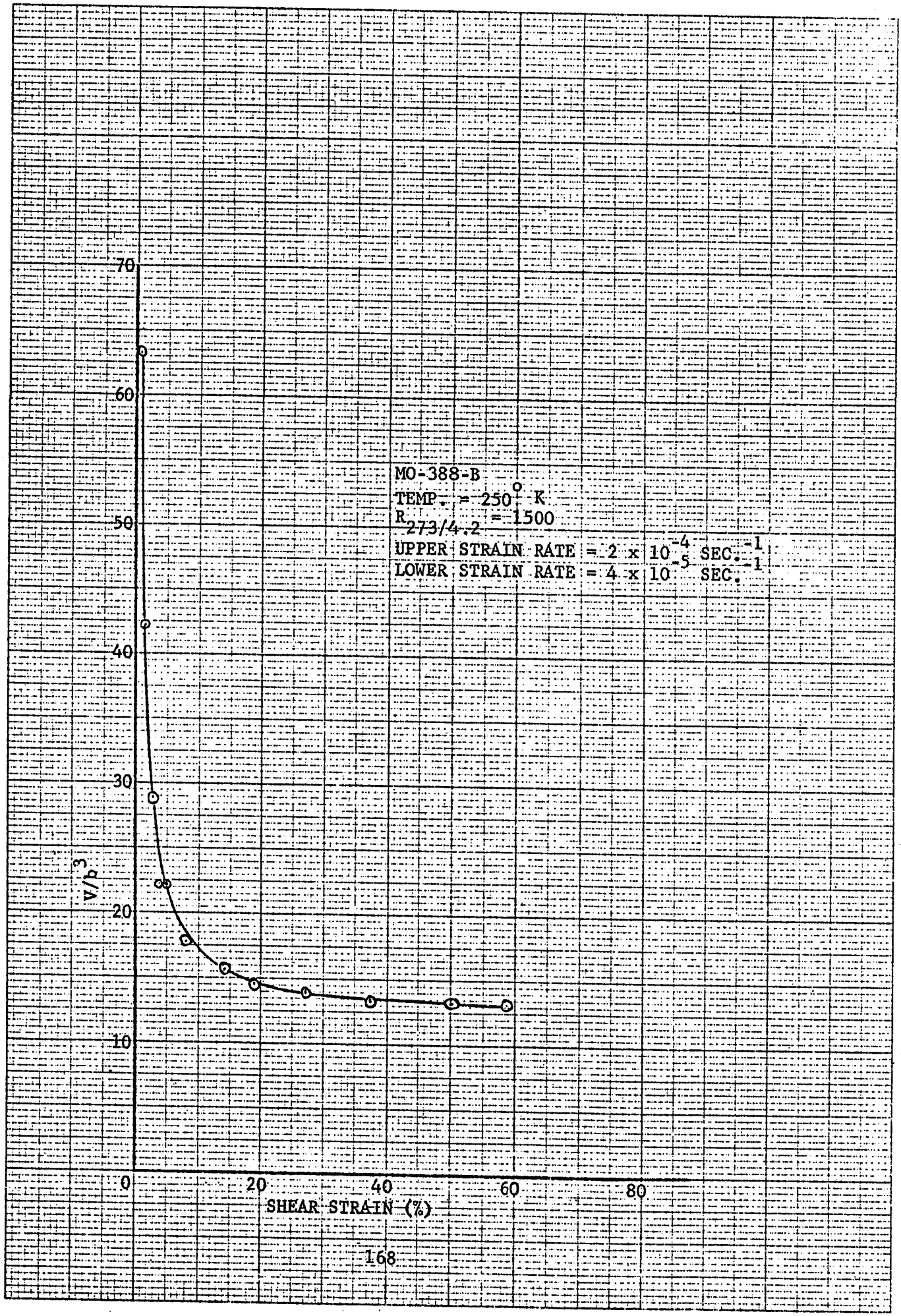

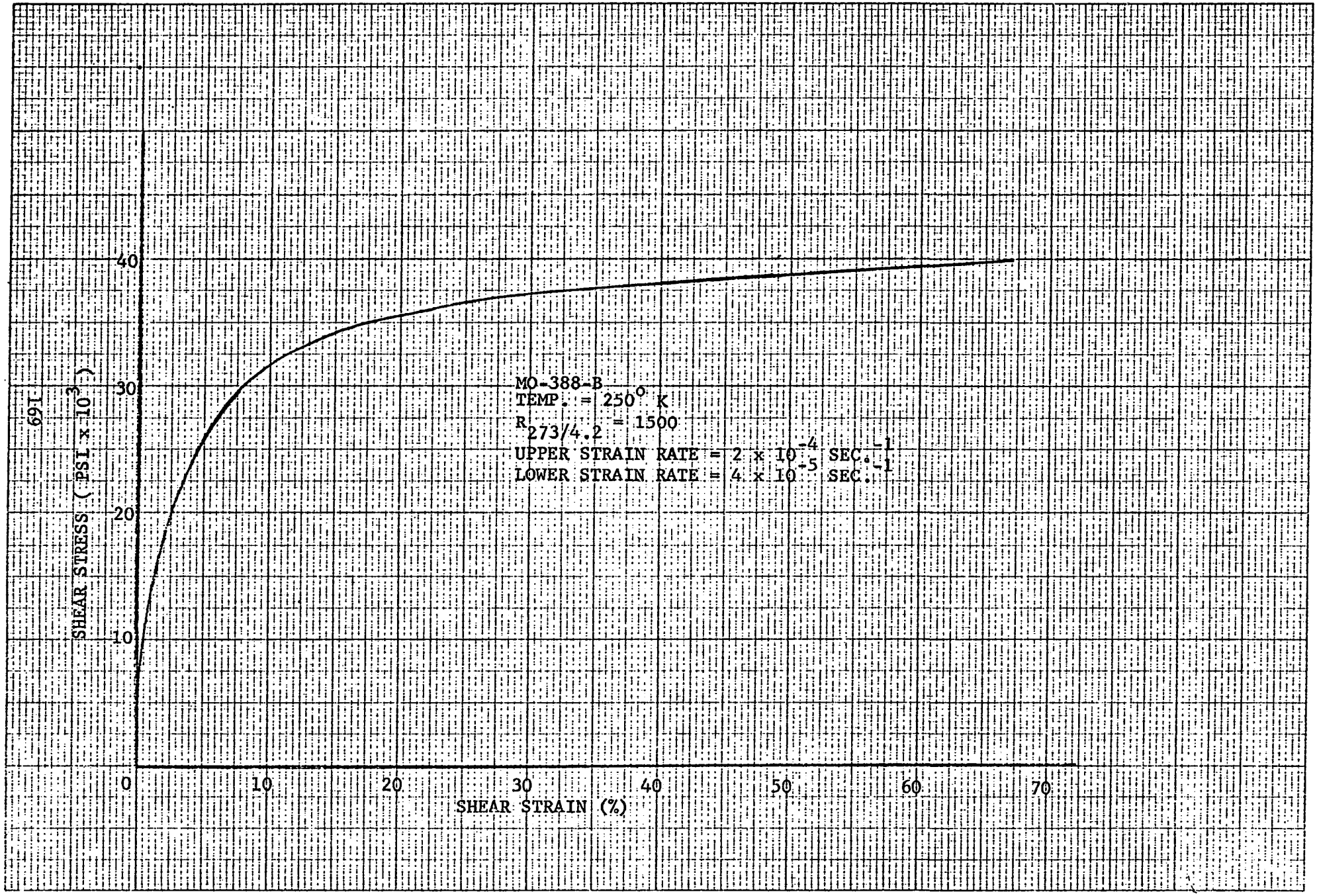

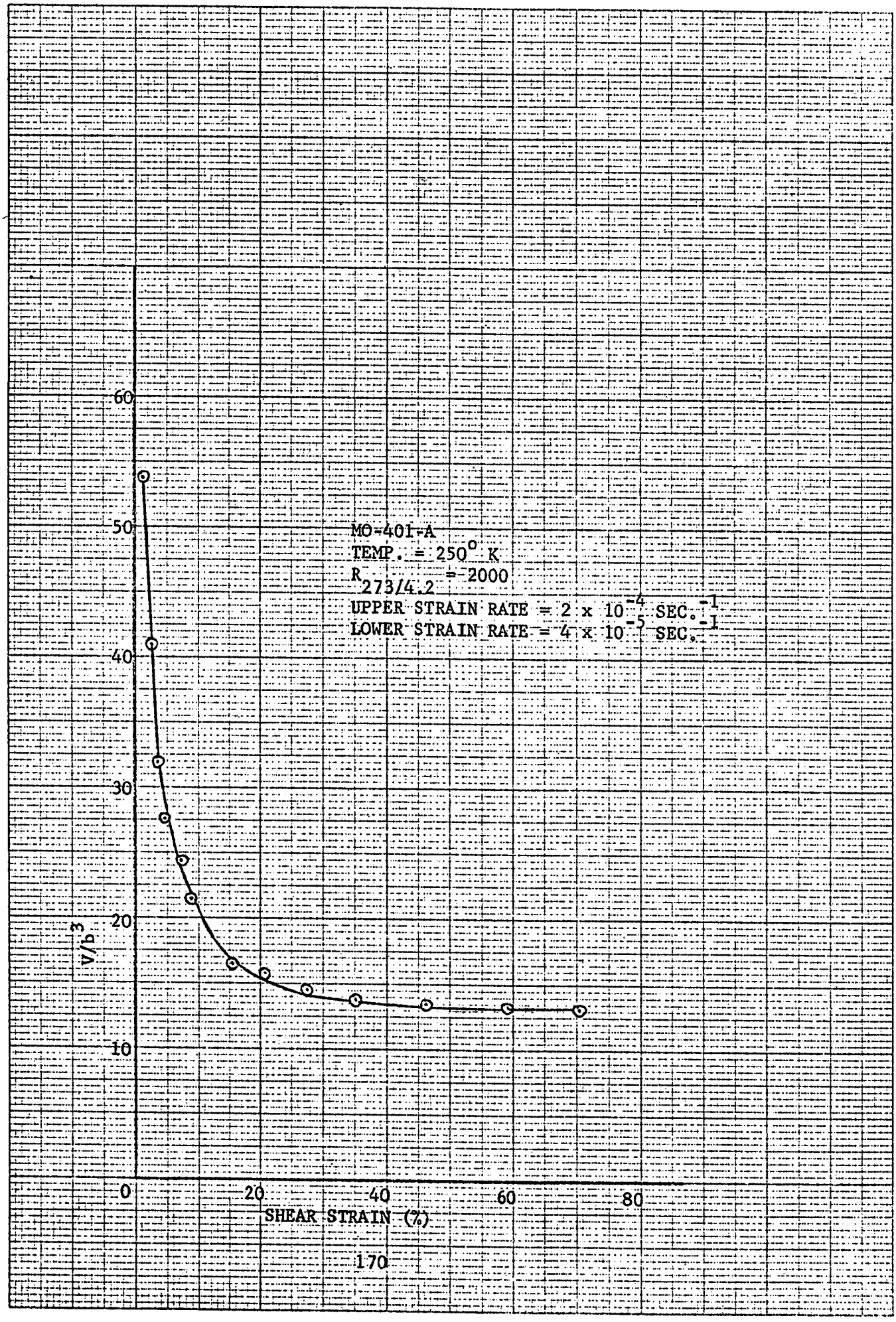

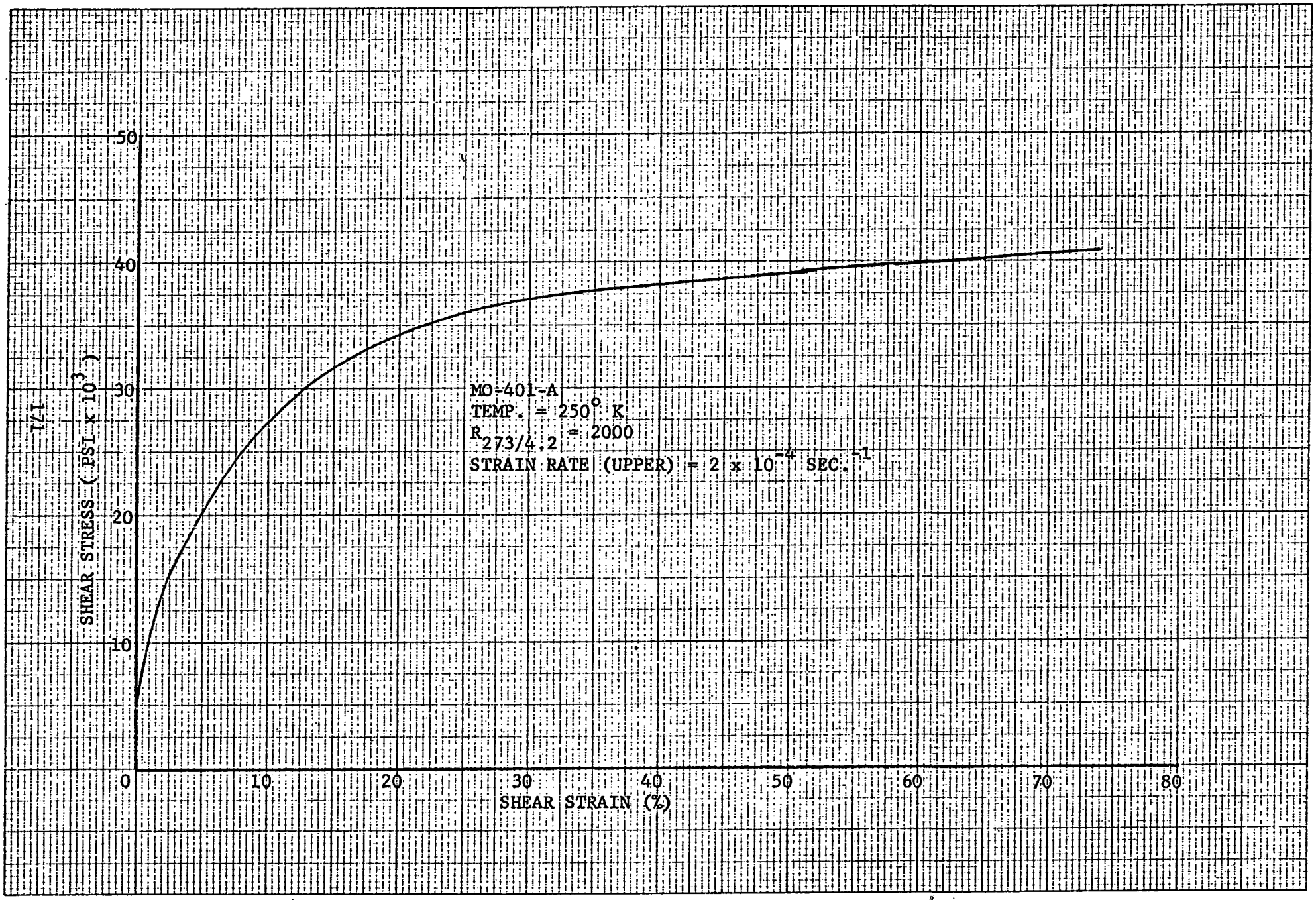

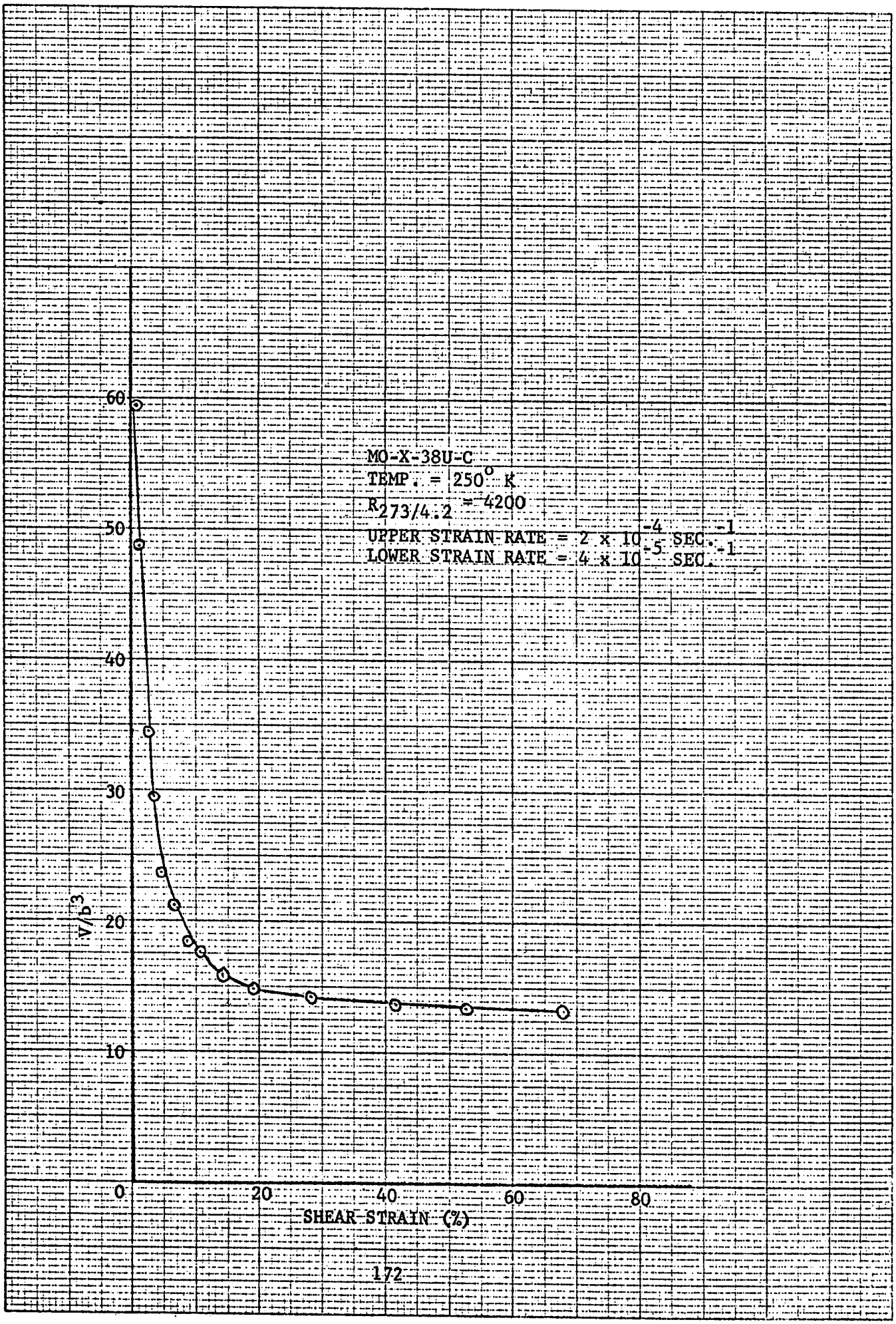

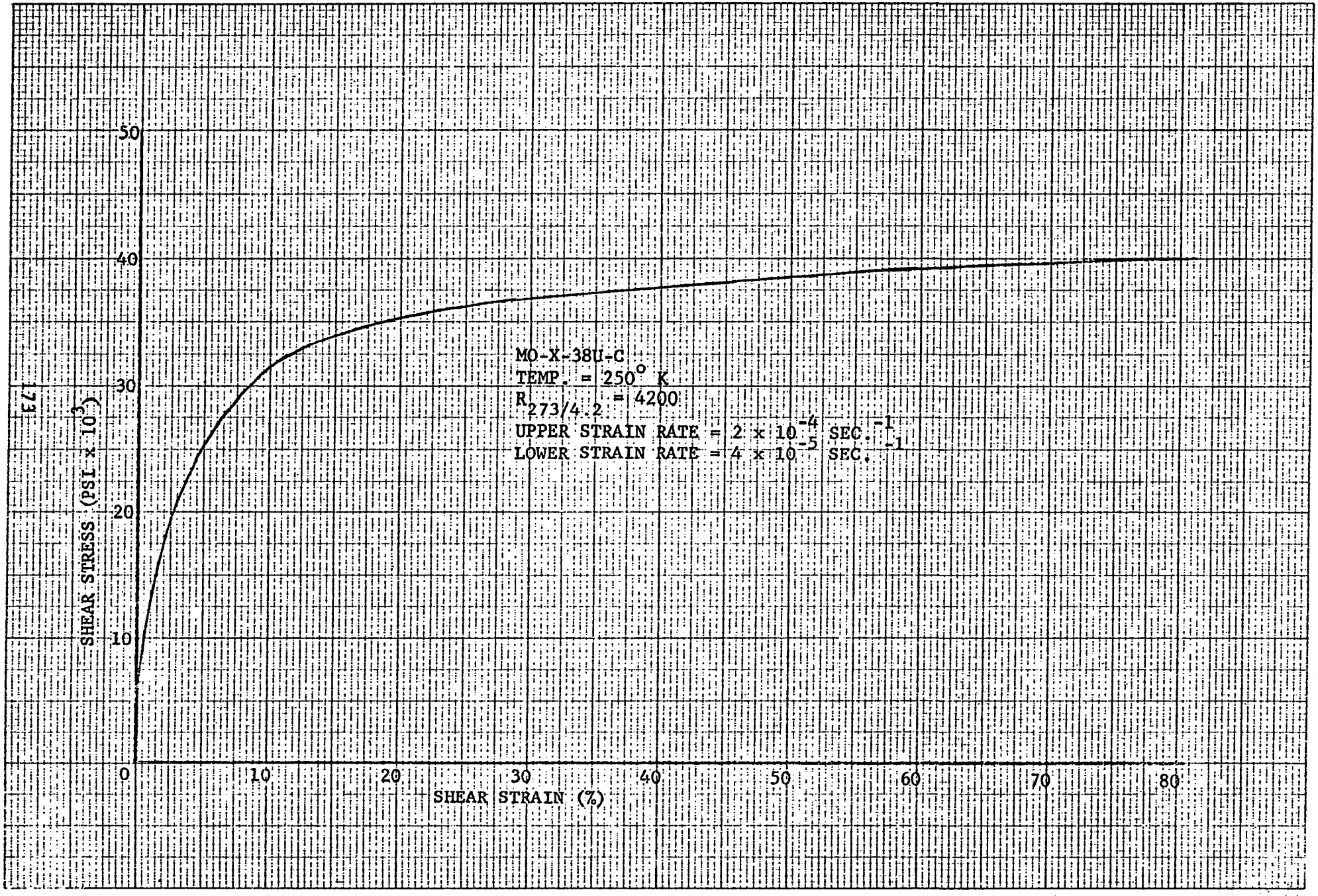

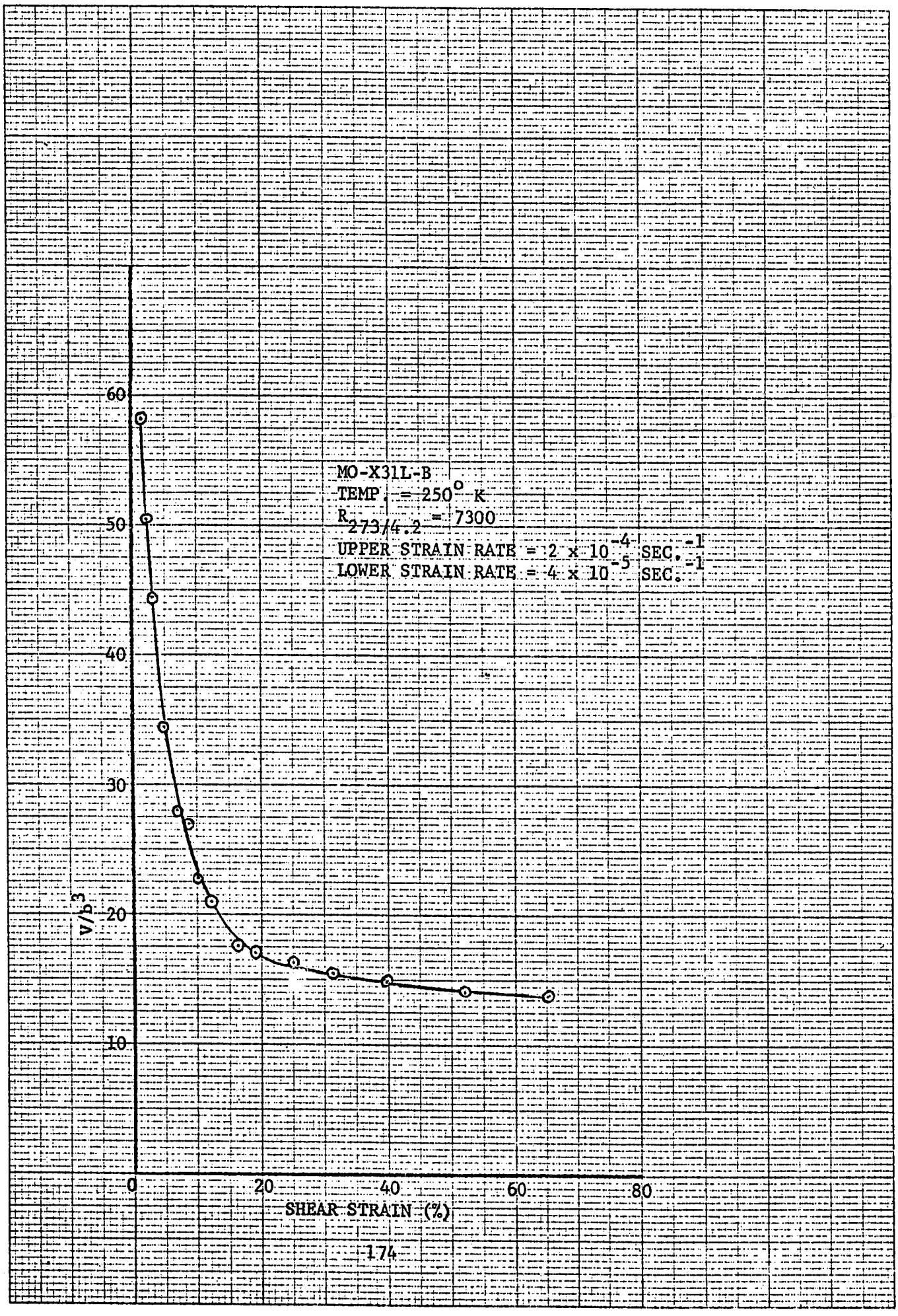

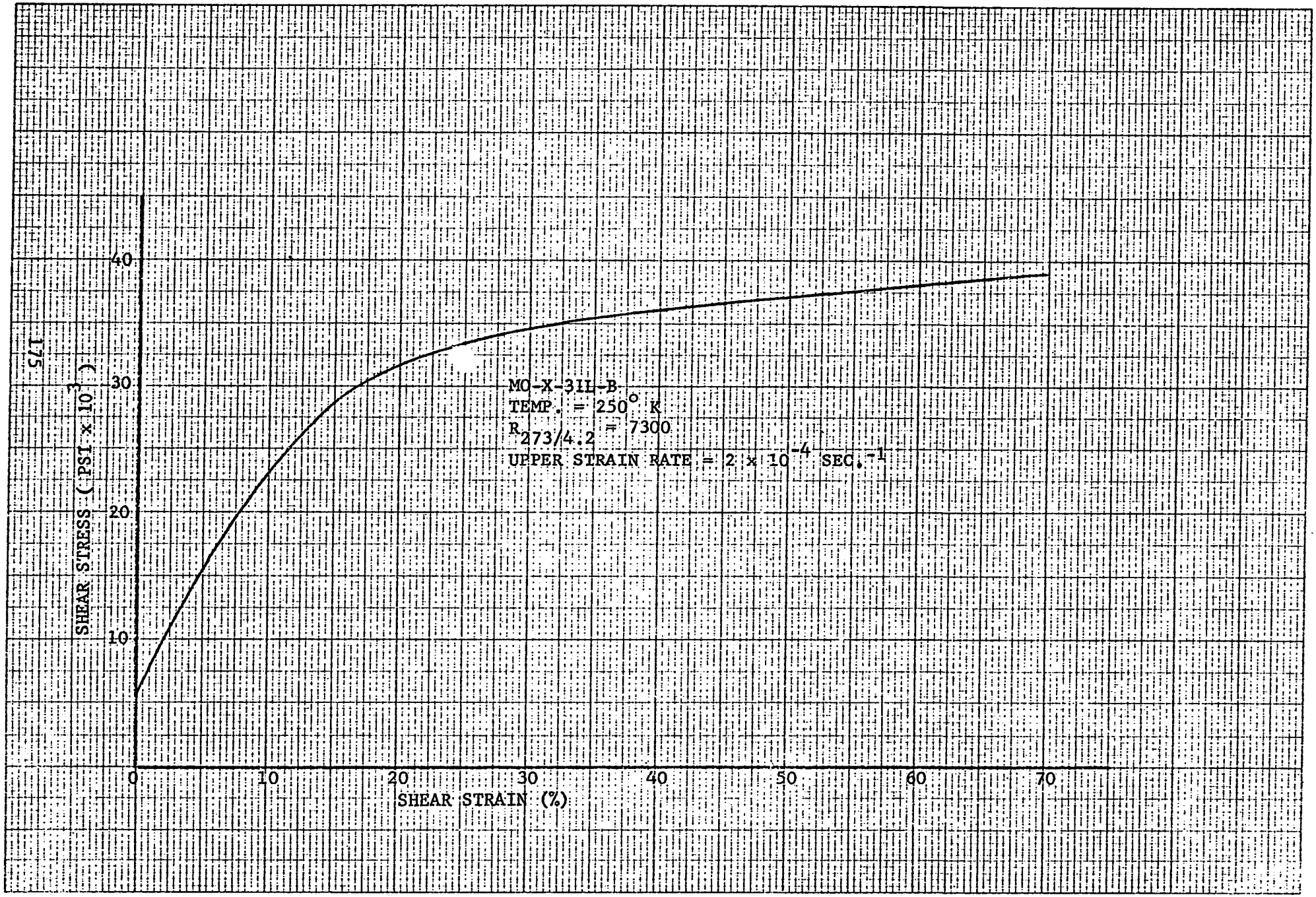

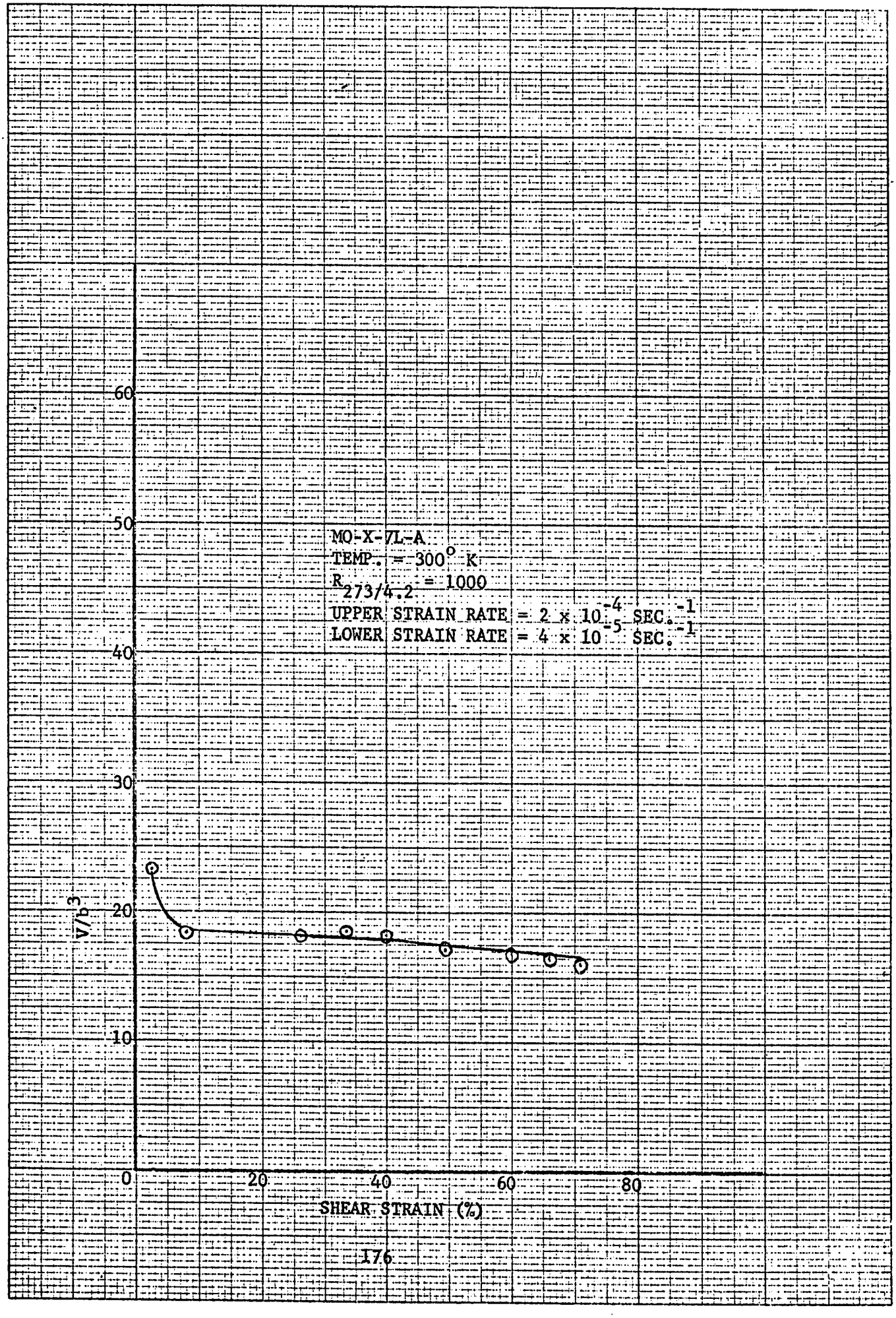

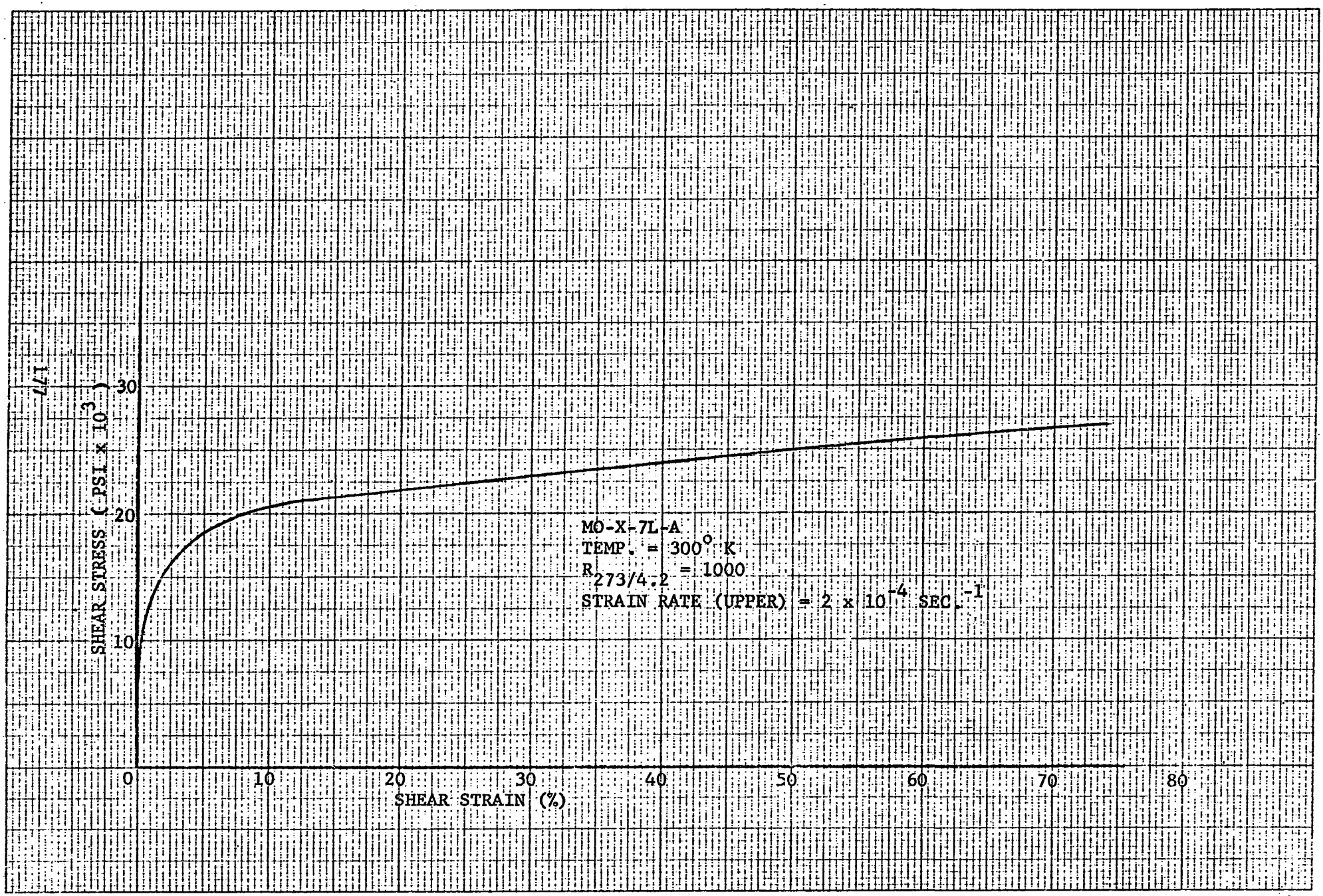

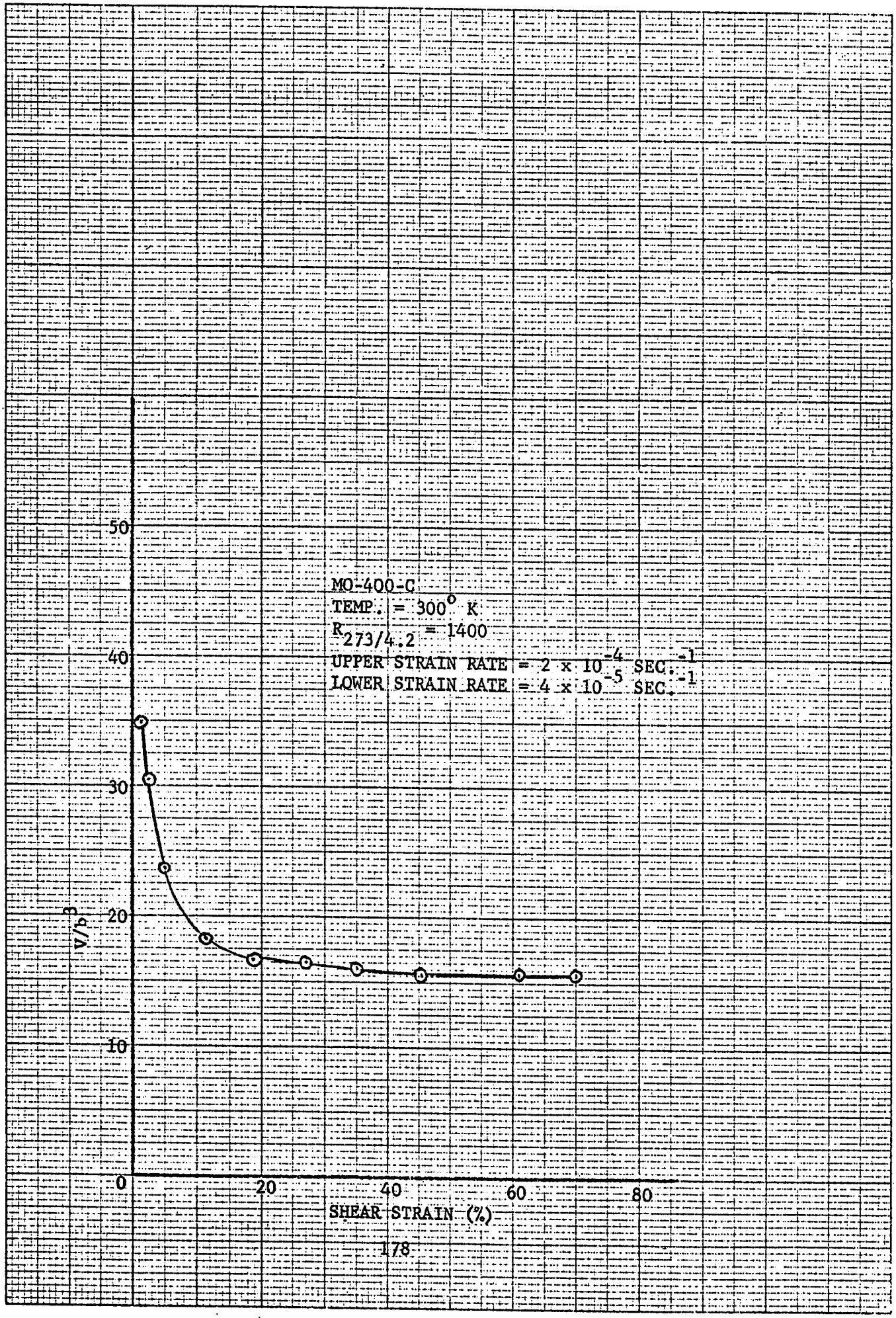

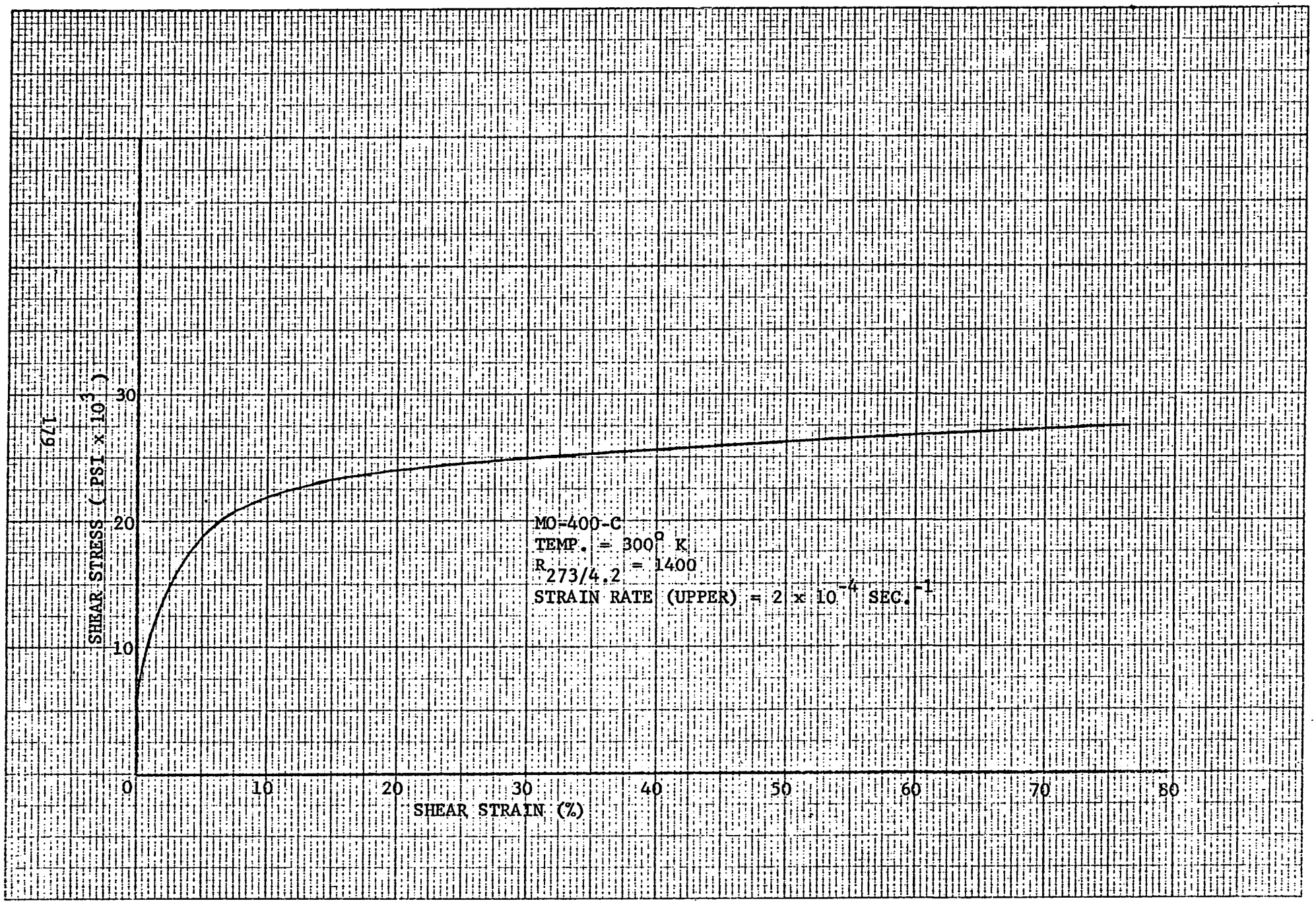

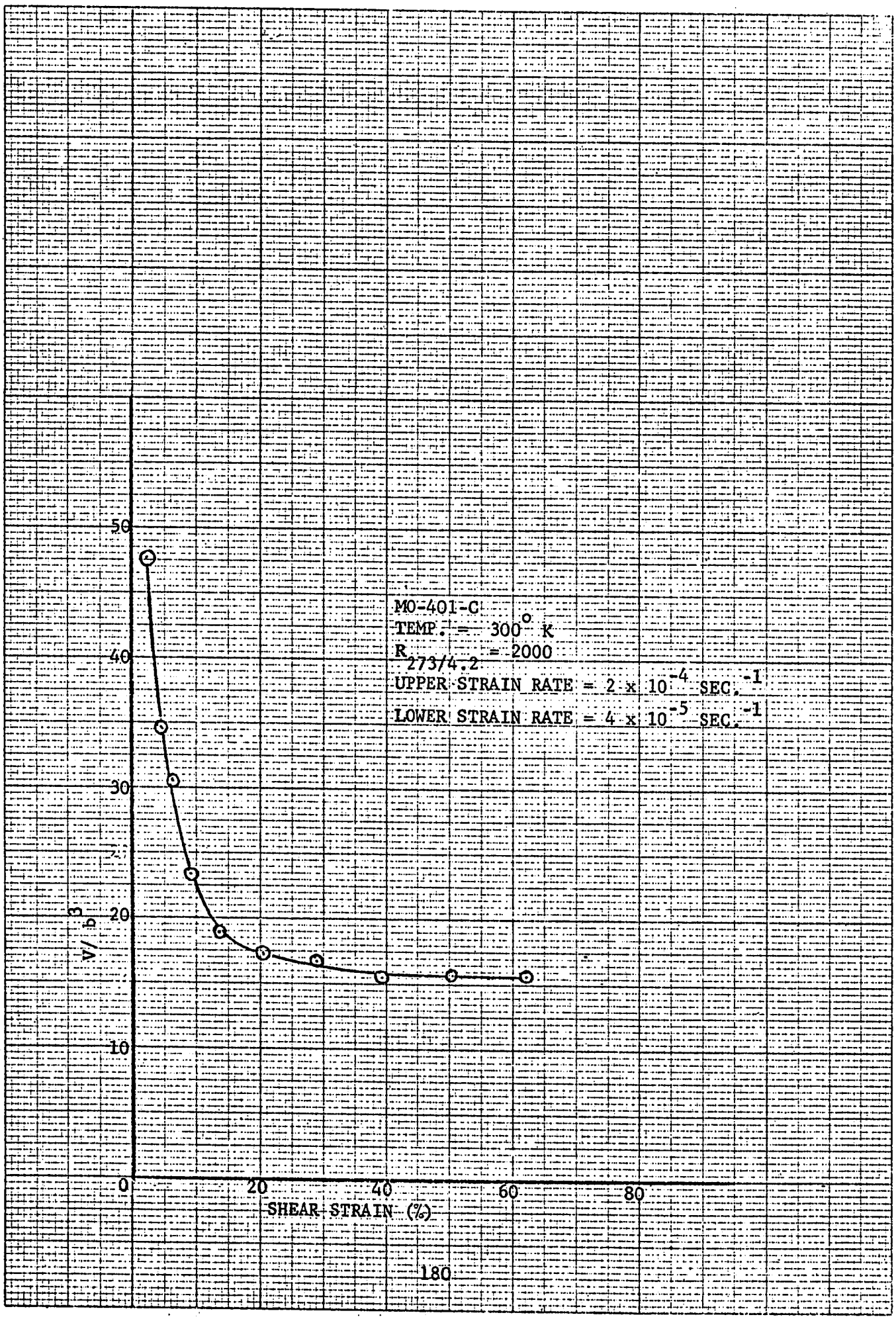

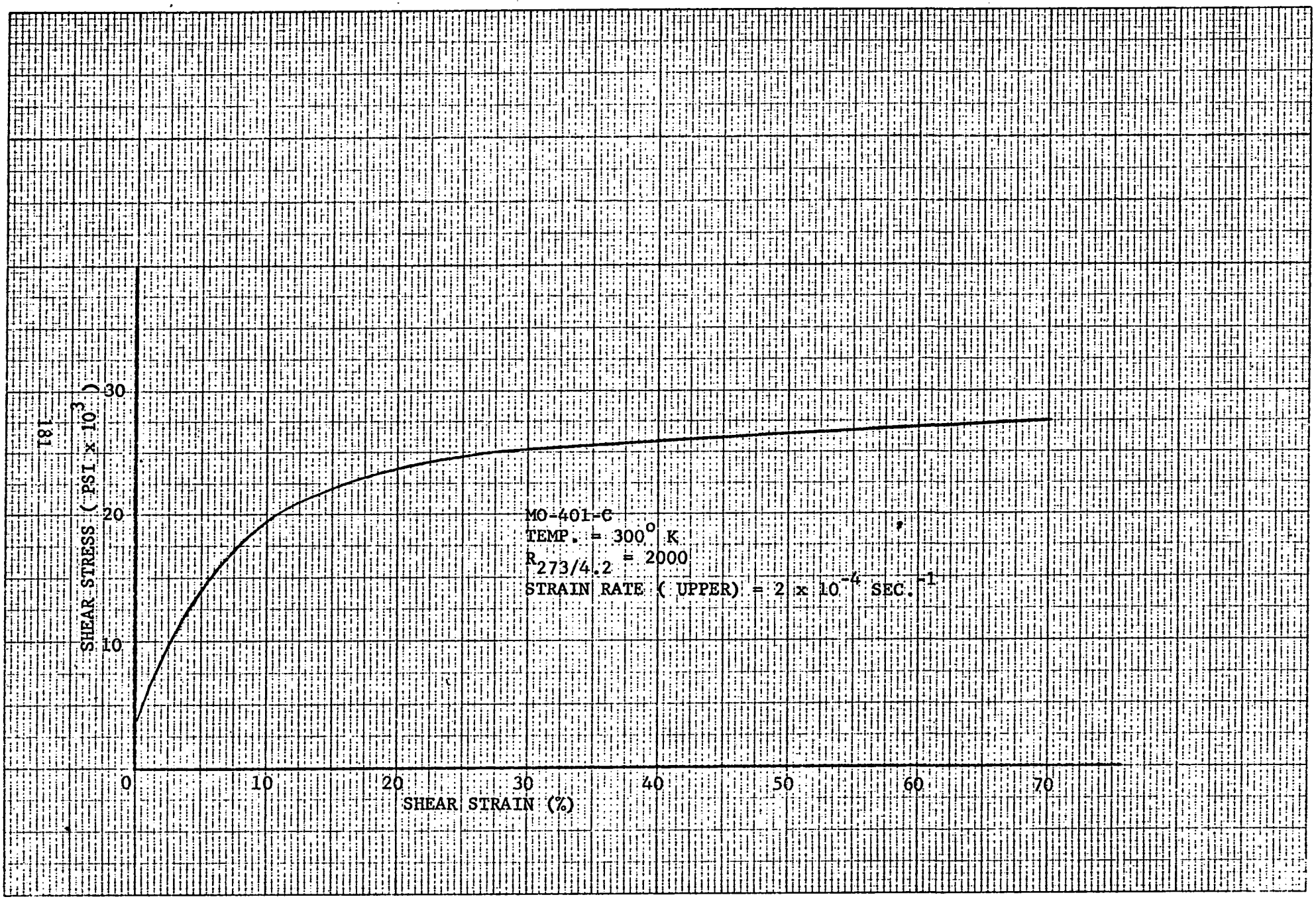

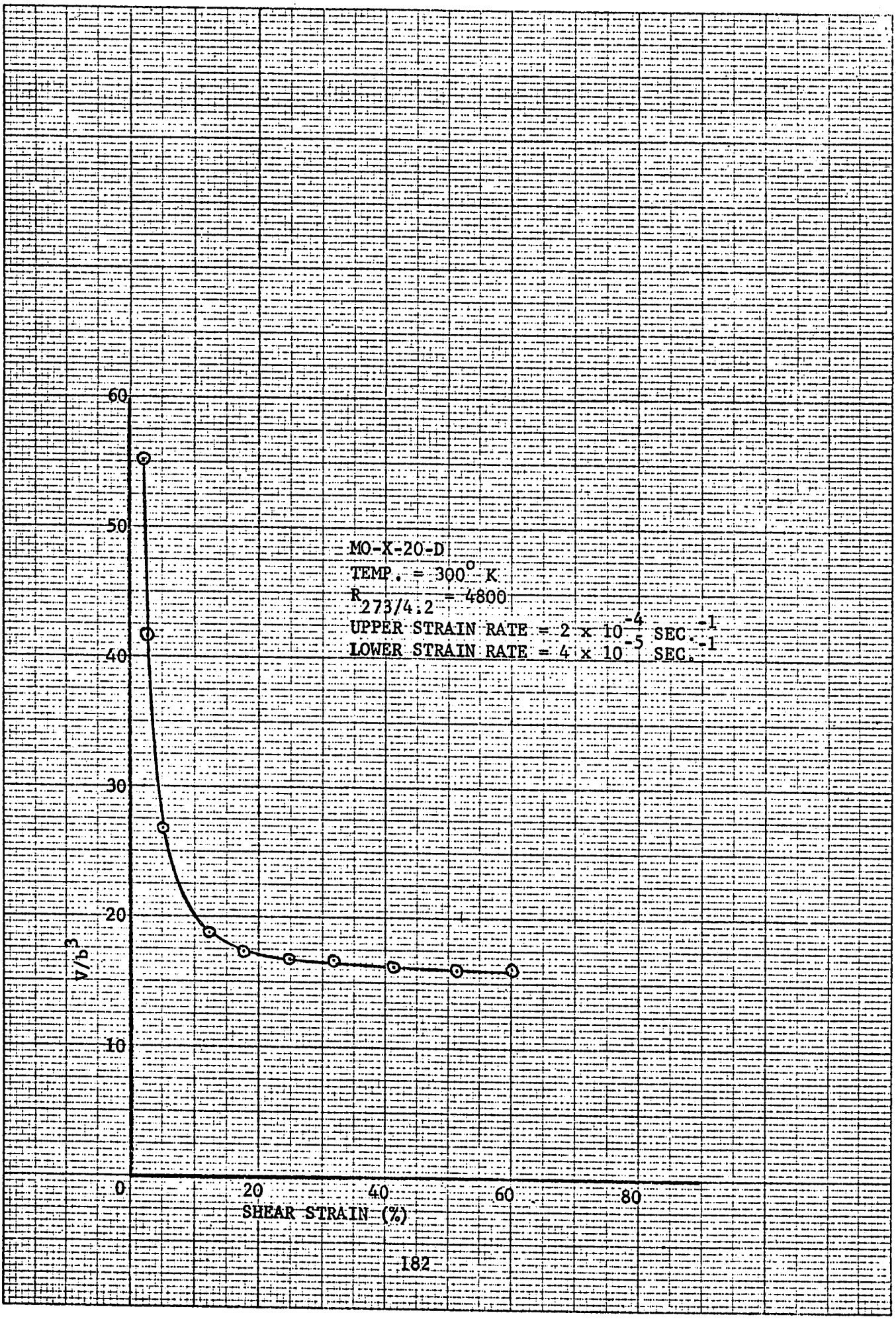

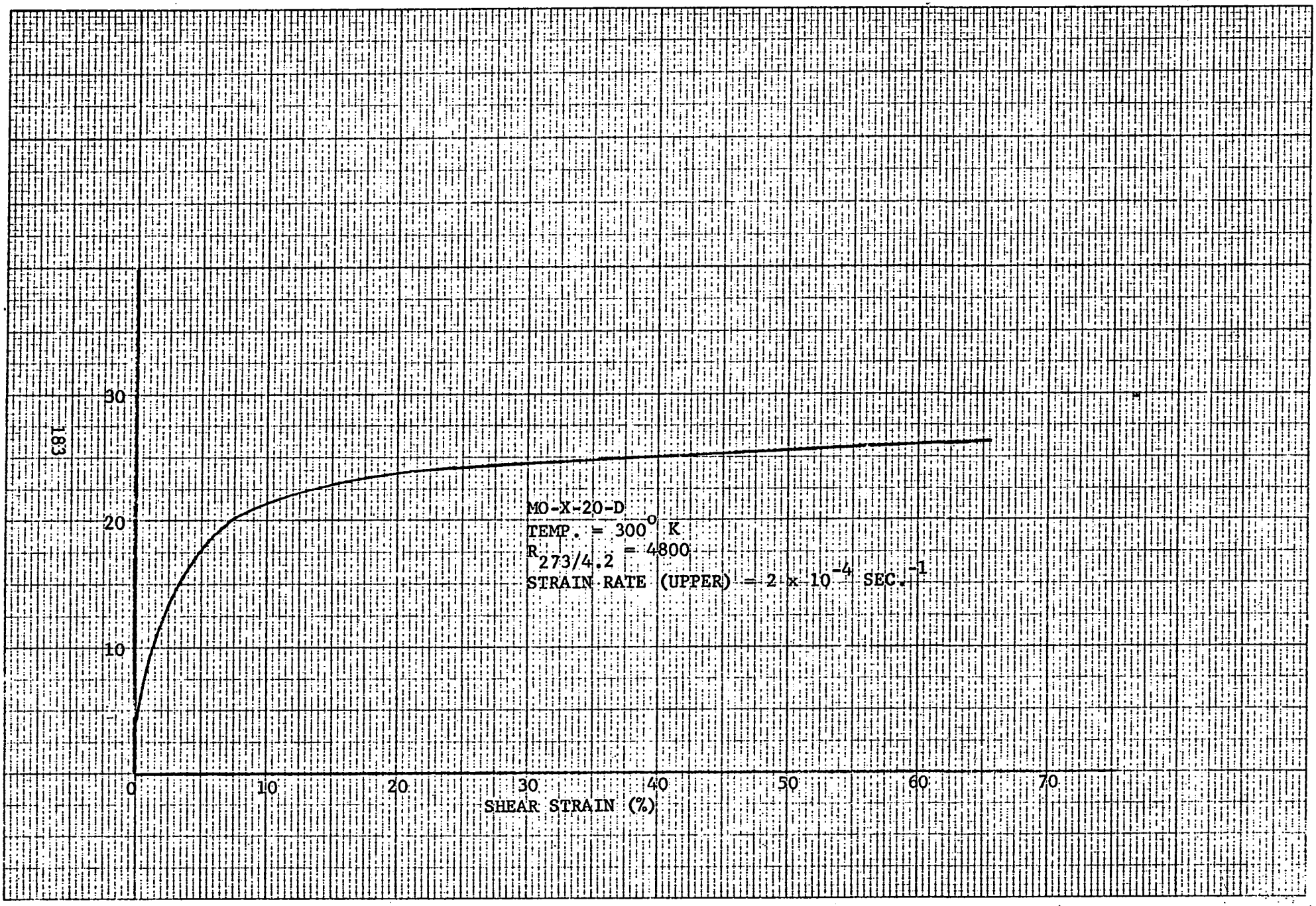

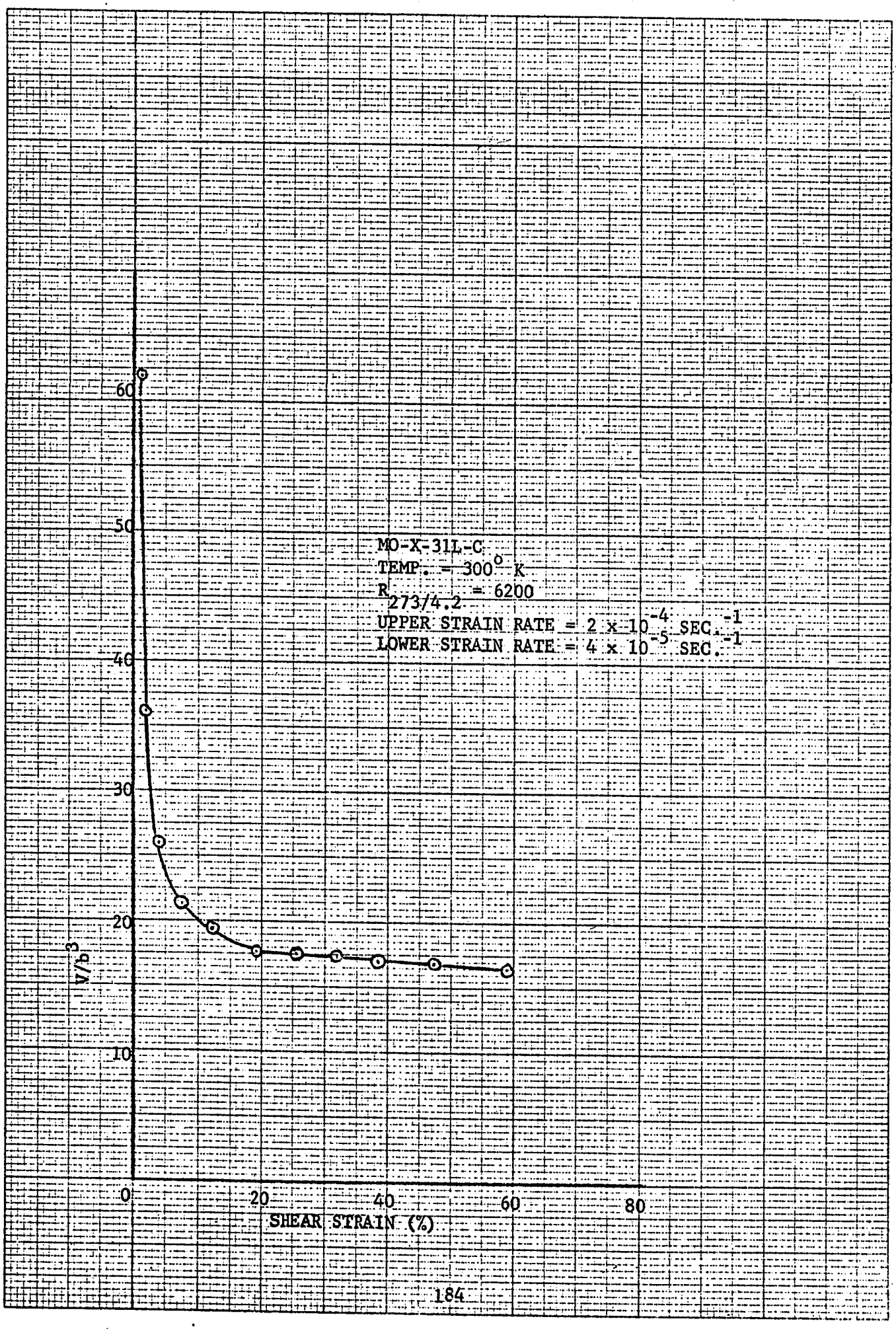

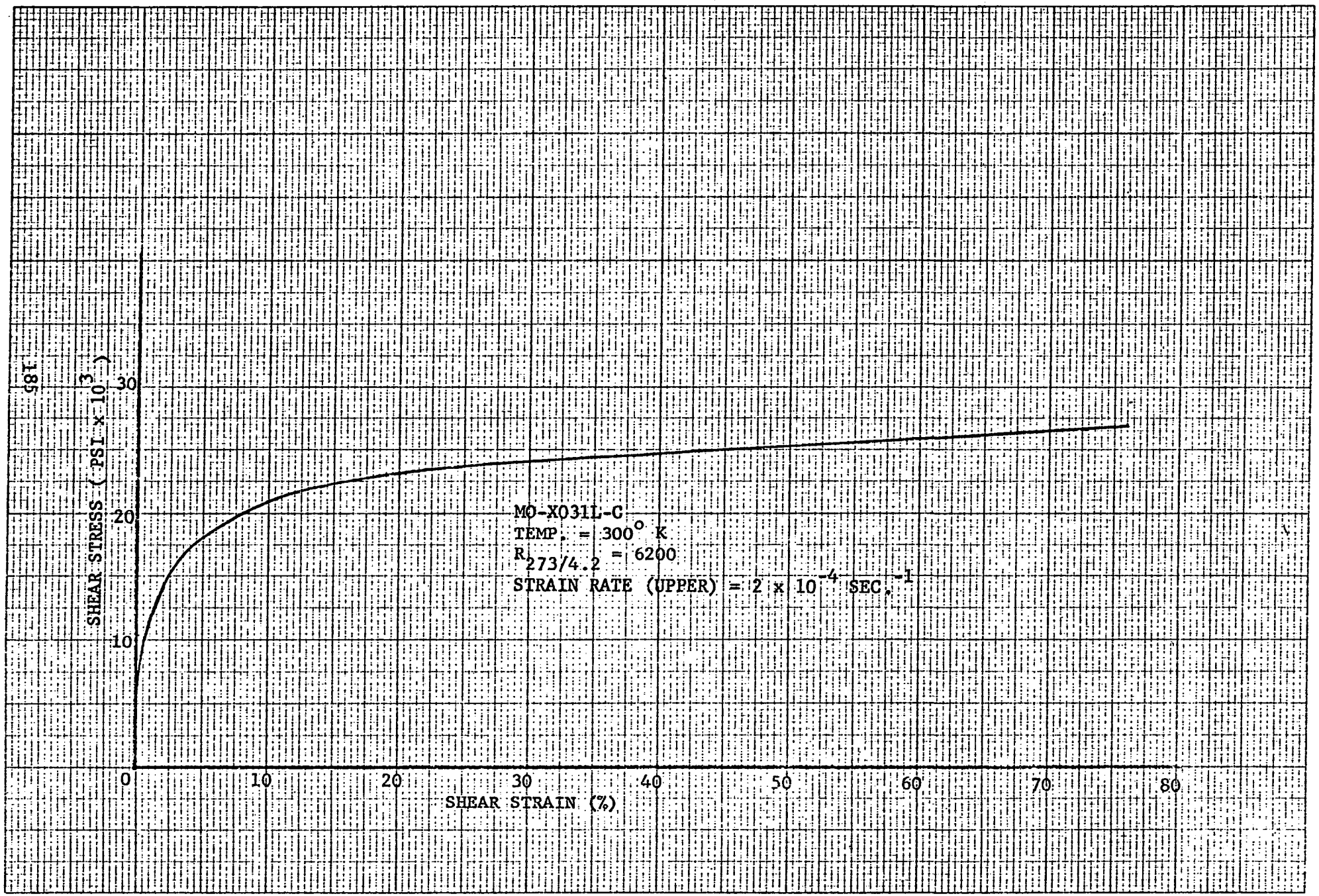

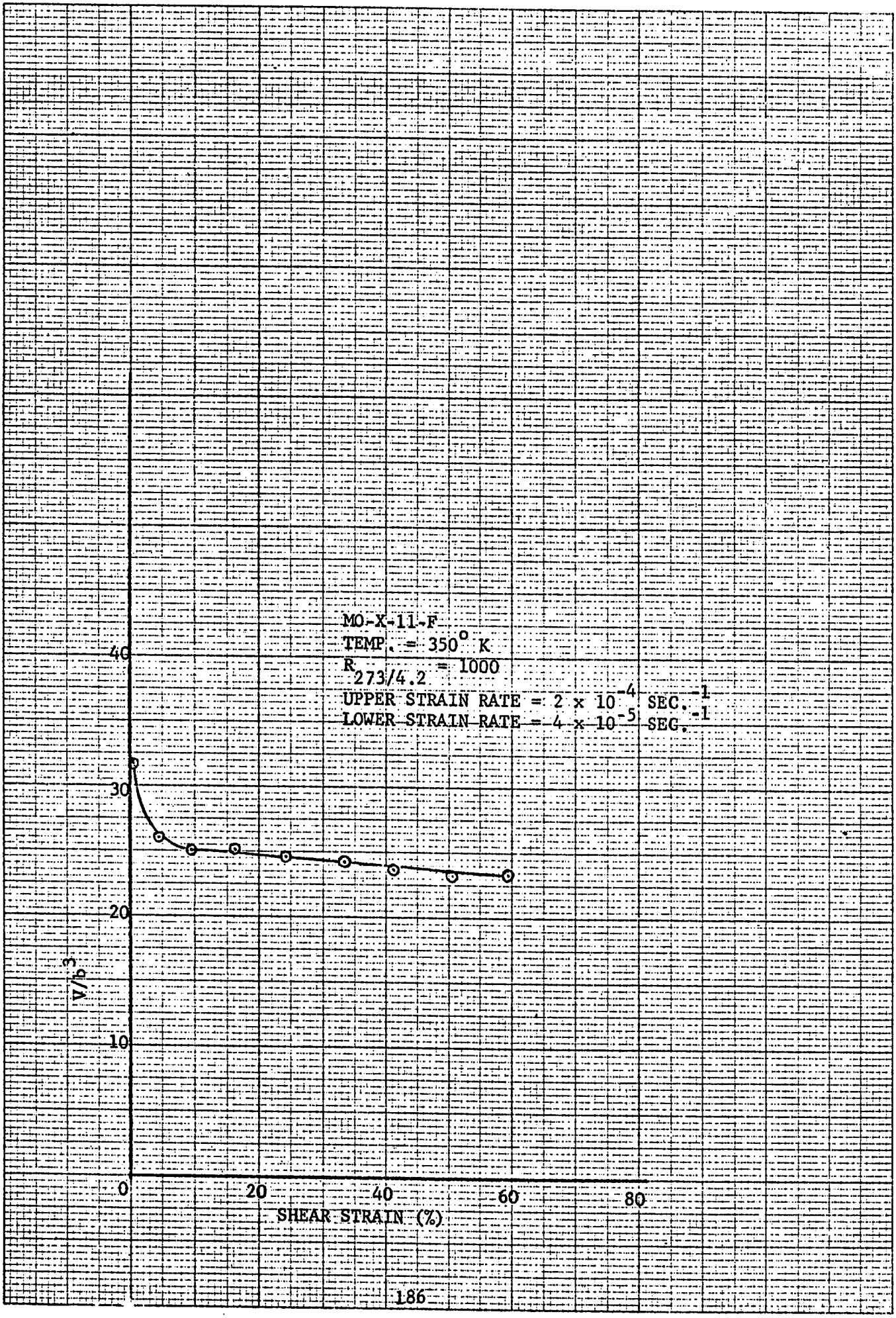

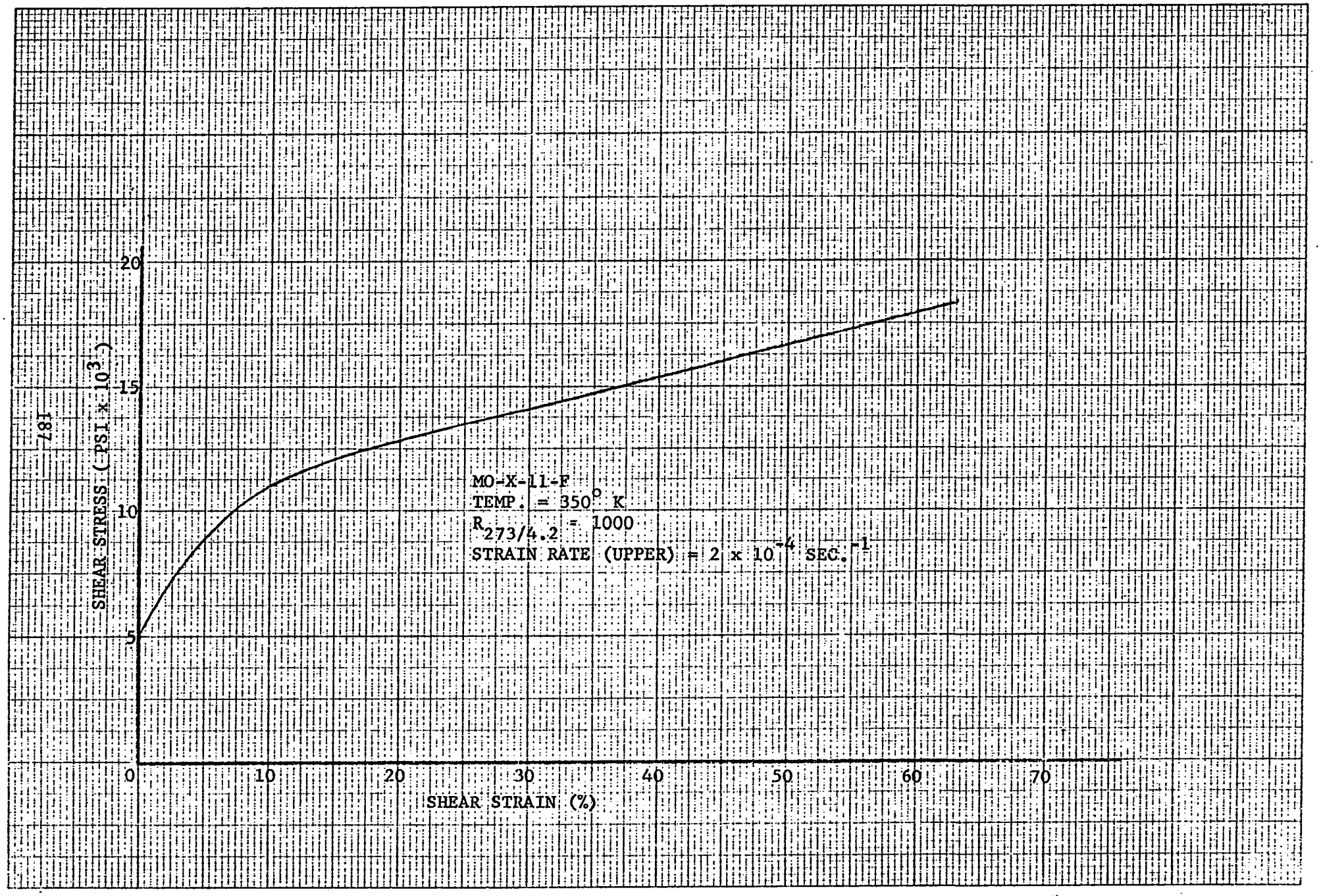

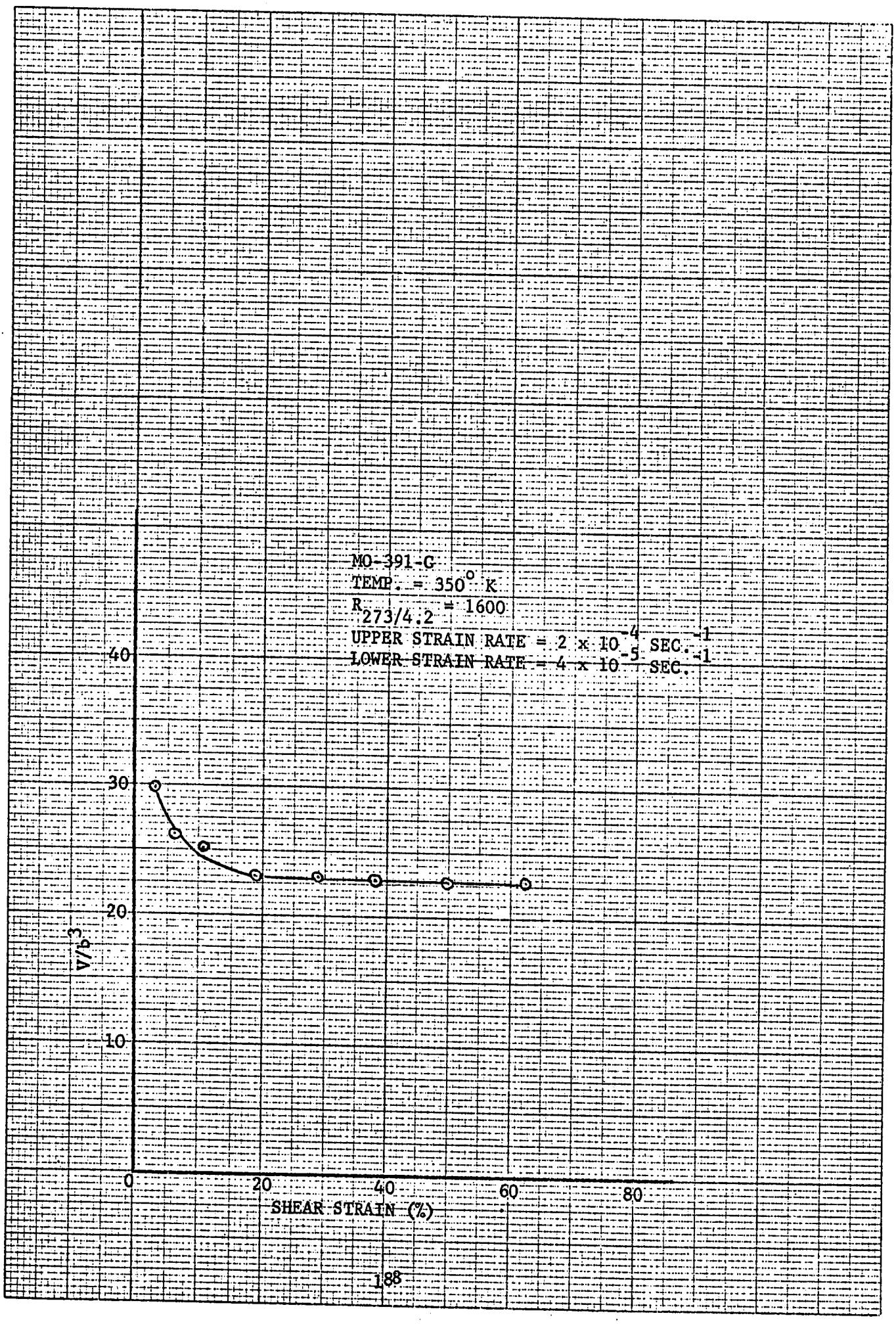

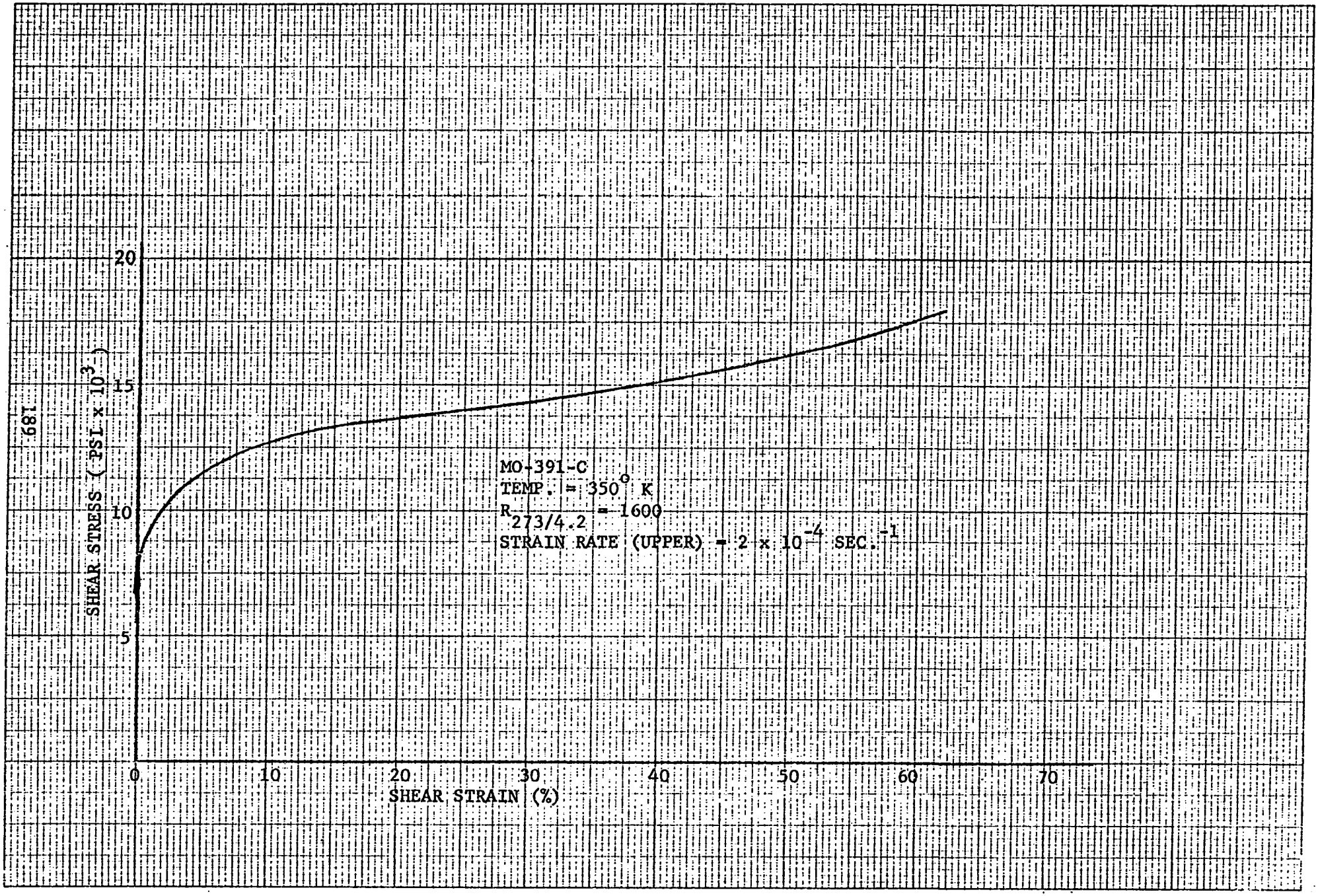

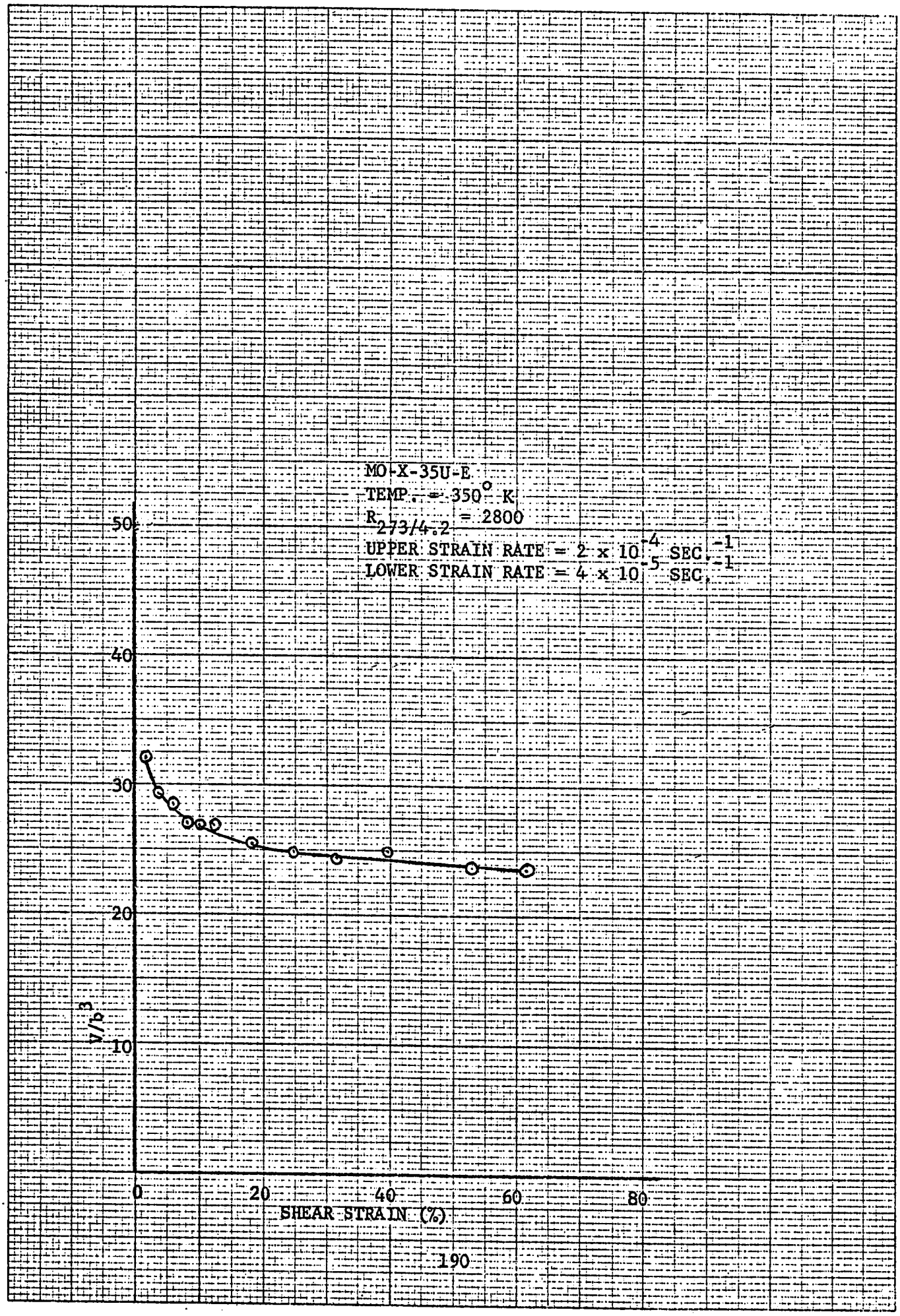

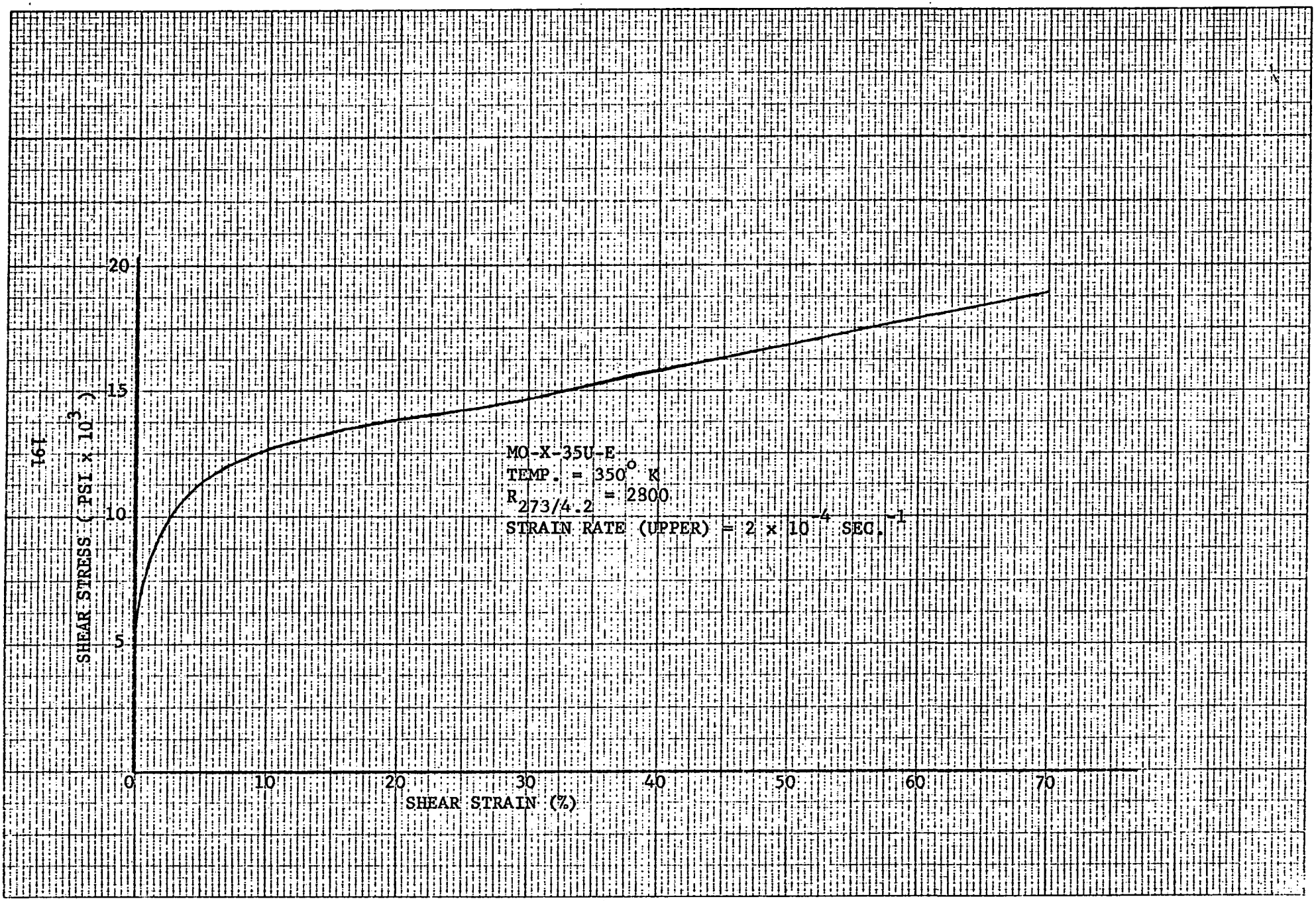

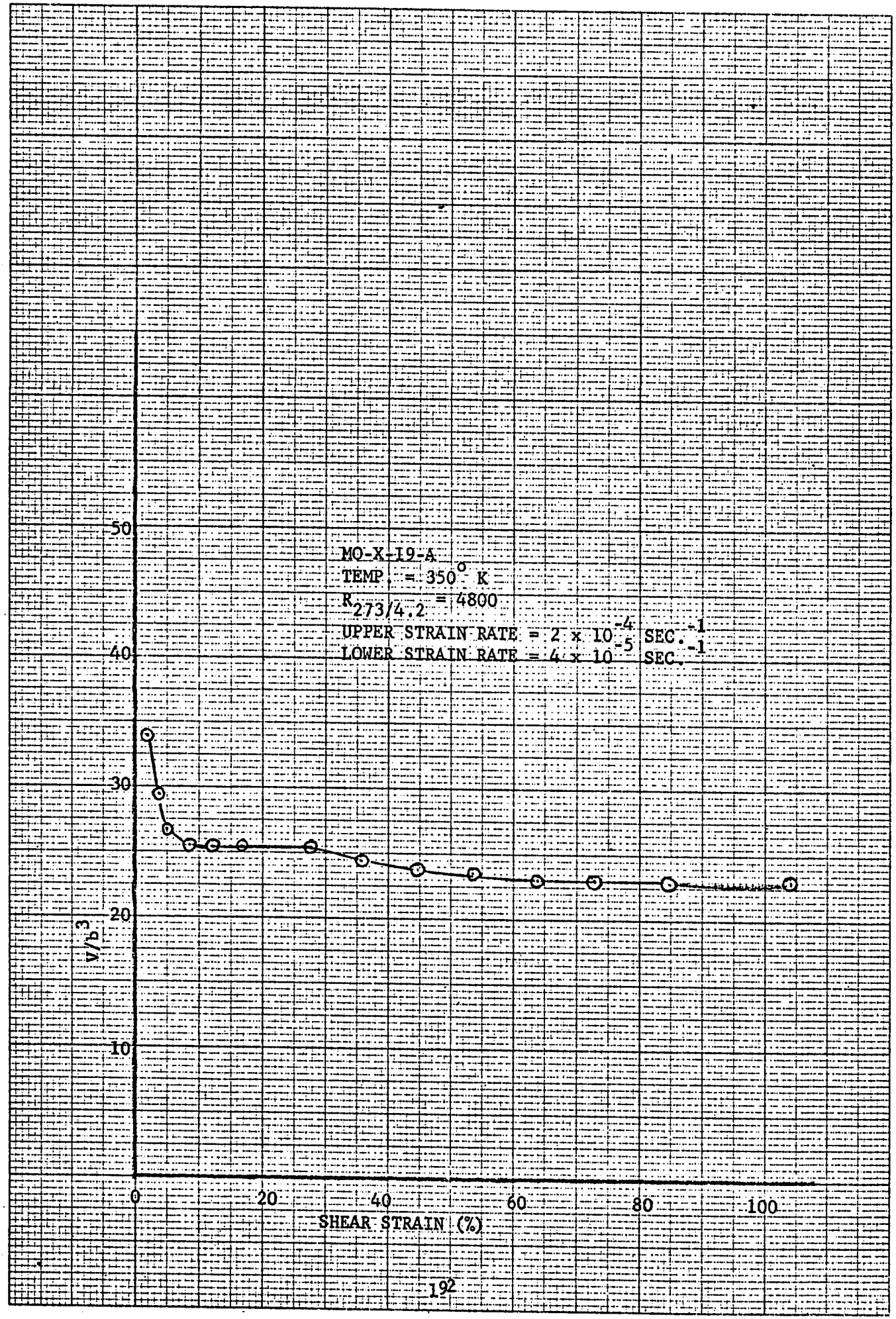

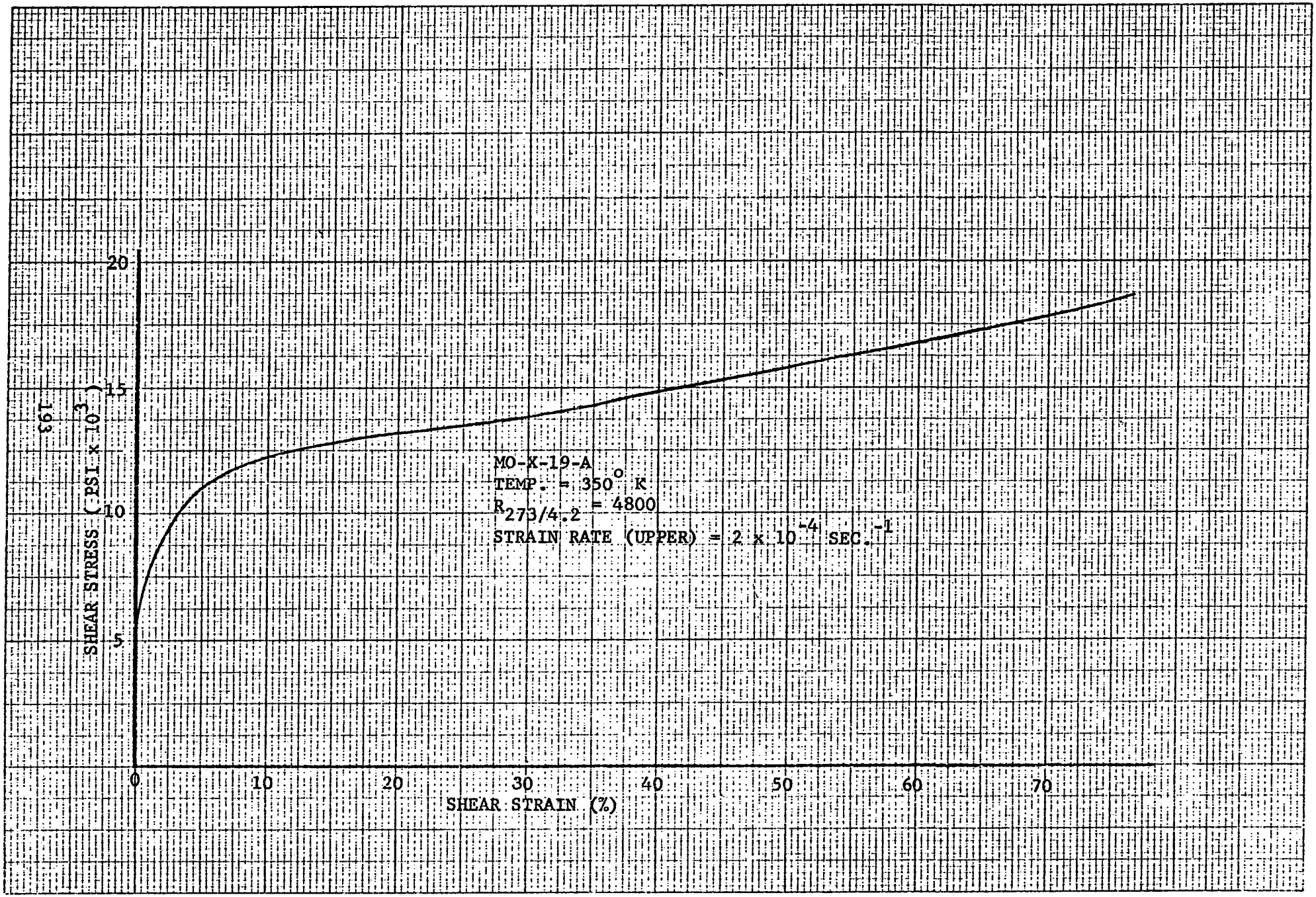

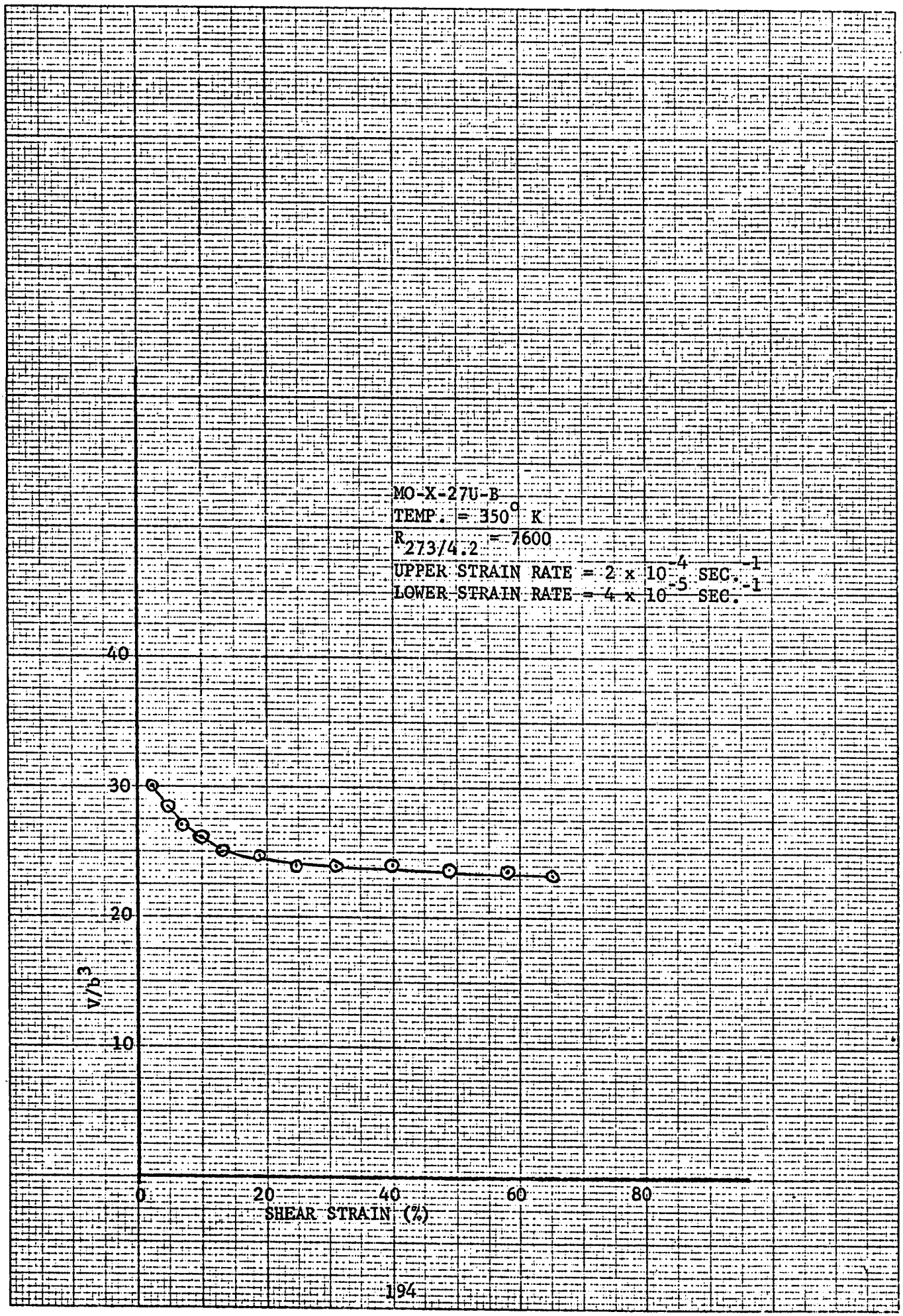

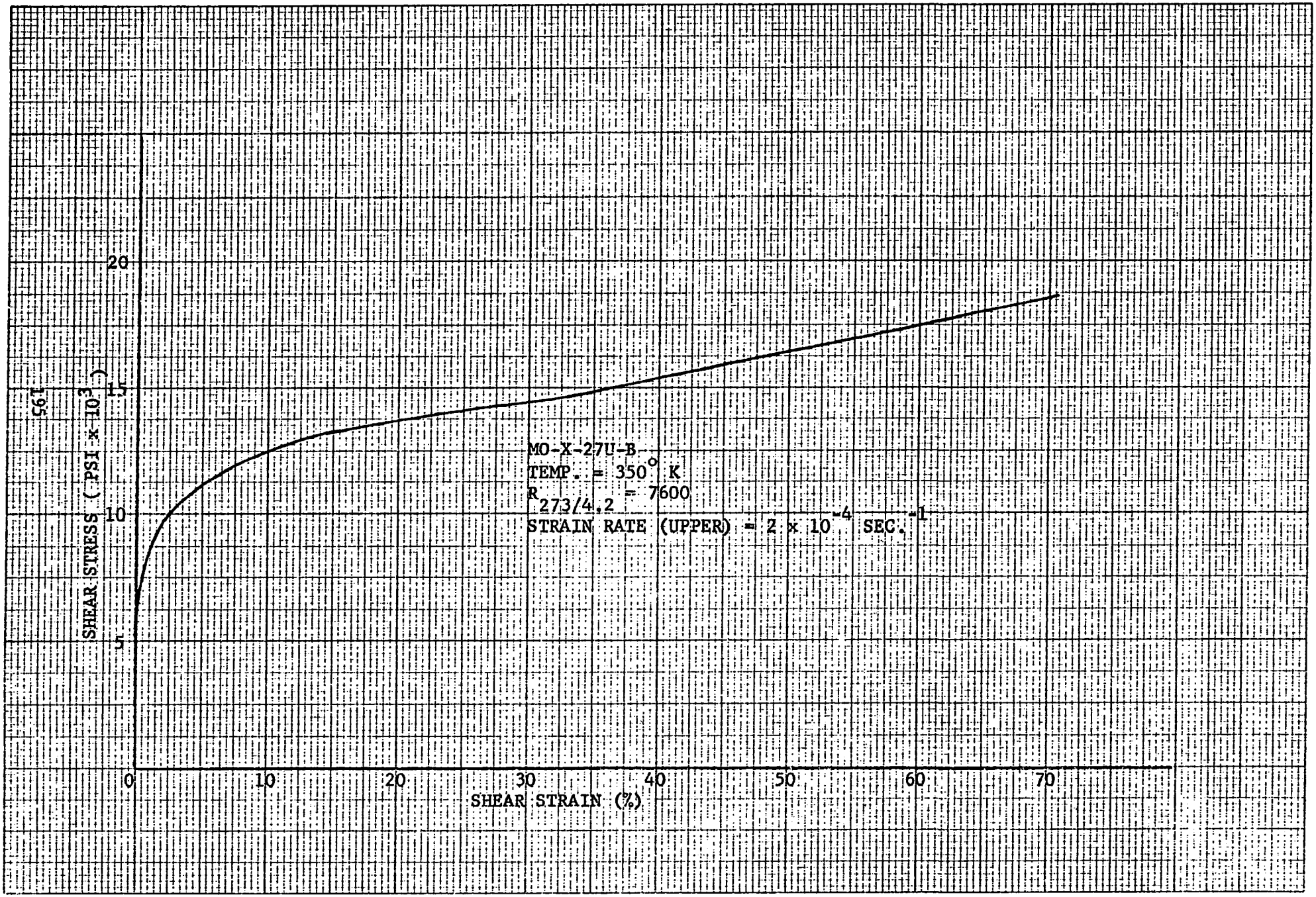

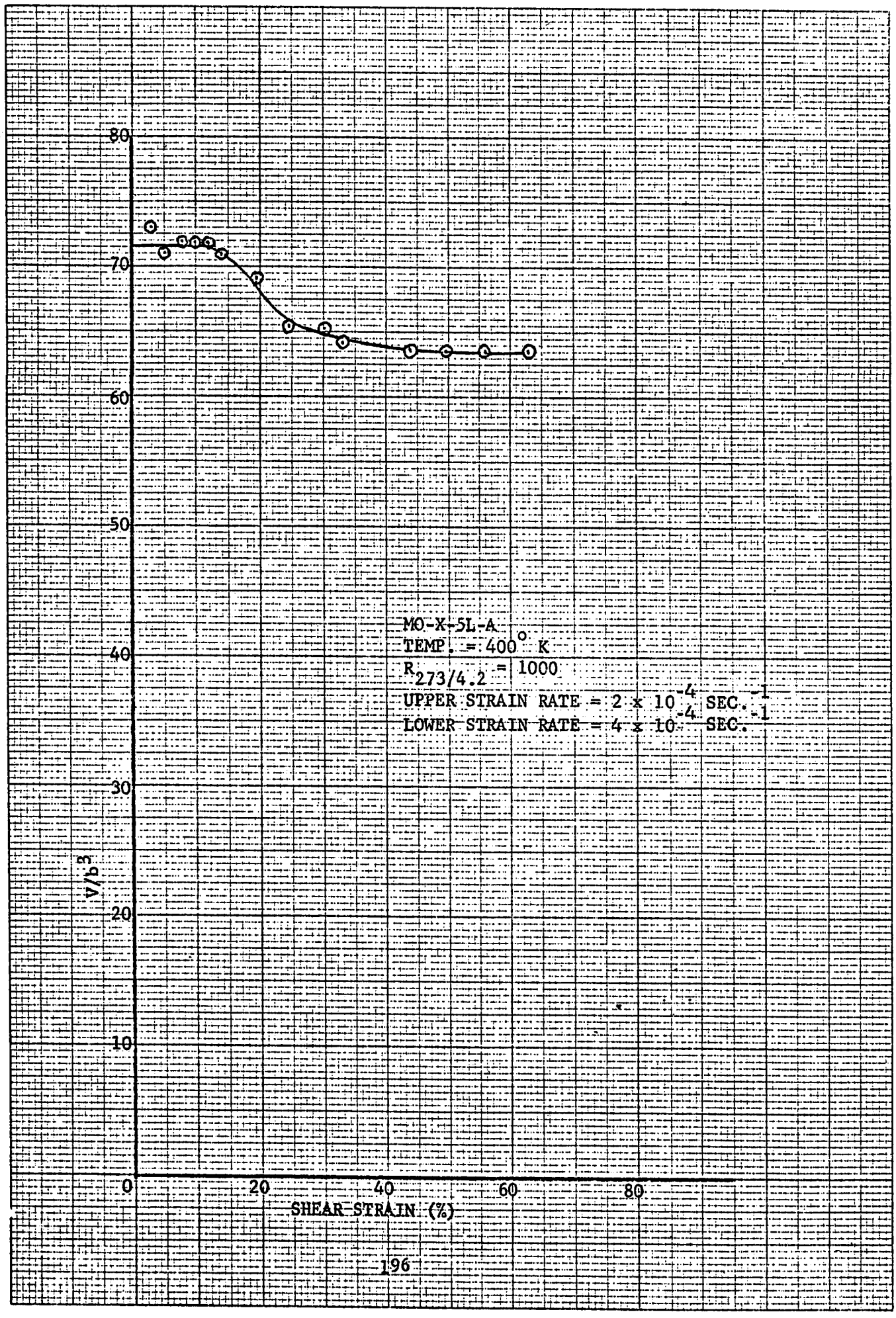

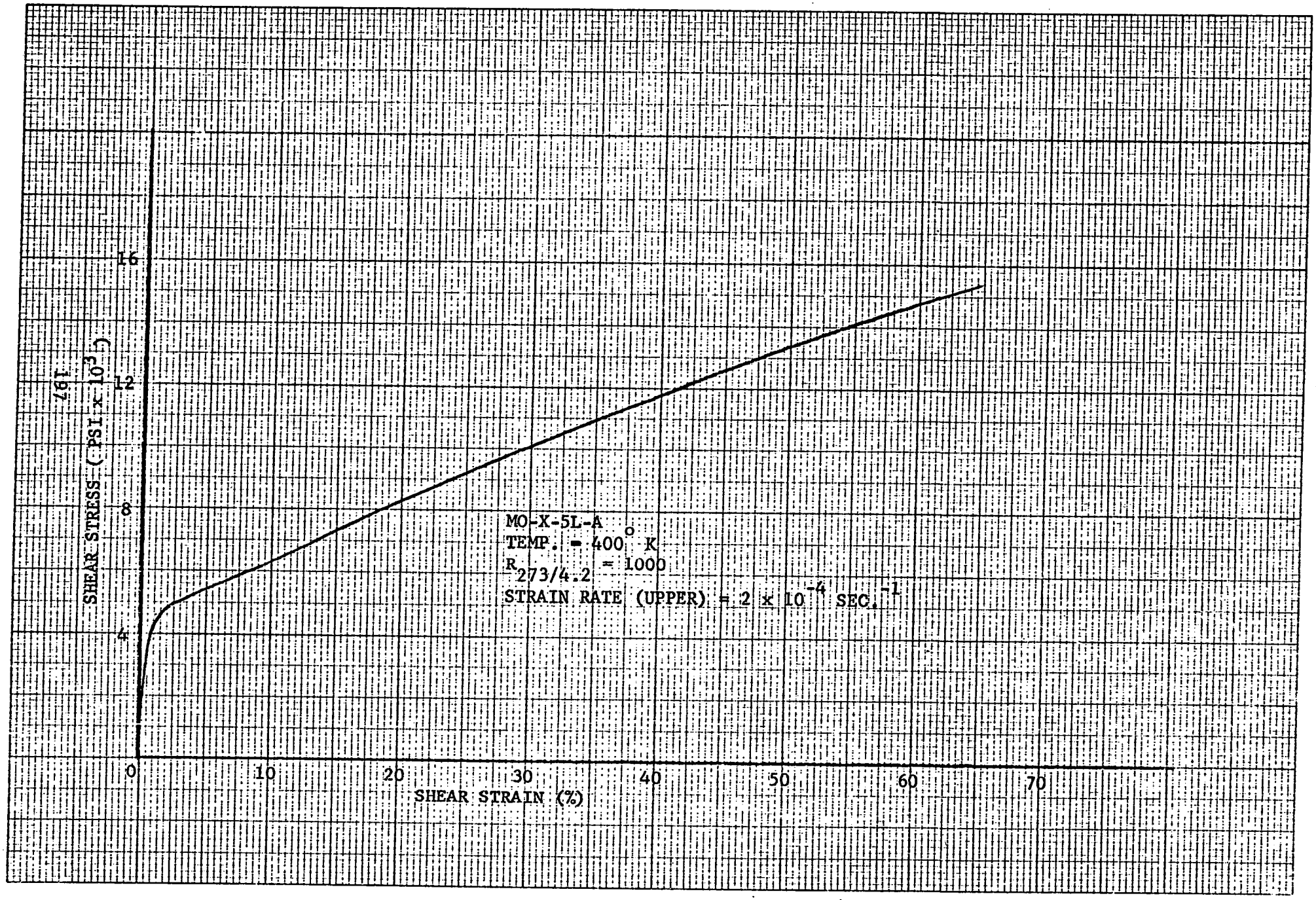

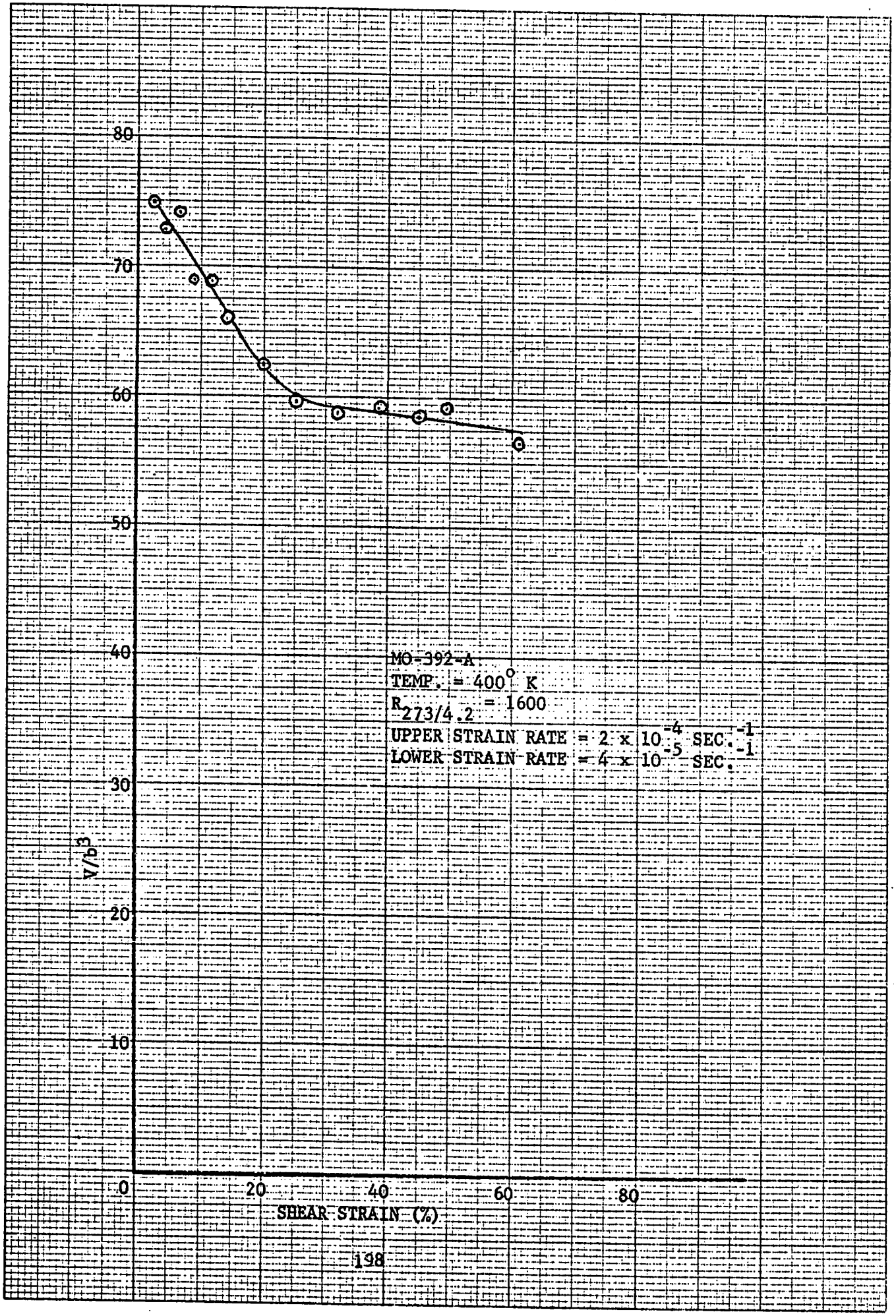

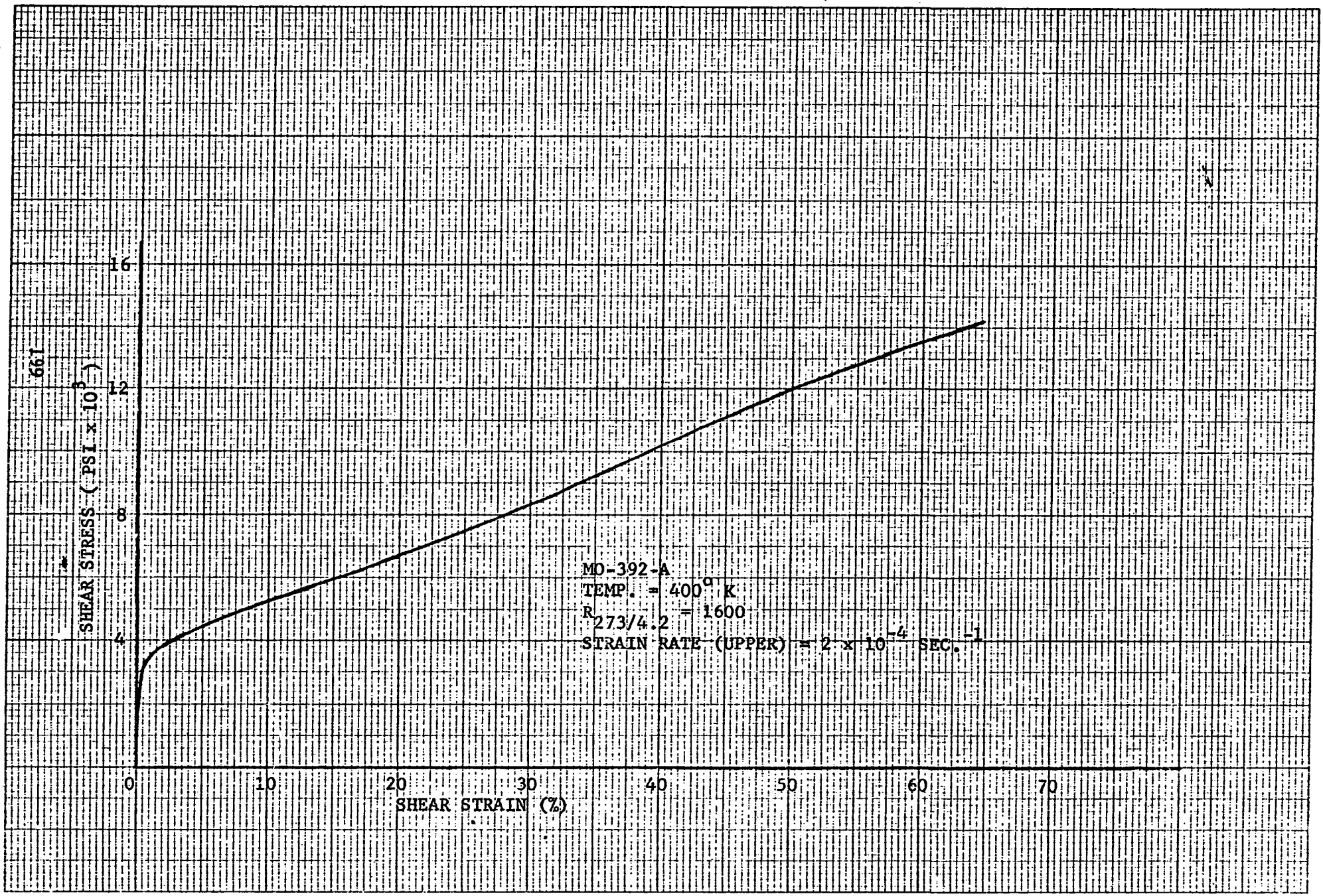

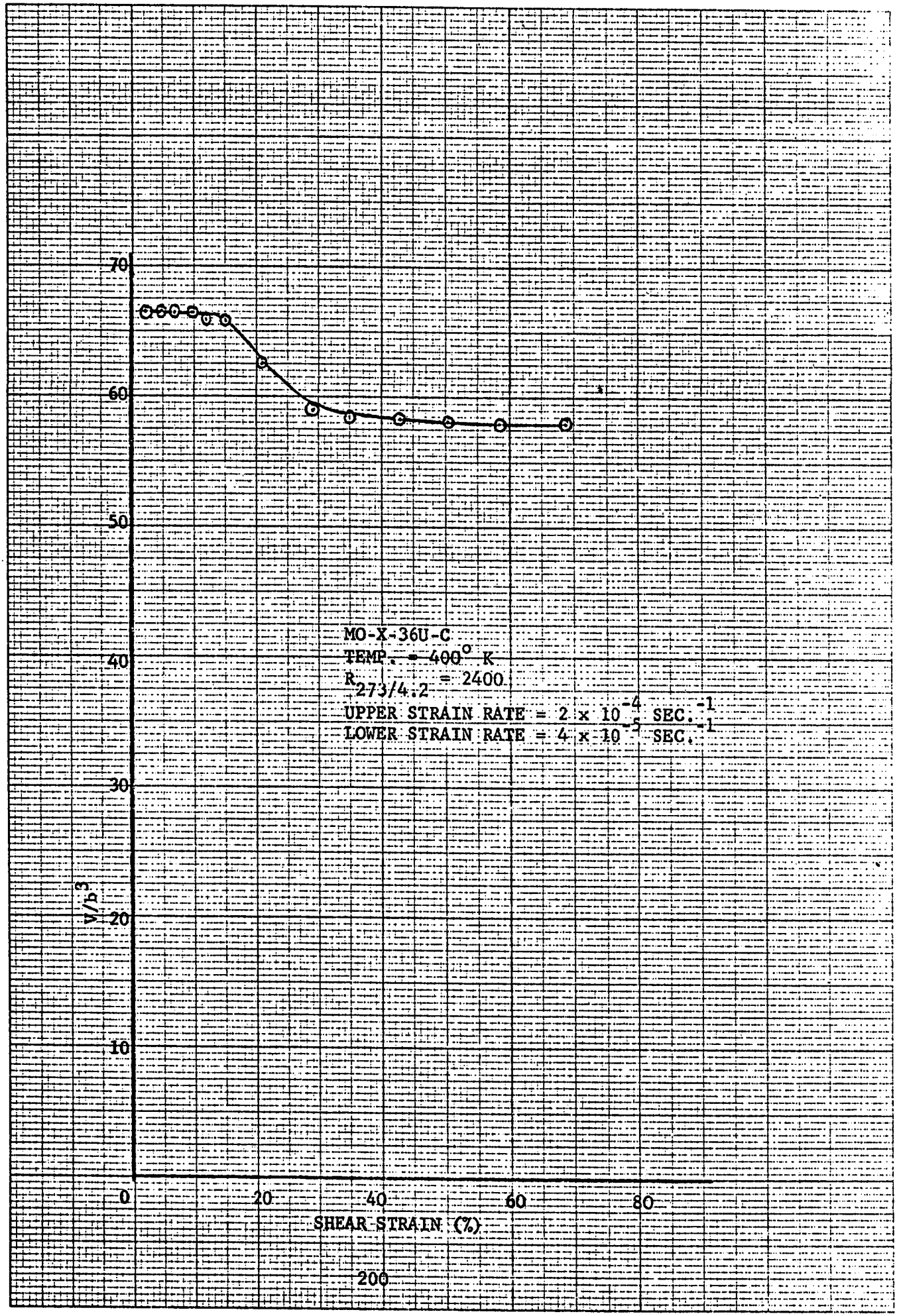

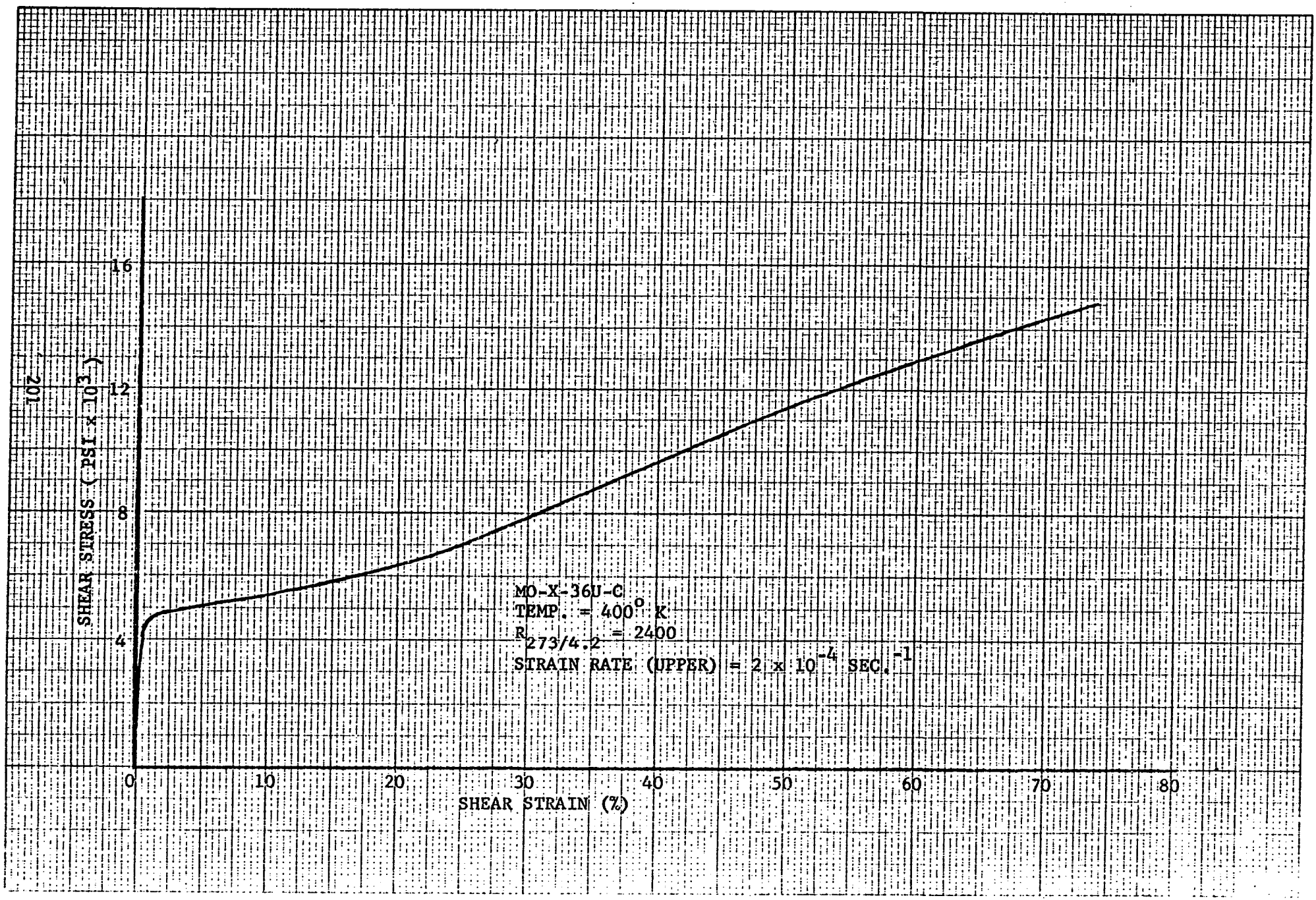

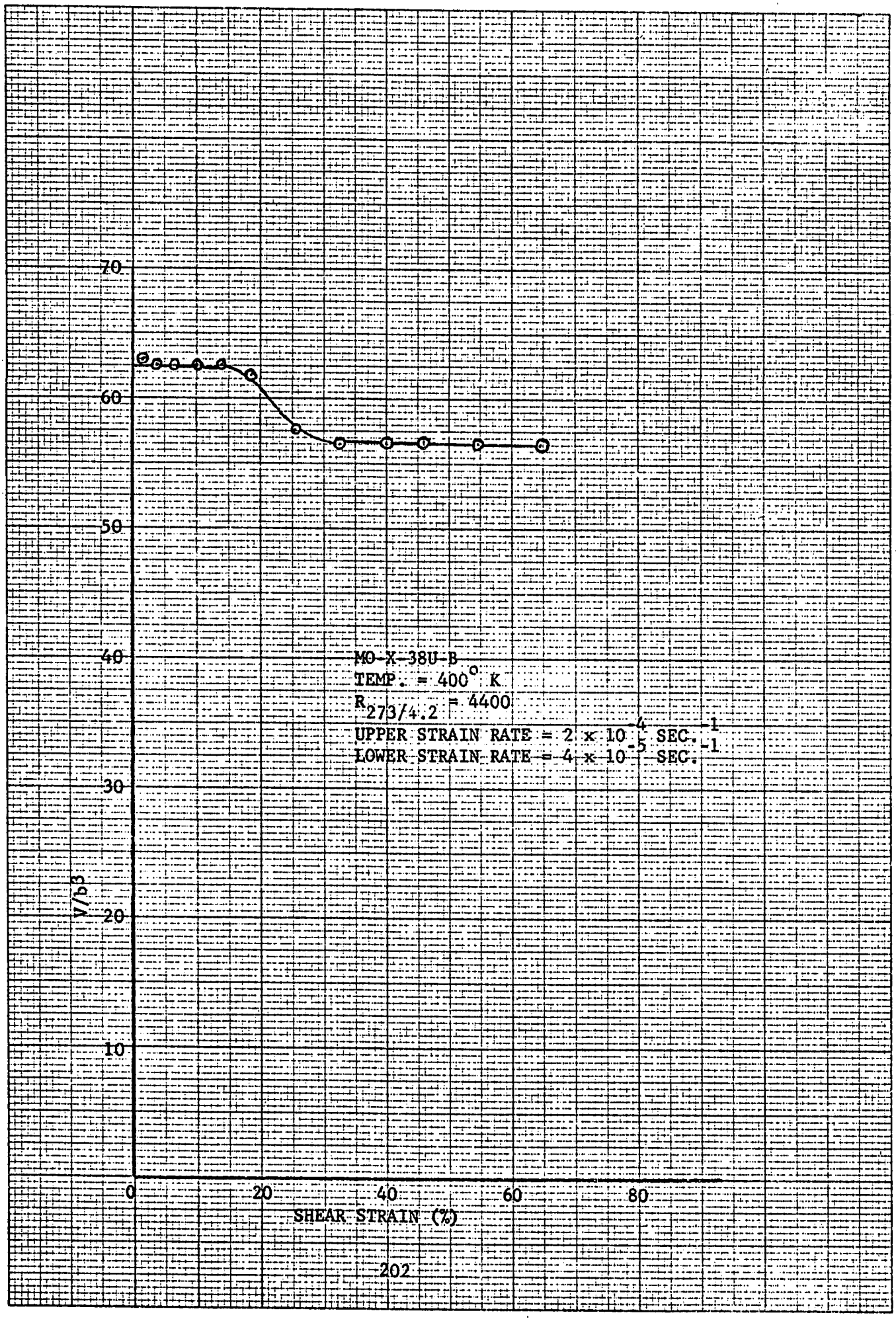

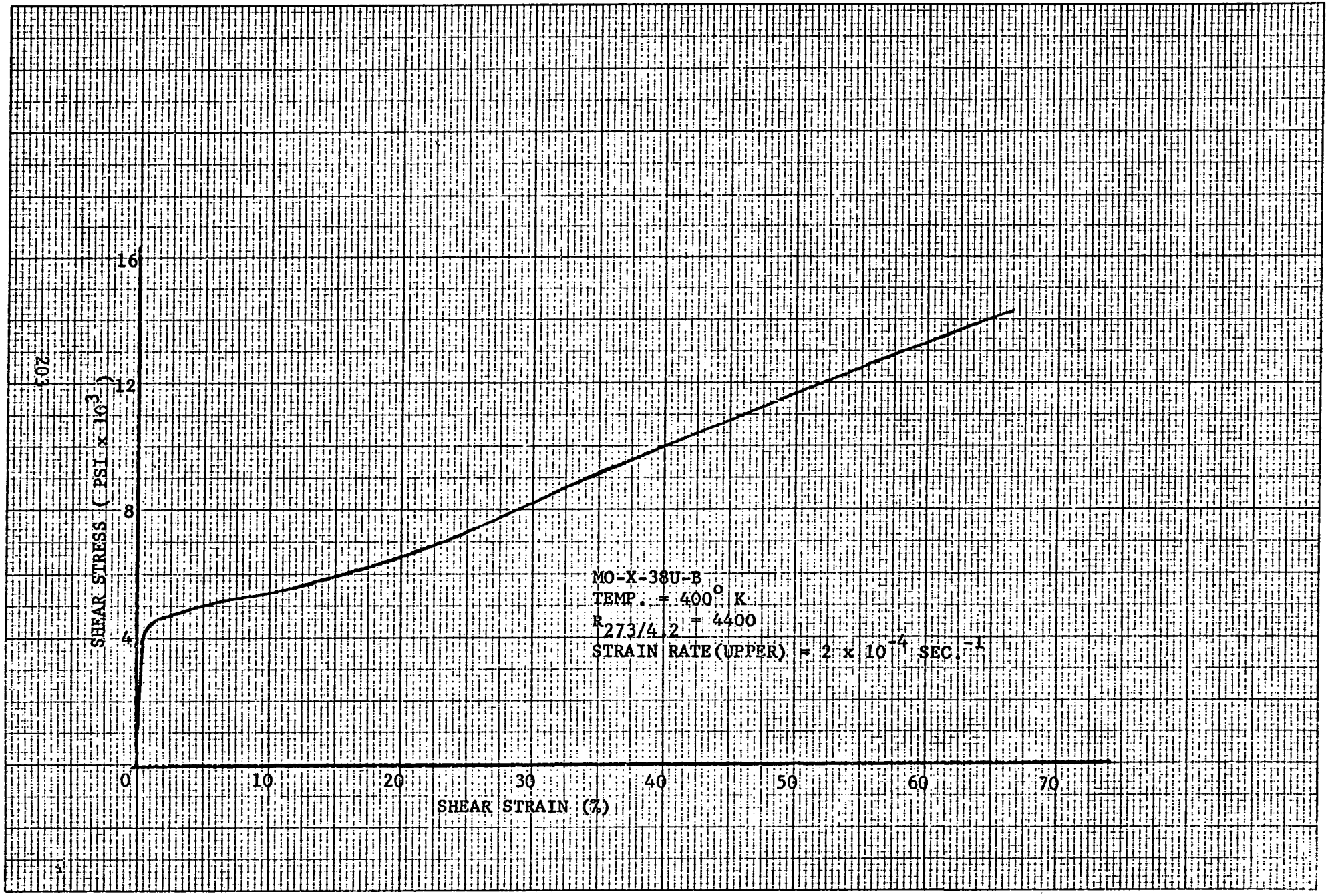

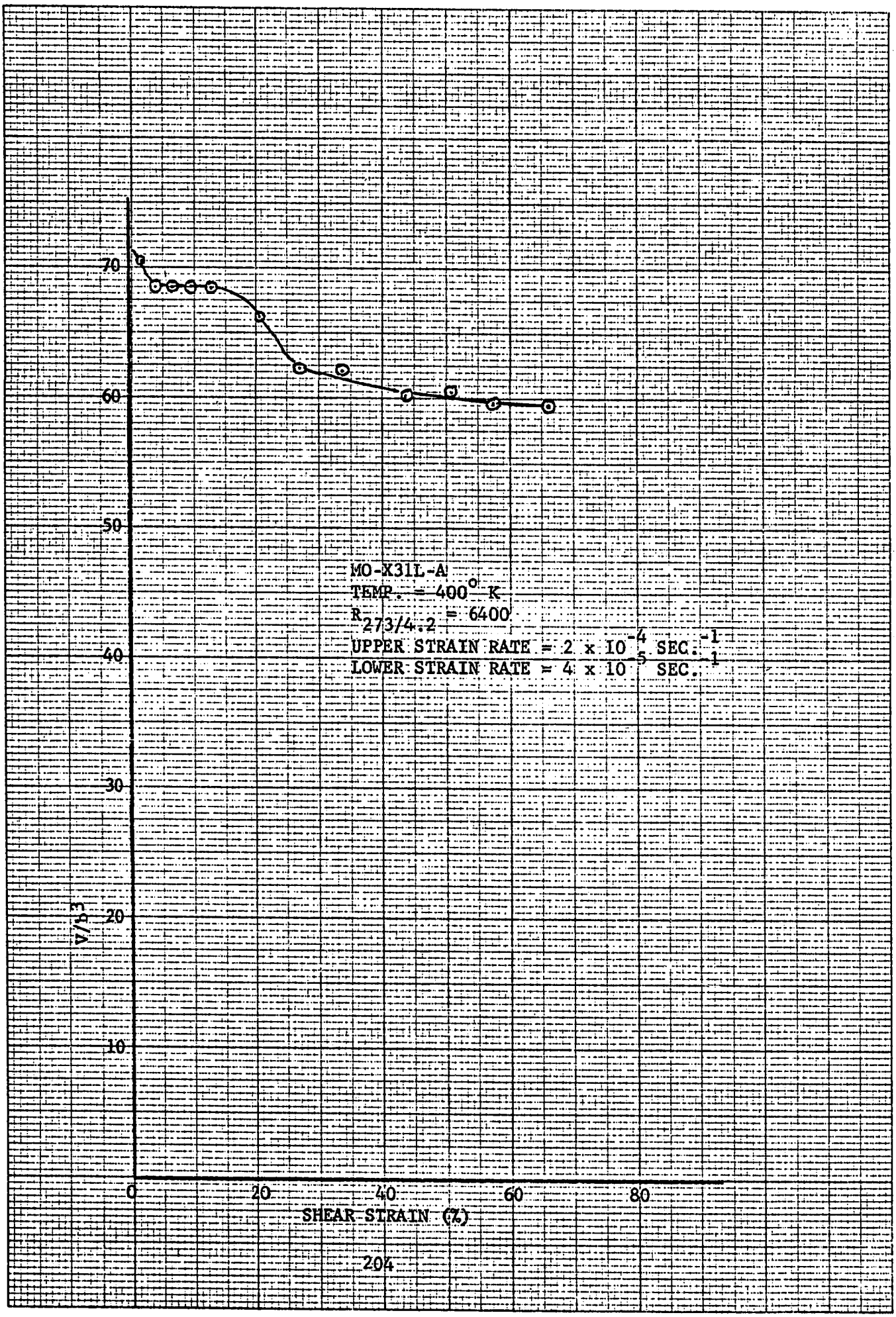

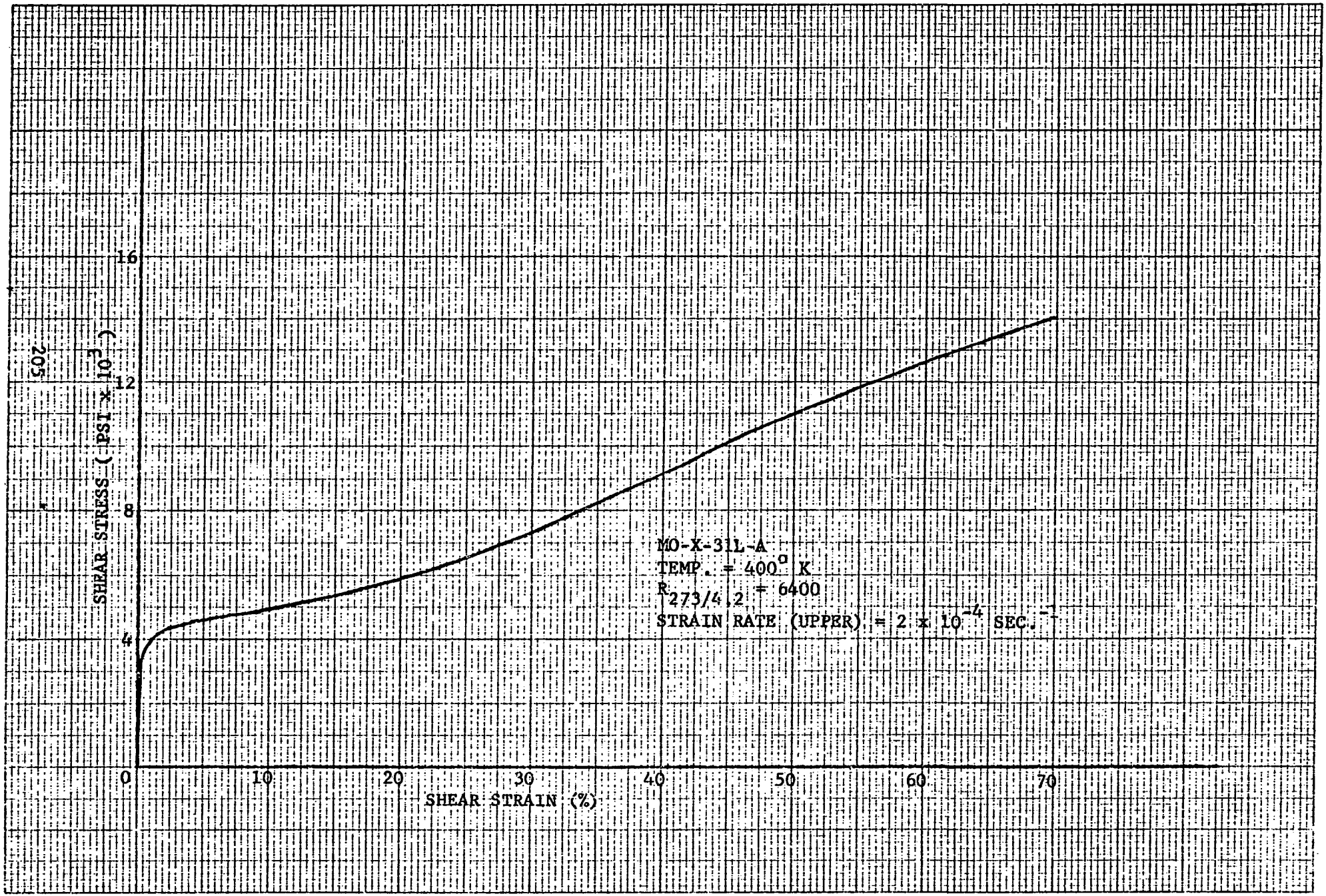

205